

# UNIVERSITÉ FRANÇOIS – RABELAIS DE TOURS

**ÉCOLE DOCTORALE EMSTU**

**E.A. 6293 GéoHydroSystèmes COntinentaux**

**THÈSE** présentée par :

**Elie DHIVERT**

Soutenue le : **04 décembre 2014**

pour obtenir le grade de : **Docteur de l'université François – Rabelais de Tours**

Discipline/ Spécialité: **Géosciences - Environnement**

**Mécanismes et modalités de la distribution spatiale et temporelle des métaux dans les sédiments du bassin versant de la Loire**

**THÈSE dirigée par :**

**Cécile Grosbois** - Professeur, université François – Rabelais de Tours

**Marc Desmet** - Professeur, université François – Rabelais de Tours

**RAPPORTEURS :**

**Fabrice Monna** - Professeur, université de Bourgogne, Dijon

**Jean-Marie Mouchel** - Professeur, université Pierre et Marie Curie, Paris 6

---

**JURY :**

**Ondrej Bábek** - Professeur, université de Palacky, République Tchèque

**Xavier Bourrain** - Expert, Agence de l'eau Loire Bretagne

**Marc Desmet** - Professeur, université François – Rabelais de Tours

**Cécile Grosbois** - Professeur, université François – Rabelais de Tours

**Fabrice Monna** - Professeur, université de Bourgogne, Dijon

**Emmanuelle Montarges-Pelletier** – CR, université de Lorraine, Nancy

**Jean-Marie Mouchel** - Professeur, université Pierre et Marie Curie, Paris 6





## **Remerciements :**

Ce travail de thèse résulte de la collaboration fructueuse entre différents acteurs de la recherche environnementale. Il n'est pas le simple fait de la contribution individuelle de chacun, mais de la synergie d'un groupe à un effort de recherche commun. A ce titre, je tiens doublement à remercier mes deux encadrants Cécile Grosbois et Marc Desmet pour leur aide et leur soutien, mais aussi pour avoir initié et animé ce projet de recherche pluridisciplinaire. Je tiens également à remercier tous les collaborateurs de ces travaux : Alexandra Coynel, Alexandra Courtin-Nomade, Irène Lefèvre, Stéphane Rodrigues, les laboratoires ArteHis - UMR 6298 et CRPG - UMR 7358. Je remercie aussi Lauren Valverde, la coordinatrice du réseau d'observation des sédiments de la Loire et de ses affluents (OSLA) dont fait partie ce projet scientifique. J'adresse un sincère remerciement aux gestionnaires du bassin, l'Agence de l'Eau Loire Bretagne en la personne de Xavier Bourrain et l'établissement public Loire (EPL), qui au-delà de financer cette étude ont aussi participé aux réflexions et fourni des informations particulièrement utiles. Je remercie également les membres du comité de pilotage de cette thèse que je n'ai pas encore cité : Dominique Boust, Jean-François Chiffolleau, Florence Curie et Michel Meybeck. Je tiens aussi à adresser mes remerciements à Fabrice Monna et Jean-Marie Mouchel les rapporteurs de ce travail de thèse ainsi qu'à Ondrej Bábek et Emmanuelle Montarges-Pelletier les membres du jury de thèse qui n'ont pas encore été cités. Je souhaite aussi tout particulièrement remercier mes collègues doctorants, techniciens et ingénieurs qui ont aussi pris une part importante à cette étude non seulement pour leur bonne humeur et leur soutien, mais aussi pour leurs idées constructives et leur aide. Je remercie fortement ma famille, mes amis, Aurélie pour leur présence de tous les instants. Pour finir, j'adresse un grand merci à la grande motivation de la fin de cette thèse !

## Résumé :

Dans le but d'étudier la distribution spatiale et temporelle des contaminations métalliques dans les sédiments du bassin de la Loire, une approche intégrée à l'ensemble du bassin a été menée. Ces travaux s'intéressent non seulement à la contribution des sources historiques de contamination, mais aussi aux processus géomorphologiques et hydrosédimentaires qui régissent le transport et l'archivage des sédiments et éléments traces associés. Ce manuscrit est organisé en trois parties expliquant la démarche et les résultats de cette étude.

La première partie propose un état des lieux des connaissances concernant l'enregistrement sédimentaire des contaminations métalliques en milieu fluviatile. Elle permet de faire émerger les problématiques scientifiques de l'étude concernant la variabilité spatiale de l'archivage des sédiments et contaminants associés à l'échelle de l'environnement fluviatile et du bassin versant de la Loire

La seconde partie permet de répondre à des verrous scientifiques concernant la représentativité des enregistrements sédimentaires. Les travaux qui la constituent visent à comprendre l'influence de l'environnement de dépôts sur l'enregistrement des signaux géochimiques. Les résultats sont présentés sous forme de deux articles. Le premier traite de la contribution des dépôts de crues dans le remplissage sédimentaire d'un réservoir de barrage et de l'influence de ces événements hydrosédimentaires sur l'enregistrement des contaminations. Un second article s'intéresse à l'influence des environnements fluviatiles d'une plaine alluviale sur l'archivage des sédiments et contaminants associés.

La troisième partie met en évidence la variabilité spatiale de l'archivage des contaminations sédimentaires à l'échelle du bassin de la Loire. D'autre part, les sources historiques de contaminations y sont caractérisées à l'échelle du bassin et sur période couvrant l'ère industrielle.

## **Abstract:**

This study is an integrated approach at the entire Loire basin (France) scale of the spatial and temporal variability of metallic contaminations in sediments. This study takes into account the history of contamination sources and also geomorphological processes controlling the transport and the archiving of sediments and associated trace elements. This manuscript is organized in three sections.

The first one provides a state of the art concerning the archiving of sedimentary contaminations in fluvial environments. In this section, scientific issues are formulated concerning the spatial variability of the sedimentary contamination archiving at different scales, the fluvial environment and at the entire basin scale.

The second section of the study has methodological purposes concerning the representation of sedimentary records. It aims to highlight influences of depositional environments on recorded geochemical signals. Results are mentioned in two papers. The first one points out contributions of flood events in the sedimentary infill of a dam reservoir and influences of these hydrosedimentary events on the archiving of geochemical signals. The second deals with influences of fluvial environments on the archiving of sediments and associated contaminants in a floodplain.

The third section is dedicated to the spatial variability of recorded temporal evolutions of sedimentary contaminations at the entire Loire basin scale. In addition, historical contamination sources are characterized at basin scale and over a time interval covering the industrial period.

## Tables des matières :

Contexte et enjeux de l'étude .....	10
Partie 1 – Distribution spatiale et temporelle des contaminants métalliques dans les sédiments : données disponibles sur le bassin de la Loire et problématiques scientifique....	17
Chapitre 1 - Histoire de la contamination métallique des sédiments .....	18
1.1. Evolution temporelle des contaminations sédimentaires .....	18
1.2. Activités polluantes aux cours de l'ère industrielle .....	22
Chapitre 2 - Facteurs de contrôle de la distribution spatiale et temporelle des contaminations sédimentaires en milieu fluviatile.....	28
2.1. Variabilité spatiale des fonds géochimiques.....	28
2.2. Variabilité spatiale des mécanismes d'archivage des sédiments et contaminants associés.....	32
Chapitre 3 - Problématiques scientifiques et plan de la thèse .....	37
Partie 2 - Influences de l'environnement de dépôt sur l'archivage des sédiments et des contaminants associés .....	49
Chapitre 4 - Synthèse .....	50
4.1. Objectifs et méthodes analytiques .....	51
4.2. Principaux résultats .....	52
4.3. Conclusion .....	55
Chapitre 5 - Influences of major flood sediment inputs on sedimentary and geochemical signals archived in a reservoir core (Upper Loire basin, France) .....	57
5.1. Introduction.....	59
5.2. Study area and methodology .....	60
5.3. Results and discussion.....	63
5.4. Conclusions.....	80
Chapitre 6 - Influence of fluvial environments on sediment archiving processes and temporal pollutant dynamics (Upper Loire River, France) .....	87
6.1. Introduction:.....	89
6.2. Study area and methods .....	90
6.3. Results and discussion.....	95
6.4. Conclusions.....	117
Partie 3 - Variabilité spatiale de l'enregistrement sédimentaire des contaminations à l'échelle du bassin de la Loire .....	124
Chapitre 7 - Synthèse .....	125
7.1. Objectifs et méthodes analytiques .....	127
7.2. Principaux résultats .....	128
7.3. Conclusion .....	132
Chapitre 8 – Spatial variability of trace element sedimentary contaminations archived in sediments of the Loire basin .....	133
8.1. Introduction.....	135
8.2. Study area and methodology .....	136
8.3. Results .....	145
8.4. Discussion .....	159
8.5. Conclusions.....	175
Conclusions et perspectives .....	187

## **Liste des tableaux :**

Tab. 2.1 : Concentrations sédimentaires de référence	28
Tab. 5.1 : Composition géochimique des sédiments de l'archive de Villerest	67
Tab. 6.1 : Composition géochimique des sédiments de l'archive de Decize (berge)	100
Tab. 6.2 : Composition géochimique des sédiments de l'archive de Decize (paléochenal)	102
Tab. 6.3 : Concentrations sédimentaires préindustrielles à Decize	114
Tab. 8.1 : Facteurs d'enrichissement des sédiments de l'archive de Decize	153
Tab. 8.2 : Facteurs d'enrichissement des sédiments de l'archive d'Apremont	155
Tab. 8.3 : Facteurs d'enrichissement des sédiments de berge du bassin de la Loire	164

## Liste des figures :

Fig. 1 : Carte géologique et industrielle du bassin de la Loire	14
Fig. 1.1 : Comparaison interbassin de l'évolution temporelle des contaminations	21
Fig. 1.2 : Histoire industrielle du basin de la Loire	27
Fig. 2.1 : Comparaison inter et intrabassin des états de référence	31
Fig. 2.2 : Facteurs de variabilité spatiale des contaminations sédimentaires	34
Fig. 5.1 : Carte du bassin et hydrologie de la Loire en amont du barrage de Villerest	64
Fig. 5.2 : Log sédimentaire de l'archive de Villerest	69
Fig. 5.3 : Diagramme CM de l'archive de Villerest	70
Fig. 5.4 : Modèle d'âge de l'archive de Villerest	74
Fig. 5.5 : Evolution temporelle des facteurs d'enrichissement à Villerest	76
Fig. 5.6 : Composition géochimique des séquences de crue dans l'archive de Villerest	79
Fig. 6.1 : Description du site de carottage de Decize	91
Fig. 6.2 : Log sédimentaires et diagrammes CM pour les archives de Decize	96
Fig. 6.3 : Modèles d'âge des archives de Decize	107
Fig. 6.4 : Profil vertical de Si/Al, Hf, COT et ST dans les archives de Decize	109
Fig. 6.5 : Evolution temporelle des facteurs d'enrichissement à Decize	115
Fig. 8.1 : Carte des sites d'échantillonnages sédimentaires dans le basin de la Loire	138
Fig. 8.2 : Description du site de carottage d'Apremont-sur-Allier	142
Fig. 8.3 : Comparaison des signatures géochimiques des sédiments de fond et de berge	146
Fig. 8.4 : Evolution temporelle des facteurs d'enrichissement à de Decize et Apremont	149
Fig. 8.5 : Comparaison amont-aval des signaux géochimiques archivés	157
Fig. 8.6 : Comparaison interbassin des signaux géochimiques archivés	160
Fig. 8.7 : 1910-1930 - association Sb-Sn dans les sédiments de la Loire Amont	162
Fig. 8.8 : 1940-1950 - association Sb-COT dans les sédiments la Loire Amont et l'Allier	166
Fig. 8.9 : 1940-1950 - association Bi-Cd dans les sédiments du bassin de la Loire	173
Fig. 8.10 :> 1980 – association Cd-Hg dans les sédiments du barrage de Villerest	176

## Contexte et enjeux de l'étude

Depuis le XIX<sup>ème</sup> siècle et l'avènement de l'ère industrielle, **les activités anthropiques** ont profondément modifié les cycles naturels à l'échelle globale, définissant ainsi une nouvelle ère géologique : l'Anthropocène (Crutzen, 2000 ; Steffen *et al*, 2007 ; Steffen *et al*, 2011). Dans ce contexte, les réponses aux crises systémiques engendrées par les activités humaines (perturbation des équilibres géologiques, géochimiques, écosystémiques et climatiques) constituent des **enjeux de civilisation** à appréhender selon différentes échelles d'espace et de temps. Les caractères intégrateurs et interconnectés des systèmes naturels imposent non seulement de maîtriser nos **impacts actuels** à l'échelle globale, mais aussi de tenir compte de **l'héritage des dégradations environnementales passées**, notamment en ce qui concerne les substances chimiques non dégradables comme les éléments traces (ET) ou les polluants organiques persistants.

A l'échelle mondiale, la mortalité liée à **l'exposition aux substances chimiques toxiques** est importante (4.9 millions de

personnes soit 8.3% de décès en 2004; Prüss-Ustün *et al*, 2011). Elle constitue aussi la troisième cause d'érosion de la biodiversité à l'échelle mondiale (Ramade, 2007). De nos jours, **les dynamiques temporelles des contaminations** sont différentes entre les pays émergents où le développement économique et démographique se traduit par une augmentation exponentielle des niveaux de contaminations et les pays anciennement industrialisés où la transition économique ainsi que le traitement des rejets industriels et urbains ont permis une amélioration significative de la qualité des milieux depuis les années 1980 (ex. Meybeck et Helmer, 1989; Stern, 1998 ; Hettige *et al*, 2000 ; Meybeck, 2002 ; Stern, 2004). Dans les pays où les rejets anthropiques sont contrôlés, **les retombées atmosphériques globales et la remobilisation des stocks de contaminants** prennent une place non négligeable dans la contamination de l'environnement, pouvant localement représenter d'importants risques toxiques pour les populations et les écosystèmes (ex. Nriagu, 1990; Pruvot *et al*, 2006; Mourier *et al*, 2011). Dans cette

## Etats de références

Pour quantifier des niveaux de contaminations dans les sédiments, des valeurs guides sont nécessaires. Ces références peuvent être basées sur des notions de risques toxiques pour les écosystèmes et les sociétés humaines. Bien que permettant l'établissement de concentrations seuils pour la gestion des sédiments, de telles valeurs rendent difficilement compte de la réalité du risque toxique. En effet, selon la minéralogie des sédiments, une partie plus ou moins importante des métaux est non disponible puisque constitutive des réseaux cristallins, résistants au cours du transport solide et des alterations.

Une approche différente a été mise en place dans ce travail consistant à établir des états de références correspondant aux concentrations géogéniques. Pour ce faire, les apports lithologiques peuvent être déterminés à partir des concentrations sédimentaires dans des bassins monolithologiques non impactés ou par l'analyse de sédiments datant de l'époque préindustrielle à l'aval des bassins. Cette dernière approche permet de reconstituer des concentrations représentatives de la contribution des différentes sources naturelles au sein des bassins.

perspective, la reconstitution des dynamiques temporelles des contaminations constitue un objectif de recherche majeur, permettant d'étudier *a posteriori* les évolutions à long terme de la qualité environnementale des milieux. Le calcul des niveaux de contaminations nécessite l'établissement **d'états de références** spécifiques des matrices étudiées (*voir encadré ci-contre*). La détermination de concentrations préindustrielles permettant d'évaluer le degré de contaminations des milieux constitue là aussi un enjeu scientifique majeur.

Dans le cadre de la Directive Cadre sur l'Eau (directive européenne 2000/60 du 23 octobre 2000), la Loire comme tous les **bassins hydrographiques** de l'Union européenne doit atteindre d'ici 2015 "le bon état écologique des milieux". De nos jours, le **domaine fluviatile de la Loire** est faiblement urbanisé et industrialisé comparé à sa partie estuarienne (agglomérations de Nantes et Saint Nazaire). A ce titre, les études des contaminations métalliques des environnements aquatiques ont surtout été focalisées sur sa partie estuarienne et le nord du Golf de Gascogne (Negrel, 1997 ; Waeles *et al*, 2004). Or, la partie

amont du bassin de la Loire est considérée par les historiens comme **l'un des principaux foyers d'émergence de la Révolution industrielle en France** (Woronoff, 1994). Depuis la seconde moitié du XIX<sup>ème</sup> siècle jusqu'à la fin des années 1950, l'extraction massive du charbon et des métaux a fourni énergie et matières premières à une industrie lourde implantée à proximité des districts miniers. A cette époque, les rejets de ces activités anthropiques n'étaient pas maîtrisés. Parallèlement à cela, **le transport sédimentaire** a fortement été perturbé au sein du bassin, suite à l'aménagement du lit du fleuve et de ces principaux affluents (Babonaux, 1970 ; Leteinturier *et al.*, 2000 ; Rodrigues *et al.*, 2007 ; Détriché *et al.*, 2010 ; Grivel et Gauthier, 2012). Le stockage à long terme des sédiments et des contaminants associés induit un risque pour les sociétés et les écosystèmes du bassin. D'autre part, la rétention des sédiments contaminés au cours de l'ère industrielle permet de reconstituer **les évolutions temporelles des contaminations sédimentaires** résultant de l'histoire industrielle et minière du bassin (Grosbois *et al.*, 2012).

Dans le cadre du programme d'observation des sédiments de la Loire et

de ses affluents (OSLA), les projets de recherche "MetOrg" visent à reconstituer les dynamiques temporelles des contaminations sédimentaires du bassin de la Loire et à caractériser les sources historiques. Il est dirigé par Pr. Cécile Grosbois et Pr Marc Desmet au sein du laboratoire GéHCO (EA 6293 université F. Rabelais de Tours) ainsi que Dr Jérôme Labanowski du laboratoire IC2MP (UMR CNRS 7285 – université de Poitiers) et est financé par l'Agence de l'Eau Loire Bretagne. Le projet comporte deux parties, l'une focalisée sur les éléments traces (ET; MetOrg 1) et l'autre s'intéressant aux polluants organiques persistants (MetOrg 2). Cette thèse s'inscrit dans le volet traitant des contaminations métalliques des sédiments.

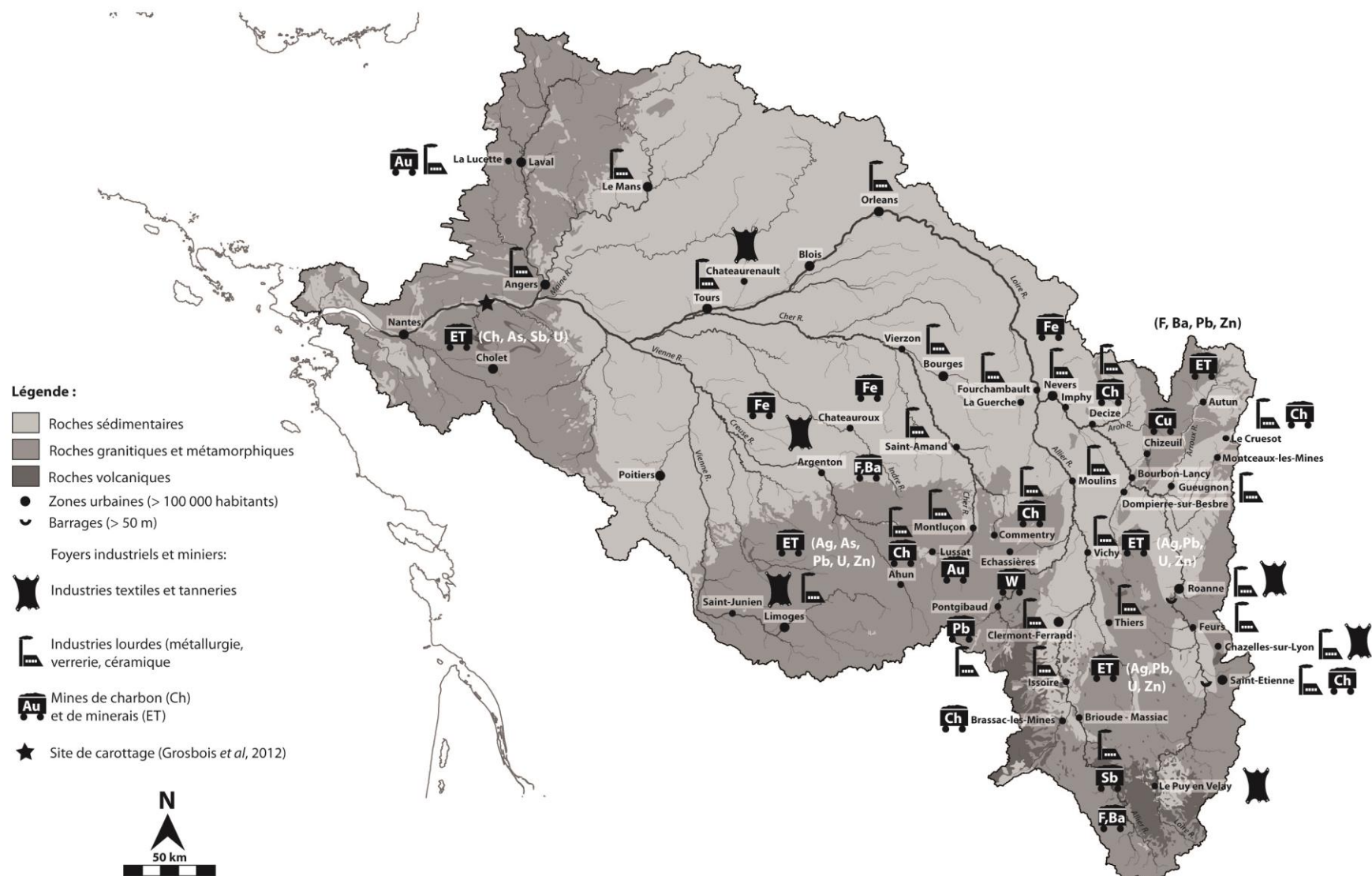
A l'échelle du bassin de la Loire, les complexes industriels et miniers sont essentiellement localisés dans le Massif Central, dans la partie amont de la Loire et de ces principaux affluents (Fig. 1 ; voir encadré p.19 pour une description physique du bassin). Cette distribution géographique des activités anthropiques est représentative des systèmes économiques basés sur l'exploitation locale des ressources géologiques. Dans ce

contexte, la reconstitution historique des contaminations sédimentaires à l'échelle du bassin doit tenir compte à la fois **de la distribution spatiale et temporelle des contaminants.**

D'autre part, la Loire et de ses principaux affluents sont des cours d'eau sablo-graveleux présentant **des morphologies diversifiées**, alternant entre cours d'eau aux tracés rectilignes ou méandriformes, à chenaux uniques ou

multiples, plus ou moins contraints par des aménagements (Lapatie, 2011 ; Latapie *et al*, 2014). Dans ce contexte, les éléments géomorphologiques constituant les **environnements fluviaires** sont multiples au sein du corridor fluviaire. A ce titre, la variabilité spatiale **des mécanismes d'archivage** des contaminations sédimentaires à l'échelle de l'environnement de dépôts constitue là aussi un aspect important de cette étude.

**Page suivante - Fig.1 : a)** Carte du bassin de la Loire montrant : (i) le réseau hydrographique (Agence de l'eau Loire Bretagne), (ii) la géologie (BRGM), (iii) les zones urbaines de plus de 100 000 habitants (INSEE), (iv) les principaux foyers industriels et miniers et (v) le site de carottage de l'archive sédimentaire ayant permis de reconstituer l'historique des contaminations métalliques au cours du XX<sup>ème</sup> siècle (Grosbois *et al*, 2012) ; **b)** Localisation du bassin de la Loire en Europe de l'Ouest



## Bibliographie :

Babonaux Y., 1970. Le lit de la Loire - Etude d'hydrodynamique fluviale, Paris, Bibliothèque Nationale, 252 p.

Crutzen P. J., Stoermer E. F., 2000. The Anthropocene. Global Change Newslett. 41.17–18.

Dacharry M., 1974. Hydrologie de la Loire en amont de Gien. Paris, N.A.L., 2 vol. 334 & 285 p.

Détriché, S., Rodrigues, S., Macaire, J.-J., Bonté, P., Bréhéret, J.-G., Bakyono, J.-P., Jugé, P., 2010. Caesium-137 in sandy sediments of the River Loire (France): Assessment of an alluvial island evolving over the last 50 years: Geomorphology, 115, 11–22

Grivel, S., Gauthier, E., 2012, Mise en place des îles fluviales en Loire moyenne, du 19<sup>e</sup> siècle à aujourd'hui, Cybergeo. URL : <http://cybergeo.revues.org/25451>

Grosbois, C., Meybeck, M., Lestel, L., Lefèvre, I., Moatar, F., 2012. Severe and contrasted polymetallic contamination patterns (1900–2009) in the Loire River sediments (France). Science of the Total Environment, 435, 290–305.

Hettige, H., Mani, M., Wheeler, D., 2000. Industrial pollution in economic development: the environmental Kuznets curve revisited. Journal of Development Economics, 62, 445–476.

Latapie, A., Camenen, B., Rodrigues, S., Paquier, A., Bouchard, J.P., Moatar, F., 2014. Assessing channel response of a long river influenced by human disturbance, Catena, 121, 1–12.

Latapie, A., 2011. Modélisation de l'évolution morphologique d'un lit alluvial: application à la Loire moyenne. PhD thesis, Tours univ., 277 pp.

Leteinturier B., Engels P., Petit F., Chiffaut A., Malaisse F., 2000. Morphodynamisme d'un tronçon de Loire bourbonnaise depuis le XVIII<sup>e</sup> siècle / Changing dynamics of the Loire river in Burgundy (France) during the last 200 years. In: Géomorphologie : relief, processus, environnement, 6, 239–251.

Meybeck, M., 2002. Riverine quality at the Anthropocene: Propositions for global space and time analysis, illustrated by the Seine River. Aquatic Sciences, 64, 376–393.

Meybeck, M., Helmer, R., 1989. The quality of rivers: from pristine stage to global pollution. Global and Planetary Change, 1, 283–309.

Mourier, B., Fritsch, C., Dhivert, E., Gimbert, F., Cœurassier, M., Pauget, B., Scheifler, R., 2011. Chemical extractions and predicted free ion activities fail to estimate metal transfer from soil to field land snails. Chemosphere, 85, 1057–1065.

Negrel, P., 1997. Multi-element Chemistry of Loire Estuary Sediments: Anthropogenic vs. Natural Sources. Estuarine, Coastal and Shelf Science, 44, 395–410.

Nriagu, J. O., 1990. Global metal pollution: poisoning the biosphere?. Environment: Science and Policy for Sustainable Development, 32, 7–33.

Prüss-Ustün, A., Vickers, C., Haefliger, P., Bertollini, R., 2011. Knowns and unknowns on burden of disease due to chemicals: a systematic review. Environmental Health, 10, 9.

Pruvot, C., Douay, F., Hervé, F., Waterlot, C., 2006. Heavy Metals in Soil, Crops and

Grass as a Source of Human Exposure in the Former Mining Areas. *Journal of Soils and Sediments*, 6, 215-220.

Ramade, F., 2007. Introduction à l'écotoxicologie: fondements et applications. Tec & Doc. 618p.

Rodrigues S, Bréhéret JG, Macaire JJ, Greulich S, Villar M., 2007. In-channel woody vegetation controls on sedimentary processes and the sedimentary record within alluvial environments: a modern example of an anabranch of the River Loire, France. *Sedimentology*, 54, 223–242.

Steffen, W., Grinevald, J., Crutzen, P., McNeill, J., 2011. The Anthropocene: conceptual and historical perspectives. *Philosophical Transactions of the Royal Society A: Mathematical, Physical and Engineering Sciences*, 369, 842-867.

Steffen, W., Crutzen, P. J., McNeill, J. R., 2007. The Anthropocene: are humans now overwhelming the great forces of nature. *Ambio: A Journal of the Human Environment*, 36, 614-621.

Stern, D. I., 2004. The rise and fall of the environmental Kuznets curve. *World development*, 32, 1419-1439.

Stern, D. I., 1998. Progress on the environmental Kuznets curve?. *Environment and Development Economics*, 3, 173-196.

Waeles, M., Riso, R. D., Maguer, J. F., Le Corre, P., 2004. Distribution and chemical speciation of dissolved cadmium and copper in the Loire estuary and North Biscay continental shelf, France. *Estuarine, Coastal and Shelf Science*, 59, 49-57.

Woronoff Denis, *Histoire de l'industrie en France, Du 16e siècle à nos jours*, Paris, Le Seuil, 1994, 671 p.



Felix Thiollier

**Partie 1 – Distribution spatiale et temporelle des contaminants métalliques dans les sédiments : données disponibles sur le bassin de la Loire et problématiques scientifique**

## Chapitre 1 - Histoire de la contamination métallique des sédiments

### 1.1. Evolution temporelle des contaminations sédimentaires

Les sédiments archivent partiellement ou totalement les traces des contaminations passées. A ce titre, ils jouent un rôle **enregistreur des paléopollutions**, témoignant de l'évolution temporelle des perturbations environnementales liées aux activités humaines.

Pour avoir accès à l'histoire des contaminations métalliques à l'échelle de l'**Holocène** on étudie généralement des archives sédimentaires prélevées dans des tourbières, des lacs, des terrasses alluviales ou des prodeltas (ex. Pavoni *et al.*, 1987 ; Buckley, 1995 ; Shotyk *et al.*, 1998 ; Kober *et al.*, 1999 ; Monna *et al.*, 2000; Monna *et al.*, 2004ab ; Negrel *et al.*, 2004 ; Schettler et Romer, 2006 ; De Vleeschouwer *et al.*, 2007 ; Küttner *et al.*, 2014). Ces archives nous informent qu'en Europe occidentale, les premiers enrichissements anthropiques en ET datent de l'**Age du Bronze** (troisième millénaire av. J.-C.), suivis de trois phases

de contaminations généralisées à l'échelle du continent correspondant aux périodes de fortes croissances économiques et démographiques *i.e.* l'**Empire Romain** (entre le dernier siècle av. J.-C. et le V<sup>ème</sup> siècle apr. J.-C.), le **Moyen Age Central** (entre le XI<sup>ème</sup> et la XIII<sup>ème</sup> siècle) et l'**ère industrielle** depuis le XIX<sup>ème</sup> siècle. Les premières phases temporelles de contaminations concernent majoritairement Pb et Cu, présentant de faibles niveaux de contaminations comparés aux enregistrements au cours de l'ère industrielle. Cependant, depuis l'Age de Bronze de forts enrichissements ont pu être archivés aux environs des anciens sites miniers et métallurgiques (Monna *et al.*, 2004 ab).

En ce qui concerne le **bassin de la Loire**, une carotte sédimentaire prélevée dans une terrasse alluviale en Loire Moyenne a permis de reconstituer une chronoséquence couvrant une période comprise entre 8400 et 1000 ans BP (Garcin *et al.*, 1999 ; Garcin *et al.*, 2001). Cette archive fait état de faibles apports anthropiques en Pb depuis environ 5000 ans BP (Négrel *et al.*, 2004).

## La Loire : le plus long fleuve de France

La Loire est le plus long fleuve de France mesurant 1012 km entre sa source au mont Gerbier-de-Jonc et l'entrée dans l'estuaire à Ancenis, pour un bassin d'une superficie de 117 800 km<sup>2</sup> (21% de la superficie de la France métropolitaine). Le domaine fluviatile est subdivisé en sous-bassins délimités par la confluence avec l'Allier (superficie 14 310 km<sup>2</sup>). Le bassin amont de la Loire (17 570 km<sup>2</sup>) est caractérisé par de fortes pentes et l'encaissement du corridor fluviatile dans des gorges en amont des retenues de Grangent et Villerest. En Loire Moyenne les pentes sont faibles et c'est dans cette partie que sont localisées les confluences avec le Cher (13 390 km<sup>2</sup>), l'Indre (3428 km<sup>2</sup>), la Vienne (21 161 km<sup>2</sup>) et la Maine (23 314 km<sup>2</sup>).

Le cycle hydrologique annuel du bassin est influencé par les précipitations atlantiques et cévenoles en hiver et en automne ainsi que par la fonte des neiges au printemps (Dacharry, 1974). La station de mesure hydrologique la plus aval du domaine fluviatile est située à Montjean-sur-Loire et présente un débit moyen mensuel maximal de 1530m<sup>3</sup>.s<sup>-1</sup> en février, le débit d'étiage est de 250 m<sup>3</sup>.s<sup>-1</sup> en aout. Sur cette station, les débits journaliers en période de crue atteignent 3100 m<sup>3</sup>.s<sup>-1</sup> pour une crue biennale, 5200 m<sup>3</sup>.s<sup>-1</sup> pour une crue décennale et 7000 m<sup>3</sup>.s<sup>-1</sup> pour une crue cinquantennale (statistiques calculées sur la période 1863 et 2013, [www.hydro.eaufrance.fr](http://www.hydro.eaufrance.fr)).

Au cours de l'**ère industrielle**, les pollutions sont polymétalliques, Cd, Cu, Hg, Pb, Sb et Zn étant les métaux les plus enrichis à l'échelle globale (ex. [www.unep.org](http://www.unep.org) ; Nriagu, 1990 ; Hong *et al*, 1994 ; Shotyk *et al*, 1998 ; Martinez-Cortizas *et al*, 1999 ; Monna *et al*, 2000 ; Arnaud *et al*, 2006). Les plus anciens et les plus importants foyers industriels et urbains étant localisés dans l'hémisphère Nord et les échanges atmosphériques étant limités entre les deux hémisphères, les contaminations y sont plus anciennes et plus fortes (Niragu, 1990).

Les séquences sédimentaires prélevées dans des **environnements fluviatiles** comme les plaines d'inondation, les îles ou les réservoirs de barrage permettent de reconstituer l'évolution temporelle des contaminations à l'échelle des bassins versants et sur une période comprise entre la décennie et le siècle (ex. Grousset *et al*, 1999, Audry *et al*, 2004a ; Gocht *et al*, 2001 ; Chillrud *et al*, 2003 ; Förstner, 2004 ; Castelle *et al*, 2007 ; Conrad *et al*, 2007 ; Berner *et al*, 2012 ; Le Cloarec *et al*, 2011 ; Ferrand *et al*, 2012 ; Desmet *et al*, 2012 ; Mourier *et al*, 2014). Pour l'ensemble de ces archives sédimentaires prélevées dans **des pays anciennement industrialisés**, les plus

importants niveaux de contaminations ont été enregistrés au cours des Trente Glorieuses (fin des années 1940 - fin des années 1970). Depuis les années 1980, le contrôle des rejets anthropiques a grandement amélioré la qualité des milieux aquatiques continentaux (ex. Meybeck et Helmer, 1989 ; Vink *et al.*, 1999 ; Meybeck, 2002).

A l'inverse, depuis la fin des années 1970, le déplacement géographique des industries lourdes des pays anciennement industrialisés vers **les pays émergents** a induit une augmentation accélérée et de très forte ampleur des pollutions sédimentaires (ex. Ip *et al.*, 2004, Xue *et al.*, 2009 en Chine ; Ayyamperumal *et al.*, 2006 en Inde). Dans les anciens pays de l'URSS au contraire, l'effondrement de l'économie soviétique au début des années 1990 a permis une diminution importante des niveaux de contaminations sédimentaires (ex. Bábek *et al.*, 2008 ; Bábek *et al.*, 2011 en République Tchèque).

La figure 1.1 permet d'illustrer ces **différences interbassins**. Sont représentées ici les dynamiques temporelles des métaux présentant les plus forts indices de géoaccumulation dans les archives sédimentaires

sélectionnées (Igeo ; Müller, 1979). Cet indice est calculé d'après l'équation (eq. 1.1).

$$Igeo = \log_2 \left( \frac{[ET]ech.}{1.5 [ET]ref.} \right) \quad (\text{eq. 1.1})$$

où  $[ET]ech.$  correspond aux concentrations sédimentaires en ET dans l'échantillon considéré et  $[ET]ref.$  les états de références (ici les concentrations préindustrielles dans les archives sédimentaires). Cette comparaison logarithmique permet d'interpréter les degrés de contamination en définissant les ordres de grandeur des enrichissements sédimentaires :

- $Igeo < 1$  = sédiments non pollués
- $1 < Igeo < 3$  = sédiments modérément pollués
- $3 < Igeo < 5$  = sédiments fortement pollués
- $Igeo > 5$  = sédiments extrêmement pollués

Les dynamiques temporelles enregistrées dans le bassin de la Seine (Fig. 1.1.) sont représentatives des pays anciennement industrialisés et montrent les plus forts niveaux de contaminations (Meybeck *et al.*, 2007 ; Le Cloarec *et al.*, 2011).

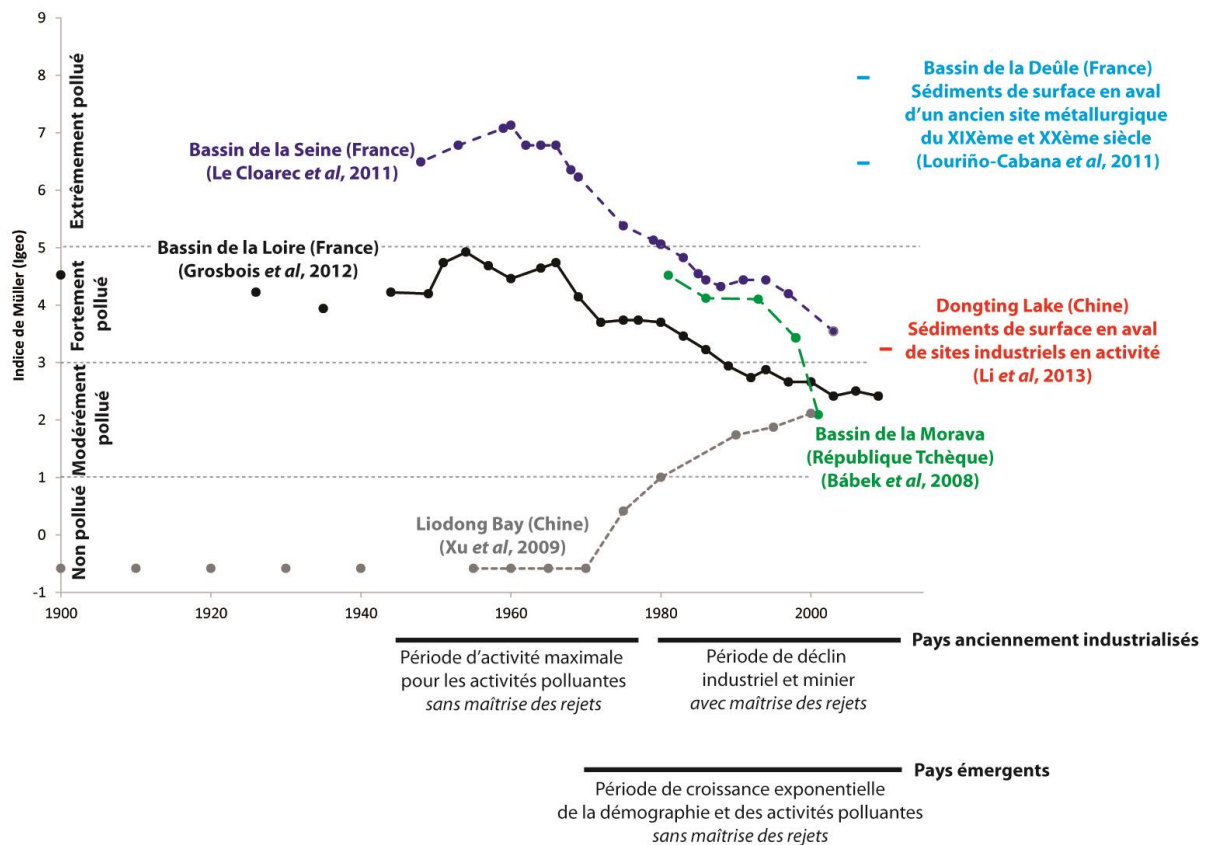


**Fig. 1.1. : Evolution temporelle de l'indice de géoaccumulation de Müller (maximum de tous les métaux) dans les sédiments de la Loire (Igeo du Hg, Grosbois et al, 2012) ainsi que dans d'autres bassins représentatifs de différentes régions du monde i.e. Igeo de Hg dans les sédiments de la Seine (Le Cloarec et al, 2011) et de Cd dans les sédiments de surface en aval d'un ancien site métallurgique du Nord de la France (Louriño-Cabana et al, 2011) pour les pays les plus anciennement industrialisés ; Igeo de Cd dans la Morava River en République Tchèque (Bábek et al, 2008) pour les pays de l'ex URSS ; Igeo eu Cd dans la Liodong Bay (Xu et al, 2009) et dans les sédiments de surface du Dongting Lake (Li et al, 2013) en Chine pour les pays émergents**

Pour comparaison, les niveaux de contaminations dans les sédiments de surface en aval d'un ancien site métallurgique considéré comme

extrêmement polluant ont été représentés (ancienne usine MetalEurop de Noyelles-Godault, Louriño-Cabana et al, 2011).

Une archive sédimentaire a été prélevée en amont de l'estuaire de la Loire à Montjean-sur-Loire en 2009, couvrant l'ensemble du XX<sup>ème</sup> siècle (Grosbois *et al*, 2012, Fig. 1.1.). L'évolution temporelle des contaminations enregistrées en aval du bassin de la Loire est synchrone avec celles archivées en aval des bassins anciennement industrialisés (Fig. 1.1). Les niveaux de contaminations maximum sont forts entre les années 1950 et la fin des années 1970, mais tout de même moins élevés que sur la Seine. Les enrichissements dans les sédiments du bassin de la Loire sont comparables à ceux enregistrés dans les bassins voisins du Rhône ou de la Garonne (Grosbois *et al*, 2012).

## 1.2. Activités polluantes aux cours de l'ère industrielle

Au cours du XX<sup>ème</sup> siècle, la demande mondiale en métaux a suivi une croissance exponentielle qui a perduré jusqu'aux chocs pétroliers des années 1970. A la fin des années 1970, les productions mondiales avoisinaient les 8000 kt/an pour Cu, 1000 kt/an pour Ni, 6000 kt/an pour le Pb et le Zn par exemple (Tilton, 1990, Rogich et Matos, 2008). En

ce qui concerne Hg, la production mondiale a été maximale durant les années 1960-1970 (90 kt/an) avant de diminuer suite à la prise de conscience de la toxicité de cet élément (Lumb, 1995 ; Hylander et Meili, 2003 ; Bank, 2012). Au cours de cette période, l'essentiel de la production mondiale en métaux alimentait **les pays les plus anciennement industrialisés**.

Depuis la fin des années 1970, la consommation mondiale en métaux suit une plus faible augmentation. De nos jours, la plus grande partie de cette production converge vers **les pays émergents**. Pour information, en 2013 le cumul mondial des extractions de métaux était de 18000 kt pour Cu, 2400 kt pour Ni, 5000 kt pour Pb et 13000 kt pour Zn ([www.minerals.usgs.gov](http://www.minerals.usgs.gov); Annexe 1). Dans les années 2000, la demande mondiale en Hg était de 1,8 kt/an (Hylander et Meili, 2003).

**A l'échelle de la France**, on observe des dynamiques comparables en ce qui concerne les demandes en métaux. La consommation annuelle des métaux a peu augmenté depuis les années 1970 où elle avoisinait les 1 à 2 kt/an pour Cd, 500 à 600 kt/an pour Cu et 200 à 300 kt/an

pour Pb et Zn (Lestel *et al*, 2007). D'après ces sources, les demandes en Hg ont drastiquement diminué de 0.4 kt/an dans les années 1960 à une consommation quasi nulle de nos jours. Les rejets anthropiques n'étant pas contrôlés et le recyclage peu développé avant les années 1980, l'évolution temporelle des contaminations métalliques est corrélée à la demande en métaux dans certains bassins hydrographiques (ex. pour le bassin de la Seine : Meybeck *et al*, 2007 ; Lestel *et al*, 2007 ; Le Cloarec *et al*, 2011). Différentes sources ont pu contribuer à la contamination de l'environnement au cours de l'ère industrielle.

**L'extraction minière** des minerais a été particulièrement intense à l'échelle mondiale, pour fournir l'importante demande en métaux. Sur le territoire français l'extraction des ET représentait un secteur économique important, présentant une production cumulée depuis le XIX<sup>ème</sup> siècle de 0.3 kt pour As, 1,7 kt pour Bi, 2,9 kt pour Cd, 70 kt pour Cu, 1,8 kt pour Pb, 100 kt pour Sb, 12 kt pour Sn, 78 kt pour U et 2400 kt pour Zn ([www.sigminesfrance.brgm.fr](http://www.sigminesfrance.brgm.fr)). D'autre part, le développement industriel et démographique du XIX<sup>ème</sup> et du XX<sup>ème</sup> siècle a été accompagné d'une demande

croissante en énergie, en partie issue des combustibles fossiles et notamment des charbons (Woronoff, 1994 ; [www.charbonnagesdefrance.fr](http://www.charbonnagesdefrance.fr)). En France métropolitaine, le cumul de la production des charbons est de  $4.9 \cdot 10^6$  kt depuis le XVIII<sup>ème</sup> siècle ([www.sigminesfrance.brgm.fr](http://www.sigminesfrance.brgm.fr)). Or, les métaux chalcophiles peuvent être enrichis dans les charbons (par rapport à la croûte continentale), généralement associés à la pyrite (ex. As, Cd, Hg et Sb ; Finkelman, 1993 ; Yudovick et Ketrus, 2005ab ; Seredin et Finkelman, 2008; Qi *et al*, 2008 ; Kolker, 2012). Les effluents et les poussières issues des mines ainsi que le transport et l'altération des phases porteuses d'ET issus des exhaures miniers ont constitué et demeurent toujours une importante source de pollution, non seulement en ce qui concerne les métaux associés aux substances extraites (minerais et charbons) mais aussi aux procédées d'exactions (ex. As, Bi, Cd, Hg ; Tiwary et Dhar, 1994ab ; Ghose et Majee, 2000ab ; Covelli *et al*, 2001 ; Jung *et al*, 2002 ; Miller *et al*, 2003 ; Courtin-Nomade *et al*, 2005 ; Grosbois et al, 2007 ; Mishra *et al*, 2008 ; Oyarzun *et al*, 2011 ; Lecey et Pavlowsky, 2014 ; Reslonges *et al*, 2014).

D'autre part, l'utilisation massive des combustibles fossiles dans l'industrie et les zones urbanisées est depuis le début de l'ère industrielle la principale source de pollutions atmosphériques à l'échelle globale. En effet, la combustion des charbons constitue le principal pôle d'émission atmosphérique en Hg à l'échelle mondiale (volatilisation lors de la combustion ; 67% des 2,2 kt de mercure émises en 2000 ; Querol *et al*, 1995 ; Hylander et Meili, 2003 ; Mukherjee *et al*, 2008). L'utilisation du pétrole dans l'industrie a été plus tardive (à partir des années 1930). L'adjonction de Pb dans les essences jusque dans les années 1980 a constitué là aussi une importante source de contamination à l'échelle du globe (ex. Hong *et al*, 1994 ; Shotyk *et al*, 1998 ; Monna *et al*, 2000 ; Arnaud *et al*, 2006 ; Garçon *et al*, 2012).

L'utilisation de ces métaux dans l'industrie a aussi grandement contribué aux contaminations métalliques enregistrées au cours de l'ère industrielle. Les industries lourdes ont été particulièrement polluantes au cours de cette période comme :

- (i) les industries de l'acier, des métaux non ferreux et des

traitements de surface qui ont pu constituer des sources des contaminations polymétalliques dépendantes des alliages fabriqués et des procédés de fabrication (Verner *et al*, 1996 ; Audry *et al*, 2004; Ettler *et al*, 2005 ; Alleman *et al*, 2010 ; Jasminka et Robert, 2011 ; Louriño-Cabana *et al*, 2011),

- (ii) les industries du verre et de la céramique dont les rejets atmosphériques peuvent être fortement enrichis en As, Hg, Pb et Sn (Querol *et al*, 2007 ; Le Cloarec *et al*, 2011),
- (iii) les industries textiles et notamment les procédés de tannage des peaux, de feutrage de la laine et de pigmentation potentiellement responsable d'importants rejets en Cr et Hg (Neal, 1938; Lumb, 1995 ; Sreeram et Ramasami, 2003 ; Möller et Einax, 2013) et
- (iv) les industries chimiques et notamment la synthèse du chlore qui ont constitué et sont toujours l'une des principales sources d'émission de Hg à l'échelle mondiale (Lumb, 1995; Heaven *et al*, 2000 ; Hylander et Meili, 2003).

**Les zones urbaines** concentrent de fortes densités d'industries, de population et de bâtiments. Elles peuvent constituer à la fois des sources de contaminations ponctuelles *via* les unités de traitement des eaux usées ou diffuses en considérant :

- (i) les retombées locales des polluants atmosphériques (Garnaud *et al.*, 1999 ; Li *et al.*, 2013)
- (ii) le ruissellement des eaux sur les toits et les chaussées ainsi que le débordement des réseaux d'assainissement lors des épisodes de fortes pluies (Estèbe *et al.*, 1997 ; Meybeck *et al.*, 2004 ; Meybeck *et al.*, 2007 ; Le Cloarec *et al.*, 2011 ;).

De la même manière, les produits phytosanitaires, fertilisants et facteurs de croissance utilisés dans l'**agriculture** peuvent être des sources diffuses de contaminations en Cu et Zn essentiellement (Xue *et al.*, 2003 ; Legros *et al.*, 2013).

Dans **le bassin de la Loire**, différentes sources potentielles de contaminations ont été recensées au cours du XX<sup>ème</sup> siècle

(Grosbois *et al.*, 2012 ; annexe 1.1). Entre la seconde moitié du XIX<sup>ème</sup> siècle et la fin des années 1950, l'économie du bassin dépendait essentiellement de l'exploitation des ressources géologiques et de leurs utilisations locales (Woronof, 1994 ; Fig. 1.2). Par conséquent, l'industrialisation et l'urbanisation du bassin de la Loire ont été essentiellement centralisées autour de **complexes industriels et miniers** implantés dans le Massif Central (Fig. 1). L'extraction minière des charbons et des ET ont été les principaux moteurs du développement économique du bassin. Les principaux districts miniers sont localisés dans les sous-bassins de la Loire Amont, de l'Allier, du Cher, de la Vienne et de la Maine. L'exploitation industrielle de ces ressources géologiques a débuté dans la seconde partie du XIX<sup>ème</sup> siècle pour atteindre un maximum entre les années 1945 et la fin des années 1950 ([www.charbonnagesdefrance.fr](http://www.charbonnagesdefrance.fr) ; [www.sigminesfrance.brgm.fr](http://www.sigminesfrance.brgm.fr)). Des industries lourdes se sont implantées à proximité de ses sources d'approvisionnement en énergie et de matières premières. Jusqu'à la fin des années 1950, ces foyers industriels et miniers ont compté parmi les principaux producteurs d'acières, de verres et de

céramiques à l'échelle nationale (Woronoff, 1994 ; [www.acier.org](http://www.acier.org)). Au début des années 1960, les activités minières ont diminué et les industries lourdes ont été relocalisées vers les ports internationaux. Depuis les années 1980, les activités potentiellement les plus polluantes du bassin ne sont plus en fonctionnement ou les rejets environnementaux sont maîtrisés. Par conséquent, cette étude est essentiellement focalisée sur l'influence des sources de contamination au cours de la période d'activité minière et industrielle maximale.

**La densité de population** est faible dans le bassin par rapport à la moyenne nationale (8.4M d'habitants en 2008 pour une densité de 72 hab.km<sup>-2</sup> contre 115 hab.km<sup>-2</sup> à l'échelle de la France métropolitaine ; [www.insee.fr](http://www.insee.fr)). Il n'existe pas de grandes aires urbaines comme les métropoles de Paris, Lyon, Toulouse ou Bordeaux dans les bassins voisins. On reconnaît 3 principaux foyers de populations, installés aux abords des anciens complexes industriels et miniers *i.e.* l'agglomération de St Etienne (508 847 hab. en 2010) constituant la plus importante aire urbaine du bassin localisée en Loire Amont, l'agglomération

de Clermont-Ferrand (468 891 hab.) dans le bassin de l'Allier et l'agglomération de Limoges (282 873 hab.) dans le bassin de la Vienne. D'autres foyers de population sont aussi implantés le long du corridor ligérien en Loire Moyenne avec les aires urbaines d'Orléans (419 271 hab.) de Tours (477 438 hab.) et d'Angers (397 435 hab.).

A la différence d'autres bassins hydrographiques comme la Seine ou le Rhin, il n'existe pas de gradient amont-aval croissant en ce qui concerne la distribution géographique des foyers industriels et urbains dans le bassin de la Loire. L'économie ayant été essentiellement basée sur l'exploitation et l'utilisation locale des ressources géologiques, les anciens foyers industriels et miniers sont situés dans la partie amont du bassin et des principaux affluents du fleuve (Fig. 1). Par conséquent, la distribution spatiale des sources potentielles de contaminations peut être un facteur de **variabilités spatiales des enregistrements sédimentaires** des contaminations métalliques. Il est ainsi proposé d'étudier la distribution spatiale et temporelle des contaminations sédimentaires à l'échelle du bassin de la Loire.

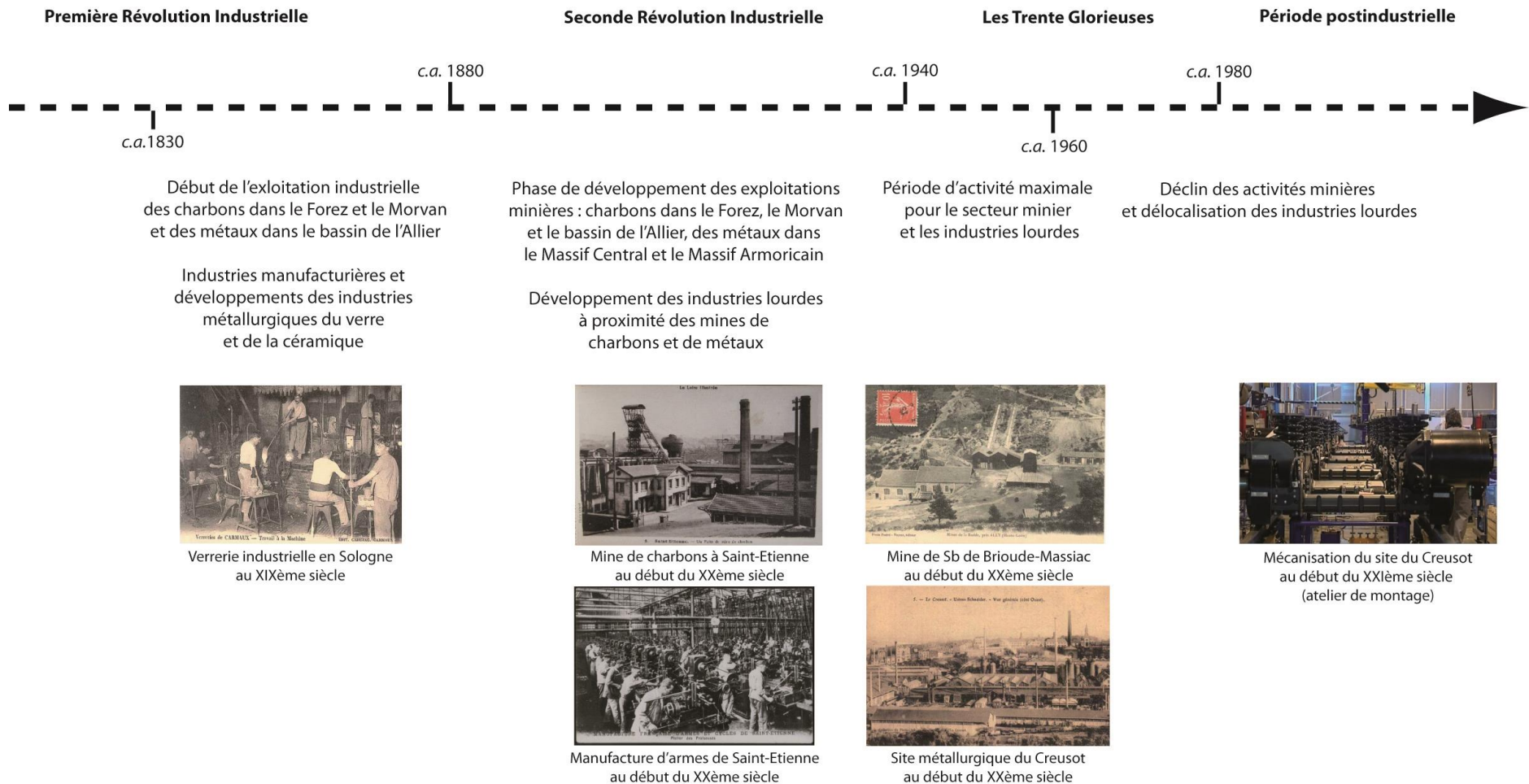


**Fig. 1.2. : Histoire industrielle du bassin de la Loire (d'après Woronoff, 1994 ; source des photographies : [www.delcampe.fr](http://www.delcampe.fr))**

## Chapitre 2 - Facteurs de contrôle de la distribution spatiale et temporelle des contaminations sédimentaires en milieu fluviatile

### 2.1. Variabilité spatiale des fonds géochimiques

A l'échelle d'un hydrosystème, la **distribution spatiale des contaminations sédimentaires** est modulée par **différents facteurs environnementaux** (géologiques, géomorphologiques, hydrologiques et biologiques) pouvant influencer à la fois les niveaux de contaminations et les dynamiques temporelles archivées. Lorsqu'on s'intéresse à la variabilité spatiale de l'enregistrement sédimentaire des contaminations, il est important de comprendre l'influence de ces facteurs de contrôle pour établir des chroniques représentatives de l'impact des activités anthropiques.

Pour quantifier des niveaux de contaminations, **des états de références** sont nécessaires (*voir encadré page 11*). Des concentrations préindustrielles représentatives de l'ensemble des sources naturelles du bassin de la Loire ont été déterminées dans la partie aval du domaine fluviatile (Grosbois *et al*, 2012 ; Tab. 2.1). Ces concentrations sédimentaires ont été mesurées dans la fraction < 63 µm à partir de sédiments anciens non datés, notés << 1900. Ce niveau sédimentaire est localisé entre 360 et 400 cm de profondeur dans l'archive la plus aval du bassin, où les 200 premiers cm permettent de couvrir le XX<sup>ème</sup> siècle.

	Sédiments fluviatiles <<1900 Bassin de la Loire		Valeurs guides écotoxicologiques (Concentrations maximales sans effet observé)	Valeurs seuils pour les sédiments dragués et stockés à terre en France Art. 1 arrêté 09/08/2006 Code env.
	360-380 cm	380-400 cm		
As	19.8	19.4	7.2	30
Cd	0.3	0.4	0.7	2
Cr	109	89	52	150
Cu	18.6	21.3	19	100
Hg	0.02	0.02	0.13	1
Ni	32.6	24.2	15.9	50
Pb	37	33	30.2	100
Zn	90	97	124	300

**Tab.2.1. : Concentrations préindustrielles dans les sédiments de la Loire (<<1900, Grosbois *et al* 2012) ; valeurs guides écotoxicologiques (Mc Donald *et al*, 2000) et valeurs seuils pour le stockage à terre en France ; valeur en ppm**

Les concentrations naturelles en As, Cr, Ni et Pb dans les sédiments du bassin de la Loire sont supérieures aux seuils écotoxiques couramment utilisés (Mc Donald *et al*, 2000 ; Tab. 2.1). Des réserves doivent donc être prises concernant la représentativité de ces **valeurs guides** pour les sédiments du bassin de la Loire. D'autre part, il faut souligner que la norme environnementale en vigueur (article 1 de l'arrêté du 08/06/2006 du code de l'environnement ; Tab. 2.1) autorise des niveaux de contaminations particulièrement élevés.

La figure 2.1. permet une **comparaison inter- et intrabassins** des états de références déterminés en aval du bassin de la Loire. Une double normalisation est ici utilisée (calcul des ratios ET/Al sur la fraction < 63µm) permettant de limiter les influences granulométriques minéralogiques. Cette analyse est basée sur le calcul des facteurs d'enrichissement par rapport aux états de références déterminés en aval du domaine fluviaile de la Loire (EF, eq. 2.1)

$$EF(ET) = \frac{ET/Al\_{ech.}}{ET/Al\_{ref.}} \quad (eq. 2.1)$$

où  $ET/Al\_{ech.}$  correspond au ratio des concentrations sédimentaires en l'ET

considéré dans l'échantillon et  $ET/Al\_{ref.}$  le ratio de référence.

Les états de référence calculés dans la partie aval du domaine fluviaile de la Loire sont ici comparés sont ceux déterminés :

- (i) dans les sédiments préhistoriques prélevés en Loire Moyenne (Grosbois *et al*, 2012) et dans le bassin de la Seine (Meybeck *et al*, 2004, 2007)
- (ii) ainsi que dans les sédiments de surface des bassins monolithologiques non impactés du bassin de la Loire (Grosbois *et al*, 2012).

Pour la plupart des ET, les ratios préindustriels calculés en aval du bassin de la Loire sont proches des ceux déterminés dans **les sédiments préhistoriques** du bassin de la Loire et de la Seine ( $0.8 < EF < 1.9$  ; Fig. 2.1). Hg présente un EF de 5 dans le bassin de la Seine, mais les concentrations sédimentaires sont similaires (0.04 ppm pour la Seine, 0.02 ppm pour la Loire). Les ratios Sb/Al sont presque 6 fois supérieurs dans les sédiments préhistoriques de la Loire par rapport aux états de référence en Loire Aval. Cette différence peut être le

## Géologie du bassin de la Loire

Trois unités géologiques sont drainées dans le bassin de la Loire:

(i) les chaînes cristallines du Massif Central et du Massif Armoricain, constituées de roches plutoniques et métamorphiques issues de l'orogénèse hercynienne (450 - 300 Ma), sont drainées par les sous bassins de la Loire Amont, de l'Allier, du Cher, de la Vienne de l'Indre et de la Maine.

(ii) en amont du bassin de la Loire et de l'Allier, sont présentes des roches issues d'un volcanisme actif depuis l'ère Tertiaire jusqu'au Quaternaire,

(iii) la partie médiane du bassin de la Loire est localisée dans le Bassin de Paris, un remplissage sédimentaire initié au Trias et qui s'est poursuivi jusqu'à la fin de l'ère Tertiaire.

Les roches granitiques, volcaniques et métamorphiques occupent 58% de l'espace ligérien et constituent l'ensemble des têtes de bassins.

Résultat de l'affinité particulière de l'élément pour la matière organique dans cet environnement de dépôt tourbeux.

Les médianes des ratios dans **les bassins monolithologiques non impactés** sont proches des de ceux calculés en aval du bassin (à l'exception là aussi de Hg et Sb ; Fig. 2.1). Cependant on constate une forte variabilité spatiale dans ces bassins monolithologiques non impactés.

Cette caractéristique est à relier à la nature de la géologie du bassin (*voir encadré ci-contre; Fig. 1*). En effet, l'inventaire géochimique des sédiments, réalisé par le BRGM en 2005 ([www.sigminesfrance.brgm.fr](http://www.sigminesfrance.brgm.fr)), fait état d'importantes anomalies géochimiques dans les massifs hérités de l'ancienne chaîne hercynienne. Ces enrichissements géogéniques atteignent localement des valeurs extrêmes *i.e.* jusqu'à 600 ppm pour Cr, Ni, 1000 ppm pour Cu sur substratum volcanique, jusqu'à 2000 ppm pour As dans le bassin de la Vienne et jusqu'à 500 ppm pour Zn et 4000 ppm pour Pb dans le bassin de la Loire Amont et l'Allier. La genèse de ces gisements métallifères a différentes origines:

(i) sédimentaires durant la période éo-varisque (450-400 Ma), aboutissant

- à la formation des gisements en Ba, F, Pb et Zn comme dans les districts miniers de Chavaniac (Haute-Loire) ou Chillac (Indre),
- (ii) d'origine volcano-sédimentaire ou hydrothermale et liée à une minéralisation sulfurée durant la période méso-varisque (400-350 Ma) comme pour le district de Chizeuil (Saône et Loire) correspondant à un gisement de Fe (Pyrite), Zn (Sphalérite), Cu (Chalcopyrite), Pb (Galène), Mo (Molybdénite), Sn (Stamoïdite), Bi (Bismuthinite) ainsi que Ag, Sb et As (Freibergite)
- (iii) et d'origine hydrothermale durant la période néo-varisque (350-3020 Ma), sur le pourtour des granites ou le long des failles, correspondant à des enrichissements en W-As-Au-Sb-U largement exploités dans le district aurifère de La Lucette (Mayenne), les mines d'Sb dans le district de Brioude-Massiac (Haute-Loire) ou d'U dans le Limousin (Delfour *et al*, 1984 ; Sizaret, 2002).

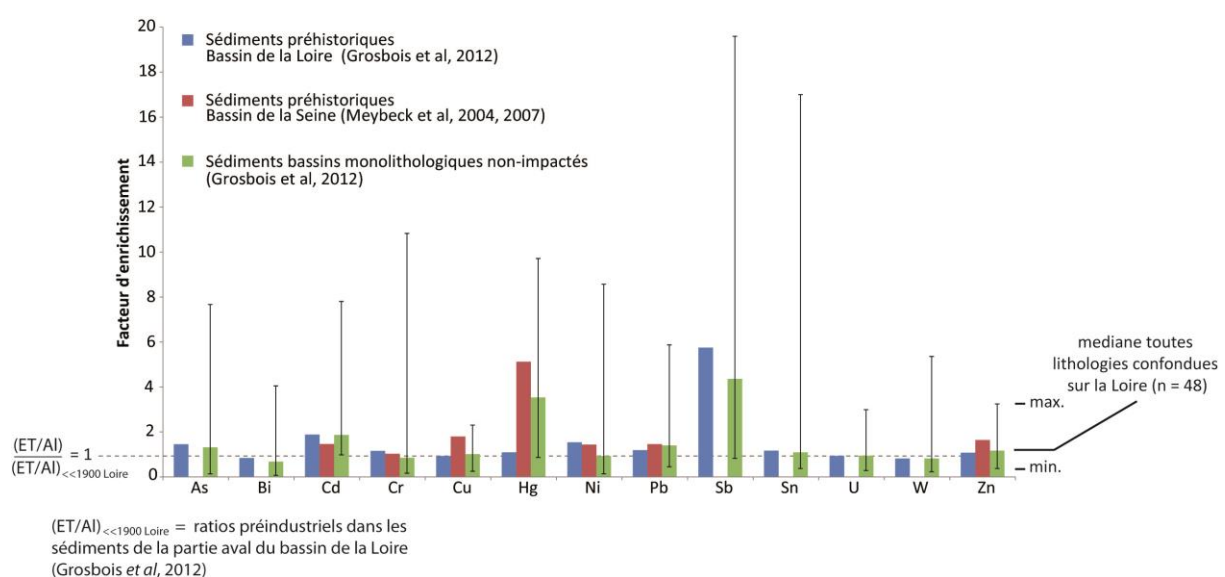


**Fig. 2.1. : Comparaison des états de références mesurés dans les sédiments fluviatiles de la partie aval du bassin de la Loire (Grosbois *et al*, 2012) avec des niveaux sédimentaires préhistoriques du bassin de la Loire (Grosbois *et al*, 2012) et de la Seine (Meybeck *et al*, 2004, 2007), ainsi qu'avec les bassins monolithologiques non impactés (Grosbois *et al*, 2012).**

La géologie contrastée du bassin de la Loire s'accompagne donc d'une importante variabilité spatiale des fonds géochimiques dans les sédiments. D'autre part, la contribution relative des différentes lithologies dans la composition minéralogique et géochimique des sédiments transportés par l'hydrosystème ligérien dépend de l'érosion des versants et du transport sédimentaire (Négrel *et al*, 1999 ; Négrel *et al*, 2004 ; Macaire *et al*, 2013). Dans ce contexte, l'analyse de la variabilité spatiale des états de référence est une étape préalable à l'établissement des niveaux de contaminations sédimentaires à l'échelle du bassin.

## 2.2. Variabilité spatiale des mécanismes d'archivage des sédiments et contaminants associés

Au cours de l'ère industrielle, l'évolution temporelle des flux de contaminants transportés jusqu'aux estuaires a non seulement été conditionnée par l'histoire des sources de contaminations, mais aussi par l'évolution temporelle du stockage sédimentaire au sein même des bassins (Walling et Owens, 2003 ; Audry *et al*, 2004 ; Meybeck *et al*, 2007; Lestel *et al*, 2007; Thévenot *et al*,

2007). Une partie des rejets anthropiques a donc été stockée à plus ou moins long terme avec les sédiments déposés dans les environnements fluviaires *i.e.* :

- (i) dans les sédiments de fond (Walling *et al*, 2003 ; Estrany *et al*, 2011 ; Reis *et al*, 2014),
- (ii) dans les plaines d'inondation et les îles (Bradley et Cox, 1990 ; Martin, 2000 ; Heaven *et al*, 2000 ; Walling *et al*, 2003 ; Lecee et Pavlowsky, 2014)
- (iii) et dans les réservoirs de barrages (Ye *et al*, 2011 ; Vukovic *et al*, 2014).

Suite à l'aménagement des cours d'eau, depuis le XIX<sup>ème</sup> siècle, le stockage sédimentaire a été amplifié en amont des retenues et dans les berges (Vörösmarty *et al*, 2003 ; Arnaud-Fassetta, 2003 ; Bridge, 2003 ; Houben, 2007).

Dans ce contexte, les processus géomorphologiques jouent un rôle important en ce qui concerne la dispersion des sédiments contaminés à l'échelle du bassin (Miller, 1997; Walling *et al*, 2003 ; Macklin *et al*, 2006 ; Fig. 2.2a). En effet, par un phénomène de cascade

sédimentaire, le transport des sédiments des zones de production jusqu'aux estuaires comporte une alternance de phases de stockages et d'érosions contrôlées par des facteurs naturels et anthropiques (Burt et Allisson, 2010). La distribution spatiale et temporelle des contaminations sédimentaires à l'échelle de l'hydrosystème ne dépend donc pas seulement de l'histoire des sources de contaminations, mais aussi de la variabilité spatiale et temporelle des phénomènes de stockage/déstockage des sédiments contaminés (Macklin and Klimek, 1992 ; Lecce and Pavlowsky, 1997 ; Birch *et al*, 2000 ; Walling *et al*, 2003 ; Förstner, 2004 ; Coynel *et al*, 2007 ; Estarany *et al*, 2011 ; Bednarova *et al*, 2013 ; Lecce and Pavlowsky, 2014 ; Reis *et al*, 2014).

D'autre part, la diversité des macroformes au sein des environnements fluviatiles peut induire des différences à l'échelle stationnelle des conditions de dépôts et de stockage des sédiments et contaminants associés. En effet, la texture, les taux de sédimentation, l'intensité des phénomènes d'érosion et les niveaux de contaminations des sédiments déposés peuvent être spatialement et temporellement hétérogènes à l'échelle de

l'environnement fluviatile (Horowitz et Elrick, 1987 ; Bradley et Cox, 1990 ; Walling *et al*, 1997 ; Walling *et al*, 1998 ; Matrin, 2000 ; Baborowski *et al*, 2007 ; Dieras *et al*, 2013 ; Hostache *et al*, 2014 ; Fig. 2.2b). Ces facteurs peuvent influencer les signaux géochimiques archivés avec les sédiments (Bábek *et al*, 2008 ; Grygar *et al*, 2010 ; Vrel *et al*, 2013 ; Grygar *et al*, 2014). Outre cela, après le dépôt sédimentaire des processus de remobilisation des ET sont susceptibles de modifier la distribution verticale et horizontale des contaminations. Le brassage et le lessivage des particules liés aux processus de pédogénèse peuvent être des facteurs de redistribution de la contamination au sein de la colonne sédimentaire (Fujikawa *et al*, 2000 ; Palumbo *et al*, 2000). De la même manière, la spéciation des métaux peut évoluer au cours du temps et des variations physicochimiques du milieu et de l'activité biologique. Ainsi les échanges entre phase particulaire et phase dissoute modifient la répartition initiale des contaminants (Van Griethuysen *et al*, 2005 ; Koretsky *et al*, 2006 ; Audry *et al*, 2010 ; Selim Reza *et al*, 2010 ; Charriaud *et al*, 2011 ; Schulz-Zunkel *et al*, 2013). Différents processus sont à l'origine de ces remobilisations comme l'évacuation des

eaux interstitielles lors de la diagenèse, la minéralisation de la matière organique, la précipitation ou la dissolution des oxydes

et des sulfures ou même l'altération des minéraux porteurs (Fig. 2.2c).

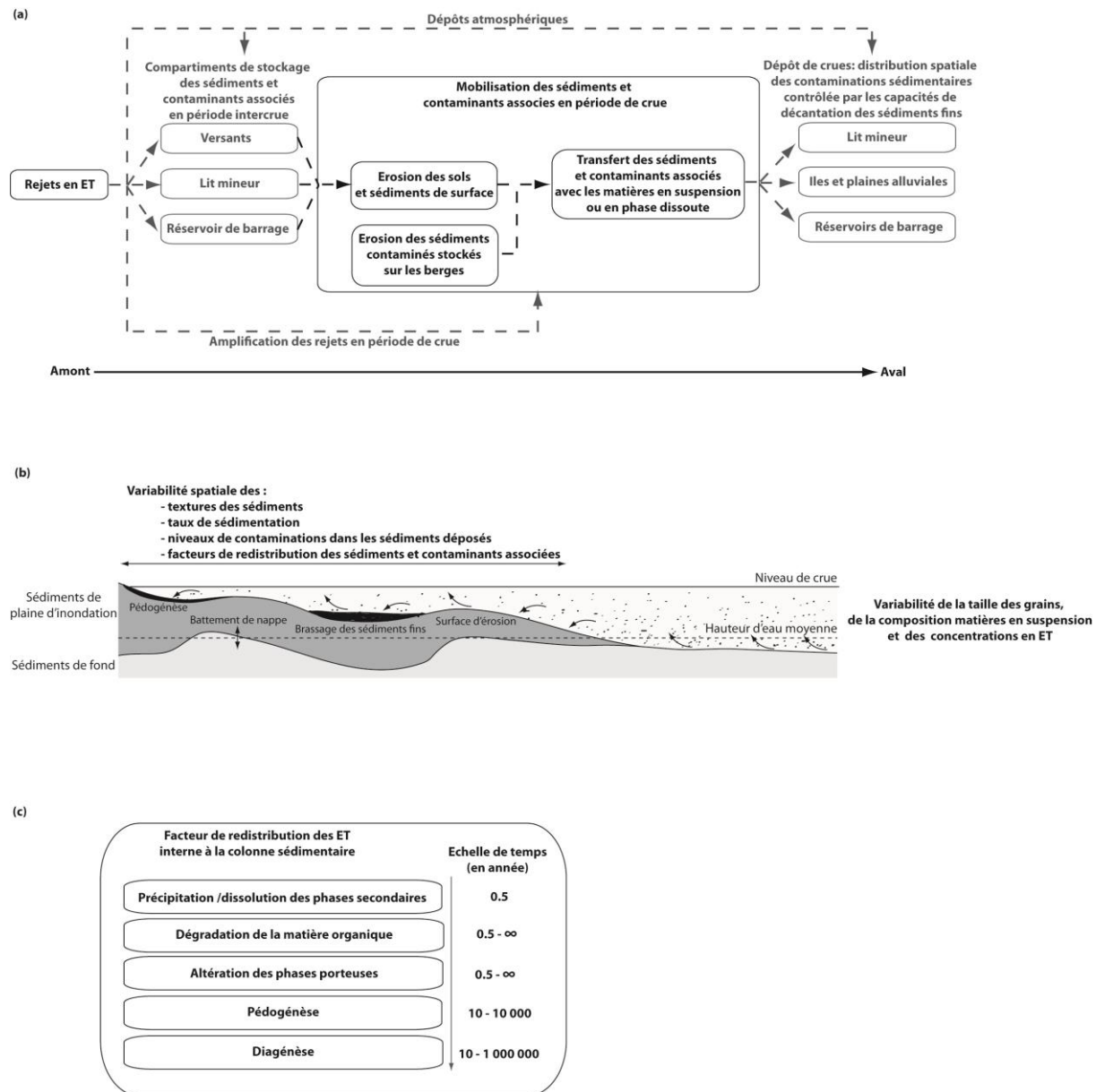


**Fig. 2.2 : a - Processus de dispersion des sédiments et contaminants associés à l'échelle du bassin versant ; b - facteurs de variabilité spatiale des processus d'archivage et de redistribution des sédiments et ET associés à l'échelle de l'environnement fluviatile ; c - processus de redistribution des ET interne à la colonne sédimentaire**

## Sédiments de la Loire

Les sédiments du lit de la Loire sont essentiellement composés de sables hétérométriques (Brossé, 1968 ; Babonaux, 1970 ; Valverde *et al*, 2013). On ne reconnaît pas de gradient amont-aval en ce qui concerne la taille des grains, et la variabilité transversale est comparable à celle longitudinale (Valverde *et al*, 2013).

Les sables de Loire sont en grande partie composés de fragments de roches (70%) essentiellement issus des facies plutoniques et métamorphiques, ainsi que des basaltes (Macaire *et al*, 2013). Les grains mono-minéraux sont constitués en majorité de quartz et d'une plus faible proportion de feldspath potassiques, de micas et de minéraux lourds (zircons).

Dans le bassin de la Loire, l'anthropisation du corridor fluviatile a fortement perturbé le **transport sédimentaire** au cours de l'ère industrielle. En effet, les premiers aménagements datent du XII<sup>ème</sup> siècle, mais c'est depuis la fin du XVIII<sup>ème</sup> siècle que la plupart des obstacles transversaux et longitudinaux permettant de se protéger des crues et d'assurer la navigation ont été construits (digues, seuils, épis et canaux ; Dion, 1961 ; Lino *et al*, 2000). Au cours du XX<sup>ème</sup> siècle, ces ouvrages ont été complétés par des retenues permettant la production d'électricité, l'écrêtage des débits de crues et garantissant un étiage minimal pour les centrales nucléaires construites en aval ; Grangent, Villerest et Naussac sont les plus importantes (Fig. 1). D'autre part, les extractions de granulats ont été particulièrement importantes dans le corridor fluviatile de la Loire. Entre 1955 et 1980 plus 5 Mm<sup>3</sup> de granulats alluvionnaires ont été extraits à un rythme 20 fois supérieur au charriage annuel (400 000 t/a Claude *et al*, 2012, [www.eau-loire-bretagne.fr](http://www.eau-loire-bretagne.fr)).

En conséquence, depuis plus d'un siècle on assiste à la **stabilisation et à l'expansion des îles et des berges**, liées conjointement à leur végétalisation

(déprise agricole dans le lit et arrêt de la navigation), à l'artificialisation des lignes d'eau et à l'absence de crues majeures (Babonaux, 1970 ; Leteinturier *et al*, 2000 ; Rodrigues *et al*, 2007 ; Détriché et al, 2010 ; Grivel et Gauthier, 2012). D'autre part, le contrôle des crues, la canalisation du lit et les extractions massives de sédiments ont eu pour conséquence d'accélérer **l'incision du fleuve** et de ces principaux affluents (Gasowski, 1994 ; Latapie, 2011 ; Latapie *et al*, 2014). Ce phénomène est particulièrement intense en amont de l'estuaire où l'incision atteint 3.1m à Ancenis depuis le début du XX<sup>ème</sup> siècle

(Latapie *et al*, 2014 ; [www.loire-estuaire.org](http://www.loire-estuaire.org)).

Lorsque l'on s'intéresse à la variabilité spatiale de l'enregistrement des contaminations sédimentaires, il est important de comprendre les **mécanismes et les modalités de l'archivage des sédiments et contaminants associés**. Au cours de cette étude, les facteurs de contrôle des variabilités spatiale et temporelle des contaminations sédimentaires seront analysés à différentes échelles d'espace (celle du bassin versant et celle de l'environnement de dépôt) et de temps (de l'événement hydrosédimentaire au siècle).

## Chapitre 3 - Problématiques scientifiques et plan de la thèse

Au cours de l'ère industrielle, les activités anthropiques ont influencé la géochimie des sédiments et le transport sédimentaire au sein des systèmes fluviaux. De nos jours, les archives sédimentaires prélevées dans les environnements de dépôts donnent accès aux dynamiques temporelles des contaminations métalliques. Cependant, l'hétérogénéité de la distribution géographique des sources peut être un facteur de variabilité spatiale des contaminations sédimentaires. D'autre part, la dispersion des sédiments et contaminants associés est contrôlée par des processus géomorphologiques et géochimiques pouvant **induire une variabilité spatiale et temporelle des signaux géochimiques archivés à l'échelle du bassin comme à celle de l'environnement fluviatile.**

Le bassin de la Loire présente des caractéristiques intéressantes pour analyser les facteurs de contrôle de la distribution spatiale et temporelle contaminations sédimentaires. En effet, l'industrialisation du bassin ayant été basée sur l'exploitation locale des

ressources naturelles, les activités anthropiques potentiellement polluantes sont essentiellement réparties dans les parties amont du fleuve et de ses principaux affluents. De surcroit, les environnements fluviatiles sont diversifiés au sein du bassin et l'aménagement des cours d'eau a conduit à de fortes évolutions morphologiques au cours des deux derniers siècles.

Cette étude correspond donc à une analyse de la variabilité spatiale des enregistrements sédimentaires des contaminations métalliques à l'échelle du bassin de la Loire. Différents verrous scientifiques ont été identifiés :

- L'influence de l'environnement de dépôt sur l'archivage des sédiments et ET associés
- La représentativité des états de références à l'échelle du bassin
- La conservation des signaux géochimiques lors du transport des sédiments contaminés depuis les sous-bassins sources vers la partie aval de l'hydrosystème
- La caractérisation des sources de contaminations

Dans le cadre de cette étude, une démarche multiscalaire, intégrant des approches géochimiques et sédimentologiques a été menée. Cette thèse présente les résultats de ces travaux autour de deux parties composées d'articles scientifiques et de synthèses présentant les principaux résultats généralisables.

La partie 2, intitulé « Influences de l'environnement de dépôt sur l'archivage des sédiments et contaminants associés», est dédiée à la variabilité spatiale et temporelle des mécanismes d'archivages des sédiments et contaminants associés dans les environnements de dépôts. Elle permet d'analyser la représentativité des signaux géochimiques archivés. Les résultats sont présentés sous la forme de deux articles. Le premier « Influences of major flood sediment inputs on sedimentary and geochemical signals archived in a reservoir core (Upper Loire basin, France) » a été soumis dans la revue Catena en janvier 2014 et accepté avec corrections majeures en juillet 2014. Il traite de l'influence des dépôts de crue dans le réservoir de Villerest en termes de contribution au remplissage sédimentaire et de contaminations

métalliques des sédiments. Le second article s'intitule « Influence of fluvial environments on sediment archiving processes and temporal pollutant dynamics (Upper Loire River, France) ». Il a été soumis dans la revue Science of the Total Environment en juillet 2014 et accepté en septembre 2014. Cet article montre l'influence des environnements de dépôts sédimentaires sur l'archivage des sédiments et contaminants associés au sein même d'une plaine d'inondation.

La partie 3 s'intitule « Variabilité spatiale de l'enregistrement sédimentaire des contaminations à l'échelle du bassin de la Loire ». Dans cette partie, une analyse de la variabilité spatiale des enregistrements sédimentaires des contaminations a été menée à l'échelle du bassin de la Loire. Cette étude est basée sur une comparaison des signaux géochimiques archivés dans la partie amont du bassin - la plus industrialisée - et la partie aval du domaine fluviatile. D'autre part, les sources ayant contribué aux contaminations des sédiments au cours de l'ère industrielle sont caractérisées dans cette partie.

## Bibliographie :

Alleman, L. Y., Lamaison, L., Perdrix, E., Robache, A., Galloo, J. C., 2010. PM10 metal concentrations and source identification using positive matrix factorization and wind sectoring in a French industrial zone. *Atmospheric Research*, 96, 612-625.

Arnaud, F., Serralongue, J., Winiarski, T., Desmet, M., Paterne, M., 2006. Pollution au plomb dans la Savoie antique (II-III<sup>e</sup> s. ap. J.-C.) en relation avec une installation métallurgique de la cité de Vienne. *Comptes Rendus Géosciences*. 338, 244-252.

Arnaud-Fassetta, G., 2003. River channel changes in the Rhone Delta (France) since the end of the Little Ice Age: geomorphological adjustment to hydroclimatic change and natural resource management. *Catena*. 51, 141–172.

Audry, S., Grosbois, C., Bril, H., Schäfer, J., Kierczak, J., Blanc, G., 2010. Post-depositional redistribution of trace metals in reservoir sediments of a mining/smelting-impacted watershed (the Lot River, SW France). *Applied Geochemistry*, 25, 778–794.

Audry, S., Schäfer, J., Blanc, G., Jouanneau, J. M., 2004. Fifty-year sedimentary record of heavy metal pollution (Cd, Zn, Cu, Pb) in the Lot River reservoirs (France). *Environmental Pollution*, 132, 413-426.

Ayyamperumal, T., M. P. Jonathan, S. Srinivasalu, J. S. Armstrong-Altrin, and V. Ram-Mohan, 2006. Assessment of acid leachable trace metals in sediment cores from River Uppanar, Cuddalore, Southeast coast of India.: Environmental pollution (Barking, Essex : 1987), 143, 34–45.

Bábek, O., Faměra, M., Hilscherová, K., Kalvoda, J., Dobrovolný, P., Sedláček, J., Machát, J., Holoubek, I., 2011. Geochemical traces of flood layers in the fluvial sedimentary archive; implications for contamination history analyses. *Catena*. 87, 281–290.

Bábek, O., Hilscherová, K., Nehyba, S., Zeman, J., Famera, M., Francu, J., Holoubek, I., Machát, J., Klánová, J., 2008. Contamination history of suspended river sediments accumulated in oxbow lakes over the last 25 years. *Journal of Soils and Sediments*. 8, 165–176.

Babonaux Y., 1970. Le lit de la Loire - Etude d'hydrodynamique fluviale, Paris, Bibliothèque Nationale, 252 p.

Baborowski, M., Büttner, O., Morgenstern, P., Krüger, F., Lobe, I., Rupp, H., Tümling, W. V., 2007. Spatial and temporal variability of sediment deposition on artificial-lawn traps in a floodplain of the River Elbe. *Environmental Pollution*, 148, 770-778.

Bank, M. S., 2012. Mercury in the environment: pattern and process. Univ of CaliforniaPress. 237p.

Berner, Z. A., Bleeck-Schmidt, S., Stüben, D., Neumann, T., Fuchs, M., Lehmann, M. 2012, Floodplain deposits: A geochemical archive of flood history – A case study on the River Rhine, Germany. *Applied Geochemistry*. 27, 543–561.

Birch, G. F., Taylor, S. E., Matthai, C., 2001. Small-scale spatial and temporal variance in the concentration of heavy metals in aquatic sediments: a review and some new concepts. *Environmental Pollution*, 113, 357-372.

Bradley, S. B., Cox, J. J., 1990. The significance of the floodplain to the cycling of metals in the river Derwent catchment,

UK. Science of the Total Environment, 97, 441-454.

Bridge, J. S., 2003. Rivers and floodplains: forms, processes, and sedimentary record. John Wiley & Sons. 491 p

Brossé, R., 1968. Localisation des sables du lit majeur de la Loire (entre les Ponts de Cé et Nantes) en fonction de leur granulométrie. Norois, 58, 279-284.

Buckley, D. E., Smith, J. N., Winters, G. V., 1995. Accumulation of contaminant metals in marine sediments of Halifax Harbour, Nova Scotia: environmental factors and historical trends. Applied Geochemistry, 10, 175-195

Burt, T. P., Allison, R. J., 2010. Sediment cascades in the environment: An integrated approach. Sediment cascades: An integrated approach, 449 p.

Castelle, S., Schäfer, J., Blanc, G., Audry, S., Etcheber, H., Lissalde, J. P., 2007. 50-year record and solid state speciation of mercury in natural and contaminated reservoir sediment. Applied Geochemistry, 22, 1359-1370.

Charriaud, A., Lesven, L., Gao, Y., Leermakers, M., Baeyens, W., Ouddane, B., Billon, G., 2011. Trace metal behaviour in riverine sediments: Role of organic matter and sulfides. Applied Geochemistry, 26, 80–90.

Chillrud, S. N., S. Hemming, E. L. Shuster, H. J. Simpson, R. F. Bopp, J. M. Ross, D. C. Pederson, D. A. Chaky, L.-R. Tolley, Estabrooks, F., 2003. Stable lead isotopes, contaminant metals and radionuclides in upper Hudson River sediment cores: implications for improved time stratigraphy and transport processes: Chemical Geology, 199, 53–70.

Claude, N., Rodrigues, S., Bustillo, V., Bréhéret, J.-G., J.-J. Macaire, Jugé, P., 2012. Estimating bedload transport in a large sand–gravel bed river from direct sampling, dune tracking and empirical formulas. Geomorphology, 179, 40–57.

Conrad, C. F., Fugate, D., Daus, J., Chisholm-Brause, C. J., Kuehl, S. A., 2007. Assessment of the historical trace metal contamination of sediments in the Elizabeth River, Virginia.: Marine pollution bulletin, 54, 385–95.

Courtin-Nomade, A., Grosbois, C., Bril, H., Roussel, C., 2005. Spatial variability of arsenic in some iron-rich deposits generated by acid mine drainage. AppliedGeochemistry, 20, 383-396.

Covelli, S., Faganeli, J., Horvat, M., Brambati, A., 2001. Mercury contamination of coastal sediments as the result of long-term cinnabar mining activity (Gulf of Trieste, northern Adriatic sea). AppliedGeochemistry, 16, 541-558.

Coynel, A., Schäfer, J., Blanc, G., Bossy, C., 2007. Scenario of particulate trace metal and metalloid transport during a major flood event inferred from transient geochemical signals. Applied Geochemistry, 22, 821–836.

De Vleeschouwer, F., Gérard, L., Goormaghtigh, C., Mattielli, N., Le Roux, G., Fagel, N., 2007. Atmospheric lead and heavy metal pollution records from a Belgian peat bog spanning the last two millennia: human impact on a regional to global scale. Science of the total environment, 377, 282-295.

Delfour J., Isnard P., Lecuyer E., Lemiere B., Lhote F., Moine B., Piboule M., Picot P., Ploquin A., Tegyey M. (1984) - Etude du gîte de pyrite de Chizeuil (Saône-et-Loire)

et de son environnement volcano-sédimentaire dévonien et dinantien. Document BRGM, n° 73, 37 p.

Desmet, M., Mourier, B., Mahler, B.J., Van Metre, P.C., Roux, G., Persat, H., I. Lefèvre, Peretti, A., Chapron, E., Simonneau, A., Miège, C., Babut, M. 2012. Spatial and temporal trends in PCBs in sediment along the lower Rhône River, France. *The Science of the total environment*, 433, 189–97.

Détriché, S., Rodrigues, S., Macaire, J.-J., Bonté, P., Bréhéret, J.-G., Bakyno, J.-P., Jugé, P., 2010. Caesium-137 in sandy sediments of the River Loire (France): Assessment of an alluvial island evolving over the last 50 years: *Geomorphology*, 115, 11–22

Dieras, P. L., Constantine, J. A., Hales, T. C., Piégay, H., Riquier, J., 2013. The role of oxbow lakes in the off-channel storage of bed material along the Ain River, France. *Geomorphology*, 188, 110–119.

Dion, R., 1961. *Histoire des levées de la Loire*. Paris, 312 p.

Estèbe, A., Boudries, H., Mouchel, J. M., Thévenot, D. R., 1997. Urban runoff impacts on particulate metal and hydrocarbon concentrations in river Seine: suspended solid and sediment transport. *Water Science and Technology*, 36, 185–193.

Estrany, J., Garcia, C., Walling, D. E., Ferrer, L., 2011. Fluxes and storage of fine-grained sediment and associated contaminants in the Na Borges River (Mallorca, Spain). *Catena*, 87, 291–305.

Ettler, V., Vaněk, A., Mihaljevič, M., Bezdička, P., 2005. Contrasting lead speciation in forest and tilled soils heavily polluted by lead metallurgy. *Chemosphere*, 58, 1449–1459.

Ferrand, E., Eyrolle, F., Radakovitch, O., Provansal, M., Dufour, S., Vella, C., Raccasi, G., Gurriaran, R., 2012. Historical levels of heavy metals and artificial radionuclides reconstructed from overbank sediment records in lower Rhône River (South-East France). *Geochimica et Cosmochimica Acta*. 82, 163–182.

Finkelman, R. B., 1993. Trace and minor elements in coal. In *Organic geochemistry*). Springer US., 593–607.

Förstner, U., 2004. Sediment dynamics and pollutant mobility in rivers: an interdisciplinary approach. *Lakes & Reservoirs: Research & Management*, 9, 25–40.

Fujikawa, Y., Fukui, M., Kudo, A., 2000. VERTICAL DISTRIBUTIONS OF TRACE METALS IN NATURAL SOIL. *Water, Air and Soil pollution*, 123, 1–21.

Garcin, M., Farjanel, G., Giot, D., 2001. Eléments radiochronologiques et palynologiques sur les alluvions du lit majeur de la Loire (Val d'Avaray, Loir-et-Cher, France)/Radiocarbon dating and palynology of alluvial deposits in the Loire flood plain (Val d'Avaray, Loir-et-Cher, France). *Quaternaire*, 12, 69–88.

Garcin, M., Giot, D., Farjanel, G., Gourry, J. C., Kloppmann, W., Negrel, P., 1999. Géométrie et âge des alluvions du lit majeur de la Loire moyenne, exemple du val d'Avaray (Loir-et-Cher, France). *Comptes Rendus de l'Académie des Sciences-Series IIA-Earth and Planetary Science*, 329, 405–412.

Garçon, M., Chauvel, C., Chapron, E., Fain, X., Mingfang L., Campillo, S., Bureau, S., Desmet, M., Bailly-Maitre, M.C., Charlet, L., 2012. Silver and lead in high altitude lake sediments : proxies for

climate changes and human activities. *Applied geochemistry*, 27, 760-773

Garnaud, S., Mouchel, J. M., Chebbo, G., Thévenot, D. R., 1999. Heavy metal concentrations in dry and wet atmospheric deposits in Paris district: comparison with urban runoff. *Science of the total environment*, 235, 235-245.

Gasowski, Z., 1994. L'enfoncement du lit de la Loire/The entrenchment of the Loire's river bed. *Revue de géographie de Lyon*, 69, 41-45.

Ghose, M. K., Majee, S. R., 2000. Assessment of the impact on the air environment due to opencast coal mining—an Indian case study. *Atmospheric Environment*, 34, 2791-2796.

Ghose, M. K., Majee, S. R., 2000. Sources of air pollution due to coal mining and their impacts in Jharia coalfield. *Environment international*, 26, 81-85.

Gocht, T., Moldenhauer, K. M., Püttmann, W., 2001. Historical record of polycyclic aromatic hydrocarbons (PAH) and heavy metals in floodplain sediments from the Rhine River (Hessisches Ried, Germany). *Applied Geochemistry*, 16, 1707-1721.

Grivel, S., Gauthier, E., 2012, Mise en place des îles fluviales en Loire moyenne, du 19<sup>e</sup> siècle à aujourd'hui, Cybergeo. URL : <http://cybergeo.revues.org/25451>

Grosbois, C., Meybeck, M., Lestel, L., Lefèvre, I., Moatar, F., 2012. Severe and contrasted polymetallic contamination patterns (1900–2009) in the Loire River sediments (France). *Science of the Total Environment*, 435, 290-305.

Grosbois, C., Courtin-Nomade, A., Martin, F., Bril, H., 2007. Transportation and evolution of trace element bearing phases in stream sediments in a mining – Influenced basin (Upper Isle River, France). *Applied Geochemistry*, 22, 2362-2374

Grousset, F. E., Jouanneau, J. M., Castaing, P., Lavaux, G., Latouche, C., 1999. A 70 year Record of Contamination from Industrial Activity Along the Garonne River and its Tributaries (SW France). *Estuarine, Coastal and Shelf Science*. 48, 401–414.

Grygar, M.T., Elznicová, J., Bábek, O., Hošek, M., Engel, Z., Kiss, T., 2014. Obtaining isochrones from pollution signals in a fluvial sediment record: A case study in a uranium-polluted floodplain of the Ploučnice River, Czech Republic. *Applied Geochemistry*. in press

Grygar, T., Světlík, I., Lisá, L., Koptíková, L., Bajer, A., Wray, D. S., Smetana, M., 2010. Geochemical tools for the stratigraphic correlation of floodplain deposits of the Morava River in Strážnické Pomoraví, Czech Republic from the last millennium. *Catena*. 80, 106-121.

Heaven, S., Ilyushchenko, M. A., Kamberov, I. M., Politikov, M. I., Tanton, T. W., Ullrich, S. M., Yanin, E. P., 2000. Mercury in the River Nura and its floodplain, Central Kazakhstan: II. Floodplain soils and riverbank silt deposits. *Science of the Total environment*, 260, 45-55.

Hong, S., Candelone, J. P., Patterson, C. C., Boutron, C. F., 1994. Greenland ice evidence of hemispheric lead pollution two millennia ago by Greek and Roman civilizations. *Science*, 265, 1841-1843.

Horowitz, A. J., Elrick, K. A., 1987. The relation of stream sediment surface area, grain size and composition to trace

- element chemistry. *Applied Geochemistry*, 2, 437-451.
- Hostache, R., Hissler, C., Matgen, P., Guignard, C., Bates, P., 2014. A 2-D hydro-morphodynamic modelling approach for predicting suspended sediment propagation and related heavy metal contamination in floodplain: a sensitivity analysis. *Hydrology and Earth System Sciences Discussions*. 11, 1741-1776.
- Houben, P., 2007. Geomorphological facies reconstruction of Late Quaternary alluvia by the application of fluvial architecture concepts. *Geomorphology*. 86, 94–114.
- Hylander, L. D., Meili, M., 2003. 500 years of mercury production: global annual inventory by region until 2000 and associated emissions. *Science of the Total Environment*, 304, 13-27
- Ip, C. C. M., X. D. Li, G. Zhang, J. G. Farmer, O. W. H. Wai, Li, Y. S., 2004. Over one hundred years of trace metal fluxes in the sediments of the Pearl River Estuary, South China.: Environmental pollution , 132, , 157–172.
- Jasminka, A., Robert, Š., 2011. Distribution of chemical elements in an old metallurgical area, Zenica (Bosnia and Herzegovina). *Geoderma*, 162, 71-85.
- Jung, M. C., Thornton, I., Chon, H. T., 2002. Arsenic, Sb and Bi contamination of soils, plants, waters and sediments in the vicinity of the Dalsung Cu-W mine in Korea. *Science of the Total Environment*, 295, 81-89.
- Kober, B., Wessels, M., Bollhöfer, A., Mangini, A., 1999. Pb isotopes in sediments of Lake Constance, Central Europe constrain the heavy metal pathways and the pollution history of the catchment, the lake and the regional atmosphere. *Geochimica et Cosmochimica Acta*, 63, 1293-1303.
- Kolker, A., 2012. Minor element distribution in iron disulfides in coal: a geochemical review. *International Journal of Coal Geology*, 94, 32-43.
- Koretsky, C. M., Haas, J. R., Miller, D., Ndenga, N. T., 2006. Seasonal variations in pore water and sediment geochemistry of littoral lake sediments (Asylum Lake, MI, USA).: *Geochemical transactions*, 7, 1-11.
- Küttner, A., Mighall, T. M., De Vleeschouwer, F., Mauquoy, D., Martínez Cortizas, A., Foster, I. D., Krupp, E., 2014. A 3300-year atmospheric metal contamination record from Raeburn Flow raised bog, south west Scotland. *Journal of Archaeological Science*, 44, 1-11.
- Latapie, A., Camenen, B., Rodrigues, S., Paquier, A., Bouchard, J.P., Moatar, F., 2014. Assessing channel response of a long river influenced by human disturbance, *Catena*, 121, 1-12.
- Latapie, A., 2011. Modélisation de l'évolution morphologique d'un lit alluvial: application à la Loire moyenne. PhD thesis, Tours univ., 277 p.
- Le Cloarec, M. F., Bonte, P. H., Lestel, L., Lefèvre, I., Ayrault, S., 2011. Sedimentary record of metal contamination in the Seine River during the last century. *Physics and Chemistry of the Earth*, 36, 515-529.
- Lecce, S. A., Pavlowsky, R. T., 2014. Floodplain storage of sediment contaminated by mercury and copper from historic gold mining at Gold Hill, North Carolina, USA. *Geomorphology*. 206, 122-132.
- Lecce, S. A., Pavlowsky, R. T., 1997. Storage of mining-related zinc in floodplain sediments, Blue River,

Wisconsin. Physical Geography. 18, 424-439.

Legros, S., Doelsch, E., Feder, F., Moussard, G., Sansoulet, J., Gaudet, J. P., Bottero, J. Y., 2013. Fate and behaviour of Cu and Zn from pig slurry spreading in a tropical water-soil-plant system. Agriculture, Ecosystems & Environment, 164, 70-79.

Lestel, L., Meybeck, M., Thevenot, D. R., 2007. Metal contamination budget at the river basin scale: an original Flux-Flow Analysis (F2A) for the Seine River. Hydrology and earth system sciences, 11, 1771-1781.

Leteinturier B., Engels P., Petit F., Chiffaut A., Malaisse F., 2000. Morphodynamisme d'un tronçon de Loire bourbonnaise depuis le XVIIIe siècle / Changing dynamics of the Loire river in Burgundy (France) during the last 200 years. In: Géomorphologie : relief, processus, environnement, 6, 239-251.

Li, F., Huang, J., Zeng, G., Yuan, X., Li, X., Liang, J., Bai, B., 2013. Spatial risk assessment and sources identification of heavy metals in surface sediments from the Dongting Lake, Middle China. Journal of Geochemical Exploration, 132, 75-83.

Li, Z., Feng, X., Li, G., Bi, X., Zhu, J., Qin, H., Sun, G., 2013. Distributions, sources and pollution status of 17 trace metal/metalloids in the street dust of a heavily industrialized city of Central China. Environmental Pollution, 182, 408-416.

Lino, M., Mériaux, P., Royet, P., 2000. Méthodologie de diagnostic des digues appliquée aux levées de la Loire moyenne. Editions Quae.

Louriño-Cabana, B., Lesven, L., Charriaud, A., Billon, G., Ouddane, B., Boughriet, A.,

2011. Potential risks of metal toxicity in contaminated sediments of Deûle river in Northern France. Journal of hazardous materials, 186, 2129-2137.

Lumb, A. J., 1995. Mercury (a Review with Special Emphasis on Pollution Effects from Gold Mining). British Geological Survey ,19p.

Macaire, J. J., Gay-Ovejero, I., Bacchi, M., Cocirat, C., Patryl, L., Rodrigues, S., 2013. Petrography of alluvial sands as a past and present environmental indicator: Case of the Loire River (France). International Journal of Sediment Research. 28, 285-303.

Macklin, M. G., Brewer, P. A., Hudson-Edwards, K. A., Bird, G., Coulthard, T. J., Dennis, I. A., Turner, J. N., 2006. A geomorphological approach to the management of rivers contaminated by metal mining. Geomorphology, 79, 423-447.

Macklin, M. G., Klimek, K., 1992. Dispersal, storage and transformation of metal contaminated alluvium in the upper Vistula basin, southwest Poland. Applied Geography. 12, 7-30.

Martin, C. W., 2000. Heavy metal trends in floodplain sediments and valley fill, River Lahn, Germany. Catena, 39, 53-68.

Martin, J. M., Meybeck, M., 1979. Elemental mass-balance of material carried by major world rivers. Marine chemistry, 7, 173-206.

Martínez-Cortizas, A., Pontevedra-Pombal, X., García-Rodeja, E., Novoa-Munoz, J. C., Shotyk, W. (1999). Mercury in a Spanish peat bog: archive of climate change and atmospheric metal deposition. Science, 284, 939-942.

- MacDonald, D. D., Ingersoll, C. G., Berger, T. A., 2000. Development and evaluation of consensus-based sediment quality guidelines for freshwater ecosystems. *Archives of Environmental Contamination and Toxicology*, 39, 20-31.
- Meybeck, M., Lestel, L., Bonté, P., Moilleron, R., Colin, J. L., Rousselot, O., Thévenot, D. R., 2007. Historical perspective of heavy metals contamination (Cd, Cr, Cu, Hg, Pb, Zn) in the Seine River basin (France) following a DPSIR approach (1950–2005). *Science of the Total Environment*, 375, 204-231.
- Meybeck M, Horowitz A, Grosbois C., 2004. The geochemistry of Seine River basin particulate matter: distribution of an integrated metal pollution index. *Science of the Total Environment*, 328, 219–36.
- Meybeck, M., 2002. Riverine quality at the Anthropocene: Propositions for global space and time analysis, illustrated by the Seine River. *Aquatic Sciences*, 64, 376-393.
- Meybeck, M., Helmer, R., 1989. The quality of rivers: from pristine stage to global pollution. *Global and Planetary Change*, 1, 283-309.
- Miller, J. R., Lechner, P. J., Bridge, G., 2003. Mercury contamination of alluvial sediments within the Essequibo and Mazaruni river basins, Guyana. *Water, Air, and Soil Pollution*, 148, 139-166.
- Miller, J. R., 1997. The role of fluvial geomorphic processes in the dispersal of heavy metals from mine sites. *Journal of Geochemical Exploration*, 58, 101-118.
- Mishra, V. K., Upadhyaya, A. R., Pandey, S. K., Tripathi, B. D., 2008. Heavy metal pollution induced due to coal mining effluent on surrounding aquatic ecosystem and its management through naturally occurring aquatic macrophytes. *Bioresource technology*, 99, 930-936.
- Möller, S., Einax, J. W., 2013. Metals in sediments—spatial investigation of Saale River applying chemometric tools. *Microchemical Journal*, 110, 233-238.
- Monna, F., Petit, C., Guillaumet, J. P., Jouffroy-Bapicot, I., Blanchot, C., Dominik, J., Château, C., 2004. History and environmental impact of mining activity in Celtic Aeduan territory recorded in a peat bog (Morvan, France). *Environmental science & technology*, 38, 665-673.
- Monna, F., Galop, D., Carozza, L., Tual, M., Beyrie, A., Marembert, F., Grousset, F. E., 2004. Environmental impact of early Basque mining and smelting recorded in a high ash minerogenic peat deposit. *Science of the Total Environment*, 327, 197-214.
- Monna, F., Clauer, N., Toulkeridis, T., Lancelot, J. R., 2000. Influence of anthropogenic activity on the lead isotope signature of Thau Lake sediments (southern France): origin and temporal evolution. *Applied Geochemistry*, 15, 1291-1305.
- Mourier, B., Desmet, M., Van Metre, P. C., Mahler, B. J., Perrodin, Y., Roux, G., Bedell, J.-P., Lefèvre, I., Babut, M., 2014. Historical records, sources, and spatial trends of PCBs along the Rhône River (France). *The Science of the total environment*. 476-477, 568–576.
- Mukherjee, A. B., Zevenhoven, R., Bhattacharya, P., Sajwan, K. S., Kikuchi, R., 2008. Mercury flow via coal and coal utilization by-products: A global perspective. *Resources, Conservation and Recycling*, 52, 571-591.

- Müller G., 1979. Schwermetalle in den Sedimenten des Rheins-Veränderungenseit 1971.Umschau;79: 778–783
- Neal, P. A., 1938. Mercury Poisoning from the Public Health Viewpoint\*.American Journal of Public Health and the Nations Health, 28, 907-915.
- Negrel, P., Kloppmann, W., Garcin, M., Giot, D., 2004. Lead isotope signatures of Holocene fluvial sediments from the Loire River valley. Applied geochemistry, 19, 957-972.
- Négrel, P., Grosbois, C., Kloppmann, W., 2000. The labile fraction of suspended matter in the Loire River (France): multi-element chemistry and isotopic (Rb-Sr and C-O) systematics. Chemical Geology, 166, 271-285.
- Négrel, P., Kloppman, W., Garcin, M., Giot, D., 1999. Strontium isotopic record of signatures of Holocene fluvial sediments in the Loire valley, France. Hydrology and Earth System Sciences, 6, 849-858.
- Nriagu, J. O., 1990. Global metal pollution: poisoning the biosphere?.Environment: Science and Policy for Sustainable Development, 32, 7-33.
- Oyarzun, R., Lillo, J., López-García, J. A., Esbrí, J. M., Cubas, P., Llanos, W., Higueras, P., 2011. The Mazarrón Pb-(Ag)-Zn mining district (SE Spain) as a source of heavy metal contamination in a semiarid realm: Geochemical data from mine wastes, soils, and stream sediments. Journal of Geochemical Exploration, 109, 113-124.
- Palumbo, B., Angelone, M., Bellanca, A., Dazzi, C., Hauser, S., Neri, R., Wilson, J., 2000. Influence of inheritance and pedogenesis on heavy metal distribution in soils of Sicily, Italy. Geoderma. 95, 247–266.
- Pavoni, B., Donazzolo, R., Marcomini, A., Degobbis, D., Orio, A. A., 1987. Historical development of the Venice Lagoon contamination as recorded in radiodated sediment cores. Marine pollution bulletin, 18, 18-24.
- Qi, C., Liu, G., Chou, C. L., Zheng, L., 2008. Environmental geochemistry of antimony in Chinese coals. Science of the total environment, 389, 225-234.
- Querol, X., Viana, M., Alastuey, A., Amato, F., Moreno, T., Castillo, S., Zabalza, J., 2007. Source origin of trace elements in PM from regional background, urban and industrial sites of Spain. Atmospheric Environment, 41, 7219-7231.
- Querol, X., Fernández-Turiel, J., Lopez-Soler, A., 1995. Trace elements in coal and their behaviour during combustion in a large power station. Fuel, 74, 331-343.
- Reis, A., Parker, A., Alencoão, A., 2014. Storage and origin of metals in active stream sediments from mountainous rivers: A case study in the River Douro basin (North Portugal). Applied Geochemistry, 44, 69-79.
- Resongles, E., Casiot, C., Freydier, R., Dezileau, L., Viers, J., Elbaz-Poulichet, F., 2014. Persisting impact of historical mining activity to metal (Pb, Zn, Cd, Tl, Hg) and metalloid (As, Sb) enrichment in sediments of the Gardon River, Southern France. Science of the Total Environment, 481, 509-521.
- Rodrigues S., Bréhéret J.G., Macaire J.J., Greulich S., Villar M., 2007. In-channel woody vegetation controls on sedimentary processes and the sedimentary record within alluvial environments: a modern example of an

- anabranch of the River Loire, France. *Sedimentology*, 54, 223–242.
- Rogich, D. G., Matos, G. R., 2008. Global Flows of Metals and Minerals.US Department of the interior, US Geological Survey.11 p.
- Schettler, G., Romer, R. L., 2006. Atmospheric Pb-pollution by pre-medieval mining detected in the sediments of the brackish karst lake An Loch Mór, western Ireland. *Applied geochemistry*, 21, 58-82.
- Schulz-Zunkel, C., Krueger, F., Rupp, H., Meissner, R., Gruber, B., Gerisch, M., & Bork, H. R. (2013). Spatial and seasonal distribution of trace metals in floodplain soils. A case study with the Middle Elbe River, Germany. *Geoderma*. 211, 128-137.
- Selim Reza, A H. M., Jean, J.-S., Yang, H.-J., Lee, M.-K., Woodall, B., Liu, C.-C., Lee, J.-F., Luo, S.-D., 2010, Occurrence of arsenic in core sediments and groundwater in the Chapai-Nawabganj District, northwestern Bangladesh.: *Water research*, 44, 2021–37.
- Seredin, V. V., Finkelman, R. B., 2008. Metalliferous coals: a review of the main genetic and geochemical types. *International Journal of Coal Geology*, 76, 253-289.
- Shotyk, W., Weiss, D., Appleby, P. G., Cheburkin, A. K., Frei, R., Gloor, M., Van Der Knaap, W. O., 1998. History of atmospheric lead deposition since 12,370 14C yr BP from a peat bog, Jura Mountains, Switzerland. *Science*, 281, 1635-1640.
- Sizaret, S., 2002. Genèse du système hydrothermal à fluorine-barytine-fer de Chaillac, (Indre, France) (Doctoral dissertation, Université d'Orléans). 260 p.
- Sreeram, K. J., Ramasami, T., 2003. Sustaining tanning process through conservation, recovery and better utilization of chromium. *Resources, conservation and recycling*, 38, 185-212.
- Thévenot, D. R., Moilleron, R., Lestel, L., Gromaire, M. C., Rocher, V., Cambier, P., Meybeck, M., 2007. Critical budget of metal sources and pathways in the Seine River basin (1994–2003) for Cd, Cr, Cu, Hg, Ni, Pb and Zn. *Science of the total environment*, 375, 180-203.
- Tilton, J. E., 1990. World metal demand: trends and prospects. *Resources for the Future*.345 p.
- Tiwary, R. K., Dhar, B. B., 1994. Effect of coal mining and coal based industrial activities on water quality of the river Damodar with specific reference to heavy metals. *International Journal of Surface Mining and Reclamation*, 8, 111-115.
- Tiwary, R. K., Dhar, B. B., 1994. Environmental pollution from coal mining activities in Damodar River Basin, India. *Mine water and the Environment*, 13, 1-10.
- Valverde, L., Jugé, P., Handfus, T., 2013. Résultats granulométriques et localisation des points dures en Loire, rapport InfoSed 2, p. 180
- Van Griethuysen, C., Luitwieler, M., Joziasse, J., Koelmans, A. A., 2005. Temporal variation of trace metal geochemistry in floodplain lake sediment subject to dynamic hydrological conditions. *Environmental Pollution*. 137, 281-294.
- Verner, J. F., Ramsey, M. H., Helios-Rybicka, E., Jedrzejczyk, B., 1996. Heavy metal contamination of soils around a PbZn smelter in Bukowno, Poland. *Applied Geochemistry*, 11, 11-16.

- Vink, R., Behrendt, H., Salomons, W., 1999. Development of the heavy metal pollution trends in several European rivers: an analysis of point and diffuse sources. *Water Science and Technology*, 39, 215-223.
- Vörösmarty, C. J., Meybeck, M., Fekete, B., Sharma, K., Green, P., Syvitski, J. P., 2003. Anthropogenic sediment retention: major global impact from registered river impoundments. *Global and Planetary Change*, 39, 169-190.
- Vrel, A., Boust, D., Lesueur, P., Deloffre, J., Dubrulle-Brunaud, C., Solier, L., Rozet, M., Thouroude, C., Cossonet, C., Thomas, S., 2013. Dating of sediment record at two contrasting sites of the Seine River using radioactivity data and hydrological time series. *Journal of environmental radioactivity*. 126, 20-31
- Vukovic, D., Vukovic, Z., Stankovic, S., 2014. The impact of the Danube Iron Gate Dam on heavy metal storage and sediment flux within the reservoir. *Catena*, 113, 18-23.
- Walling, D. E., He, Q., 1997. Use of fallout <sup>137</sup>Cs in investigations of overbank sediment deposition on river floodplains. *Catena*. 29, 263-282.
- Walling, D. E., Owens, P. N., 2003. The role of overbank floodplain sedimentation in catchment contaminant budgets. *Hydrobiologia*, 494, 83-91.
- Walling, D. E., Owens, P. N., Carter, J., Leeks, G. J. L., Lewis, S., Meharg, A. A., Wright, J., 2003. Storage of sediment-associated nutrients and contaminants in river channel and floodplain systems. *Applied Geochemistry*, 18, 195-220.
- Walling, D. E., Owens, P. N., G. J.L. Leeks., 1998. The role of channel and floodplain storage in the suspended sediment budget of the River Ouse, Yorkshire, UK. *Geomorphology*. 22, 225–242.
- Walling, D.E., Owens, P.N., Leeks, G.J.L., 1997. The characteristics of overbank deposits associated with a major flood event in the catchment of the River Ouse, Yorkshire, UK. *Catena*. 31, 53–75.
- Woronoff D., Histoire de l'industrie en France, Du 16e siècle à nos jours, Paris, Le Seuil, 1994, 671 p.
- Xue, H., Nhat, P. H., Gächter, R., Hooda, P. S., 2003. The transport of Cu and Zn from agricultural soils to surface water in a small catchment. *Advances in Environmental Research*, 8, 69-76.
- Xu, B., Yang, X., Gu, Z., Zhang, Y., Chen, Y., Lv, Y., 2009. The trend and extent of heavy metal accumulation over last one hundred years in the Liaodong Bay, China. *Chemosphere*, 75, 442-446.
- Ye, C., Li, S., Zhang, Y., Zhang, Q., 2011. Assessing soil heavy metal pollution in the water-level-fluctuation zone of the Three Gorges Reservoir, China. *Journal of hazardous materials*, 191, 366-372.
- Yudovich, Y. E., Ketris, M. P., 2005. Arsenic in coal: a review. *International Journal of Coal Geology*, 61, 141-196.
- Yudovich, Y. E., Ketris, M. P., 2005. Mercury in coal: a review: Part 1. *Geochemistry. International Journal of Coal Geology*, 62, 107-134.



E.A. 6293 - GeHCO

## Partie 2 - Influences de l'environnement de dépôt sur l'archivage des sédiments et des contaminants associés

## **Chapitre 4 - Synthèse**

### **Points importants :**

- Etude des mécanismes d'archivage des sédiments et contaminants associés
- Variabilité spatiale du signal géochimique à l'échelle de l'environnement de dépôt
- Influence des apports de crues sur l'enregistrement du signal géochimique

### **Mots clés :**

archivage sédimentaire, plaine alluviale, réservoir de barrage, dynamique temporelle, éléments traces

#### **4.1. Objectifs et méthodes analytiques**

Les archives sédimentaires permettent de reconstituer les dynamiques temporelles des contaminants à l'échelle d'un bassin versant. L'objectif principal de ce second chapitre est de répondre aux verrous méthodologiques concernant la **représentativité de ces enregistrements.**

L'hétérogénéité de la géologie du bassin de la Loire peut être un facteur de variabilité spatiale des fonds géochimiques. Or il est nécessaire d'établir **un état de référence représentatif** des apports naturels pour quantifier les niveaux de contaminations sédimentaires.

D'autre part, les environnements de dépôt sont variés au sein du corridor fluviaile et soumis à des évolutions géomorphologiques à plus ou moins long terme. Ces facteurs peuvent induire **une variabilité spatiale et temporelle de l'archivage des sédiments et ET associés** à l'échelle de stationnelle.

Cette étude correspond à une **approche intégrée des processus sédimentologiques et géochimiques** pouvant influencer l'enregistrement des contaminations sédimentaires du bassin

de la Loire. Les variabilités spatiale et temporelle de différents paramètres sont ici étudiées à l'échelle de l'environnement fluviaile :

- (i) les mécanismes de dépôts sédimentaires,
- (ii) les taux d'aggradation,
- (iii) la continuité de l'archivage sédimentaire,
- (iv) l'origine des sédiments archivés
- (v) et les processus de redistribution des ET au sein de la colonne sédimentaire.

Afin d'étudier ces facteurs de variabilité, trois archives sédimentaires ont été échantillonnées dans des environnements fluviaux différents en Loire Amont. Le premier site de carottage a été défini **dans le réservoir de la retenue** de Villerest. Une archive sédimentaire y a été prélevée en 2010. Les deux autres archives ont été échantillonnées en 2012 **dans un paléochenal et la berge de la plaine d'inondation** à Decize. Les analyses sédimentologiques et géochimiques ont été réalisées à une résolution de 2 cm.

En premier lieu, l'évolution géomorphologique des environnements de dépôts a été reconstituée à l'aide d'un

## Influence des processus hydrosédimentaires

Après de fortes crues, les niveaux de contaminations des dépôts sédimentaires peuvent être différents de ceux archivés après des événements moins importants.

Trois séquences de crues associées à des événements majeurs représentent une part importante du remplissage sédimentaire du réservoir de Villerest. Ces séquences de crue permettent de mettre en évidence un important stockage de sédiments fortement contaminés lors de ces événements.

Malgré la sélection de la fraction < 63µm des sédiments et la normalisation à l'aluminium, on observe une variabilité des facteurs d'enrichissements au sein des séquences de crue en lien avec l'évolution de la granularité et de la minéralogie des sédiments déposés au cours de l'hydrogramme de crue.

L'analyse de l'évolution à long-terme des contaminations a permis de mettre en évidence une diminution des niveaux de contaminations enregistrée dans les séquences déposées entre ces crues et la sollicitation événementielle d'importantes sources de contamination lors de ces épisodes hydrosédimentaires majeurs.

La variabilité du signal géochimique enregistrée pendant ces crues majeures n'est pas représentative de l'évolution à long-terme des niveaux de contaminations.

diagramme C-M de Passegae, adapté à la Loire Amont. Cette méthode permet de reconstituer les environnements de dépôt sédimentaire en définissant graphiquement des domaines caractérisant des processus de dépôts à l'aide de l'évolution de la distribution de la taille des grains. Suite à cela, les modèles d'âge et les taux d'aggradation des archives ont été calculés entre des niveaux sédimentaires datés (profils de  $^{137}\text{Cs}$  et séquences de crues historiques). Les analyses géochimiques des éléments majeurs et traces ont été réalisées sur la fraction < 63µm après digestion totale des sédiments. Dans cette étude, les niveaux de contaminations sont exprimés en facteur d'enrichissement (*cf.* EF ; eq. 2.1). Les annexes 1 et 2 montrent l'étude préliminaire qui a permis de localiser les sites de carottages et les résultats des analyses géochimiques et sédimentologiques.

### 4.2. Principaux résultats

L'analyse sédimentologique et la datation des archives sédimentaires permettent de mettre en exergue des différences inter et intra environnements fluviaires concernant les mécanismes de

dépôts sédimentaires, les taux d'aggradation et la continuité des enregistrements. Deux processus de sédimentation ont contribué au remplissage sédimentaire du réservoir de Villerest :

- (i) une décantation de particules fines en période intercrue
- (ii) et des apports massifs en éléments plus grossiers lors des épisodes de crues majeurs en 1996, 2003 et 2008 (> temps de retour de 20 ans).

**Le taux d'aggradation n'est pas linéaire dans le réservoir**, ces épisodes de crues contribuant à hauteur de 43 %m. de la colonne sédimentaire accumulée depuis le fonctionnement du barrage en 1984.

De la même manière, **différents mécanismes d'alluvionnement se sont succédés lors de l'édification de la plaine alluviale** à Decize. Une séquence sableuse datant de la fin du Petit Age Glaciaire constitue la base de l'archive prélevée en berge et présente un granoclassement associé à la progressive déconnexion de l'environnement de dépôt. La partie sommitale de cette archive est essentiellement composée de sédiments fins décantés lors des épisodes de

débordements. De manière synchrone, le remplissage sédimentaire du paléochenal résulte essentiellement de la décantation de particules fines. Malgré cela, **des différences existent quant à la continuité des enregistrements** entre la berge et le paléochenal. En effet, 4 séquences de crues datant 1846, 1856, 1866 et 1907 ont été archivées dans le paléochenal et sont absentes de la carotte en berge. Une meilleure préservation des sédiments archivés est ainsi mise en évidence dans le paléochenal. D'autre part, après l'exhaussement du barrage de Decize en 1933, les taux de sédimentation ont diminué pour les deux environnements, mais avec une intensité plus importante sur la berge.

Ces différences spatiales et temporelles des processus d'alluvionnement et de préservation des sédiments archivés ont une influence sur l'enregistrement des signaux géochimiques. Dans les sédiments du réservoir de Villerest, une tendance à la diminution des enrichissements est archivée dans les sédiments déposés en période d'intercrue. A l'inverse, les sédiments déposés lors des épisodes de crues présentent des enrichissements en ET bien plus importants, attestant de

## Influence des environnements de dépôt

Entre les environnements fluviatiles, l'hétérogénéité des processus d'apport sédimentaire mais aussi d'archivage des sédiments et contaminants associés sont des facteurs de la variabilité des enregistrements à l'échelle stationnelle.

Deux archives sédimentaires ont été prélevées au sein de la plaine alluviale de la Loire Amont à Decize à proximité l'une de l'autre, la berge et le paléochennal. La comparaison des enregistrements permet de mettre en évidence l'influence de l'environnement de dépôt sur l'archivage des sédiments et contaminants associés.

D'une part, l'enregistrement sédimentaire est plus préservé dans le paléochennal que dans la berge, le signal sédimentaire étant plus complet et la continuité de l'archive meilleur.

D'autre part on observe une importante divergence de l'évolution tendancielle des contaminations entre les deux environnements, liée à la fois à une différence de nature des sédiments archivés et à des processus de redistribution des contaminants au sein de la colonne sédimentaire en berge.

A Decize, l'enregistrement en berge n'est pas représentatif de l'évolution à long terme des contaminations du bassin amont.

**l'activation ou la réactivation de sources spécifiques de contaminations.** De plus, durant ces épisodes hydrosédimentaires, le dépôt de sédiments plus grossiers et l'apport massif de matériel détritique influencent les niveaux de contaminations enregistrés même après sélection de la fraction < 63µm et normalisation à l'aluminium.

En ce qui concerne la plaine alluviale de Decize, cette étude met en évidence d'importantes variabilités spatiales des signaux géochimiques enregistrés. En effet, alors que les concentrations préindustrielles sont comparables entre les parties amont et aval du bassin en ce qui concerne les sédiments fins (excepté l'influence locale des anomalies géochimiques), les concentrations sont significativement différentes entre les sédiments déposés dans la partie proximale de la plaine d'inondation (sédiments sableux) et dans sa partie distale (sédiments fins). Ces résultats soulignent la représentativité à l'échelle du linéaire de la Loire des états de références mesurés et montrent **l'influence du tri minéralogique lié au processus de dépôts sédimentaires sur le signal géochimique** au sein de la plaine d'inondation.

La meilleure préservation des sédiments déposés dans le paléochenal conduit à **une plus grande résolution sur les évolutions à court terme des niveaux de contaminations**. D'autre part, lors de l'archivage sédimentaire, **une sélection différente des sédiments contaminés** opère entre les deux environnements de dépôts. Cette différence se traduit en berge par l'enregistrement d'un signal géochimique moins complet que dans le paléochenal. De surcroit, des processus de pédogénèse induisent aussi une forte **redistribution des contaminants au sein de la colonne sédimentaire** en berge.

#### 4.3. Conclusion

Cette étude montre l'influence des processus hydrosédimentaires et géomorphologiques associés aux environnements de dépôts sur l'archivage des signaux géochimiques.

Les résultats de cette étude montrent ainsi une variabilité spatiale à l'échelle de l'environnement fluviatile des concentrations préindustrielles. Pour

autant, les concentrations pristines mesurées en amont et en aval du domaine fluviaile de la Loire sont comparables si l'on s'intéresse à des environnements de dépôts similaires (zone de décantation des particules fines).

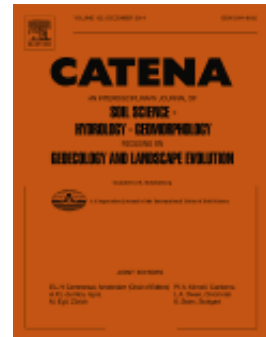
**Le choix du site de carottage détermine aussi la représentativité de l'enregistrement sédimentaire.** Dans le cadre du réservoir de Villerest, les dépôts intercrues permettent de reconstituer les évolutions tendancielles des niveaux de contaminations alors que les séquences de crues attestent de l'activation événementielle de sources de contaminations. Au niveau de la plaine d'inondation de Decize, le remplissage sédimentaire du paléochenal permet une reconstitution plus représentative de l'évolution à long terme des contaminations sédimentaires. En effet, l'archivage en berge est soumis à une plus grande sélection des particules déposées, à des événements d'érosion et à des processus de redistributions des ET au sein de la colonne sédimentaire.



**Illustration 1 :** Photographie aérienne du barrage de Villerest (Loire Amont) durant la crue de novembre 2008 (> temps de retour de 50 ans ; source : EPL)

## **Chapitre 5 - Influences of major flood sediment inputs on sedimentary and geochemical signals archived in a reservoir core (Upper Loire basin, France)**

Published in: Catena, 2015, 126, 75-85



E. Dhivert <sup>a</sup>, C. Grosbois <sup>a</sup>, A. Coynel <sup>b</sup>, I. Lefèvre <sup>c</sup>, M. Desmet <sup>a</sup>

<sup>a</sup> Université François Rabelais de Tours. EA 6293 GéHCO. Parc de Grandmont. 37200 Tours. France

<sup>b</sup> Université de Bordeaux. UMR 5805 CNRS EPOC. Av. des universités. 33405 Talence cedex. France.

<sup>c</sup> Laboratoire des Sciences du Climat et de l'Environnement, UMR CNRS/CEA/UVSQ 1572 – IPSL. 91198 Gif –sur–Yvette. France.

*Received on October the 20<sup>th</sup> of 2014 and accepted on October the 27<sup>th</sup> of 2014*

### **Highlights:**

- Conservative trace element and grain-size variations inform about flood dynamics
- Sediment-laden underflows during major floods magnify annual aggradation rate
- Contamination levels of sediments are enhanced during flood events
- Solid anthropogenic inputs are diluted by detrital material inputs during flood events

## **Abstract:**

The Villerest flood-control reservoir was built in the Upper Loire River (France) during the early 1980s, downstream from the most important industrial and coal-mining area of the basin. This reservoir has constituted an important trap for sediments and associated pollutants since its operation in 1984. A 154-cm-long core was recovered in 2010 in the deepest area of the reservoir and shows the influence of sedimentary infill processes on aggradation rates and selected chemical patterns. During dam operations, the lacustrine aggradation rate is not linear because of three turbiditic-like layers resulting from sediment-laden underflows during major flood events in 1996, 2003 and 2008. These three events contribute to 43% of the  $151 \text{ kg.m}^{-2}$  of accumulated sediments over the 1984-2010 period. Trace element solid sources are activated during these floods as selected metals present the highest enrichment factors, levels never reached during interflood periods. In addition, sedimentological and detrital geochemical signals during these events influence anthropogenic trace element signals by a variable dilution effect (maximum during the increasing discharge stage). Hence, coupling sedimentological and geochemical approaches allows us to understand the sedimentary infill dynamics and, more specifically, to take into account the influence of floods on the temporal trajectories of pollutants.

**Keywords:** Loire basin, sedimentary archive, age model, flood event, detrital trace elements, Villerest dam reservoir

## 5.1. Introduction

At the basin scale, the spatial distributions of the sedimentary contamination of metallic pollutants are largely controlled by the settling capacity of fine-grained sediments (< 63 µm; Horowitz and Elrick, 1987; Walling *et al*, 2003). Over the last 50 years, dam constructions highly modified the transfer of sediments in hydrosystems by constituting storage areas for transported sediments (Vörösmarty *et al*, 2003). The coarsest sediments are mostly deposited in the delta part of the reservoirs, while the finest sediments settle in the deepest area (Fan and Morris, 1992; Ziegler and Nisbet, 1995; Morris *et al*, 2008). Potentially polluted sediments trapped in reservoirs can then become a source of contamination for biota, interstitial and surface waters by pollutant diffusion at the water-sediment interface, by organic matter mineralization, or by reworking within pollutant-bearing phases during dam exploitation (maintenance, dredging and/or emptying, dam flushing) (Coynel *et al*, 2007; Audry *et al*, 2010). However, these reservoirs also offer good opportunities – as do lakes – to find preserved contamination records (Audry *et al*, 2004; Castelle *et al*, 2007),

particularly in fluvial systems where the high spatial and temporal variability of aggradation rates managed floodplain edifications (Walling *et al*, 1997; Walling and He, 1997; Bábek *et al*, 2008; Desmet *et al*, 2012; Mourier *et al*, 2014). This is particularly important for rivers affected by artificial width contraction (Arnaud-Fassetta, 2003). Numerous studies address the annual and seasonal sediment trapping yield of large dam reservoirs (e.g., Yang *et al*, 2002; Dai *et al*, 2008) and associated-sediment pollutant dynamics over time, especially during high discharge events (Ye *et al*, 2011; Vukovic *et al*, 2014), but sedimentary infill processes and their influence on aggradation rates and sediment chemical temporal patterns are poorly understood. Thus, the origins of the trapped sediment and settling conditions constitute a key point towards building the temporal trends of pollutants, anthropogenic sources and their variations at a basin scale.

The Villerest flood-control reservoir, built in the Upper Loire River (France) downstream from an important industrial and coal-mining area (Saint Etienne; Fig. 5.1), largely contributes to the retention of potentially polluted sediments,

complementing the other large dam in the basin (Grangent dam, Fig. 5.1). The present study uses sedimentological and geochemical approaches to characterize the sediment dynamics and associated TE during infilling processes in a high-order stream reservoir and shows the main influence of high discharge events on TE temporal trends.

## 5.2. Study area and methodology

### 5.2.1. Main geographical and geological characteristics of the study area

The Loire River basin ( $117,800 \text{ km}^2$ ) is among the ten largest W-European basins and the largest in France. The Upper Loire (Strahler stream order of 6), upstream from the studied station at the Villerest dam, is 260 km long and drains a basin of  $6516 \text{ km}^2$ . According to the French geological survey (infoterre.brgm.fr, 2013), it contains four main geological units (Fig. 5.1):

- (i) Variscan plutonic rocks (granites, gneiss and micaschists, aged between 500 and 300 Ma) covering 63% of the basin area;
- (ii) volcanism between 20 Ma and 300 ka, representing approximately

- 15% of the basin area and only located in the S-E part;
- (iii) sedimentary bedrock of Carboniferous (mainly sandstones) and Oligocene-Miocene age (fluviacustrine deposits such as sands, marls and clays), corresponding to 4 and 12 %, respectively, of the upper basin surface; and
- (iv) Quaternary alluvia along the river covering 5 % of the surface.

According to the Villerest dam managers (EPL, [www.eptb-loire.fr](http://www.eptb-loire.fr), 2013), the hydrolic structure was built between the late 1970s and 1983, and water filling operations occurred by steps between 1983 and 1984. The dam has been in operation since 1984 with a mean water reservoir of  $128 \text{ Mm}^3$ , approximately 36 km long (influencing 14% of the upstream main channel length) and no wider than 900 m with a maximum depth of 60 m. The water level varies by 11 m over a year as the current exploitation of the reservoir allows two operating modes in relation to the hydrological cycle:

- (i) during the spring and autumn, the water level is at the minimum to control winter flood outflows;

(ii) conversely, at the beginning of summertime, the water level is at the maximum to guarantee a minimal low flow (at least  $12 \text{ m}^3.\text{s}^{-1}$  at the Villerest gauging station, 1 km downstream from the dam). The Villerest dam is also a hydroelectric power plant that remains in operation all year.

The hydrological regime in the upper basin is a balance of oceanic and Mediterranean influences with additional snow-melt in the spring (Dacharry, 1974). The resulting annual hydrological cycle at the Feurs gauging station, 19 km upstream of the dam's influence, is characterized by winter high flows with floods in the autumn, winter and/or spring. During the high flow for the 1984-2010 period, the highest monthly discharge was  $64.3 \text{ m}^3.\text{s}^{-1}$  and the summer low flows show a minimum of  $10.5 \text{ m}^3.\text{s}^{-1}$  ([www.hydro.eaufrance.fr](http://www.hydro.eaufrance.fr), 2013). Since the beginning of the dam's construction, several major flood events occurred (Fig. 5.1b):

(i) 3 major floods with a greater than 50-year flood average daily discharge calculated over the period ( $1400 \text{ m}^3.\text{s}^{-1}$ ) in November 1976 ( $1410 \text{ m}^3.\text{s}^{-1}$ ), December 2003

( $1570 \text{ m}^3.\text{s}^{-1}$ ) and November 2008 ( $1490 \text{ m}^3.\text{s}^{-1}$ );

- (ii) (ii) a greater than 20-year flood average daily discharge ( $1200 \text{ m}^3.\text{s}^{-1}$ ) in May 1983 ( $1340 \text{ m}^3.\text{s}^{-1}$ ), just before water filling operations started in the Villerest dam;
- (iii) (iii) additional important floods occurred in May 1977 ( $1050 \text{ m}^3.\text{s}^{-1}$ ) and September 1980 ( $1060 \text{ m}^3.\text{s}^{-1}$ ).

All of these major floods resulted from heavy rainfall episodes in the upstream basin. They usually took place throughout the basin with maximum discharges at the same time in the Loire main stream and its major tributaries.

### **5.2.3. Analytical methods**

The coring site ( $45^{\circ}58'54''\text{N}, 4^{\circ}2'15''\text{E}$ ) is located 200 m upstream from the Villerest dam in the deepest zone of the reservoir (57 m deep at the coring site) when the water level in the reservoir was the lowest. The core was recovered from a platform ship in September 2010 with a UWITEC gravity corer fitted with a 2-m long and 90-mm diameter plastic liner. At the laboratory, only sediments from the middle of the liner were sampled in 2 cm-slices with a ceramic knife. The slices were then stored in acid-washed plastic

containers to prevent metallic contamination. Neither gas bubbles nor living organisms and/or bioturbation features were clearly observed when slicing. The dry bulk density ( $\text{kg.m}^{-3}$ ) was determined as the weight of dry material divided by the volume of the container, and the water content (%) was calculated from the weight difference between the fresh and dry sediments. Particle size analyses were performed after a 1-min ultrasonic step with a Malvern Mastersizer 2000 laser diffraction microgranulometer on each fresh 2-cm core slice (measurement range between 0.02 and 2000  $\mu\text{m}$ ). Although leaf and brushwood remains were present in low amounts in the studied core, they disturbed the measured grain-size signal, so macroscopic organic remains were manually removed before the measurements. The grain-size median ( $D_{50}$ ), the ten percentile ( $D_{10}$ ), the ninety percentile ( $D_{90}$ ) and the cumulative volumetric percentage of clay (<2  $\mu\text{m}$ ), silt (2–63  $\mu\text{m}$ ) and sand (>63  $\mu\text{m}$ ) were computed with a Gradistat spreadsheet (Blott and Pye, 2001) using the Folk and Ward geometric method (Folk and Ward, 1957).

The radiometric analyses were performed on approximately 50 g of < 2 mm core material in air-tight plastic boxes for a 24 h gamma-counting. Very low-background detectors, namely, coaxial HP Ge N-types, were used for gamma spectrometry (8000 channels, low background). The efficiencies and backgrounds were periodically controlled with internal soil and sediment standards, pure KCl samples, and IAEA standards (Soil 6, 135 and 375).  $^{137}\text{Cs}$  was detected with an energy peak at 661 keV in a spectrum area free of any interference. The activities were corrected to the time of the collection period, and the uncertainty of the measurements was approximately 0.5% with a detection limit of 0.3 Bq/kg. The  $^{137}\text{Cs}$  artificial radionuclide activity is commonly used in bed sediments as a time calibration, using 3 events in Western Europe:

- (i) its introduction in 1950 in the atmosphere by the first important nuclear weapon tests (NWT),
- (ii) the maximum  $^{137}\text{Cs}$  atmospheric fallout in 1964 (atmospheric  $^{137}\text{Cs}$  emissions decreased after 1964 thanks to the October 1963 nuclear test ban treaty, Walling

and Bradley, 1990; Klaminder *et al*, 2012)

- (iii) and the 1986 fallout peak following the Chernobyl nuclear power plant disaster (C-NPPD).

We also used the top of the core between 2 and 0 cm, which corresponds to the sampling period (2010 here).

Part of each air-dried material slice was sieved through <63 µm disposable Nylon mesh. The chemical composition was also determined with the <63 µm fraction to limit the grain-size and associated mineralogical influence. The selection of fine-grained sediments for the geochemical analyses is particularly important in the Loire River context, where the sandy fraction is very heterometric and the mineralogical composition of the sediments depends on the grain-size of the particles (Macaire *et al*, 2013; Valverde *et al*, 2013). Representative 0.5 g of dry <63 µm material was digested in a Teflon beaker in a tunnel oven with LiBO<sub>2</sub>-Li<sub>2</sub>B<sub>4</sub>O<sub>7</sub>. After the samples were dried, the residues were completely re-dissolved with HNO<sub>3</sub> acid. Additional splits of 0.2 g were digested by hot Aqua Regia (95°C) for the determination of trace element (TE) abundances. The total contents of the

major and minor elements were analyzed by ICP-AES (Jobin-Yvon 70; Govindaraju and Mevelle, 1987), and the trace elements were analyzed by ICP-MS (Perkin Elmer 5000, Govindaraju *et al*, 1994), except for Hg, which was analyzed by cold vapor AAS (Perkin Elmer 5100). The total carbon (TC) and total sulfur (TS) were analyzed by O<sub>2</sub> flow combustion at 1000°C using a LECO SC 144 DR. All of the digestion processes and analyses were quality-checked by the analyses of one sample out of every ten and internal reference materials. The accuracy was within 5% of the certified values and the analytical errors better than 10% rsd for the TE concentrations (Tab. 5.1).

### 5.3. Results and discussion

#### 5.3.1. Characterization of depositional conditions

##### 5.3.1.1. Sedimentary description of the Villerest core

The sedimentological analysis of the 154 cm long core consists of a visual and textural description (Fig. 5.2) in addition to a comparison of the grain-size distribution in the sedimentary layers with the C-M diagram (Passeggi, 1957; 1964; Fig. 5.3).

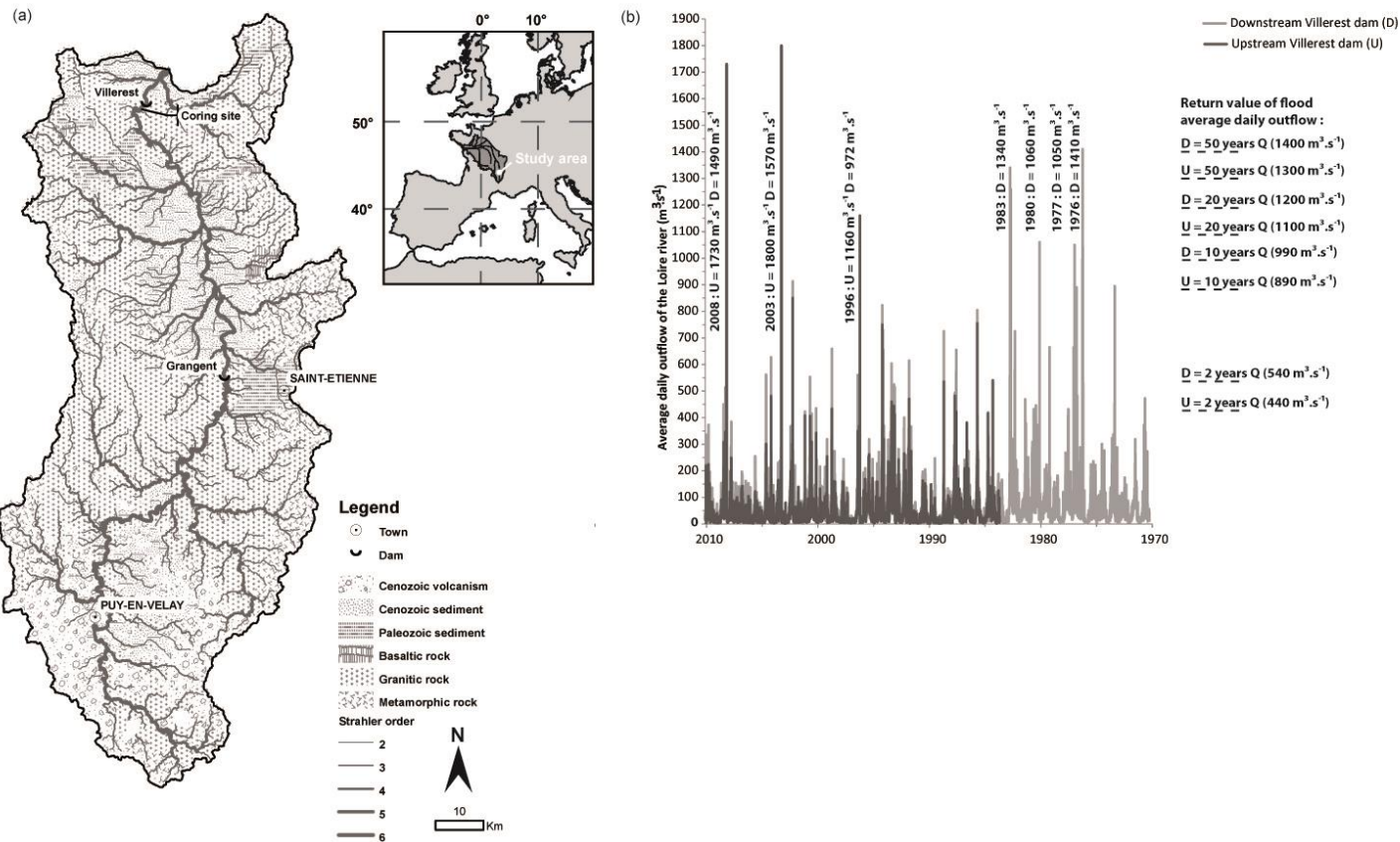


**Fig. 5.1:** **a-** Localization of the studied area, the coring site in the Villerest reservoir, the geology and the 2 main towns (Saint Etienne >500 000 inhabitants; Le Puy en Velay > 60 000 inhabitants); **b-** Daily discharge variations upstream and downstream of the studied dam site since 1970 (data from [www.hydro.eaufrance.fr](http://www.hydro.eaufrance.fr)).

This diagram allows the characterization of the particle depositional conditions according to the ninety-nine percentile ( $D_{99}$ ) and the median grain-size ( $D_{50}$ ) distribution, called the C and M parameters, respectively. In this approach, the higher the C and M values are and the more the grain-size distribution is parallel to the C-M line, the more energetic the depositional environment is. The grain-size distribution of these studied sediments, measured with a laser granulometer, should be considered with caution because of their fine-grained and very poorly sorted texture (Pye and Blott, 2004). Because the grain-size measurement reproducibility was low for  $D_{99}$ ,  $D_{90}$  was used as the C parameter to be more representative. Throughout the entire core, three sedimentary units have been identified:

- The deepest unit 3 (128-154 cm), is also the coarsest unit. It is composed of very coarse silts to fine sands ( $59 < D_{50} < 284 \mu\text{m}$ ) (Fig. 5.2). The percentage of sand ranges from 48% (126-128 cm) to 88% (136-138 cm) with the highest  $D_{90}$  of the entire core (312-632  $\mu\text{m}$ ). According to the Valverde *et al.* study (2013), which defines the

characteristics of stream sediments in the Upper Loire sub-basin ( $D_{50} > 1000 \mu\text{m}$  and  $D_{90} > 1100 \mu\text{m}$ ), and Bravard *et al.*'s (2014) interpretations of the CM image, the grain-size distribution of this sedimentary layer looks like a river bank deposit in a proximal position from the river channel (low variability of  $D_{90}$  compared to  $D_{50}$ , characteristic of the RS segment; Fig. 5.3). Hence, unit 3 can represent the fluvial domain, *i.e.*, sediments deposited in energetic conditions, but they may also have been reworked during the dam construction.

- On the other side, the upper unit 1, from 84 cm up to the surface, corresponds to the finest very poorly sorted particles, mainly silts with clays (73-87% silts, Tab. 5.1). The  $D_{50}$  ranges from 7.3  $\mu\text{m}$  (64-66 cm deep) to 19.8  $\mu\text{m}$  (42-44 cm). Immediately after the core opening, laminated sedimentary layers were visually identified at the 54-84 cm ( $7 < D_{50} < 14 \mu\text{m}$ ); 50-58 cm ( $8 < D_{50} < 12 \mu\text{m}$ ); 19-30 cm ( $10 < D_{50} < 14 \mu\text{m}$ ), except within 22-24 cm; and 0-6 cm depths ( $9 < D_{50} < 10 \mu\text{m}$ ; Fig. 5.2), showing centimeter alternations of lighter and darker bands. In these sedimentary layers, the alternation of sediment colors is not

associated with textural variations. The grain-size distribution of these sequences is not parallel to the C-M line (Fig. 5.3). Therefore, they consist of fine-grained sediments that settled in a lentic environment since the dam began operation in 1984. Organic matter was not characterized, but darker layers should correspond to death biomass depositions after summertime. In addition, well-defined coarser and lighter layers at the 58-64 cm, 30-50 cm and 6-19 cm depths (Fig. 5.2) do not fit in the predefined domain. All of these stacked intervals also present a larger grain-size distribution than the respective unit with a higher sand percentage. They all note various depositional processes. The 6-19 cm level presents vertical grain-size sorting (18.5% down to 8.6% sand with upward coarsening at the beginning until 14 cm deep), whereas the two other coarse levels show a hysteresis in the C-M diagram from fine to coarse grains and back to fine particles (10.0% up to 19.7% of sands with maximum grain size at 60-62 cm and 40-42 cm deep) (Fig. 3).

- Units 1 and 3 limit sharp grain-size transitions at 84 cm and 128 cm deep, which correspond to unit 2's boundaries. The color and textural composition of this sedimentary layer are homogenous. The percentage of silt clearly decreases downcore (from 78 % down to 50%; Tab. 5.1), although the percentage of sand and  $D_{50}$  increases at the same time (up to 48% and to 56  $\mu\text{m}$ , respectively; Fig. 5.2; Tab. 5.1). The grain-size distribution of this sedimentary unit draws a middle domain between the lacustrine and the fluvial domains, which are not described in literature (Fig. 5.3). This can occur during dam water filling when the water level increases progressively. At the bottom of unit 2 (104-128 cm), the archived sediments are clearer and the grain-size distribution of this sedimentary layer presents similarities with the coarsest and lightest sequences of unit 1. Indeed, they are involved in the same domain in the C-M diagram, and the vertical grain-size sorting shows a similar hysteresis (Fig. 5.3.).

Depth (cm)	<sup>137</sup> Cs (2s)		D <sub>50</sub>	Sand (%)	Silt (%)	Clay (%)	Si %	Al %	Ca %	Fe %	K %	Mg %	Mn %	Na %	P %	Ti %	TC %	TS %	Ba ppm	Hf ppm	La ppm	Rb ppm	Sm ppm	Th ppm	U ppm	Zr ppm	As ppm	Bi ppm	Cd ppm	Cr ppm	Cu ppm	Hg ppm	Mo ppm	Ni ppm	Pb ppm	Sb ppm	Sn ppm	W ppm	Zn ppm
	(Bq.kg <sup>-1</sup> )	(μm)	(%)	(%)	(%)	(%)	(%)	(%)	(%)	(%)	(%)	(%)	(%)	(%)	(%)	(%)	(%)	(%)	(ppm)	(ppm)	(ppm)	(ppm)	(ppm)	(ppm)	(ppm)	(ppm)	(ppm)	(ppm)	(ppm)	(ppm)	(ppm)	(ppm)	(ppm)	(ppm)	(ppm)	(ppm)			
0-2	10±0,9	10,0	7,3	84,8	7,9		16,72	8,44	0,64	4,91	2,27	1,04	0,09	0,48	0,28	0,50	5,58	0,27	531	3,2	34,8	191,3	5,72	13,1	7,6	114,8	44,7	2,1	1,7	116	52,3	0,22	0,9	39,4	87,8	1,0	18	5,6	217
2-4		9,5	5,0	86,9	8,1		16,74	9,42	0,89	5,05	2,59	1,24	0,09	0,68	0,21	0,65	3,70	0,11	589	3,8	38,0	212,8	6,33	13,8	7,5	139,3	29,4	1,9	1,5	130	45,3	0,19	0,8	42,0	72,7	0,6	15	5,5	215
4-6		11,0	5,9	87,0	7,1		16,90	9,31	0,89	4,83	2,61	1,21	0,09	0,75	0,21	0,65	3,99	0,07	573	4,7	39,8	207,1	6,62	15,8	7,3	174,7	27,5	2,2	1,5	130	50,2	0,23	0,8	41,3	69,0	0,7	18	6,4	206
6-8		12,7	8,6	85,4	5,9		16,57	9,42	1,11	5,07	2,66	1,30	0,08	0,76	0,20	0,74	3,22	0,08	588	4,0	36,8	222,5	6,19	12,4	6,6	151,9	21,5	1,3	0,9	144	41,6	0,12	0,8	46,9	51,1	0,4	13	4,8	168
8-10		15,8	11,5	83,7	4,8		16,87	9,17	1,00	4,91	2,56	1,22	0,09	0,76	0,20	0,72	4,51	0,07	594	4,7	37,9	214,9	6,30	13,4	7,1	171,1	28,8	2,3	2,0	130	54,9	0,26	1,1	43,8	72,5	0,8	20	6,6	221
10-12	15±0,8	18,6	15,2	80,4	4,3		16,87	8,81	0,91	4,58	2,50	1,16	0,09	0,79	0,21	0,66	5,09	0,1	573	5,8	38,7	202,7	6,63	15,3	7,8	191,1	28,8	2,3	2,0	130	54,9	0,26	1,1	43,8	72,5	0,8	20	6,6	221
12-14		20,9	17,5	78,6	3,9		17,42	8,51	0,79	4,15	2,51	1,05	0,09	0,88	0,23	0,58	5,23	0,11	597	6,5	44,3	183,0	7,27	19,8	8,3	236,2	36,9	3,7	2,6	116	63,3	0,43	1,2	41,6	84,8	1,2	22	8,3	257
14-16		18,4	16,6	78,8	4,6		17,27	8,22	0,75	4,00	2,42	0,99	0,09	0,88	0,23	0,54	5,56	0,11	608	6,8	45,5	176,7	7,46	20,0	8,2	229,3	38,2	4,3	2,1	103	66,2	0,37	1,2	38,6	88,3	1,2	23	8,1	269
16-19		15,5	18,5	75,4	6,0		17,60	8,72	0,72	4,29	2,45	1,04	0,10	0,81	0,25	0,55	5,41	0,12	626	5,8	45,2	187,3	7,40	21,5	8,7	211,5	41,4	4,3	2,2	103	61,7	0,40	1,1	37,6	92,9	1,2	21	8,5	254
19-20		14,3	15,5	79,0	5,5		n.d.	n.d.	n.d.	n.d.	n.d.	n.d.	n.d.	n.d.	n.d.	n.d.	n.d.	n.d.	n.d.	n.d.	n.d.	n.d.	n.d.	n.d.	n.d.	n.d.	n.d.	n.d.	n.d.	n.d.	n.d.	n.d.	n.d.	n.d.					
20-22	14±1,6	16,9	22,6	72,7	4,7		16,10	8,81	0,69	4,89	2,24	1,06	0,12	0,50	0,35	0,50	<d.l.	<d.l.	567	3,4	38,8	183,4	6,37	16,6	8,0	110,8	42,2	3,7	2,1	123	55,7	0,29	0,8	40,9	101,8	1,0	17	6,1	243
22-24		13,4	17,7	76,6	5,7		17,10	8,33	0,69	4,82	2,26	1,04	0,11	0,56	0,36	0,50	5,94	0,25	561	3,9	39,7	179,2	6,57	17,4	9,1	133,2	51,1	3,2	1,7	116	59,2	0,29	0,9	40,0	96,2	1,0	15	6,2	227
24-26	12±0,9	10,1	5,9	86,5	7,6		17,38	9,21	0,70	4,97	2,51	1,15	0,10	0,59	0,27	0,56	4,55	0,24	598	3,6	39,6	200,6	6,50	17,4	8,3	128,1	51,4	2,4	1,8	123	55,1	0,28	1,0	43,1	86,8	1,0	17	6,4	215
26-28		11,0	9,5	83,4	7,1		17,30	9,62	0,76	4,80	2,70	1,24	0,09	0,66	0,19	0,61	3,79	0,14	618	4,1	40,2	213,0	6,59	18,6	8,1	141,5	40,6	2,1	1,7	123	52,6	0,30	0,8	43,6	79,9	1,0	17	6,6	214
28-30		9,7	4,2	87,4	8,5		17,27	9,69	0,97	5,02	2,79	1,38	0,09	0,70	0,20	0,67	3,30	0,09	603	4,4	39,6	248,2	6,48	16,3	8,2	150,4	35,1	1,6	1,5	123	50,4	0,25	0,8	46,7	72,0	0,7	19	6,7	204
30-32	12±1,0	14,7	13,0	81,7	5,3		17,22	9,59	1,06	4,86	2,86	1,40	0,08	0,74	0,17	0,68	3,01	0,09	588	4,5	38,8	252,4	6,67	16,0	7,5	135,3	31,9	1,5	1,1	123	44,6	0,22	0,9	46,3	61,1	0,7	20	6,3	169
32-34		14,9	11,7	82,7	5,6		17,17	9,61	1,04	5,07	2,80	1,37	0,09	0,82	0,21	0,71	4,36	0,11	656	5,5	43,7	239,4	7,20	17,5	8,0	193,8	33,1	1,7	1,9	144	54,5	0,34	1,1	49,9	73,9	0,9	24	7,5	209
34-36	16±1,0	15,8	12,0	82,9	5,1		17,85	9,33	0,99	4,82	2,79	1,31	0,09	0,86	0,21	0,68	4,47	0,11	658	6,3	44,2	233,1	7,42	19,2	8,5	212,0	36,6	1,9	2,6	144	63,5	0,49	1,2	54,7	82,9	1,0	26	8,9	247
36-38		16,7	13,4	81,6	5,0		17,54	8,89	0,91	4,48	2,66	1,19	0,09	0,85	0,22	0,62	4,76	0,13	665	6,9	45,9	223,2	7,70	23,0	9,0	236,9	38,9	1,9	2,7	151	70,2	0,48	1,4	55,5	90,0	1,1	26	9,5	278
38-40		19,9	17,6	78,4	4,1		18,66	8,85	0,86	4,38	2,68	1,13	0,11	0,91	0,28	0,59	5,07	0,13	682	8,2	52,4	217,6	8,45	23,7	9,7	127,5	41,3	1,8	3,2	151	73,5	0,53	1,5	56,8	97,2	1,3	27	10,2	293
40-42	15±1,0	21,2	19,7	76,3	4,0		18,39	8,28	0,81	3,96	2,56	1,02	0,10	0,93	0,26	0,55	4,68	0,11	659	8,9	53,7	215,4	8,73	25,7	9,7	297,4	38,3	1,8	2,9	137	69,2	0,47	1,4	52,8	89,4	1,1	23	9,6	275
42-44		19,8	17,9	77,7	4,4		20,61	8,42	0,85	3,61	2,87	0,96	0,09	1,16	0,24	0,56	3,47	0,09	702	13,6	70,2	211,8	11,18	35,2	10,6	471,9	31,2	1,3	2,2	123	55,3	0,38	1,1	44,9	74,5	1,1	20	9,0	229
44-46		18,5	14,3	81,6	4,1		18,66	8,69	0,83	4,20	2,58	1,06	0,11	0,91	0,29	0,58	5,00	0,13	677	7,8	51,7	211,2	8,45	24,8	9,6	277,7	38,1	1,6	2,8	144	76,4	0,46	1,5	54,2	93,7	1,2	25	10,8	289
46-48		12,2	10,0	83,6	6,3		17,79	7,80	0,76	4,30	2,52	1,09	0,09	0,75	0,25	0,59	5,35	0,13	692	6,7	46,9	222,0	7,71	21,6	9,5	227,0	43,3	1,8	3,2	144	83,9	0,53	1,5	56,9	103,4	1,2	25	10,3	326
48-50		12,4	12,9	81,0	6,1		17,29	8,67	0,66	4,43	2,43	1,07	0,10	0,59	0,28	0,53	5,17	0,12	633	4,4	41,7	227,1	6,56	19,3	9,1	150,9	44,1	1,6	2,2	116	75,5	0,42	<d.l.	53,5	95,8	1,1	19	8,0	291
50-52	13±0,9	9,0	14,5	75,1	10,4		17,01	7,86	0,61	4,63	2,06	0,95	0,12	0,42	0,41	0,46	<d.l.	<d.l.	554	3,5	37,4	212,9	5,99	15,9	9,5	113,0	46,5	1,3	1,3	96	68,9	0,27	1,1	51,8	95,3	1,1	15	6,1	229
52-54		10,0	11,6	80,4	8,0		16,47	9,52	0,62	4,86	2,50	1,14	0,10	0,49	0,30	0,52	4,36	0,14	664	3,8	41,6	255,9	6,65	18,3	8,9	125,7	37,9	1,4	1,6	109	57,5	0,27	1,0	47,2	90,2	1,2	17	6,7	243
54-56		12,3	14,9	79,3	5,8		16,99	9,14	0,69	4,85	2,57	1,12	0,10	0,53	0,32	0,54	4,15	0,18	646	4,6	42,9	257,2	6,79	18,5	9,3	149,1	42,7	1,5	1,5	123	60,9	0,23	0,9	52,2	90,1	1,1	16	6,9	227
56-58		7,8	6,8	82,9	10,3		16,71	8,90	0,74	4,98	2,44	1,10	0,12	0,54	0,38	0,56	4,74	0,23	651	3,8	42,8	237,6	6,88	17,9	9,2	139,3	49,3	1,											

Depth (cm)	<sup>137</sup> Cs (2s) (Bq.kg <sup>-1</sup> )	D <sub>50</sub> (μm)	Sand (%)	Silt (%)	Clay (%)	Si %	Al %	Ca %	Fe %	K %	Mg %	Mn %	Na %	P %	Ti %	TC %	TS %	Ba ppm	Hf ppm	La ppm	Rb ppm	Sm ppm	Th ppm	U ppm	Zr ppm	As ppm	Bi ppm	Cd ppm	Cr ppm	Cu ppm	Hg ppm	Mo ppm	Ni ppm	Pb ppm	Sb ppm	Sn ppm	W ppm	Zn ppm
84-86	9±0,8	44,1	40,2	56,0	3,8	19,69	8,11	0,91	3,88	2,85	1,05	0,07	1,05	0,17	0,52	4,27	0,24	707	10,5	59,1	217,6	10,03	28,4	10,3	371,3	39,8	2,2	3,1	144	46,1	0,36	1,3	55,7	69,7	1,0	33	11,8	194
86-88		39,9	36,9	58,8	4,3	20,15	8,37	0,95	3,60	3,02	1,09	0,06	1,13	0,14	0,53	3,90	0,09	708	10,9	59,5	224,6	10,09	30,7	9,6	379,7	28,7	1,9	1,7	123	38,1	0,36	1,1	40,8	58,9	0,8	27	9,6	152
88-90		50,7	43,5	52,7	3,8	20,85	8,09	0,94	3,41	3,08	1,01	0,05	1,25	0,14	0,50	3,28	0,07	729	10,9	59,8	219,1	10,28	31,9	9,0	387,5	25,9	1,6	1,8	130	33,2	0,22	1,2	37,9	53,9	1,1	23	9,4	149
90-92	4±0,4	55,9	46,4	50,2	3,4	20,84	7,95	0,94	3,32	3,14	0,99	0,05	1,25	0,14	0,47	2,99	0,06	754	10,5	57,2	219,4	9,42	29,8	9,0	364,2	26,2	1,7	1,9	116	32,6	0,20	1,1	39,5	53,0	0,9	31	9,3	156
92-94		27,1	25,5	69,8	4,7	20,83	7,78	0,94	3,24	3,07	0,99	0,05	1,24	0,13	0,46	3,78	0,08	727	9,9	54,4	222,6	9,33	29,5	8,8	347,7	24,8	1,6	1,7	116	30,5	0,18	1,2	37,7	48,9	0,8	19	7,9	146
94-96		25,8	24,8	70,1	5,1	19,04	8,66	1,05	4,05	2,99	1,19	0,08	0,98	0,15	0,57	3,93	0,09	733	8,9	52,2	233,9	8,68	25,6	9,4	307,1	33,0	2,6	2,7	151	42,6	0,33	1,2	43,4	65,8	0,8	29	9,7	178
96-98		28,7	28,4	66,7	4,9	19,03	8,67	1,06	4,19	2,98	1,21	0,08	0,96	0,16	0,59	3,91	0,08	729	8,6	50,2	236,2	8,65	25,4	9,5	318,4	34,5	2,5	3,0	157	46,1	0,37	1,2	46,7	68,5	0,9	31	9,7	188
98-100		54,7	45,2	50,8	3,9	20,37	8,16	0,94	3,51	3,00	1,01	0,06	1,16	0,14	0,54	3,93	0,07	758	11,2	61,8	225,3	10,10	30,7	9,6	397,7	30,3	2,0	2,4	137	37,2	0,27	1,2	42,4	61,9	1,0	23	9,0	170
100-102	6±0,6	42,7	39,5	56,5	3,9	21,26	7,79	0,91	3,22	2,97	0,92	0,06	1,31	0,16	0,50	3,02	0,06	675	11,6	68,7	196,9	11,39	33,8	10,1	401,3	31,2	1,5	3,2	144	36,0	0,41	1,5	48,0	60,2	1,1	19	8,2	194
102-104		26,0	26,2	69,2	4,6	21,14	8,01	0,86	3,30	2,95	0,93	0,07	1,26	0,17	0,47	3,83	0,07	661	9,0	57,4	201,3	9,35	27,4	8,8	335,0	31,5	1,7	4,7	151	40,1	0,57	1,0	51,3	62,3	1,0	22	8,6	217
104-106-		20,8	19,0	76,1	4,9	18,74	8,67	1,04	4,24	2,91	1,21	0,09	0,92	0,16	0,59	3,60	0,06	636	8,2	47,0	224,7	8,11	23,3	8,8	281,4	34,7	2,5	3,0	164	45,8	0,46	1,2	52,4	72,0	1,0	28	8,3	198
106-108		20,5	19,0	76,1	4,8	18,14	8,72	1,09	4,52	2,84	1,25	0,11	0,88	0,19	0,60	4,76	0,07	671	7,6	46,6	223,2	8,03	23,0	9,1	253,9	43,2	3,2	5,7	212	61,7	0,49	1,5	64,0	90,0	1,5	36	10,2	267
108-110		33,3	34,7	61,5	3,8	18,46	8,60	1,02	4,26	2,82	1,18	0,10	0,96	0,20	0,58	4,52	0,07	655	7,9	49,3	216,9	8,46	25,5	9,2	274,0	39,9	2,8	6,0	198	60,3	0,59	1,6	67,8	88,3	1,4	30	9,0	275
110-112	9±0,5	31,3	32,0	64,2	3,8	19,27	8,34	0,96	3,96	2,81	1,08	0,09	1,15	0,21	0,55	5,16	0,08	704	9,2	51,1	206,0	9,02	25,6	9,0	322,3	38,5	2,6	5,6	212	59,7	0,55	1,8	71,8	87,1	1,7	29	10,1	275
112-114		25,3	25,9	70,0	4,1	17,44	8,26	0,94	4,41	2,61	1,07	0,15	0,91	0,31	0,55	6,74	0,09	743	7,7	50,6	207,9	8,56	24,5	10,3	259,7	56,3	3,5	13,2	301	92,3	0,61	2,1	104,3	125,1	1,6	37	12,4	474
114-116		18,0	13,4	81,8	4,8	18,40	8,32	1,04	4,44	2,75	1,13	0,16	0,96	0,26	0,56	5,23	0,11	707	8,9	49,4	215,6	8,38	24,1	9,4	305,6	40,8	3,1	10,3	260	77,4	0,50	2,0	100,4	106,3	1,5	40	11,8	386
116-118		15,4	11,4	83,0	5,5	18,16	8,34	0,95	4,48	2,68	1,10	0,17	0,93	0,30	0,55	5,33	0,12	740	8,7	52,4	213,4	9,05	24,7	9,9	298,9	45,8	3,6	14,6	281	92,7	0,64	2,4	114,8	125,1	1,5	44	14,5	474
118-120		15,8	12,5	82,6	4,9	17,06	8,91	0,90	4,80	2,56	1,21	0,16	0,75	0,31	0,56	5,79	0,14	749	5,6	43,1	222,6	7,51	19,9	9,5	201,4	56,3	4,2	18,4	328	113,5	0,79	2,8	155,7	147,9	1,9	53	15,0	588
120-122	8±0,9	16,7	13,3	82,0	4,7	17,69	8,54	0,80	4,55	2,43	1,13	0,16	0,72	0,33	0,55	< d.l.	< d.l.	655	6,1	44,2	212,5	7,72	20,0	8,7	219,8	43,5	3,3	13,2	267	86,6	0,51	1,7	121,1	125,1	1,3	37	11,1	454
122-124		19,8	16,9	79,0	4,1	17,10	8,64	0,76	4,58	2,43	1,15	0,17	0,68	0,31	0,54	5,50	0,12	645	5,4	43,1	220,9	7,58	20,6	8,8	193,3	46,1	3,2	14,1	267	92,1	0,58	1,6	121,6	127,0	1,1	38	10,5	463
124-126		19,4	17,3	77,9	4,8	17,46	8,58	0,79	4,61	2,39	1,11	0,17	0,72	0,35	0,55	5,23	0,18	647	6,1	45,8	213,9	7,88	22,5	9,1	209,6	48,6	3,4	13,7	267	85,7	0,49	1,6	167,3	132,3	1,3	35	10,3	461
126-128		59,2	48,9	48,0	3,1	17,42	8,45	0,84	4,28	2,41	1,08	0,10	0,80	0,26	0,57	5,43	0,1	711	6,5	44,1	209,0	7,68	21,5	10,8	214,4	52,4	3,4	13,0	335	81,0	0,49	2,1	145,2	131,1	1,4	37	9,8	460
128-130		140,9	69,8	28,2	2,0	18,75	8,99	0,93	4,50	2,76	1,18	0,09	0,96	0,21	0,58	3,99	0,08	753	7,7	49,4	211,4	8,46	23,6	10,4	263,2	45,4	3,8	5,6	287	65,6	0,47	< d.l.	98,7	120,8	1,9	33	9,8	321
130-133	4±0,6	120,9	66,2	31,7	2,0	18,42	9,39	0,85	4,97	2,81	1,27	0,10	0,81	0,24	0,55	< d.l.	< d.l.	710	6,2	47,3	228,5	7,90	23,6	10,0	218,3	36,9	4,1	4,4	267	55,8	0,30	1,9	97,5	111,5	1,1	32	9,9	264
133-134		119,9	67,6	30,3	2,1	17,68	9,64	0,83	5,27	2,80	1,32	0,11	0,64	0,24	0,60	3,13	0,04	690	8,6	56,4	237,7	9,56	30,1	10,8	284,4	21,8	1,9	2,4	274	30,8	0,32	< d.l.	56,4	57,5	0,9	35	9,6	166
134-136		100,4	61,4	36,2	2,3	18,46	9,20	0,88	4,85	2,77	1,23	0,10	0,82	0,26	0,59	5,33	0,04	721	9,5	58,2	227,3	9,74	30,0	11,2	323,5	39,8	3,6	3,7	267	50,7	0,47	< d.l.	96,4	98,6	1,4	33	10,4	261
136-138		284,4	88,4	10,8	0,8	17,45	9,75	0,87	5,14	2,77	1,30	0,10	0,68	0,23	0,60	4,51	0,07	745	7,3	50,5	230,7	8,52	25,6	10,3	261,8	51,4	4,1	7,1	335	62,2	0,46	< d.l.	108,4	116,1	1,5	40	13,0	335
138-140		179,8	78,2	20,4	1,3	18,18	10,13	0,85	5,52	3,00	1,44	0,12	0,62	0,23	0,55	3,70	0,06	776	6,3	46,9	241,0	7,94	23,9	10,5	207,7	49,3	5,0	4,4	308	76,0	0,41	< d.l.	91,2	123,0	1,3	42	10,8	377
140-142	4±0,3	236,7	83,2	15,6	1,2	18,02	9,78	0,90	5,42	2,92	1,34	0,12	0,70	0,24	0,61	4,00	0,1	865	7,8	52,7	235,4	8,78	25,9	11,1	278,1	55,9	4,7	5,3	308	51,4	0,33	< d.l.	157,6	109,5	1,3	40	11,2	291
142-144		155,4	71,2	27,0	1,8	17,36	9,65	0,92	5,22	2,75	1,																											

### 5.3.1.2. Stratigraphic evidence of flood sequences

A detailed sedimentological analysis of the upper unit of the core allows us to enhance the sediment layers that settled in a lacustrine context and possibly came from events with important sedimentary loads. The coarser and lighter layers at the 58-64 cm, 30-50 cm and 6-19 cm depths look like turbidites, as they are described in lakes (Sturm and Matter, 1978; Giovanoli, 1990) and reservoirs

(Ambers, 2001), when associated with important flood events and massive material transport. During important discharge events entering the reservoir, the riverine sediment load is transported according to the grain-size of the particles, river flow density and water density stratification. The coarsest sediments are mainly deposited in the reservoir delta and the residual flow generates fine sediment-laden under- and overflows deposited further in the reservoir floor.

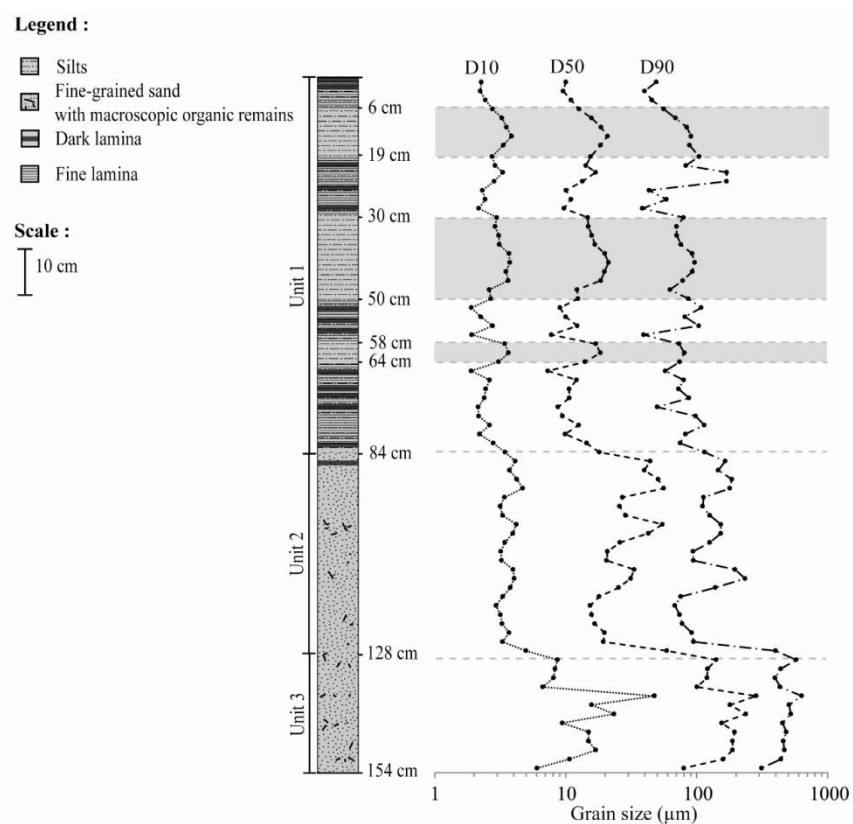


**Fig. 5.2:** Sedimentary log with grain-size parameters ( $D_{10}$ ,  $D_{50}$  and  $D_{90}$ ) in each 2-cm thick layer.

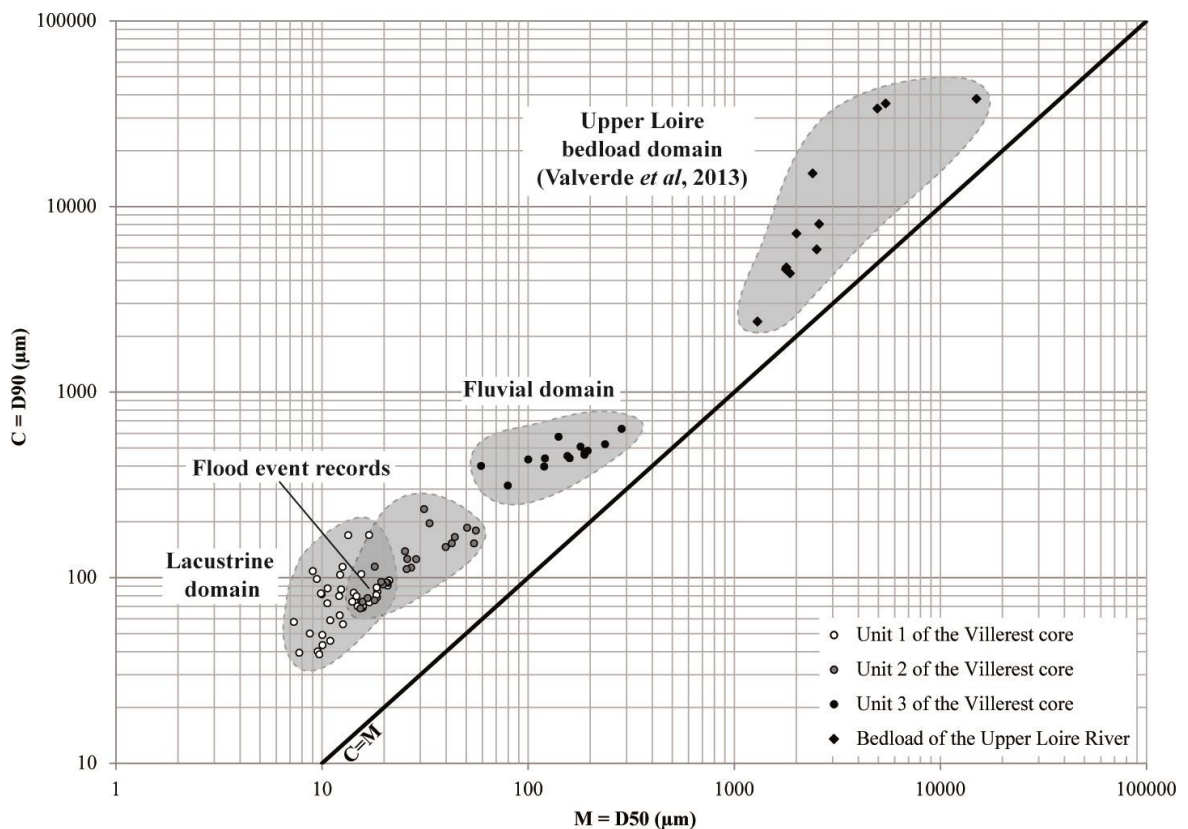


**Fig.5.3:** The C-M diagram for the 3 core units and associated depositional condition domains according to Passegia (1957, 1964).

For these turbidite-like layers, well-marked  $D_{50}$  and  $D_{90}$  patterns in the C-M diagram (total grain-size hysteresis for the 58- to 64-cm and 30- to 50-cm-deep layers and a partial hysteresis for the 6- to 19-cm sequence) can be associated with underflow-related depositional processes (Giovanoli, 1990; Gilli *et al.*, 2013). These flood sequences would correspond to the most important events since the dam began operation in 1984, *i.e.*, the 58- to 64-cm interval to the 1996 flood, the 30- to 50-cm interval to the 2003 flood and the 6- to 19-cm interval to the 2008 flood. In particular, this 2008 flood event was

not managed like the two previous ones. The dam gates usually open gradually to regulate downstream runoff according to the upstream flood hydrograph. However, in 2008, the reservoir water level was already high before the flood event and the dam gates were opened the same time the flood began (H. Xhaard, EPL, pers.com.). This dam management may be related to the incomplete hysteresis in the 6- to 19-cm interval ( $D_{50}$  and  $D_{90}$  are only correlated up to 14 cm deep in a decreasing trend, Fig. 5.2). In unit 2, which was deposited during the reservoir water infilling, the 104- to 128-cm interval could

correspond to the major 1983 flood with a greater than 20-year flood average daily outflow.

### **5.3.2. Age model definition**

#### **5.3.2.1. $^{137}\text{Cs}$ dating**

The  $^{137}\text{Cs}$  activity shows a well-marked maximum ( $124.2 \pm 1.4 \text{ Bq}.\text{kg}^{-1}$ ) at 80-82 cm (Tab. 5.1). This  $^{137}\text{Cs}$  peak is preceded by  $\gamma$  activities between  $5.6 \pm 0.7$  and  $19.6 \pm 1.2 \text{ Bq}.\text{kg}^{-1}$ . The bottom of the lacustrine sedimentary record at 82-84 cm is assumed to be synchronous with the Villerest dam's full operation beginning in 1984. In these circumstances, the  $^{137}\text{Cs}$  peak can correspond to the C-NPPD fallout in 1986. The detection of some  $^{137}\text{Cs}$  in units 2 and 3, ranging between  $4.1 \pm 0.3$  and  $9.2 \pm 0.5 \text{ Bq}.\text{kg}^{-1}$  (Tab. 5.1), indicates that these deposits belong to the post-1950 period. Nonetheless, the post-depositional mobilization of the  $^{137}\text{Cs}$  during diagenesis and the resulting down migration of this radionuclide in the sedimentary column could disturb the dating (Smith *et al*, 2000; Benoit and Rozan, 2001). In particular, unit 2 is associated with the reservoir water infilling. According to the dam managers, the water infilling period lasted from the end of the dam's construction in 1983 to 1984. The heavy aggradation rate of this

unit should reflect important local sedimentary inputs in the downstream part of the reservoir during the water filling operation. Two hypotheses can be formed regarding the sediment origin in unit 3:

- (i) these sediments were part of a former river bank of the Loire River before the dam's construction, and the absence of the NWT maximum fallout (1964  $^{137}\text{Cs}$  peak) is then related to sediments younger than 1964;
- (ii) or the sediments from unit 3 could have been partly reworked during the dam construction starting in the late 1970s. The lack of the 1964  $^{137}\text{Cs}$  peak would then be due to a sediment hiatus in the bottom unit 3 as parts of these channel sediments were scoured and exported during the dam construction. The sediments from unit 3 could not have been more precisely dated.

#### **5.3.2.2 Age model calculation**

To take into account the temporal variations in the sedimentation processes, the flood events' influence on sedimentary infill and the compaction

variations with depth during coring, an age model was precisely built on the calculation of mass accumulation rates (MAR,  $\text{kg} \cdot \text{m}^{-2} \cdot \text{y}^{-1}$ ; Van Metre *et al*, 2004) using the two absolute depth-date markers and flood markers.

This age model is first based on the dry mass parameter (DM;  $\text{kg} \cdot \text{m}^{-2}$ ), calculated as follows:

$$DM = (1-n) \cdot DS \cdot Th \quad (\text{equation 5.1})$$

with  $n$  as the porosity (%; the volume of water contained in a well-known volume of fresh sediments),  $DS$  as the apparent density of the sediments ( $\text{kg} \cdot \text{m}^{-3}$ ; the dry mass material contained in the defined volume) and  $Th$  as the thickness of the sampled layer (m).

The MAR is then expressed between each date-bounded interval by dividing the cumulative dry mass (cum) with the time interval (TI; year) as follows:

$$MAR = \text{cum}/\text{TI} \quad (\text{equation 5.2}).$$

Therefore, the corresponding age of the sediment (Date) at a level  $i$  is calculated as follows from the top of the core (= coring date; 2010 in the study case) to the first time marker:

$$Date_i = \text{coring date} - (\text{cum}_i/MAR) \quad (\text{equation 5.3})$$

For sediment layers  $j$  older than the first time marker  $i$ , equation 4 is then applied:

$$Date_j = \text{marker date}_i - (\text{cum}_j - \text{cum}_i)/MAR_j \quad (\text{equation 5.4})$$

The cumulative dry mass slope varies according to the depth from  $1.9 \text{ kg} \cdot \text{m}^{-2} \cdot \text{cm}^{-1}$  in unit 1 to  $4.2 \text{ kg} \cdot \text{m}^{-2} \cdot \text{cm}^{-1}$  in unit 2 and  $8.0 \text{ kg} \cdot \text{m}^{-2} \cdot \text{cm}^{-1}$  in unit 3 (Fig. 5.4). These variations correspond to the 3 aforementioned sediment units. In particular, unit 1 shows light variations in the cumulative dry mass slope associated with the 3 identified major floods in the sediment sequence. The MAR was then adjusted in the upper unit 1:

- (i) when considering the whole unit 1 between the 1984 and 2010 depth-date markers, the MAR reaches  $5.8 \text{ kg} \cdot \text{m}^{-2} \cdot \text{y}^{-1}$ ;
- (ii) when taking into account each flood sequence (1996, 2003 and 2008) as a depth-date marker, the MAR fluctuates between 2.0 and  $3.0 \text{ kg} \cdot \text{m}^{-2} \cdot \text{y}^{-1}$  (Fig. 5.4).

These three flood events highly contribute to the sediment budget as they

correspond to 43% of the settled sediments since the beginning of the dam's operation (total of  $151.4 \text{ kg.m}^{-2}$  of trapped sediments, calculated by cumulating DM over unit 1) with 8.3, 41.0 and  $16.3 \text{ kg.m}^{-2}$  of material, respectively, instantly deposited (5.5, 27.1 and 10.8% of the total sedimentary infill since 1984). Such an influence of large flood events on the aggradation rate has been highlighted for flood-control reservoirs built in a mountain context (low-order stream, steep slope and storm influenced climate, Ambers, 2001), but never for high-order stream draining large watersheds as in the studied reservoir.

### **5.3.3. Temporal dynamics of the trace element contaminations**

#### **5.3.3.1. Influence of flood events in the registered enriched TE trends**

The sedimentological analysis of the depositional conditions highlights the non-linear aggradation rate during the sedimentary infilling of the Villerest reservoir caused by flood event deposits. According to the detailed age model, the temporal variations in the trace element contents could then be described in the upper unit of the core. In a sedimentary archive, the trace element concentrations can vary with depth by several orders of

magnitude according to the temporal variations in both natural and anthropogenic inputs and, to a lesser extent, by chemical remobilization processes. Enrichment factors (EF) were chosen to describe the temporal dynamics of selected trace elements presenting an anthropogenic influence in the studied sediment core. They were calculated in the  $<63 \mu\text{m}$  fraction using the natural geochemical reference of the entire Loire basin (Grosbois *et al*, 2012; Tab. 5.1).

Trace elements such as *Ba*, *La*, *Th*, *Hf*, *Sm*, *U* and *Zr* present EF close to 1. These trace elements are usually considered as tracers of detrital sources as they are specifically associated with mineral hosts. *Zirconium* and *Hf* can be enriched in sediments containing zircons, *barium* in the presence of barite, and *rare earth elements* in phosphates and Ti-bearing heavy minerals (Dill, 2010). Some other trace elements such as *Cu*, *Sb*, *Sn*, *Pb* and *Zn*, which are potentially associated with diffuse and/or local anthropogenic sources (*i.e.*, Kabata-Pendias, 2000; Pacyna and Pacyna, 2001; Callender, 2003), present a light anthropogenic influence in the studied sediments as their EFs range from 2 to 4. A temporal

decline is not clearly expressed, and flood sequences are seemingly more impacted than others (Tab. 5.1). The most enriched trace elements ( $EF > 6$ ) in the studied area are *Bi*, *Cd* and *Hg*. Even if these trace elements are always

enriched throughout unit 1, their EF values appear higher in flood sequences, similar to *Cu*, *Sb*, *Sn*, *Pb* and *Zn* (Fig. 5.5; Tab. 5.1), with enrichment maxima up to 6.8 for *Bi*, 15.5 for *Cd* and 34.2 for *Hg*.

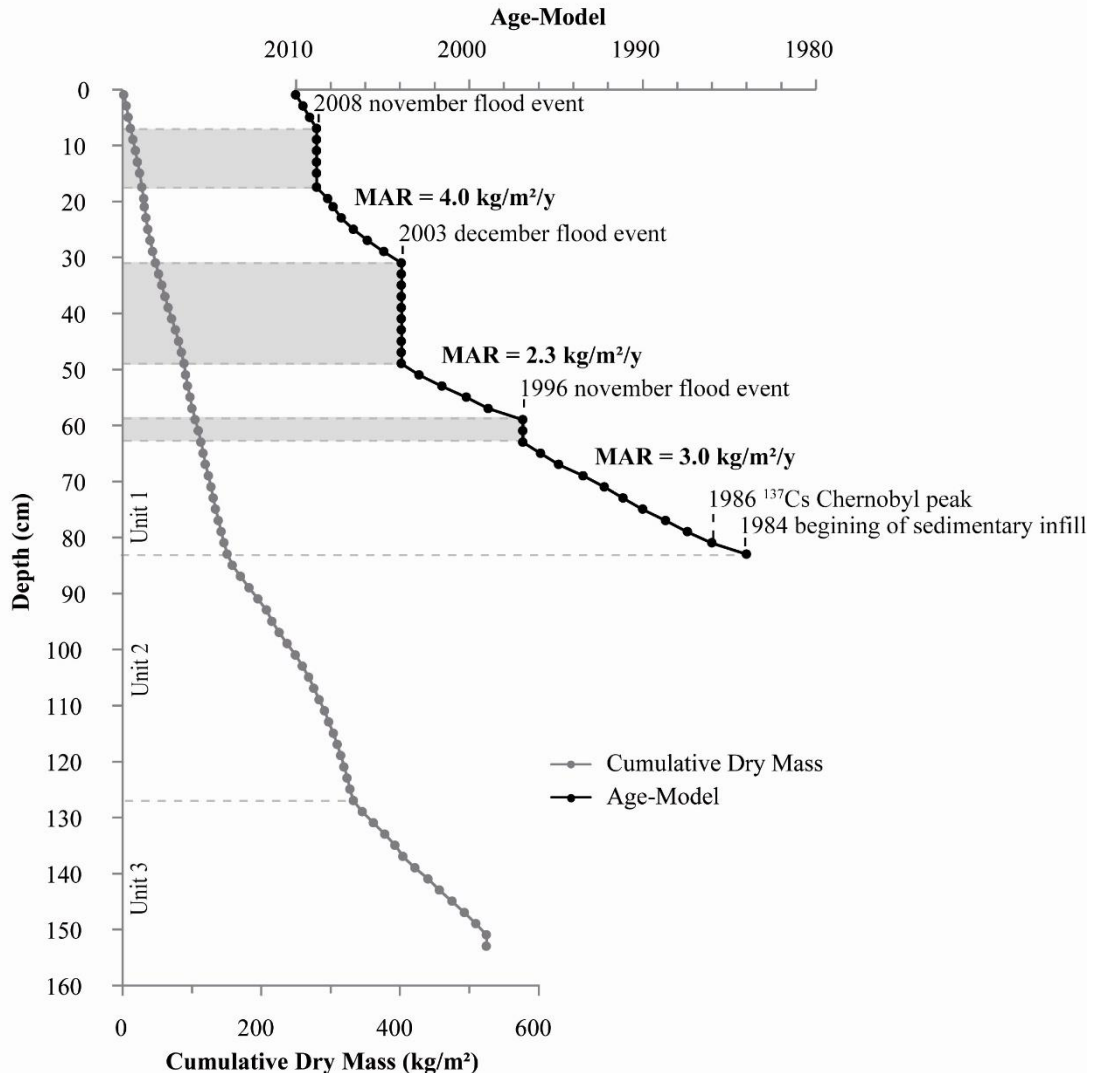


**Fig. 5.4:** The age model with the cumulative dry mass in the 3 sedimentary units and the mass accumulation rates in unit 1 from the core.

These flood events carry solid trace element-rich materials provided by various natural (*Ba, Hf, La, Sm, Th, U, Zr*) and anthropogenic sources. The temporal dynamics of the TE concentrations depend on the relative importance between mechanisms such as coarse non-impacted particle dilution, trace element chemical remobilization and anthropogenic metal sources mobilized during a flood event. In the studied flood sequences, the most enriched trace elements are *Bi, Cd* and *Hg*, and the flood periods represent the highest levels of contamination throughout the entire 1984-2010 period. Hence, additional anthropogenic sources were solicited or enhanced during these specific hydrological events. This type of enrichment maximum associated with particle transport during a flood event has been already observed for suspended matter fractions in Coynel *et al.* (2007) and for sediment archives in Babek *et al.* (2011), for instance.

In geochemical studies, age models are usually conducted with continuous sedimentation rates (*e.g., Grousset *et al.*, 1999; Audry *et al.*, 2004; Le Cloarec *et al.*, 2011; Grosbois *et al.*, 2012*

definition of the age model induces large differences. The 2 absolute depth-date markers available in this study (1986 for the 80-82 cm deep layer and 2010 for the 0-2 cm deep layer) allow us to calculate a linear sedimentation rate equal to  $3.4 \text{ cm.y}^{-1}$ . With this first age model, the flood sequences at the 58-64 cm, 30-50 cm and 6-19 cm depths are wrongly dated to the early 1990s, 1995-2001 and 2005-2009 periods, respectively. When considering this continuous sedimentation rate, the flood sequences are also wrongly associated with highly impacted periods (Fig. 5.5).

### 5.3.3.2. Chemical characteristics of detrital material inputs during flood events

The high analysis resolution for the 2003 ( $n=10$  analyzed 2-cm thick layers) and 2008 ( $n=6$ ) flood events was enough to adequately describe the chemical variations during such a hydrological event record in the studied core. Such an approach was not made for the 1996 flood record as only three 2 cm-thick sediment layers were made, nor for the 1983 flood as this flood occurred during the dam's water filling conditions.

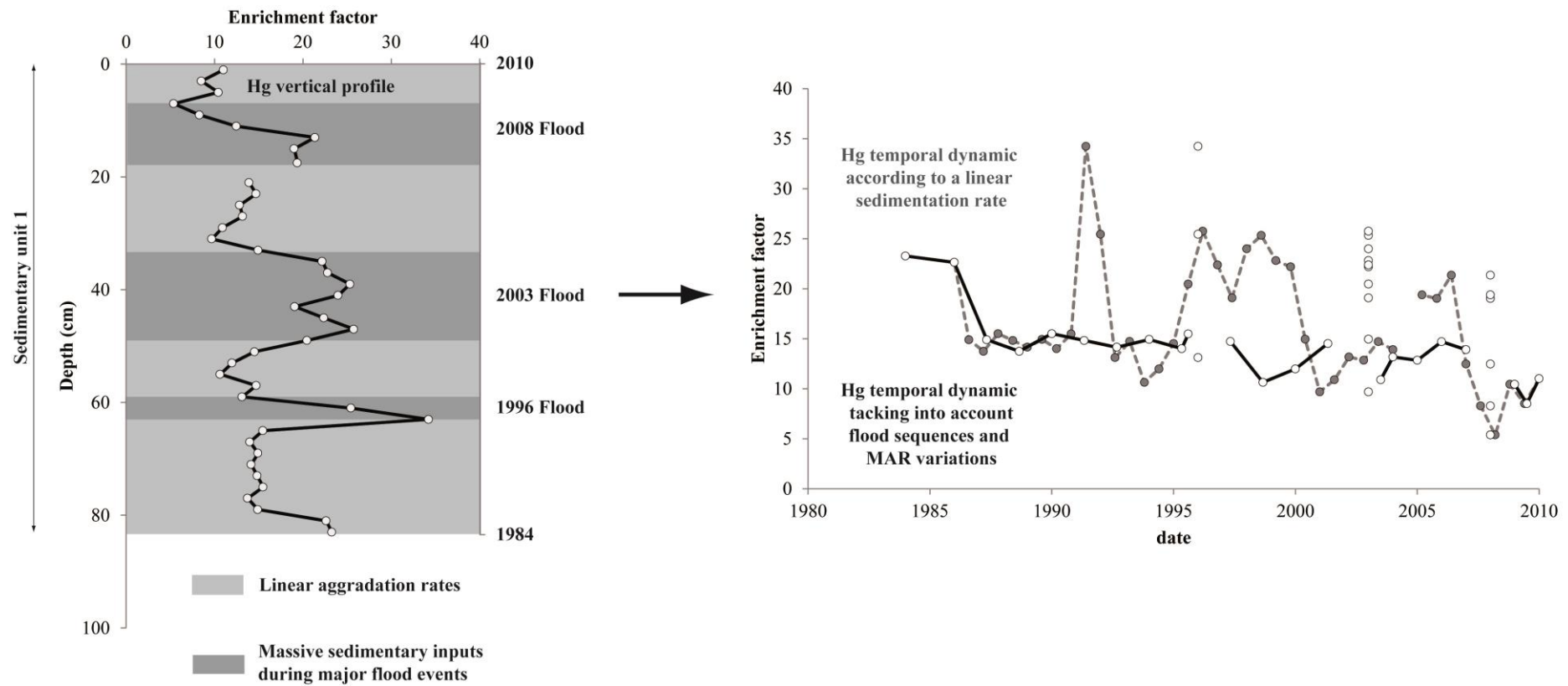


**Fig. 5.5:** Vertical profile of Cd and Hg enrichment factors (see text for calculation) in sedimentary unit 1 from the core

For the major element patterns during the 2003 flood, the *silicon* content begins to increase to a maximum peak at 42-44 cm depth (20.6% Si). The sand percentage and  $D_{50}$  also increase, but their maxima are present at 40-42 cm depth (Fig. 5.6a) and define the rising phase of the 2003 flood (named after stage I), as already described by Alvarez-Iglesias *et al.* (2007) and Babek *et al.* (2011). *Sodium* and the  $K/Rb$  ratio follow this *Si* pattern, similar to detrital trace elements such as *Ba*, *La*, *Th*, *Hf*, *Sm*, *U* and *Zr* (Tab. 5.1). In the meantime, elements such as *Al*, *Fe*, *Mg*, *TC*, *TS* and, to a lesser extent, *Ti* and *Mn* first decrease during stage I with well-marked depleted layers at 42-44 cm depth (Tab. 5.1). The *Si/Al* ratio then presents a well-defined bell-curve with a maximum centered on the 42-44 cm layer (Fig. 5.6a). A slight temporal decoupling is then observed between the *Si/Al* ratio and grain-size parameters. As the *Si/Al* ratio is usually used as a mineralogical tracer (Alvares-Iglesias *et al.*, 2007; Chen and Kandasamy, 2007; Bouchez *et al.*, 2011), stage I can be related to the solid transport of an important input of detrital material. The increase in grain-size, following the *Si/Al* variations in stage I, emphasize the coarse

characteristics of this detrital material during the flood rising phase (Walling *et al.*, 1997). However, the temporal decoupling between the geochemical detrital signature and grain-size parameters could be linked to the time gap between the runoff and bedload mobilization during the clockwise hysteresis response of a flood hydrogram in the Loire River system, as shown by Claude *et al.* (2012). The decrease in *Fe*, *Mg*, *Ti*, *TC* and *TS* at the same time can be related to a dilution by coarse and *Si*-rich detrital inputs.

In the flood sequences, a second stage can be delineated (Stage II in Fig. 5.6) that is associated with the grain-size decrease. Ratios such as *Si/Al* and  $K/Rb$  and the detrital trace element contents decrease at the same time as  $D_{50}$  and the sandy fraction. The *Manganese*, *TC* and *TS* contents start to increase (maximum at 38-40 cm for the 2003 flood) before their contents decrease until the end of the flood (from 38 to 30 cm deep). At the same time, the percentage of clayey fraction starts to increase (from 4.1% to 5.6%) and is associated with a well-marked upward increase in *Al*, *Fe*, *Mg*, *Ca* and *Ti* content. The depth level, associated with the concentration

maxima, then shifted for the 2 different element groups at 42-44 cm for the *Si/Al*, *Na*, and *K/Rb* maxima and at 32-34 cm for the *Al*, *Fe*, *Mg*, *K*, and *Ti* maxima. Stage II can be related to the end of the flood hysteresis, when underflow declined and the finest sediments in the suspension present in the water column began to settle. The increase in major elements such as *Al*, *Fe*, *Mg*, *Ca* and *Ti* indicates that these fine particles may be associated with clay and (Fe, Ti) oxyhydroxide transport.

The 2008 flood's sedimentary record is less well-defined relative to the dam's specific management when the Villerest dam was transparent during the flood rising phase. The stage I sand percentage, defined by  $D_{50}$ , and *Si/Al* increase in the 2003 flood do not seem to be as well registered for the 2008 flood. The increasing sand percentage phase is missing (Fig. 5.6b), and the *sodium* and *Si/Al* and *K/Rb* ratios only present steady levels from 19 to 14 cm deep. At the same time, the *Fe*, *Ti* and *Mg* concentrations are the lowest during the 2003 flood. Stage II's decreasing *Si/Al*,  $D_{50}$  and sand percentage are similar in both flood registered sequences with a well-marked

increase in the Fe content and clay percentage.

For these flood sequences recorded in the Villerest sediments, anthropogenic enriched trace elements present significant correlations with the *Si/Al* and *TOC* contents. A short depletion of these enriched TEs clearly corresponds to a *Si/Al* maximum during phase I (Fig. 5.6a). The influence of coarser non-impacted detrital material, such as K-feldspars, quartz and accessory minerals, on the archived anthropogenic TE signal is highlighted here. The enriched TE decreased together with the *TOC* content although the *Fe* content kept increasing (Fig. 6a and b). Hence, the flood events mobilized TE-rich material mostly associated with the organic fraction rather than detrital (*Si/Al* variations) and Fe-rich material.

All of these detailed chemical variations enhance the importance of material origins during a flood event and the influence of grain-size and associated mineralogical effects on major and trace element concentrations, even in the <63  $\mu\text{m}$  fraction. The significant relationships between the sand and clay percentages,  $D_{50}$ , *Si/Al*, *K/Rb* ratios and detrital trace elements show the presence of coarse

particles, which mainly mobilized at the beginning of a flood in a dam reservoir, although finer particles settle at the end

of the flood and influence chemical variations.

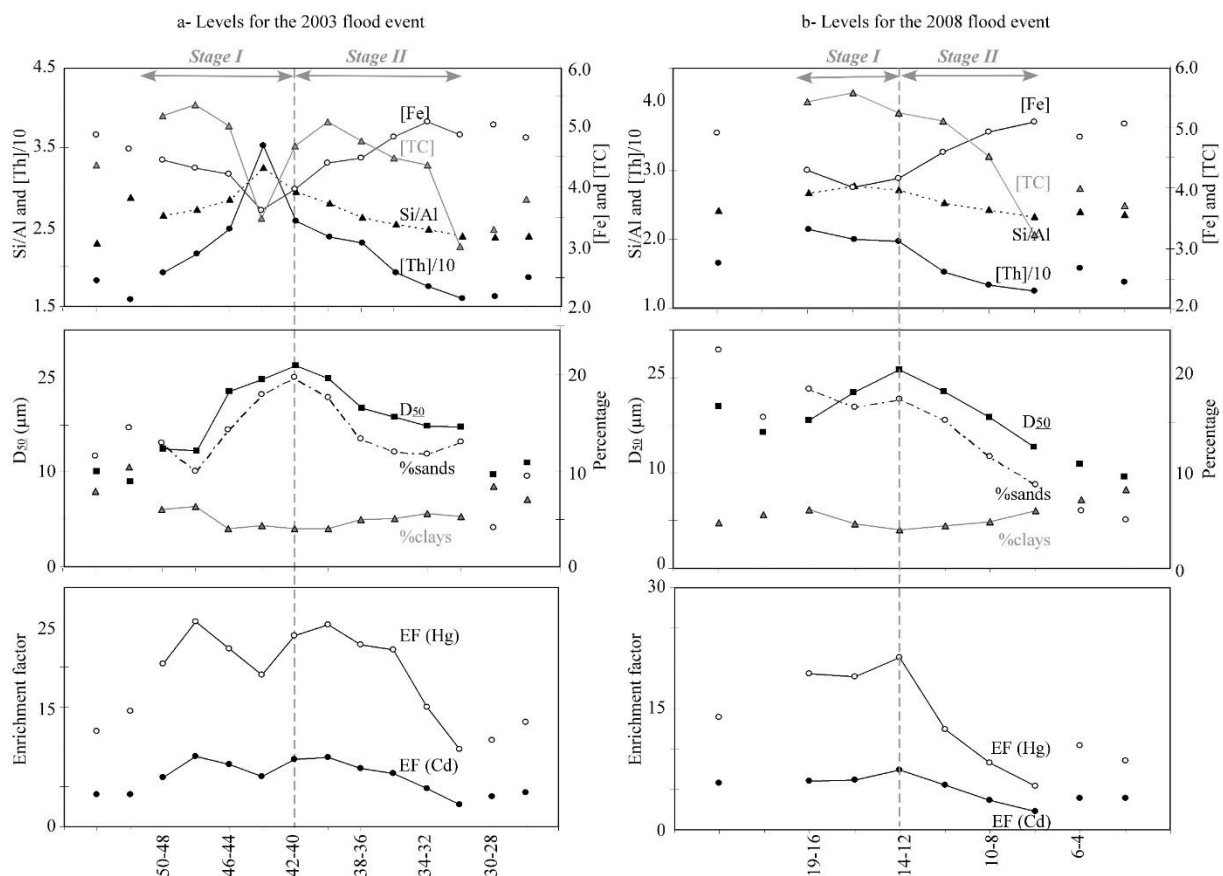


**Fig. 5.6:** Variations in selected parameters (Si/Al ratio, TOC, Fe and Th concentrations, percentage of sands and clays,  $D_{50}$ , enrichment factors of Cd and Hg) in the core sediments during a- the 2003 flood and b- the 2008 flood.

#### 5.4. Conclusions

When study areas such as the Loire River are located in artificially narrowing rivers with sandy sediment, fine-grained sediment settling spots are difficult to find and reservoirs can be considered for well-defined sedimentary archives. In the Villerest flood-control reservoir, the sedimentological analysis of the studied core allows us to highlight different settling periods relative to the dam's construction, operation phase and upstream hydrological conditions. The base of this sedimentary archive illustrates local aggradation conditions associated with dam construction and water infilling periods. Only the upper sedimentary unit, which was deposited in a lacustrine context during dam operation, can be taken into account to describe the temporal dynamics of the pollutants. In addition, major flood events during the 1984-2010 period have largely contributed to sedimentary infill (43% of the total sediment accumulation since 1984) with highly TE-impacted deposits ( $EF > 20$  for Hg and  $>10$  for Cd and Bi) compared to interflood periods. When considering a linear sedimentation rate over the period, such an influence from the flood events could not be

indicated, and the flood sequences were wrongly associated with high polluted periods and specific anthropogenic inputs. Hence, these results emphasize the importance of combining sedimentological and geochemical analyses to understand the sedimentary infilling processes and temporal trajectories of contaminants in a reservoir.

The flood sequences resulting from sediment-laden underflows present variations in the sedimentological and geochemical signals. Grain-size variations and conservative TE inputs mark two stages associated with flood hydrograms. In particular, an increasing discharge stage is associated with a coarsening phase with important detrital material inputs, although the decreasing discharge stage presents a fining particle size trend and a depletion of detrital inputs followed by Fe-rich clay deposits. For all of the flood episodes, anthropogenic TE possibly came from remnant sources, solicited and/or emphasized. In addition, even in the  $<63 \mu\text{m}$  fraction of these flood sequences, the anthropogenic TE signals appear to be controlled by the grain-size and detrital material inputs. Indeed, massive inputs of coarser and

non-impacted sediments at maximum discharge induce an underestimation of the calculated EF. In terms of river dam management, these results show the importance of flood control and limiting the spread of pollutants, though the dam reservoir also constitutes important stocks of polluted sediments, which can potentially be remobilized during reworking phases and/or storage variations.

## Acknowledgments

This work was supported by the framework EPL-Feder. The authors really appreciate help in the field of the 2 boat pilots from “Syndicat mixte du barrage de Villerest”.

## References

- Alvarez-Iglesias, P., Quintana, B. Rubio, Pérez-Arlucea, M., 2007. Sedimentation rates and trace metal input history in intertidal sediments from San Simón Bay (Ría de Vigo, NW Spain) derived from  $^{210}\text{Pb}$  and  $^{137}\text{Cs}$  chronology. *Journal of environmental radioactivity*, 98, 229–250.
- Ambers, R. K. R., 2001. Using the sediment record in a western Oregon Flood-control reservoir to assess the influence of storm history and logging on sediment yield. *Journal of Hydrology*, 244, 181-200.
- Arnaud-Fassetta, G., 2003. River channel changes in the Rhône Delta (France) since the end of the Little Ice Age: geomorphological adjustment to hydroclimatic change and natural resource management. *Catena*, 51, 141–172.
- Audry, S., Grosbois, C., Bril, H., Schäfer, J., Kierczak, J., Blanc, G., 2010. Post-depositional redistribution of trace metals in reservoir sediments of a mining/smelting-impacted watershed (the Lot River, SW France). *Applied Geochemistry*, 25, 778–794.
- Audry, S., Schäfer, J., Blanc, G., Jouanneau, J.-M., 2004. Fifty-year sedimentary record of heavy metal pollution (Cd, Zn, Cu, Pb) in the Lot River reservoirs (France). *Environmental pollution*, 132, 413–426.
- Bábek, O., Faměra, M., Hilscherová, K., Kalvoda, J., Dobrovolný, P., Sedláček, J., Machát, J., Holoubek, I., 2011. Geochemical traces of flood layers in the fluvial sedimentary archive; implications for contamination history analyses. *Catena*, 87, 281–290.
- Bábek, O., Hilscherová, K., Nehyba, S., Zeman, J., Famera, M., Francu, J., Holoubek, I., Machát, J., Klánová, J., 2008. Contamination history of suspended river sediments accumulated in oxbow lakes over the last 25 years. *Journal of Soils and Sediments*, 8, 165–176.
- Benoit G, Rozan TF., 2001.  $^{210}\text{Pb}$  and  $^{137}\text{Cs}$  dating methods in lakes : a

- retrospective study. *Journal of Paleolimnology*, 25, 455–465
- Blott, S. J., Pye, K., 2001. GRADISTAT: a grain size distribution and statistics package for the analysis of unconsolidated sediments. *Earth Surface Processes and Landforms*, 26, 1237–1248.
- Bravard, J.-P., Goichot, M., Tronchère, H., 2014. An assessment of sediment-transport processes in the Lower Mekong River based on deposit grain sizes, the CM technique and flow-energy data. *Geomorphology*. 207, 174–189
- Bouchez, J., Gaillardet, J., France-Lanord, C., Dutra-Maia, P., Maurice, P., 2011. Grain size control of river suspended sediment geochemistry: clues from Amazon river depth-profiles. *Geochem. Geophys. Geosyst.*, 12, Q03008
- Callender, E., 2003. Heavy metals in the environment. Historical trends. Treatise on geochemistry, B. Sherwood collar ed, 9, pp. 67-105.
- Castelle, S., Schäfer, J., Blanc, G., Audry, S., Etcheber H., Lissalde, J.-P. 2007. 50-Year Record and Solid State Speciation of Mercury in Natural and Contaminated Reservoir Sediment. *Applied Geochemistry*, 22, 1359–1370.
- Chen, C.-T., Kandasamy, S., 2007. Evaluation of elemental enrichments in surface sediments off southwestern Taiwan. *Environmental Geology*, 54, 1333–1346.
- Claude, N., Rodrigues, S., Bustillo, V., Bréhéret, J.-G., J.-J. Macaire, Jugé, P., 2012. Estimating bedload transport in a large sand–gravel bed river from direct sampling, dune tracking and empirical formulas. *Geomorphology*, 179, 40–57.
- Coynel, A., Schäfer, J., Blanc G., Bossy, C., 2007. Scenario of particulate trace metal and metalloid transport during a major flood event inferred from transient geochemical signals. *Applied Geochemistry*, 22, 821–836.
- Dacharry M., 1974. Hydrologie de la Loire en amont de Gien. Paris, N.A.L., 2 vol. 334 & 285 p
- Dai, S. B., Yang, S. L., Cai, M., 2008. Impacts of dams on the sediment flux of the Pearl River, southern China. *Catena*, 76, 36–43.
- Desmet, M., Mourier,B., Mahler, B.J., Van Metre, P.C., Roux, G., Persat, H., I. Lefèvre, Peretti,A., Chapron, E., Simonneau, A., Miège, C., Babut, M. 2012, Spatial and temporal trends in PCBs in sediment along the lower Rhône River, France. *The Science of the total environment*, 433, 189–97
- Dill, H. G., 2010. The “chessboard” classification scheme of mineral deposits: Mineralogy and geology from aluminum to zirconium. *Earth-Science Reviews*, 100, 1–420.
- Fan, J., Morris, G. L. 1992, Reservoir sedimentation. I: Delta and density current deposits. *Journal of Hydraulic Engineering*, 118, 354-369.
- Folk, R.L., Ward, W. C., 1957. Brazos River bar: a study in the significance of grain size

parameters. *Journal of Sedimentary Petrology*, 27, 3–26.

Gilli A., Anselmetti F.S., Glur L., Wirth, S.B., 2013. Lake sediments as archives of recurrence rates and intensities of past flood events, in: Schneuwly-Bollschweiler, M., Stoffel, M., Rudolf-Miklau, F. (Eds.), *Dating torrential processes on fans and cones - Methods and their application for hazard and risk assessment, Advances in Global Change Research*. Springer, 47, pp. 225-242.

Giovanoli F., 1990. Horizontal transport and sedimentation by interflows and turbidity currents in Lake Geneva. In: Tilzer MM, Serruya C (eds) *Large lakes: ecological structure and function*. Springer, Berlin/Heidelberg, 175–195

Govindaraju K., Potts P., Webbs J.S., Watson J., 1994. Whin sill dolerite WS-E from England and Pitscurrie microgabbro PM-S from Scotland: assessment by one hundred and four international laboratories. *Geostand Newsl*, 18, 221–300.

Govindaraju K., Mervelle G., 1987. Fully automated dissolution and separation methods for inductively coupled plasma atomic emission spectrometry rock analysis. Application to the determination of rare earth elements. *J Anal At Spectrom*, 2, 615-621.

Grosbois C., Meybeck M., Lestel L., Lefèvre I., Moatar, F., 2012. Severe and contrasted polymetallic contamination patterns (1900-2009) in the Loire River sediments (France). *The Science of the total environment*, 435-436, 290–305.

Grousset, F. E., Jouanneau, J. M., Castaing, P., Lavaux, G., Latouche, C., 1999. A 70 year Record of Contamination from Industrial Activity Along the Garonne River and its Tributaries (SW France). *Estuarine, Coastal and Shelf Science*. 48, 401–414.

Horowitz, A. J., Elrick, K. A., 1987. The relation of stream sediment surface area, grain size and composition to trace element chemistry. *Applied Geochemistry*, 2, 437-451.

Kabata-Pendias, A. 2000. Trace elements in soils and plants. 3<sup>rd</sup> ed. CRC Press.

Klaminder, J., P. Appleby, P. Crook, Renberg, I., 2012. Post-deposition diffusion of <sup>137</sup>Cs in lake sediment: Implications for radiocaesium dating. *Sedimentology*, 59, 2259–2267.

Le Cloarec M.F., Bonte P., Lestel L., Lefèvre I., Ayrault, S., 2011. Sedimentary record of metal contamination in the Seine River during the last century. *Phys Chem Earth*, 36, 515–529.

Macaire, J. J., Gay-Ovejero, I., Bacchi, M., Cocirat, C., Patryl, L., Rodrigues, S. 2013, Petrography of alluvial sands as a past and present environmental indicator: Case of the Loire River (France). *International Journal of Sediment Research*, 28, 285-303.

Morris, G. L., Annandale, G., Hotchkiss, R., 2008. Reservoir sedimentation. Sedimentation engineering process measurements, modeling and practices. Amer Soc Civil Engineer (ASCE), Reston, USA, 1-17.

- Mourier B., Desmet M., Van Metre P.C., Mahler B.J., Perrodin Y., Roux G., Bedell J.-P. Lefèvre I., Babut, M., 2014. Historical records, sources and spatial trends of PCBs along the Rhône River (France). *Science of the Total Environment*, 476-477, 568-576.
- Pacyna, J. M., Pacyna, E. G., 2001. An assessment of global and regional emissions of trace metals to the atmosphere from anthropogenic sources worldwide. *Environmental Reviews*, 9, 269–298.
- Passega, R., 1964. Grain-size representation by CM pattern as a geological tool. *J. Sediment. Petrol.*, 34, 830–847.
- Passega, R., 1957, Texture as characteristic of clastic deposition. *Bull. Am. Assoc. Pet. Geol.*, 41, 1952–1984.
- Pye, K., Blott, S. J., 2004. Particle size analysis of sediments, soils and related particulate materials for forensic purposes using laser granulometry. *Forensic science international*, 144, 19–27.
- Smith JT, Clarke RT, Saxén R., 2000. Time-dependent behavior of radiocaesium : A new method to compare the mobility of weapons test and Chernobyl derived fallout. *Journal of Environmental Radioactivity*, 79, 65-83
- Sturm M, Matter, A., 1978. Turbidites and varves in Lake Brienz (Switzerland): deposition of clastic detritus by density currents. *Spec Publ Int Assoc Sedimentol.*, 2, 147–168.
- Valverde, L., Jugé, P., Handfus, T., 2013. Résultats granulométriques et localisation des points dures en Loire, rapport InfoSed 2, pp. 180
- Van Metre, P.C., Wilson, J.T., Fuller, C.C., Callender, E., Mahler, B.J., 2004. Collection, analysis, and age-dating of sediment cores from 56 U.S. lakes and reservoirs sampled by the U.S. geological survey, 1992–2001 USGS Scientific Investigations Report–5184
- Vörösmarty, C. J., Michel Meybeck, B. Fekete, K. Sharma, P. Green, Syvitski, J. P., 2003. Anthropogenic sediment retention: major global impact from registered river impoundments. *Global and Planetary Change*, 39, 169–1907.
- Vukovic, D., Vukovic Z., Stankovic, S., 2014. The impact of the Danube Iron Gate Dam on heavy metal storage and sediment flux within the reservoir. *Catena*, 113, 18–23.
- Walling, D. E., Owens, P. N., Carter, J., Leeks, G. J. L., Lewis, S., Meharg, A. A., Wright, J., 2003. Storage of sediment-associated nutrients and contaminants in river channel and floodplain systems. *Applied Geochemistry*, 18, 195–220.
- Walling, D. E., Bradley, S. B., 1990. Some applications of caesium-137 measurements in the study of fluvial erosion, transport and deposition. in: Walling, D. E., Yair, A., Berkowicz S. (Eds), *Erosion, Transport and Deposition Processes*, (Proc. Jerusalem Workshop, April 1987), IAHS Publ. 189, IAHS Press, Wallingford, UK, pp. 179–203.

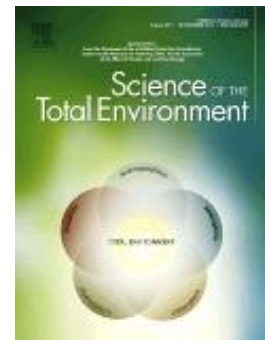
- Walling, D.E, He, Q., 1998. The spatial variability of overbank sedimentation on river floodplains. *Geomorphology*, 24, 209–223.
- Walling, D E, He, Q., 1997. Sediment deposition on river floodplains, 29, 263–282.
- Walling, D.E., Owens, P. N., Leeks, G. J. L., 1997. The characteristics of overbank deposits associated with a major flood event in the catchment of the River Ouse, Yorkshire, UK. *Catena*, 31, 53–75.
- Yang, S., Zhao, Q., Belkin, I. M., 2002. Temporal variation in the sediment load of the Yangtze River and the influences of human activities. *Journal of Hydrology*, 263, 56-71.
- Ye, C., Li, S., Zhang, Y., Zhang, Q., 2011. Assessing soil heavy metal pollution in the water-level-fluctuation zone of the Three Gorges Reservoir, China. *Journal of hazardous materials*, 191, 366–372.
- Ziegler, C. K., Nisbet, B. S. 1995, Long-term simulation of fine-grained sediment transport in large reservoir. *Journal of Hydraulic Engineering*, 121, 773-781.



**Illustration 2 :** Photographie aérienne de la la plaine alluviale de Decize (Loire Amont) montrant le paléochenal et le point bar étudié.

## **Chapitre 6 - Influence of fluvial environments on sediment archiving processes and temporal pollutant dynamics (Upper Loire River, France)**

Published in: Science of the Total Environment, 2015, 1, 121-136



E. Dhivert, C. Grosbois, S. Rodrigues, M. Desmet

Université François Rabelais de Tours. EA 6293 GéHCO. Parc de Grandmont. 37200 Tours.  
France

*Received on July the 28<sup>th</sup> of 2014 and accepted on September the 25<sup>th</sup> of 2014*

### **Highlights:**

- Divergence on long-term evolution of sedimentary pollution archived in a floodplain
- Archiving capacity depends on the connection degree to the river channel
- Archived geochemical signals depend on sampling statutes in the floodplain
- Good resolution on short-time variations of pollution in the paleochannel
- Pollution trend altered by redistribution processes in the floodplain ridge

## **Abstract:**

Floodplains are often cored to build long-term pollutant trends at the basin scale. To highlight the influences of depositional environments on archiving processes, aggradation rates, archived trace element signals and vertical redistribution processes, two floodplain cores were sampled near in two different environments of the Upper Loire River (France): (i) a river bank ridge and (ii) a paleochannel connected by its downstream end. The base of the river bank core is composed of sandy sediments from the end of the Little Ice Age (late 18<sup>th</sup> century). This composition corresponds to a proximal floodplain aggradation (< 50 m from the river channel) and delimits successive depositional steps related to progressive disconnection degree dynamism. This temporal evolution of depositional environments is associated to mineralogical sorting and variable natural trace element signals, even in the < 63-μm fraction. The paleochannel core and upper part of the river bank core are composed of fine-grained sediments that settled in the distal floodplain. In this distal floodplain environment, the aggradation rate depends on the topography and connection degree to the river channel. The temporal dynamics of anthropogenic trace element enrichments recorded in the distal floodplain are initially synchronous and present similar levels. Although the river bank core shows general temporal trends, the paleochannel core has a better resolution for short-time variations of trace element signals. After local water depth regulation began in the early 1930s, differences of connection degree were enhanced between the two cores. Therefore, large trace element signal divergences are recorded across the floodplain. The paleochannel core shows important temporal variations of enrichment levels from the 1930s to the coring date. However, the river bank core has no significant temporal variations of trace element enrichments and lower contamination levels because of a lower deposition of contaminated sediments and a pedogenetic trace elements redistribution.

**Keywords:** Loire Basin, floodplain sediments, archiving processes, depositional environments, sedimentation rate, trace elements, pollutant temporal dynamics

## 6.1. Introduction:

The grain size distribution of alluvial deposits controls the fluvial architecture and fine-grained sediments, essentially settling in out-of-channel forms (Walling *et al*, 1998; Bridge, 2003; Houben, 2007). Because metallic and organic contaminants are typically associated with the finest particles during sediment transport, floodplains play a key role in pollutant cycles, constituting short-to long-term storage areas for contaminated sediments (Bradley and Cox, 1990; Martin *et al*, 2000; Heaven *et al*, 2000; Lecee and Pavlowsky, 2014). Therefore, floodplains are often cored to study pollutant temporal trends and to identify temporal variability of natural and anthropogenic sources (e.g., Grosbois *et al*, 2012 for the Loire Basin (France) and neighboring hydrosystems: Grousset *et al*, 1999 for the Garonne Basin; Gocht *et al*, 2001, Berner *et al*, 2012 for the Rhin basin; Le Cloarec *et al*, 2011 for the Seine basin; Ferrand *et al*, 2012, Desmet *et al*, 2012, Mourier *et al*, 2014 for the Rhone basin). However, floodplains cannot be considered to be a homogenous depositional environment because of

- (i) the temporal variability of aggradation rates caused by long-

term evolutions of natural and anthropogenic influences on parameters controlling sediment deposition (Hoffmann *et al*, 2010; Hughes *et al*, 2010; Meitzen *et al*, 2013; Grygar *et al*, 2014)

- (ii) and the short-term (overbank floods) and the short-space (lateral transect) scale variability of aggradation rates, sediment textures and storage capacities (Nanson and Croke, 1992; Walling *et al*, 1997; Walling and He, 1998; Lecce and Pavlowsky, 2004; Rodrigues *et al*, 2006; Baborowski *et al*, 2007; Dieras *et al*, 2013).

This short-scale variability of sediment inputs influence contamination levels and archived temporal dynamics of pollutants (Bradley and Cox, 1990; Birch *et al*, 2001; Matrin, 2000; Heaven *et al*, 2000; Baborowski *et al*, 2007; Bábek *et al*, 2008; Grygar *et al*, 2010; Vrel *et al*, 2013; Hostache *et al*, 2014). Additionally, between morphological units of a floodplain, large differences may exist in the nature and degree of post-depositional processes managing the fate of archived pollutants. Archived contaminated sediments can be re-

mobilized during erosion episodes (Macklin and Klimek, 1992; Lecce and Pavlowsky, 1997; Förstner *et al*, 2004; Lecce and Pavlowsky, 2014). A high spatial variability exists during high discharge events of erosion intensity across floodplains (Benetti, 2003, Fuller, 2008, Dieras *et al*, 2013, Thompson and Croke, 2013). Additionally, exchanges between particulate and dissolved fractions inside the sedimentary column are an important factor managing the fate of archived contaminants. These exchanges can be controlled by organic matter degradation and seasonal variations of redox potential, which affect morphological units of floodplains differently (Griethuysen *et al*, 2005, Charriaud *et al*, 2011, Schulz-Zunkel *et al*, 2013). The vertical redistribution of contaminated particles can occur in floodplain soils where pedogenic activity has been settled (Fujikawa *et al*, 1998, Palumbo *et al*, 2000).

These variability factors question the representation at the basin scale of pollutant temporal dynamics archived in a punctual situation of a floodplain. In other words, what are the conditions allowing the building of representative pollutant trends from a floodplain core? In this

study, the influence of depositional environments on sediment archiving processes, aggradation rates and associated Trace Elements (TE) was investigated at a local scale in the Upper Loire River floodplain. The aim was to highlight mechanisms controlling the archiving of sediments and associated TE and the temporal dynamics of contaminants in two floodplain cores sampled in two different morphological units separated by less than 50 m:

- (i) a ridge of the river bank
- (ii) and a paleochannel connected at its downstream end (Fig. 6.1).

## 6.2. Study area and methods

### 6.2.1. Main characteristics of the study area

The Loire River basin ( $117,800 \text{ km}^2$  -  $1,013 \text{ km}$  long) is among the ten largest W-European basins and is the largest in France (Fig. 6.1a). The Decize station is located in the upper reach of the Loire River ( $14,752 \text{ km}^2$  -  $450 \text{ km}$  long), 30 km upstream of the Allier River confluence. This station is located close to the confluence with the Aron tributary, the Loire River lateral canal and the Seine-

Loire canal. Because of the Decize dam, built in 1836 and elevated in 1933 (Fig. 6.1), the main channel of the Loire River allows the shipping connection between these canals. The coring site ( $46^{\circ}49'36.6''N$ ,  $3^{\circ}27'38.2''E$ ) is located 1.5 km upstream from this dam and 400 m downstream from the maximum dam influence (the lock of the lateral canal). (i)

The geology of the Upper Loire (ii) Basin is different. According to the French geological survey, the upstream region of

the Loire hydrosystem essentially drains granites, gneisses and micaschists from the eastern region of the French Central Massif, an old massif inherited from the Variscan orogeny (480-290 Ma). However, two other geological units constitute bedrocks of the Upper Loire Basin:

a volcanic area from the Tertiary as the basin head of the Loire River and sedimentary basins from the Carboniferous and Oligocene-Miocene (mainly sandstones, marls and clays).

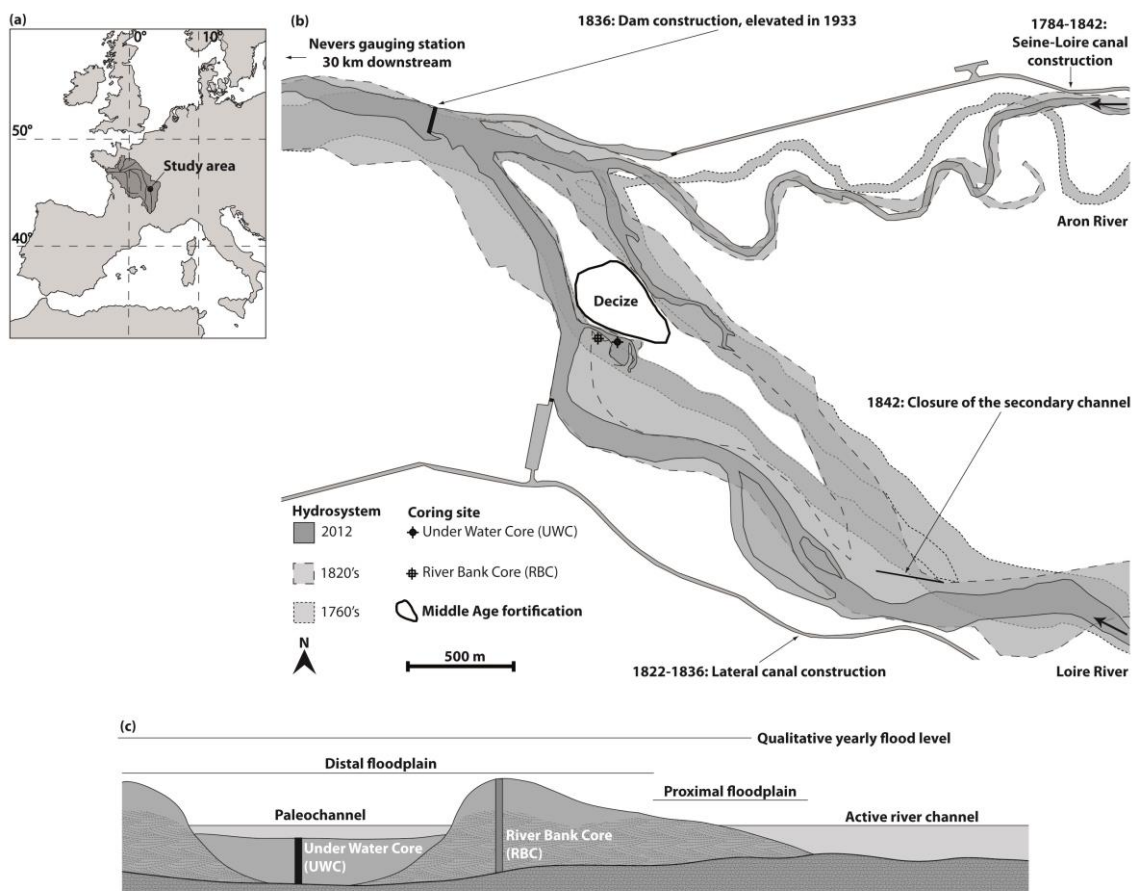


**Fig. 6.1.: a-** Location of the study area in W-Europe, **b-** morphodynamic history, hydrosystem anthropization and local industrial histories of the study area (data from [www.geoportail.fr](http://www.geoportail.fr), 2014; Decize Municipal Archive, 2014), and **c-** schematic view of the sample strategy.

The hydrology of the upper basin is influenced by a balance of oceanic and Mediterranean rainfall during autumn and winter, completed by snow-melt in spring (Dacharry, 1974). The annual hydrological cycle of the Upper Loire River, at the Nevers gauging station (30 km downstream of the coring site), is characterized by a high flow period from November to May. Monthly discharges calculated over 59 years range from 199  $\text{m}^3.\text{s}^{-1}$  to 323  $\text{m}^3.\text{s}^{-1}$ . Low flow occurs in summertime with average values ranging from 50  $\text{m}^3.\text{s}^{-1}$  to 121  $\text{m}^3.\text{s}^{-1}$  (data from [www.hydro.eaufrance.fr](http://www.hydro.eaufrance.fr)). At this gauging station, the 50-year flood peak discharge reached 2200  $\text{m}^3.\text{s}^{-1}$  (daily discharge), 1900  $\text{m}^3.\text{s}^{-1}$  for the 20-year flood, 1700  $\text{m}^3.\text{s}^{-1}$  for the 10-year flood, 1400  $\text{m}^3.\text{s}^{-1}$  for the 5-year flood and 1000  $\text{m}^3.\text{s}^{-1}$  for the 2-year flood. Four catastrophic flood events occurred in the basin after the water depth measurement began at the Decize dam gauging station (1836): 1846 (7.1 m), 1856 (6.5 m), 1866 (7.4 m) and 1907 (6.3 m) (DREAL archives, 2013; [www.vigicrues.fr](http://www.vigicrues.fr) 2013).

The studied floodplain results from a lateral migration of a relatively straight channel, which was active until the 18<sup>th</sup> century, to the present meander. This

sinuosity was initiated at the end of the Little Ice Age (LIA), between the 1760s and 1820s, and was associated with channel widening (Fig. 6.1b). This morphological evolution was described for a large number of fluvial systems all over the world (e.g., Arnaud-Fassetta, 2003; Landon, 1999 for the Rhône River; Knox, 2006 for the Upper Mississippi River) and even in the Upper Loire River for a historical meander located 10 km upstream of the study area (Leteinturier *et al*, 2000; Babonaux, 1970). These rapid changes in the river channel planform are attributed to a large sedimentary transport resulting from combined actions of important flood events associated with climate change of the end of the LIA and soil erosion magnification by human land use. Additionally, river bed modifications (embankments, dams, hydraulic structures for water-depth control), performed since the 19<sup>th</sup> century along the Loire River, triggered a narrowing of the main river channel, its incision and the development of woody vegetation (Gasowski, 1994; Rodrigues *et al*, 2006; Détriché *et al*, 2010; Latapie, 2011; Grivel and Gautier, 2012; Macaire *et al*, 2013; Latapie *et al*, 2014). Presently, the study area corresponds to a typical point bar complex characterized by a ridge and swale topography delimiting

former scroll bars. Bridge (2003) proposes a definition of point bar and scroll bar concepts by explaining that sediments are preferentially deposited in the inner part of meanders, allowing sedimentary bars to form with a scroll planform shape. The lateral migration of the river channel induces the formation of successive bars and establishes a point bar complex. In the study area, the paleochannel, which is flooded throughout the year, constitutes a remnant of the initial channel and is preserved by anthropogenic actions.

### **6.2.2. Analytical method**

The two sediment cores were sampled in May 2012, after the last spring floods. The underwater core (UWC), was sampled in the deepest area of the paleochannel (Fig. 6.1c). The top of the sedimentary infill was elevated at 189.8 m asl, under 0.5 m of water column on the coring date. A UWITEC gravity corer fitted with a 2 m long and 90 mm diameter plastic liner was used for the UWC. The river bank core (RBC), was sampled on the adjacent river bank (Fig. 6.1c), 48 m E-S-E from the UWC at the top of the closer ridge, elevated at 191.3 m asl. For this core, an Eijkelkamp mechanical percussion corer equipped with 1 m long and 63 mm diameter plastic liners was used.

Material and methods used for this study are detailed in Dhivert *et al*, (2015). All of the analyses were performed with 2 cm-slices of core sediments. To complement visual and textural descriptions of sedimentary units, temporal variations of deposition conditions were reconstructed using the C-M diagram (Passega, 1957, 1964) and specific segments were understood following universal pattern interpretations (Bravard *et al*, 2014; Arnaud Fasseta, 2003; Bravard and Peiry, 1999). The rolling domain (N-O domain, Fig. 6.2) was anchored in the Loire River context using bed load sediments sampled more than 30 km downstream of the study area (Valverde *et al*, 2013). Bed load sediments involve a broad spectrum of particles ( $D_{50}$  range between 1.3 mm and 15.0 mm) from coarse sands (1-2 mm) to medium gravels (8-16 mm). A grain size measurement was performed on fresh sediments using a Mastersizer 2000 laser diffraction microgranulometer (Malvern) as it is the only method to establish sedimentological patterns and destroy a minimum amount of material. For poorly sorted sediments, the grain size distribution of the coarsest particles must be considered carefully (Pye and Blott, 2004). Similar to Dhivert *et al*. (2015), the

replicability was low for the ninety-ninth percentile of very poorly sorted fine-grained layers. The ninetieth percentile ( $D_{90}$ ) was used as the C parameter to be more representative of the coarsest grain size, and the M value corresponded to the median grain size ( $D_{50}$ ).

Regarding the structural differences between the UWC (aquatic sediments saturated) and the RBC (terrestrial sediments showing a secondary porosity), age-models were designed to calculate mass accumulation rates (MAR,  $\text{kg} \cdot \text{m}^{-2} \cdot \text{y}^{-1}$ ; Van Metre *et al.*, 2004) to correct coring compaction. MARs are calculated, dividing cumulative dry mass (cum;  $\text{kg} \cdot \text{m}^{-2}$ ) between each date-bounded by time intervals. The dry mass parameter (DM;  $\text{kg} \cdot \text{m}^{-2}$ ) is calculated as follows:

$$DM = (1-n) \cdot DS \cdot Th \quad (\text{eq. 6.1})$$

where  $n$  represents the porosity (%) corresponding to the volume of water in a well with a known volume of sediments (here  $2.4 \cdot 10^{-5} \text{ m}^3$ ) and is calculated from the weight difference between the fresh and dried sediments.  $DS$  is the apparent density of sediments ( $\text{g} \cdot \text{m}^{-3}$ ) corresponding to the dry mass material in the defined volume and  $Th$  the thickness of the sampled layer (here  $2.0 \cdot 10^{-2} \text{ m}$ ). The age of sediments (Date) at

level  $i$  is calculated as follows from the top of the core (2012 in this study as the coring date) to the first time marker:

$$Date_i = coring\ date - cum_i / MAR \quad (\text{eq. 6.2})$$

For sediment layers  $j$ , which is older than the first time marker  $i$ , Equation 6.3 is then applied:

$$Date_j = marker\ date_i - (cum_j - cum_i) / MAR_j \quad (\text{eq. 6.3})$$

Absolute dating was based on  $^{137}\text{Cs}$  artificial radionuclide vertical distribution.  $^{137}\text{Cs}$  measurements were performed using gamma spectrometry with very low-background detectors, coaxial HP Ge N-type (8000 channels, low back-ground).

Geochemical analyses were performed on the  $< 63 \mu\text{m}$  fraction. The 190-202 cm deep layer was pooled because  $< 63 \mu\text{m}$  material was too low. Analyses were made at the SARM-CRPG laboratory ([www.helium.crpg.cnrs-nancy.fr/SARM](http://www.helium.crpg.cnrs-nancy.fr/SARM)). Material was completely digested with  $\text{LiBO}_2\text{-Li}_2\text{B}_4\text{O}_7$  on a tunnel oven and placed in an acidic solution before being analyzed by ICP-OES (ICap 6500, Thermo Scientific) for total major and minor element concentrations, and ICP-MS (Thermo Elemental X7, Thermo Scientific) for trace elements, except for

Hg, which was completed using DMA-80 (Milestone). The total organic carbon (TOC), after an HCl attack and total sulfur (TS), was analyzed by O<sub>2</sub> flow combustion at 1350°C with a SC 144-DRPC (Leco). The analytical error taking into account accuracy of digestion processes and analyses was within 1% for major elements and 10% for trace elements.

### 6.3. Results and discussion

#### 6.3.1. Archiving processes during the floodplain edification

##### 6.3.1.1 Aggradation processes in the floodplain

The texture of sediments can be used as proxy for tracing the geomorphological evolution of the floodplain and the associated aggradation processes accompanying the river bank accretion and the lateral migration of the river channel (Bravard *et al*, 2014; Passeggi, 1957, 1964).

The RBC core presents two distinct sequences: the deepest sequence (126-202 cm) rich in sand (> 63 µm) and the upper sequence (0-126 cm) composed of fine-grained sediments (< 63 µm; Fig. 6.2a). According to Walling et al. (1997)

and Walling and He (1997), during overbank floods, sandy sediments are deposited in the highly connected context of a proximal floodplain (within the first 50 m from the river channel) and fine-grained sediments settle in the lowly connected context of a distal floodplain. In this study, this distinction allows for the characterization of two large depositional environments with specific aggradation processes over space and through time (Fig. 6.2b).

The proximal floodplain sequence, archived at the base of the RBC (126-202 cm), presents a general fining upward ( $r = 0.6$ ,  $p < 0.05$ ,  $n = 33$ , Fig. 6.2b, Tab. 6.1). This is confirmation of a connection degree evolution during the aggradation period.

The deepest unit of the RBC (190-202 cm), named unit 3 (Fig. 6.2a), is composed of moderately sorted sands (Tab. 6.1). Compared to actual bed sediments with high grain size variability (N-O domain), unit 3 draws the P domain in the C-M diagram (Fig. 6.2c). This sedimentary layer can be interpreted as channel bar sediments fed by a mix between rolling and gradual suspension.

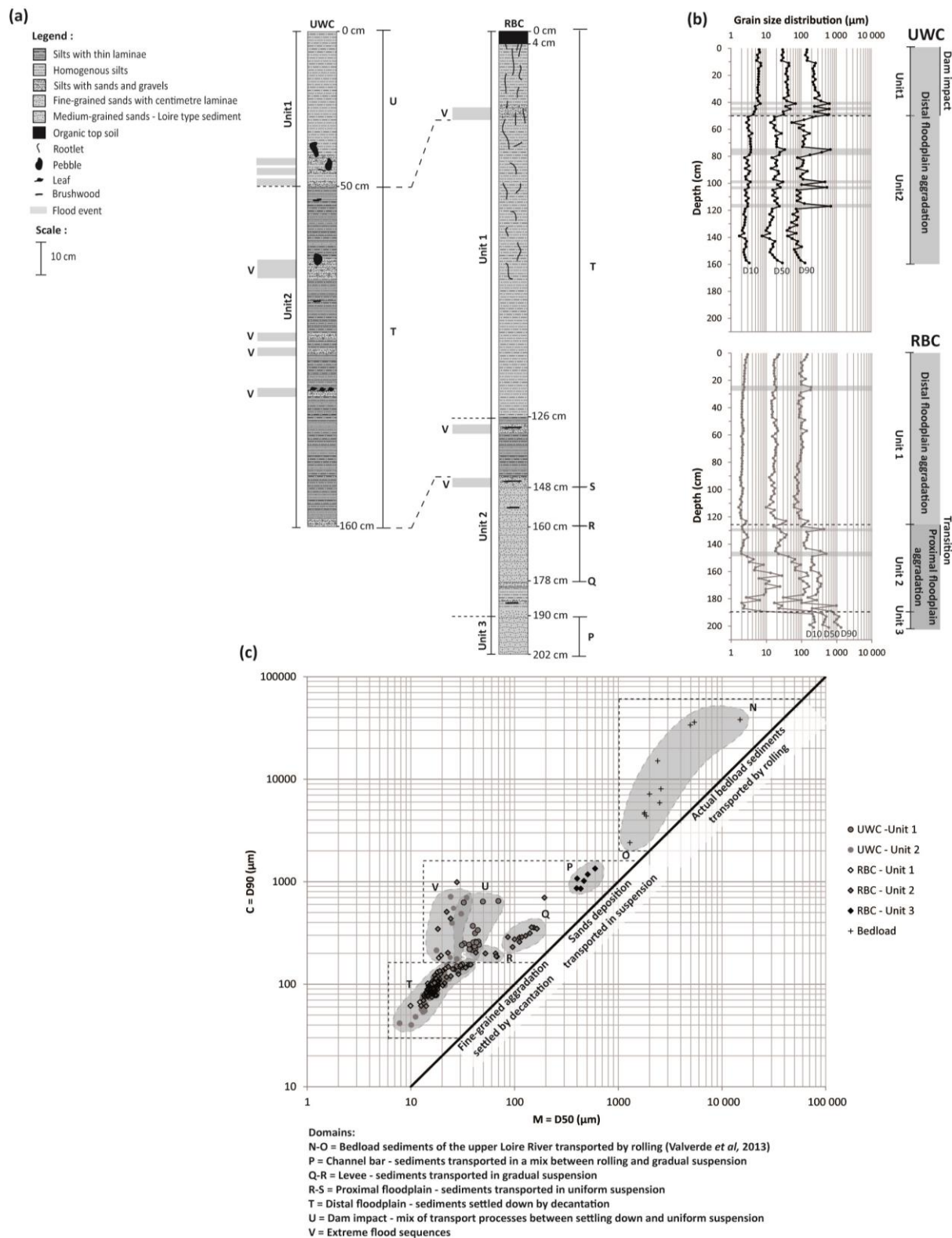


**Fig. 6.2:** **a-** Logs description, **b-** grain size distribution, and **c-** temporal evolution of settling conditions characterized with the C-M diagram (Passega, 1957, 1964).

It marks the first step of point bar formation as defined by Nanson and Page (1983).

Unit 2 (Fig. 6.2a) of the RBC (126-190 cm) is characterized by a high variability of grain size distribution delineating four progressive steps of proximal floodplain evolution. The 178-190 cm deep layer is very heterometric (composed of fine-grained sediments) and alternates with heterometric sandy layers (Tab. 6.1). This sub-unit has an erratic pattern in the C-M diagram and does not materialize specific domain. This high retention capacity of fine and coarse sediments is related to a vegetated filter effect (Rodrigues *et al*, 2007; Euler *et al*, 2014). The upper sub-unit (160-178 cm; Fig. 6.2a) is composed of fine-grained sands (Tab. 6.1). This sedimentary layer is in the Q-R domain on the C-M diagram (Fig. 6.2c) and is characterized by a distribution parallel to the C=M line. Sediments were transported by graded suspension and deposited in a levee. These first two sub-units (178-190 cm and 160-178cm) highlight the point bar accretion process during lateral migration of the river channel. The two next sub-units (148-160 cm and 126-144 cm deep) are composed of finer grained sediments. The interval at 148-160 cm deep is made

of a balanced proportion of fine-grained sands and fine-grained sediments (Tab. 6.1). In this layer, the M value varies by 56% without a specific bottom-up trend but the C value stays constant. It is located in the R-S domain in the C-M diagram (Fig 6.2c). Sediments were transported by uniform suspension during overbank floods and constituted a proximal top river bank aggradation. The last interval of unit 2 (126-144 cm; Fig. 6.2a) is a centimeter laminated and composed of fine-grained sediments (Tab. 6.1). There is less of a sandy fraction than in the sub-unit (148-160 cm), which is mainly represented by very fine-grained sands. This sub-unit transitions between uniform suspension and another domain, noted T in the C-M diagram (Fig. 6.2c), where fine-grained sediments settled during long inundation periods. These two last intervals correspond to a higher disconnection degree aggradation. The river bank begins to be too high or/and too far from the river channel to be regularly submerged by high-energy and turbulent flows transporting sediments by gradual suspension.

Sediments of the upper unit of the RBC (0-126 cm), noted unit 1 (Fig. 6.2a) and corresponding to the distal floodplain aggradation, are uniformly composed of

fine-grained sediments (Tab. 6.1). The sand fraction is low and largely composed of very fine-grained sands. This sedimentary unit fully constitutes domain T in the C-M diagram (Fig. 6.2c). Up to 80 cm deep, the exponential bottom-up increase of the TOC content combined with the relative abundance of roots and the apparent secondary porosity are evidence of soil formation. The 4 last centimeters correspond to a saturated organic top soil (water content > 87%; TOC > 3.5%).

The 160 cm long record of the UWC represents the entire column of fine-grained sediments settled in the paleochannel. The 2 last centimeters (158–160) contain heterometric sands and constitute the interface with the initial floor of this sedimentary trap. Two depositional processes occurred during the sedimentary infilling, corresponding to two sedimentary units (Fig. 6.2a).

The deepest unit of the UWC (Unit 2; 50–160 cm) is faintly laminated and has a texture comparable to the uppermost unit of the RBC (Tab. 6.2). This unit 2 is included in the same domain T of the C-M image as is the upper sequence of the RBC (Fig. 6.2c) aggraded by the settling of fine-grained sediments.

The upper unit of the UWC (Unit 1; 0–50 cm) is significantly different from unit 2, *i.e.*, a lack of laminations and a lesser abundance of fine-grained sediments (Tab. 6.2). The sandy fraction is mainly composed of fine-grained sands. Unit 1 is located in domain U in the C-M image (Fig. 6.2c), presenting coarser sediments when compared with the T domain. The aggradation of this unit results from a mix of settling of fine-grained sediments and uniform suspension of fine-grained sands. In this study, the Decize Dam was severely elevated in 1933 to increase river channel depth at the lateral canal lock. Because of this, another sedimentary process initiated and affected the UWC. The dam elevation may have induced slackwater deposition of fine-grained sands in the paleochannel by its downstream connection during high discharge levels.

As shown by Walling and He (1997) for surface sediments, long-term depositional processes are mainly influenced by the distance to the main river channel and, in a lesser way, the connection degree and floodplain topography. Low spatial and temporal variability of sediment textures inside the distal floodplain constitute a key point to sample representative sedimentary

archive. However, topography, such as local river planform changes, must be accounted for to understand sedimentary transitions, as the low topographic areas are more influenced by connection degree variations.

#### 6.3.1.2. *Extreme flood sequences as proxy of the archiving capacity*

The last domain defined in the C-M diagram, noted V (Fig. 6.2c), is characterized by a significant increase of C values, and stable M values. The V domain gathers layers enriched in heterometric sands with centimeter pebbles (Fig. 6.2a, Tab. 6.1 and 6.2). These layers are well recorded in the UWC at 114-118 cm, 102-104 cm, 98-100 cm, 74-80 cm, 48-50 cm, 44-46 cm and 40-42 cm. However, they are not well preserved in the RBC (present at 24-28 cm in the distal floodplain aggradation). RBC flood layers are also visible at 144-148 cm, 128-130 cm, corresponding to high energy inputs of sands (proximal floodplain aggradation; Fig. 6.2a).

Microfacies of archived extreme flood sequences can be related to observations from Walling et al. (1997), which highlights increasing grain sizes for the coarsest particles in contemporaneous flood deposits.

Even if the settling conditions are similar in the UWC and the RBC before dam elevation, why there are no flood sequences preserved in the RBC during distal floodplain aggradation?

In natural topographic depressions, such as abandoned channels (UWC), extreme flood records are described as sandy units composed of coarser particles than sediment deposited during standard overbank floods (Bábek *et al.*, 2011; Werritty *et al.*, 2006). The remobilization of trapped sediments is low in these former channels, even during extreme flood events, as shown by Dieras *et al.* (2013) in the Rhône River basin. However, preserving extreme flood deposits is limited in river banks (like RBC) because of strong erosion with these catastrophic discharges (Benedetti, 2003). Erosional control of river bank accretion is particularly strong for embanked rivers, as in the study area (Thompson and Croke, 2013; Fuller, 2008).

In the UWC, the preservation of flood sequences denotes a high level of archiving capacity and a nearly continuous record. In the RBC, their absence notes the importance of a topographic control on accretion and sediment preservation.

Depth (cm)	Age (y)	<sup>137</sup> Cs (Bq/kg)	D <sub>50</sub> (μm)	Sand (> 63 μm) (%)	Silt (2-63 μm) (%)	Clay (< 2 μm) (%)	Si (%)	Al (%)	TOC (%)	S tot. (%)	Hf (ppm)	As (ppm)	Bi (ppm)	Cd (ppm)	Cr (ppm)	Cu (ppm)	Hg (ppm)	Mo (ppm)	Ni (ppm)	Pb (ppm)	Sb (ppm)	Sn (ppm)	U (ppm)	W (ppm)	Zn (ppm)	
0-2	2012	7+-	0,6	23,0	25	69	6	26,50	7,33	4,03	0,08	10,9	27,9	1,3	1,0	123	32	0,195	1,1	40	72,0	2,1	20,6	9,2	6,5	196
2-4	2010	n.d.	n.d.	20,5	22	72	6	26,71	7,49	3,60	0,05	11,0	29,8	1,3	1,3	129	36	0,250	1,1	39	77,0	2,3	22,4	10,1	6,9	201
4-6	2001	n.d.	n.d.	17,0	20	74	7	26,93	7,72	3,49	0,06	10,4	31,3	1,4	1,2	132	37	0,270	1,2	40	79,1	2,4	23,7	9,5	7,1	201
6-8	1996	9+-	0,5	16,6	18	76	7	27,30	7,69	3,30	0,06	11,3	31,3	1,4	1,2	134	37	0,265	1,2	40	78,9	2,4	23,8	9,8	7,1	197
8-10	1990	n.d.	n.d.	16,2	18	75	7	27,03	7,89	3,19	0,08	10,6	32,6	1,5	1,1	139	39	0,290	1,2	43	82,6	2,5	24,6	9,7	7,6	209
10-12	1984	n.d.	n.d.	17,3	18	75	7	26,95	8,03	3,03	0,07	10,8	35,8	1,6	1,1	145	40	0,310	1,2	42	86,5	2,9	26,7	10,3	7,6	218
12-14	1978	9+-	0,4	16,9	19	74	7	26,58	8,25	2,71	0,07	10,5	40,6	1,3	1,1	133	48	0,420	1,2	43	83,8	3,0	45,3	10,4	8,0	199
14-16	1971	11+-	0,6	16,7	16	76	7	26,49	7,99	2,97	0,07	10,1	35,5	1,6	1,2	143	43	0,345	1,2	44	85,2	2,9	35,9	10,1	7,7	213
16-18	1964	12+-	0,6	17,3	19	74	8	26,48	8,02	2,99	0,07	10,6	35,3	1,6	1,1	139	44	0,365	1,3	43	83,2	2,7	32,8	10,4	7,8	208
18-20	1958	9+-	0,4	18,1	21	72	7	26,53	8,02	2,93	0,06	10,6	37,3	1,7	1,1	143	46	0,395	1,2	42	85,3	2,8	35,1	10,5	8,0	210
20-22	1952	10+-	0,5	17,3	18	74	8	26,43	8,05	2,92	0,07	11,4	40,1	1,7	1,1	150	48	0,380	1,3	45	88,5	3,1	37,9	11,2	8,5	219
22-24	1946	n.d.	n.d.	17,1	19	73	8	26,67	8,22	2,86	0,06	11,4	40,5	1,5	1,2	140	47	0,475	1,2	45	84,0	3,0	41,2	10,8	8,1	208
24-26	1940	5+-	0,3	19,6	24	68	8	26,79	8,03	2,92	0,07	10,3	36,5	1,7	1,2	150	42	0,330	1,2	45	88,8	2,8	29,9	10,3	7,9	213
26-28	1933	n.d.	n.d.	18,7	24	68	8	26,68	8,35	2,67	0,05	11,3	40,4	1,2	0,9	127	47	0,410	1,1	44	80,9	2,9	46,8	10,4	7,8	184
28-30	1931	n.d.	n.d.	15,1	18	74	9	26,68	8,40	2,60	0,06	10,5	38,5	1,2	0,8	124	46	0,400	1,0	42	78,1	2,8	46,5	10,1	7,5	172
30-32	1928	1+-	0,3	15,6	17	75	9	26,73	8,40	2,39	0,04	10,9	38,4	1,1	0,8	128	45	0,395	1,1	42	79,5	2,9	49,6	10,0	7,5	166
32-34	1925	n.d.	n.d.	17,4	21	71	8	26,37	8,57	2,32	0,05	9,8	39,4	1,1	0,7	129	44	0,405	1,1	42	80,6	3,0	53,7	9,9	7,6	167
34-36	1923	n.d.	n.d.	14,1	16	75	9	26,41	8,55	2,17	0,05	10,5	39,4	1,1	0,9	136	43	0,385	1,1	44	81,5	2,9	53,9	10,2	7,1	164
36-38	1920	< d.l.	0,5	14,2	15	76	9	26,58	8,62	1,98	0,06	11,2	37,3	1,1	0,7	131	40	0,370	1,0	43	79,1	2,8	53,2	10,1	6,7	155
38-40	1917	< d.l.	0,5	14,6	18	73	9	26,58	8,71	1,86	0,05	10,8	37,6	1,0	0,8	136	40	0,380	1,0	43	79,4	2,9	49,6	10,4	6,7	151
40-42	1914	n.d.	n.d.	14,4	16	74	9	26,47	8,69	1,79	0,05	10,7	36,4	1,0	0,8	132	37	0,350	0,9	43	75,9	2,6	41,9	10,5	6,6	144
42-44	1911	< d.l.	0,4	15,3	17	73	9	26,62	8,68	1,70	0,05	10,9	36,0	1,0	0,7	133	36	0,350	0,9	41	79,4	2,6	38,7	10,3	6,5	141
44-46	1908			14,6	16	74	10	26,63	8,65	1,62	0,02	11,8	37,0	1,0	0,9	131	36	0,340	1,0	44	76,1	2,6	32,3	10,7	7,0	138
46-48	1905			14,9	16	74	10	26,58	8,68	1,63	0,05	11,6	36,6	1,0	0,8	124	35	0,325	0,9	43	74,2	2,3	26,0	10,3	6,9	136
48-50	1902			19,3	23	68	9	27,23	8,60	1,08	0,03	13,0	32,7	0,9	0,7	106	28	0,255	0,9	41	63,8	2,0	14,4	10,7	6,3	121
50-52	1899			16,6	20	71	9	26,42	8,76	1,56	0,04	10,3	34,4	0,9	0,7	120	33	0,350	1,0	43	112,9	2,2	21,4	10,2	6,6	132
52-54	1896			18,0	20	71	9	26,61	8,71	1,55	0,04	11,9	36,3	0,9	0,7	113	32	0,395	1,0	42	66,4	2,2	19,4	10,4	6,5	129
54-56	1893			20,4	20	71	8	26,56	8,72	1,45	0,03	11,1	35,8	0,9	0,7	111	31	0,385	1,0	42	65,1	2,8	18,4	10,4	6,5	129
56-58	1891			21,5	25	67	8	26,46	8,75	1,56	0,04	10,8	34,3	0,9	0,6	106	30	0,300	0,9	42	63,2	2,1	16,1	10,4	6,6	127
58-60	1888			18,3	21	70	9	27,14	8,71	1,31	0,03	11,5	33,0	0,9	0,8	108	29	0,220	0,9	42	62,0	1,9	14,3	10,5	6,4	128
60-62	1885			14,8	18	72	10	26,49	8,66	1,59	0,04	12,5	34,9	0,9	0,7	121	33	0,315	1,0	43	182,4	2,3	25,7	10,6	6,9	133
62-64	1882			18,1	20	71	9	27,21	8,70	1,09	0,02	11,6	33,4	0,9	0,7	106	27	0,275	0,9	41	60,6	1,9	13,9	10,3	6,5	124
64-66	1879			18,7	22	69	9	27,71	8,73	0,91	0,04	12,2	31,2	0,9	0,5	103	27	0,175	0,9	41	57,6	1,8	12,7	10,2	6,2	124
66-68	1876			21,1	22	70	8	27,85	8,55	0,91	0,05	13,4	30,2	0,9	0,6	106	25	0,190	0,9	42	57,4	1,8	12,4	10,5	6,0	120
68-70	1873			19,0	22	69	9	27,69	8,66	0,86	0,05	11,4	30,5	0,8	0,6	101	27	0,180	0,9	43	55,8	1,8	11,8	10,0	6,0	122
70-72	1870			18,1	20	71	9	27,54	8,62	0,89	0,05	12,6	29,7	0,9	0,7	100	27	0,180	0,9	43	55,8	1,8	11,3	10,0	6,3	123
72-74	1867			18,5	20	71	9	27,68	8,61	0,80	0,06	12,3	30,2	0,8	0,6	101	27	0,145	0,8	43	55,7	1,8	12,2	10,3	5,9	126
74-76	1864			18,0	19	72	9	27,70	8,83	0,76	0,06	11,1	31,8	0,9	0,6	100	25	0,088	0,8	38	54,2	1,8	10,8	9,7	6,9	122
76-78	1861			15,8	18	72	10	27,48	8,84	0,70	0,06	11,6	32,0	0,9	0,6	101	25	0,079	0,8	41	53,9	1,9	10,6	9,9	5,7	121
78-80	1858			17,8	18	73	9	27,84	8,60	0,66	0,05	11,1	29,8	0,8	0,6	96	23	0,064	0,8	38	51,7	1,8	10,5	9,8	5,9	116
80-82	1855			16,4	15	75	9	27,90	8,68	0,77	0,06	11,5	29,9	0,9	0,6	99	24	0,077	0,8	39	53,4	1,8	10,6	10,3	5,9	117
82-84	1852			16,0	14	77	10	28,12	8,65	0,65	0,06	11,7	30,7	0,9	0,6	99	23	0,064	0,9	39	52,3	1,7	9,8	9,9	6,0	121
84-86	1849			16,7	15	75	9	27,77	8,69	0,68	0,04	12,1	29,0	0,9	0,5	99	23	0,073	0,9	39	51,4	2,0	10,2	9,9	5,7	114
86-88	1846			17,2	17	73	10	28,52	8,55	0,61	0,05	11,1	28,5	0,8	0,5	92	21	0,058	0,7	36	49,3	1,7	9,4	9,5	5,9	109
88-90	1844			14,6	14	76	10	27,90	8,76	0,68	0,06	11,2	29,8	0,8	0,6	96	23	0,058	0,7	38	51,8	1,9	10,0	9,8	5,9	119
90-92	1841			12,2	11	78	11	28,27	8,69	0,61	0,05	10,6	29,7	0,8	0,5	93	21	0,054	0,7	36	49,2	1,7	9,2	9,4		

**Tab. 6.1 - continued from previous page**

Depth (cm)	Age (y)	<sup>137</sup> Cs (Bq/kg)	D <sub>50</sub> (µm)	Sand (>63 µm) (%)	Silt (2–63 µm) (%)	Clay (<2 µm) (%)	Si (%)	Al (%)	TOC (%)	S tot. (%)	Hf (ppm)	As (ppm)	Bi (ppm)	Cd (ppm)	Cr (ppm)	Cu (ppm)	Hg (ppm)	Mo (ppm)	Ni (ppm)	Pb (ppm)	Sb (ppm)	Sn (ppm)	U (ppm)	W (ppm)	Zn (ppm)	
0-2	2012	6+	0,7	30,1	27	71	2	29,22	7,03	2,92	0,10	11,8	27,9	0,9	1,0	96	27	0,110	0,9	33	61,5	1,8	10,8	7,4	6,0	159
2-4	2009	n.d.	n.d.	31,2	28	70	2	28,50	7,10	3,11	0,09	11,0	29,1	1,0	1,0	101	33	0,130	0,8	35	68,4	1,8	13,4	7,9	6,7	174
4-6	2007	n.d.	n.d.	28,6	26	71	2	29,04	7,07	2,83	0,10	11,4	25,1	1,0	1,0	101	31	0,115	0,8	35	66,2	1,8	11,7	7,6	6,4	166
6-8	2005	n.d.	n.d.	31,2	29	69	2	29,98	7,01	2,49	0,09	13,1	24,4	0,9	1,0	101	29	0,120	0,7	34	65,2	1,8	11,4	8,3	6,1	160
8-10	2002	n.d.	n.d.	27,8	26	71	3	30,51	6,92	2,18	0,08	15,2	24,0	0,9	0,8	99	29	0,150	0,7	35	66,6	1,8	11,9	8,7	6,0	155
10-12	1999	7 +	1 +	44,9	41	57	2	30,56	6,94	2,09	0,08	15,0	23,7	0,9	0,8	99	28	0,105	0,8	34	66,2	1,7	12,6	8,7	6,3	149
12-14	1997	5 +	0,5	45,5	41	57	2	30,45	7,02	2,21	0,09	13,3	23,2	1,0	0,9	103	28	0,110	0,8	35	66,7	1,9	13,3	8,5	6,4	161
14-16	1994	7 +	0,8	39,2	37	60	2	30,32	7,09	2,21	0,10	15,7	24,4	1,0	1,0	119	30	0,280	0,9	40	78,9	1,9	13,5	9,6	6,5	170
16-18	1991	n.d.	n.d.	39,5	37	60	2	30,02	7,13	2,19	0,11	14,7	26,4	1,0	1,1	162	34	0,180	1,1	48	104,2	2,0	14,8	9,1	6,8	194
18-20	1987	9 +	0,5	36,8	36	62	2	30,15	7,08	2,15	0,10	16,3	25,5	1,2	1,2	167	30	0,200	1,1	50	112,2	1,9	14,8	10,1	6,5	196
20-22	1984	9 +	0,7	41,8	39	58	2	30,23	7,15	2,24	0,10	15,9	25,4	1,1	1,1	177	36	0,220	1,1	52	143,6	2,2	15,7	9,6	6,7	212
22-24	1981	n.d.	n.d.	42,1	40	58	2	30,05	7,18	2,31	0,11	15,0	28,4	1,5	1,3	209	40	0,255	1,1	57	199,5	2,2	16,9	9,1	6,8	238
24-26	1978	12 +	0,8	36,8	35	62	2	30,66	7,10	2,17	0,11	16,6	26,7	1,4	1,3	202	36	0,185	1,1	57	252,9	2,1	15,0	9,3	6,7	229
26-28	1974	13 +	0 +	41,2	39	58	2	30,75	7,16	2,05	0,11	14,9	26,8	1,6	1,2	181	35	0,185	1,1	52	255,4	2,1	17,3	9,0	7,7	225
28-30	1969	14 +	1 +	40,1	38	59	3	30,76	7,16	2,04	0,12	15,0	24,8	1,5	1,2	161	33	0,195	1,0	49	201,8	2,1	14,8	9,0	6,7	231
30-32	1964	17 +	0,8	43,1	41	57	3	30,64	7,24	1,98	0,11	16,1	25,4	2,3	1,4	156	34	0,170	1,1	47	193,7	2,2	15,4	10,0	7,2	239
32-34	1960	12 +	1 +	41,6	40	58	2	29,94	7,30	2,22	0,14	17,1	28,9	1,7	1,8	178	42	0,330	1,2	58	170,0	2,3	16,6	11,1	7,4	359
34-36	1957	12 +	1 +	44,3	41	57	2	29,99	7,39	2,68	0,20	15,4	33,6	2,7	2,4	222	57	0,255	1,4	77	133,9	3,0	21,2	10,6	7,7	536
36-38	1955	9 +	0,7	32,6	31	66	3	28,45	7,56	3,74	0,38	12,9	39,4	3,4	3,0	240	89	0,575	2,0	89	107,2	4,1	24,7	15,4	8,8	614
38-40	1952	n.d.	n.d.	39,7	39	59	2	27,61	7,69	4,61	0,47	12,0	41,7	2,9	2,8	244	110	0,720	2,4	93	106,2	4,8	29,6	19,2	8,8	599
40-42	1948	< d.l.	1 +	69,9	52	46	2	27,45	7,76	4,85	0,45	11,7	41,1	2,8	2,4	218	114	0,895	2,3	83	96,6	4,6	29,0	18,2	8,4	543
42-44	1944	n.d.	n.d.	36,4	37	60	3	28,03	7,77	4,14	0,35	16,0	33,4	1,3	1,4	129	95	0,570	1,5	51	84,9	3,7	38,1	12,2	7,2	292
44-46	1940	n.d.	n.d.	49,7	45	52	3	28,25	7,99	3,02	0,30	13,3	32,4	1,0	1,0	127	66	1,080	1,2	41	91,2	3,6	55,8	10,4	7,3	200
46-48	1936	< d.l.	1 +	31,1	32	64	3	28,24	8,03	2,62	0,18	13,7	27,6	1,0	0,9	126	52	0,410	0,9	39	87,0	2,9	60,7	10,4	6,7	180
48-50	1933	n.d.	n.d.	32,4	37	60	3	27,70	8,36	2,89	0,21	11,7	32,7	1,0	0,8	132	48	0,450	1,0	40	90,7	3,1	71,3	9,6	6,8	179
50-52	1931	n.d.	n.d.	17,7	21	74	5	26,25	8,96	2,31	0,15	8,6	30,1	1,0	0,6	171	43	0,420	0,9	45	91,7	3,0	58,9	8,3	5,8	162
52-54	1930	< d.l.	1 +	17,5	19	77	5	26,38	8,80	2,65	0,13	8,5	31,7	1,0	0,7	181	45	0,480	0,9	43	109,4	3,6	77,2	8,2	5,6	160
54-56	1928	n.d.	n.d.	13,7	8	86	6	26,14	9,03	2,58	0,11	7,5	29,3	1,1	0,6	172	69	0,505	1,0	41	114,0	3,9	81,9	8,5	6,1	181
56-58	1927	n.d.	n.d.	18,0	19	76	5	27,18	8,49	2,37	0,10	8,8	29,2	1,1	0,7	177	38	0,470	1,0	38	112,2	3,4	64,9	8,6	6,5	157
58-60	1925	< d.l.	1 +	16,7	15	79	5	27,25	8,66	2,04	0,07	8,7	23,3	0,9	0,5	159	34	0,395	0,8	41	84,2	2,5	29,0	8,7	6,0	140
60-62	1922			19,6	20	75	5	27,24	8,63	2,21	0,08	9,5	23,4	1,0	0,5	157	35	0,465	0,9	40	80,5	2,4	26,6	9,0	5,7	142
62-64	1920			27,8	31	65	4	28,09	8,33	2,12	0,07	11,7	22,9	0,9	0,6	158	33	0,435	0,8	37	79,3	2,7	22,2	9,4	5,9	132
64-66	1918			19,0	21	74	5	27,99	8,31	2,17	0,09	10,5	27,0	0,9	0,6	175	36	0,450	0,8	38	78,1	2,6	23,3	9,4	6,3	145
66-68	1917			21,1	23	73	4	27,80	8,33	2,26	0,09	10,0	29,4	1,0	0,6	165	37	0,405	0,7	39	75,1	2,3	22,1	8,8	6,0	143
68-70	1915			20,1	21	75	4	27,82	8,27	2,37	0,09	10,3	29,4	0,9	0,6	157	36	0,410	0,8	40	73,5	2,3	20,8	9,0	5,9	140
70-72	1913			20,0	21	75	4	27,38	8,37	2,26	0,10	9,8	29,7	0,9	0,6	152	36	0,385	0,8	39	73,5	2,3	20,9	9,1	6,1	141
72-74	1910			20,3	20	76	4	26,71	8,64	2,29	0,11	9,4	28,6	0,9	0,6	120	32	0,315	1,1	41	66,1	2,0	15,1	8,9	5,7	137
74-76	1907			34,5	40	56	4	27,50	8,51	1,99	0,08	10,4	26,8	0,9	0,6	97	29	0,275	0,9	37	64,6	2,0	12,7	9,5	5,8	136
76-78	1907			25,0	30	66	4	27,41	8,53	2,05	0,08	10,4	25,2	0,8	0,6	98	27	0,250	0,8	39	61,5	1,7	11,8	9,2	5,8	128
78-80	1907			24,0	29	66	5	27,26	8,42	2,12	0,08	10,7	24,1	0,8	0,5	95	25	0,225	0,7	38	58,3	1,7	10,9	8,9	6,3	122
80-82	1903			14,9	14	79	7	27,40	8,62	1,84	0,06	9,7	23,4	0,9	0,5	97	26	0,235	0,7	39	55,6	1,6	10,7	8,4	6,3	127
82-84	1899			20,7	22	72	5	27,40	8,54	1,52	0,07	11,4	25,7	0,9	0,5	92	25	0,290	0,7	37	61,4	1,8	10,9	9,2	7,4	127
84-86	1895			18,9	20	74	6	26,72	8,20	1,38	0,07	9,8	27,6	0,9	0,5	92	25	0,485	0,8	35	64,6	1,9	11,9	8,4	6,8	126
86-88	1891			20,4	20	75	5	27,93	8,24	1,29	0,06	10,4	25,7	0,8	0,5	90	24	0,555	0,6	36	63,1	1,6	10,5	8,4	6,2	121
88-90	1888			14,1	13	80	7	27,17	8,49	1,39	0,08	9,2	28,8	0,9	0,6	93	25	0,605	0,7	37	69,3	1,8	11,5	8,3	6,4	131
90-92	1885			22,4	24	72	5	28,55	8,54	1,20	0,06	12,4	34,5	1,0	0,7	98	24	0,425	0,8	37	80,3	2,1	13,			

Depth (cm)	Age (y)	<sup>137</sup> Cs (Bq/kg)	D <sub>50</sub> (µm)	Sand (> 63 µm) (%)	Silt (2-63 µm) (%)	Clay (< 2 µm) (%)	Si	Al	TOC	S tot.	Hf	As	Bi	Cd	Cr	Cu	Hg	Mo	Ni	Pb	Sb	Sn	U	W	Zn
100-102	1861		21,4	21	74	5	28,00	8,72	1,12	0,05	12,4	30,2	1,0	0,6	93	24	0,066	0,9	36	60,2	2,2	11,4	9,6	6,5	109
102-104	1856		25,9	33	62	5	27,34	8,87	1,14	0,08	9,9	31,4	1,1	0,6	91	24	0,060	0,9	37	60,2	1,9	10,8	8,5	6,6	114
104-106	1854		15,7	14	80	7	28,32	8,75	1,00	0,07	9,6	29,6	1,1	0,5	91	23	0,058	0,9	35	61,7	2,0	11,8	8,6	7,0	110
106-108	1853		18,0	17	77	6	28,11	8,71	1,08	0,06	9,7	28,4	1,0	0,6	89	23	0,063	0,8	35	59,4	1,9	10,8	8,1	6,4	109
108-110	1851		15,5	13	80	7	28,18	8,68	0,99	0,06	10,7	28,9	1,0	0,6	89	22	0,051	0,8	35	58,0	1,7	10,8	8,5	6,2	108
110-112	1850		21,3	19	76	5	27,95	8,73	0,99	0,06	10,4	31,9	1,0	0,6	101	24	0,049	0,9	41	59,6	2,0	11,4	8,9	6,0	117
112-114	1848		17,7	15	79	6	28,42	8,45	0,95	0,04	10,9	29,4	0,9	0,6	91	21	0,045	0,9	38	55,9	1,8	10,5	8,5	6,1	106
114-116	1846		21,0	22	73	5	27,44	8,96	1,07	0,04	9,2	31,7	1,0	0,6	97	25	0,067	1,0	41	58,7	1,8	10,4	8,4	5,8	120
116-118	1846		24,2	30	65	6	29,10	8,44	0,88	0,05	10,8	29,7	0,9	0,5	89	20	0,036	0,8	33	56,7	1,9	9,9	9,1	6,3	100
118-120	1843		15,1	13	80	7	27,51	8,69	1,09	0,06	8,9	33,1	1,2	0,6	90	22	0,049	0,9	37	59,2	2,0	10,9	8,4	6,3	112
120-122	1840		14,9	15	78	7	27,81	8,69	1,10	0,06	9,2	35,4	1,1	0,6	94	22	0,047	0,9	36	62,3	2,4	11,3	8,6	7,3	116
122-124	1837		12,8	9	83	8	27,87	8,73	1,08	0,06	9,2	35,6	1,1	0,6	89	23	0,045	0,9	35	63,3	2,5	10,9	8,8	7,5	118
124-126	1833		16,2	15	79	7	27,38	8,59	1,01	0,05	9,4	33,0	1,1	0,6	91	22	0,043	0,8	36	60,4	2,2	10,5	8,6	6,9	111
126-128	1830		14,7	13	80	7	27,02	8,80	1,03	0,06	8,5	32,7	1,0	0,6	92	25	0,051	0,8	36	61,4	2,1	10,9	8,6	7,1	126
128-130	1827		13,2	8	86	7	26,85	8,85	1,27	0,06	8,7	32,6	1,0	0,6	89	23	0,046	0,9	37	58,5	2,0	10,6	8,5	6,8	116
130-132	1824		13,1	13	80	7	26,59	9,18	1,13	0,07	7,7	37,1	1,1	0,5	97	26	0,050	1,0	40	60,1	2,0	11,0	7,9	6,9	127
132-134	1821		11,1	6	85	8	26,89	9,17	1,31	0,07	7,5	35,7	1,1	0,6	92	25	0,055	0,9	38	61,2	2,0	11,1	7,9	7,4	125
134-136	1819		10,1	4	87	9	26,62	9,28	1,27	0,05	7,0	36,3	1,1	0,6	93	25	0,049	0,9	38	61,4	2,1	11,7	7,8	7,4	127
136-138	1816		12,9	12	81	7	26,41	9,40	1,25	0,07	7,1	33,4	1,0	0,4	103	27	0,051	1,0	44	54,2	2,0	10,1	8,4	6,5	139
138-140	1813		7,8	6	82	12	26,68	9,36	1,23	0,07	6,8	36,5	1,0	0,5	96	26	0,044	1,0	38	58,4	2,2	10,2	8,4	6,7	132
140-142	1810		12,7	9	85	7	27,30	8,78	1,29	0,07	8,1	31,5	0,9	0,5	94	23	0,053	0,8	37	55,0	1,9	9,2	8,2	6,0	128
142-144	1807		18,1	15	79	6	28,01	8,60	1,14	0,06	10,4	28,9	0,8	0,5	95	23	0,046	0,8	36	54,7	2,0	9,8	9,0	6,0	125
144-146	1804		15,6	13	80	7	27,59	8,75	1,13	0,06	9,5	28,3	0,8	0,5	96	23	0,047	0,8	37	56,4	2,1	9,6	9,2	6,2	130
146-148	1800		16,1	17	77	6	28,41	8,63	1,01	0,05	10,7	26,7	0,8	0,5	93	22	0,042	0,7	36	52,4	1,8	8,6	9,2	5,8	119
148-150	1797		13,8	10	82	7	27,33	8,77	1,02	0,05	9,7	27,0	0,8	0,5	103	24	0,047	0,8	41	52,4	1,6	8,2	8,7	5,2	125
150-152	1794		13,0	12	80	8	27,83	8,66	0,98	0,06	10,6	26,7	0,8	0,5	99	22	0,042	0,8	39	52,7	1,6	8,0	9,0	5,3	120
152-154	1791		15,5	14	78	7	27,79	8,72	0,97	0,05	10,7	27,5	0,9	0,5	100	23	0,044	0,8	40	57,8	1,8	8,6	9,2	5,6	121
154-156	1787		17,6	17	77	7	27,92	8,72	0,88	0,02	11,2	26,5	0,8	0,4	102	22	0,039	0,9	39	51,4	1,8	8,1	9,1	5,3	117
156-158	1783		21,1	20	73	6	28,45	8,46	0,85	0,03	13,0	24,5	0,8	0,4	100	21	0,032	0,8	39	52,4	1,7	8,3	10,2	5,1	112
158-160	1778		29,7	30	66	5	29,40	8,13	0,75	0,03	18,3	23,2	0,7	0,5	98	18	0,026	0,7	36	50,9	1,7	8,1	12,8	5,5	105
d.l.																									
0,01																									
5																									
0,001																									
0,5																									
5																									
0,7																									
0,2																									
0,5																									
0,1																									
0,3																									

**Tab. 6.2 – continued from next page**

### ***6.3.2. Time correlation and mass accumulation rate comparisons***

#### ***6.3.2.1. Time correlation of sedimentary archives***

In addition to archiving capacity and accretion continuity, the aggradation rate is an important factor influencing the resolution of temporal analyses. Spatial and temporal variability of aggradation rates across the floodplain can be highlighted by comparing the two cores. The first step of this analysis consists on a time correlation using specific temporal anchoring markers.

First, based on  $^{137}\text{Cs}$  vertical profiles, specific time markers can be defined. In these cores, the  $^{137}\text{Cs}$  is not detectable less than 36 cm deep in the RBC and 40 cm deep in the UWC (Tab. 6.1 and 6.2). Sediments archived below these depths were settled before 1950, which was the date of the first important Nuclear Weapon Test (NWT). Gamma activities, measured between the surface and 36 or 40 cm deep, have large peaks at 16-18 cm deep for RBC and at 30-32 cm deep for the UWC (Tab. 6.1 and 6.2). These sedimentary layers can be associated with the NWT maximum fallouts in 1964. The study area was barely impacted by the

Chernobyl Nuclear Power Plant Disaster (C-NPPD) fallout of 1986 (De Cort *et al*, 1998). The measured  $^{137}\text{Cs}$  patterns do not involve secondary peaks related to this event.

To refine the time correlation, additional relative time markers can be determined with sedimentary records associated to well dated hydrosedimentary events, such as flood events or climate and anthropogenic river forcing. The Decize Dam elevation of 1933 should influence sedimentation up to 50 cm deep for the UWC. In the upper unit of the RBC, only one sandy layer is recorded at 24-28 cm, likely related to the Decize Dam elevation, which should have triggered better preservation conditions. This hydrosedimentary event may be correlated to the three coarsest layers archived in the dam impacted unit of the UWC (48-50 cm, 44-46 cm and 40-42 cm; Fig. 6.2). The sedimentary transition dating is consistent with the  $^{137}\text{Cs}$  absence under 40 cm (< 1950) in the UWC. However, this time correlation holds for the RBC, where the  $^{137}\text{Cs}$  vertical distribution does not conform to the common pattern described in the literature ( $^{137}\text{Cs}$  peak at 16-18 cm and some radionuclide was detected until 36

cm). In the pedogenetic context of the top 80 cm of the RBC, the  $^{137}\text{Cs}$  vertical profile has to be interpreted cautiously because of roots and macrofauna bioturbation associated with solute transport. All of these mechanisms may be responsible for the downward migration of the radionuclide (Détriché *et al.*, 2010; Matisoff *et al.*, 2011). Additionally, the four flood sequences in the deepest unit of UWC at 114-118 cm, 102-104 cm, 98-100 cm, and 74-80 cm deep, can be dated to be 1846, 1856, 1866 and 1907, respectively, which are the four catastrophic floods events documented at the Decize gauging station.

#### *6.3.2.2. Temporal and spatial variability of the mass accumulation rate*

To compare the aggradation rhythm between the two cores, age-models can be set up between time markers. Age-models are built using mass accumulation rates (MARs), calculated between each dated level. The sandy sequence of the proximal floodplain aggradation, of the RBC, is considered contemporary at the end of the LIA (between 1760 and 1820). Detailed age models are only defined for the fine-

grained sedimentation, *i.e.*, the whole UWC core and up to 144 cm for the RBC.

To refine the age-model, dates were calculated with respective MARs calculated between each date-bounded. For the UWC, a constant MAR of  $1.3 \text{ kg.m}^{-2}.\text{y}^{-1}$  can be calculated between the 2012 and the 1933 time marker, both bounding the upper unit. However, the MAR varies by 8% of this value by focusing on the 2012-1964 period or the 1964-1933 period (Fig. 6.3). The maximum error associated with these estimates is  $\pm 6$  years. For the deepest unit of the UWC, a constant MAR of  $2.3 \text{ kg.m}^{-2}.\text{y}^{-1}$  is calculated between the 1933 and the 1846 time marker. More precisely, the MAR ranges between 1.7 and  $4.4 \text{ kg.m}^{-2}.\text{y}^{-1}$  between dated flood sequences (Fig. 6.3). The maximum time deviation corresponding to this variability reaches 11 years. There is no time marker below the 118 cm deep sedimentary level (1846), but the age-model can be extended given the lack of sedimentary variations to the core bottom. Therefore, a constant MAR of  $2.3 \text{ kg.m}^{-2}.\text{y}^{-1}$  allows the dating of the core base at approximately  $1778 \pm 11$  years. This result is consistent with the previously mentioned morphodynamic evolution of the floodplain and, therefore, the UWC can be

considered as a complete sequence of fine-grained aggradation.

For RBC, accurate dating based on a constant rate of accumulation between two date-bounded lacks may be less robust because there is no linear accretion caused by erosional processes controlling the river bank vertical accretion. Without considering this limit, the MAR reaches  $2.4 \text{ kg.m}^{-2}.\text{y}^{-1}$  between the 1933 and 2012 time markers. During this period, the MAR varies a maximum of 12,5% of this value, which induces an associated error of 4 years (Fig. 6.3). To date the 28-144 cm sequence, we correlated the base of the two archives at approximately  $1778 \pm 11$  years and defined this date to be the beginning of fine-grained aggradation. In this sequence, the MAR reaches  $6.2 \text{ kg.m}^{-2}.\text{y}^{-1}$  with a maximum error of  $\pm 11$  years.

The proximal floodplain aggradation in the RBC, which lasted at least from the 1760s to the late 1770s, has a MAR of  $17.4 \text{ kg.m}^{-2}.\text{y}^{-1}$ , materializing an important sediment transport at the end of the LIA and a MAR gradient from the proximal to distal floodplain. A similar spatial variability was shown by Walling and He (1998) at a floodplain scale.

For fine-grained sedimentation, MARs estimated over the 234 years for the two archives ( $4.9 \text{ kg.m}^{-2}.\text{y}^{-1}$  for RBC and  $2.0 \text{ kg.m}^{-2}.\text{y}^{-1}$  for UWC) are comparable with values generally calculated in floodplains (e.g., 1.0 to  $6.6 \text{ kg.m}^{-2}.\text{y}^{-1}$  by Walling and He, 1997; 0.7 to  $5.9 \text{ kg.m}^{-2}.\text{y}^{-1}$  by He and Walling, 1996). In this study, the MAR is more than 2 times larger for the RBC than for UWC (3 times larger for cum). During overbank floods, important differences of sediment deposition rates exist between morphological units at the floodplain scale, not necessarily correlated to ground-level elevation (Baborowski *et al*, 2007). Walling and He (1997; 1998) explained that the large MAR variability detected in distal floodplains is usually controlled by connection degree variations (with the river channel) rather than topographical forcing. Natural depressions, such as paleochannels, do not necessarily have the highest accumulation rates because their connectivity with the main channel limits fine-grained deposition compared to their outer margins. During overbank floods, sediment deposition is less important in the UWC than the RBC because transported sediments are evacuated by the downstream connection before

settling. However, stored sediments are better preserved long-term in the paleochannel than in a river bank.

During the archived period, the MAR is not constant for the two cores. The Decize Dam elevation in 1933 moderates the MAR by 44% in the UWC and even more in the RBC (-68%), highlighting the dramatic reduction of overbank inputs for

the river bank. The reduction in the magnitude and the frequency of overbank floods, or/and decline of transported sediment recorded since the 19<sup>th</sup> century and the second part of the 20<sup>th</sup> century in many anthropized rivers, can explain this trend (Owens *et al*, 1999; Arnaud-Fassetta, 2003; Benetti, 2003; Lecce and Pavlowsky, 2004; Du and Walling, 2012).

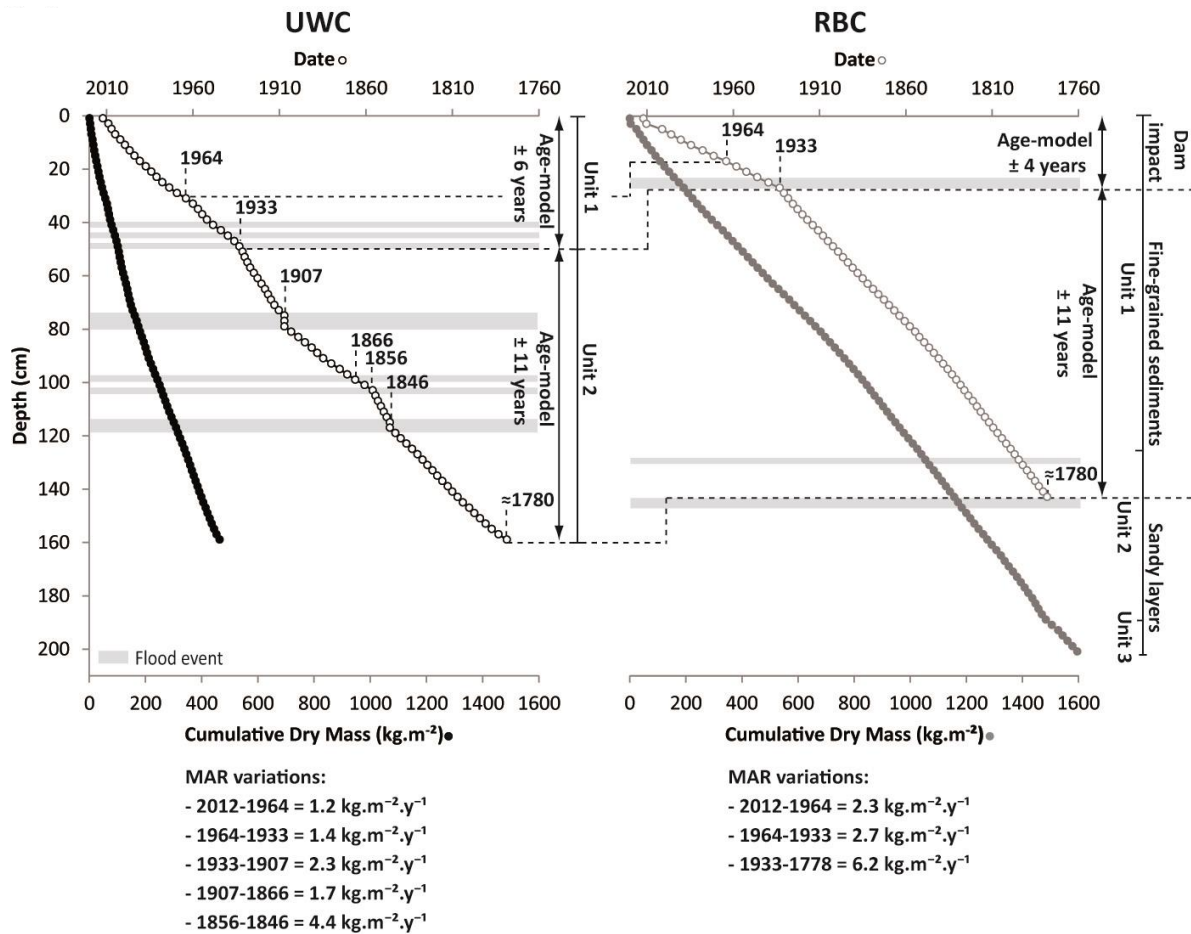


**Fig. 6.3:** Time correlation, age model definition and mass accumulation rates temporal variations in the two cores.

### **6.3.3. Influences of archiving processes on geochemical patterns**

#### **6.3.3.1. Comparison of the local geochemical background in fluvial environments**

Depositional environments influence sediment texture and aggradation rate, but can they control geochemical composition? For the sandy Loire River, variations of Si/Al ratios and some Rare Earth Elements (REE), such as Hf and Sm concentrations, can be used as tracers of silico-clastic and heavy mineral inputs, even in the < 63 $\mu$ m fraction (Dhivert *et al*, 2015).

In this study, Si/Al ratios and Hf concentrations are significantly correlated in both cores ( $r = 0.9$ ,  $p < 0.05$ ,  $n = 181$ ). However, significant differences in their geochemical profiles are observed between sediments deposited in the proximal floodplain (126-202 cm in the RBC) and those archived in the distal floodplain (0-126 cm for the RBC and 50-160 cm before the dam elevation of 1933 for the UWC; Fig. 6.4, Tab. 6.1 and 6.2).

During proximal floodplain aggradation (only in the RBC), Si/Al ratios and Hf concentrations have the maximum

values of all profiles and are highly variable (Fig. 6.4). Si/Al ratios and Hf concentrations decrease from the bottom to 126 cm according to a fining upward trend ( $r = 0.6$ ,  $p < 0.05$ ,  $n = 33$  with  $D_{50}$ ). In this dynamic environment, sediments (essentially sands) are mainly composed of Si-rich detrital particles and REE-rich heavy minerals.

During distal floodplain aggradation, both cores have lower Si/Al ratios and Hf concentrations with much smaller variations than in the proximal floodplain (Fig. 6.4). Sediments are poorer in Si-rich sands and REE-rich heavy particles in favor of fine-grained sediments, and richer in Al. Additionally, for the UWC, the 0-50 cm sediment layers, deposited after 1933, have Si/Al ratios and Hf concentrations similar to the proximal floodplain environment of the RBC (Fig. 6.4). The 0-50 cm levels are coarser compared to sediments archived below because of slackwater deposition of fine sands after the elevation of the dam.

The sandy fraction of the Loire River sediments mobilized during high discharge events are composed of Si-rich minerals, such as quartz and REE-rich heavy minerals. In the fining upward sequence recorded in the proximal

floodplain, (Si, REE)-rich sands are less present. This is the result of a bottom-up decreasing trend of the depositional environment energy. A progressive disconnection of the river bank induces a change in the grain size and mineralogical composition. However, fine-grained sediments settled in a low-energy distal floodplain in a highly disconnected environment with a homogenous mineralogical composition. After the dam elevation, the connection degree

enhanced in the UWC, and the sandy fraction composed of (Si, REE)-rich minerals is more expressively represented.

These results highlight a high variability of detrital material input, influencing the mineralogical and the geochemical signatures across a floodplain, even in the  $< 63 \mu\text{m}$  fraction. The mineral distribution depends on the connection degree in the depositional environment.

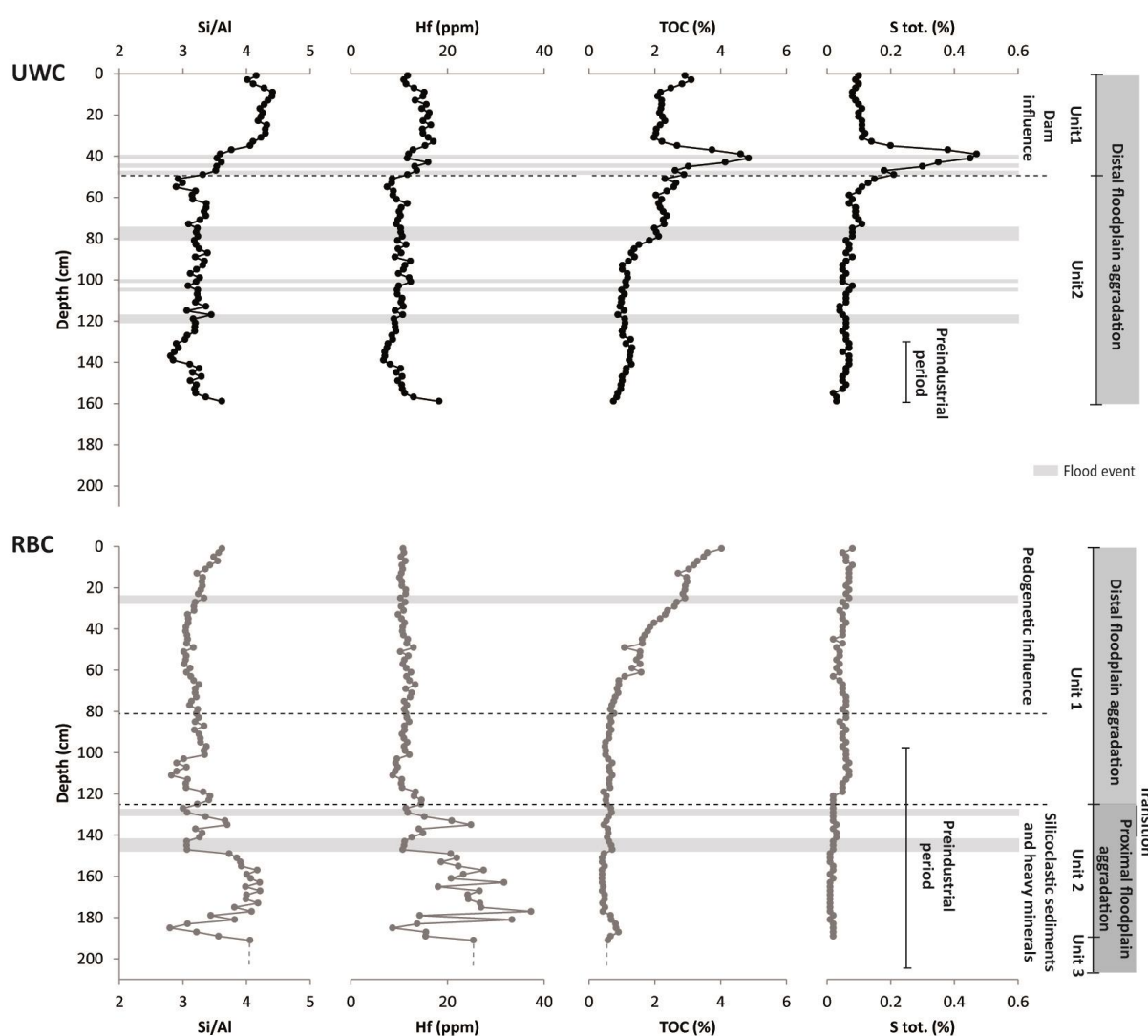


**Fig. 6.4:** Vertical profiles of Si/Al ratio, Hf, TOC and S concentrations for the two cores.

Additionally, sediments deposited during the preindustrial period allows for the definition of natural TE concentrations specific to the local geochemical background. In this study, these sediment layers can be used to highlight the influences of depositional environments on measured preindustrial concentrations. Therefore, sediments older than the 1830s (100-202 cm for the RBC; 128-160 cm for the UWC) are considered. The background levels could have been affected by the first coal mining activities in the upstream basin (Woronoff, 1994, French coal mining agency, 2013). In the distal floodplain environment, Al concentrations and TE concentrations are very similar along both cores (Tab.6.3). The two cores have similar concentrations with median differences less than 11% for all of the cited TE. No significant differences in TE distributions ( $p > 0.05$ ,  $n = 28$ ) were noted, except for Pb and U. Therefore, the local geochemical background can be well defined in this highly disconnected context because the mineralogical composition of settled fine-grained sediments is homogenous across the distal floodplain and stable over the registered period.

In the proximal floodplain sequence (only in the RBC), the chemical

composition is more variable than in the distal floodplain (Tab.6.3). This can be related to the mineralogical sorting associated with river bank accretion. This process results in accumulated sediments during overbank floods. However, the geochemical compositions of deposited sediments in the proximal floodplain depend on flood magnitudes and river morphology (Brich et al, 2000; Martin, 2000). Considering the influence of the energetic gradient on particle mineralogy and induced chemical variability in the proximal floodplain sequence, measured geochemical backgrounds are less representative than in the distal environment. Distributions of TE concentrations measured in the proximal floodplain are significantly different from those in the distal floodplain ( $p < 0.05$ ,  $n = 61$ , except for Cr and Ni). However, TE concentrations are in the same range of magnitude in both depositional environments, except for Cd, U, Hg and, to a lesser extent, Sn. They present over-ranges of 77%, 111%, 65%, and 52%, respectively, compared to the distal floodplain maximum. The differences between the two depositional environments could be related to mineralogical sorting from the proximal to distal floodplain. Cd and U are significantly

correlated to Hf concentrations ( $r = 0.9$ ,  $p < 0.05$ ,  $n = 61$ ). Cadmium and U enrichments in the proximal floodplain sediments can be explained by a higher percentage of their heavy mineral hosts in the sandy fraction, *i.e.*, zircons, barites, phosphorites and Ti-bearing heavy minerals (Dill, 2010).

Intra-site variability of natural TE concentrations exists at a local scale between sediments deposited in the proximal and the distal floodplain, but what do they represent when compared with inter-site differences? To answer this question, the defined local background concentrations can be compared to preindustrial TE levels in fine-grained sediments archived at the most downstream station of the basin (Grosbois *et al*, 2012) and are representative of an average background at the entire Loire Basin scale (Tab. 6.3). Enrichment factors (EF) were calculated using the double normalization of Al contents and the preindustrial TE levels. For Bi, Cr, Cu, Ni, Sn, U, W and Zn, the EFs are close to 1 for deposited sediments in both distal and proximal floodplain environments. The local geochemical background for this TE is then similar to the one assumed for the basin. For Cd and U unit, EFs are verified in

the distal environment, but have significant differences in the proximal environment ( $p < 0.05$ ,  $n = 61$ , EF ranged between 1 and 4 for Cd, 1 and 3 for U). In the Loire Basin, the mineralogical variability linked to proximal environment dynamics induces larger geochemical variations in the Cd and U concentrations than the upstream-downstream gradient because of heavy mineral relative abundances. For distal and proximal environments, As, Hg, Mo and Sb have light enrichments in sedimentary levels older than the 1830s (EF ranged between 1 and 6). Preindustrial Hg concentrations in the UWC and the RBC are low and similar to those archived in the downstream part of the Loire Basin. The reason for Hg enrichments is not significant (Tab. 6.3). However, for As, Mo and Sb, enrichments can be related to a local geochemical anomaly 50 km upstream of the study station, associated with Variscan hydrothermal mineralization, which could provide (As-Mo-Sb)-rich chalcopyritic bearing phases (Delfour *et al*, 1984).

Because of the mineralogical sorting in the  $< 63 \mu\text{m}$  fraction of floodplain sediments, the geochemical background measured in fine-grained

sediments settled in the distal environment can be considered more representative of the basin scale. With the exception of specific local enrichments caused by geochemical anomalies, preindustrial concentrations in the upstream part of the Loire Basin are similar to those of the downstream basin. These results provide evidence for an average background reference at the basin scale and will be further used in this study.

#### *.6.3.3.2. Influence of archiving processes on anthropogenic TE variations*

Archiving processes and associated connection degree variations influence sediment accumulation rates, major elements and natural TE levels. They can induce temporal discrepancies in anthropogenic TE variations. Because of this, archived TE temporal dynamics could be related to the sampling site choice. For the studied cores, do they allow access to a similar anthropogenic contamination history? This study focuses on distal floodplain sediments because proximal floodplain sediments are preindustrial with low to moderate enrichments of As, Cd, Mo, Sb, Sn and U, which are linked to mineralogical composition differences.

In the distal floodplain, the two cores have enrichment factors close to 1 for TEs up to the late 1860s, except for Hg, which has had a light enrichment ( $2 < EF < 4$ ) since the 1850s (Fig. 6.5), and Sb and Mo which have higher geochemical backgrounds.

After the late 1860s, three different temporal dynamics are represented by Hg, Sn and Cd. First, a synchronic EF increase is calculated for Hg and Sn (up to 30 and 8, respectively) in both cores from the 1860s until the dam elevation in 1933. The other TE (Cd) shows EFs not higher than 2-3 (Fig. 6.5). Hg, and Sn profiles are different between the two cores. In the RBC, Hg enrichments gradually increase from the 1860s and reach a maximum of 21 in the 1930s. Sn enrichment becomes significant in the early 1900s and reaches a maximum of 7 in the late 1920s. In the UWC, TE enrichment profiles are different than in the RBC and characterize short temporal variations of contamination levels (Fig. 6.5). Hg enrichment sharply increases between the early 1880s and the early 1890s with a maximum EF of 30, higher than the RBC registered maximum. The Hg EF then decreases until the late 1900s ( $EF = 11$ , similar in RBC) before a second increase in the RBC (EF close to 23 in the

early 1930s). For Sn, the EF profile is similar to the RBC variations with a light enrichment between the late 1900s and the early 1920s (EF = 4). However, this maximum EF peak is higher in the UWC (EF = 10) than in the RBC. By the 1930s, enrichment levels are similar in both cores with maximum values higher in the UWC than in the RBC.

After the dam elevation in 1933, TE enrichment trends and maxima highly differ between the two cores. In the RBC, EF temporal trends significantly decrease for Hg and Sn ( $r = 0.8$ ,  $p < 0.05$ ,  $n = 14$ ), reaching an enrichment level high for Hg in the early 2010s (EF = 11) and low for Sn (EF *c.a.* 4). For Cd, the EF starts to increase with the dam elevation (EF *c.a.* 3) and then remains stable ( $p > 0.05$ ). In the UWC, the EF temporal trends are less linear than in the RBC. All of the studied TE have a period of maximum enrichment. The Hg maximum (EF *c.a.* 57) occurred just after the dam elevation, between the early 1940s and the 1950s. The Sn maximum occurred (in the 1920s-1930s) before the dam elevation but the enrichment remains high until the 1940s (EF close to 8) and the Cd maximum occurs in the early 1950s (EF *c.a.* 9). After

these EF maxima, all of the TE enrichments slowly decrease, reaching enrichment levels less than those recorded in the RBC for Hg and Sn and similar for Cd.

These EF variations highlight the influence of settling environments on the archived anthropogenic TE history. In this studied floodplain and before water-depth control by the dam in the early 1930s, TE temporal trends are comparable in terms of trajectories and contamination levels, although the UWC has shorter-time variations and higher EF peaks. Even if the aggradation rate is higher for the RBC before 1933 (see § 3.2.3), the temporal resolution of the recorded TE chronic is not as good as for the UWC. This is linked to a better conservative environment for the trapped sediments in the paleochannel.

After the dam elevation, differences in TE temporal dynamics are enhanced, with enrichments in UWC sediments becoming more variable and with higher EF peaks than in the RBC. The spatial variability of contamination levels in sediments deposited during overbank floods depends on the transport capacity of suspended materials (Baborwski *et al.*, 2007).

	UWC - distal floodplain (n=15)			RBC - distal floodplain (n=13)			RBC - proximal floodplain (n=33)			Entire Loire basin (n=2)*		Upper Loire Basin (n=1)**
	Range	Med.	Var.	Range	Med.	Var.	Range	Med.	Var.	n.d.	n.d.	< 6000 BP
Si	26.41-28.40	27,30	7	26.02-29.39	27,10	9	25.51-31.33	29,60	20	n.d.	n.d.	20,34
Al	8.46-9.40	8,77	11	8.24-9.22	8,86	11	7.31-9.12	7,93	23	8.37	8.54	8,90
TOC	0.8-1.3	1,1	41	0.5-0.7	0,6	43	0.4-0.9	0,5	93	1.2	1.1	8,7
S tot.	0.02-0.07	0,06	83	0.02-0.07	0,06	83	0.01-0.03	0,02	100	n.d.	n.d.	0.54
As	24.5-37.1	28,9	44	26.4-38	30,8	38	16.2-46.2	25,5	118	19.8	19.4	43,4
Bi	0.8-1.1	0,9	44	0.8-0.9	0,9	18	0.6-0.9	0,8	39	0.7	0.6	1,1
Cd	0.4-0.6	0,5	43	0.4-0.6	0,5	44	0.4-1.1	0,7	101	0.3	0.4	0,8
Cr	89-103	96	15	94-104	98	10	88-110	97	22	109	89	98
Cu	21-27	23	28	21-27	24	27	14-27	20	65	19,0	21	31
Hg	0.03-0.06	0,05	50	0.04-0.06	0,05	37	0.02-0.09	0,03	226	0.02	0.02	0,09
Mo	0.7-1.0	0,8	29	0.8-1.0	0,9	23	0.6-1.1	0,8	68	0.4	0.3	2,8
Ni	36-44	38	21	34-43	39	22	27-49	34	64	33	24	87
Pb	51-61	55	18	47-58	52	20	46-69	52	43	37	33	49
Sb	1.6-2.2	2,0	31	1.6-2.4	1,8	42	1.5-2.2	1,7	44	0.5	0.3	3,2
Sn	8-12	10	38	8-11	9	30	7-17	8	128	8	7	8
U	7.8-10.2	8,7	28	9.1-10.7	9,7	17	8.8-22.1	12,1	110	8.8	7.5	12,8
W	5.1-7.4	6,0	38	5.6-6.3	5,8	13	4.6-6.3	5,5	30	6.3	5.7	4,9
Zn	112-139	125	22	105-127	120	18	81-137	100	56	90	97	118

**Tab. 6.3:** Geochemical composition of preindustrial sediments (< 1830) in the paleochannel (UWC) and river bank (RBC) cores compared to preindustrial concentrations representative of the all-natural sources at the entire Loire Basin scale (\*Grosbois et al, 2012) and prehistorical concentrations in organic sediments of the Upper Loire Basin (\*\* ARTEHIS - UMR 6298 - Dijon University, France). n.d. = not determined; Med. = Median value; Var. = Range variability compare to the median value; Unit: Si, Al, TOC, S tot. (%); As, Bi, Cd, Cr, Cu, Hg, Mo, Ni, Pb, Sb, Sn, U, W, Zn (ppm)

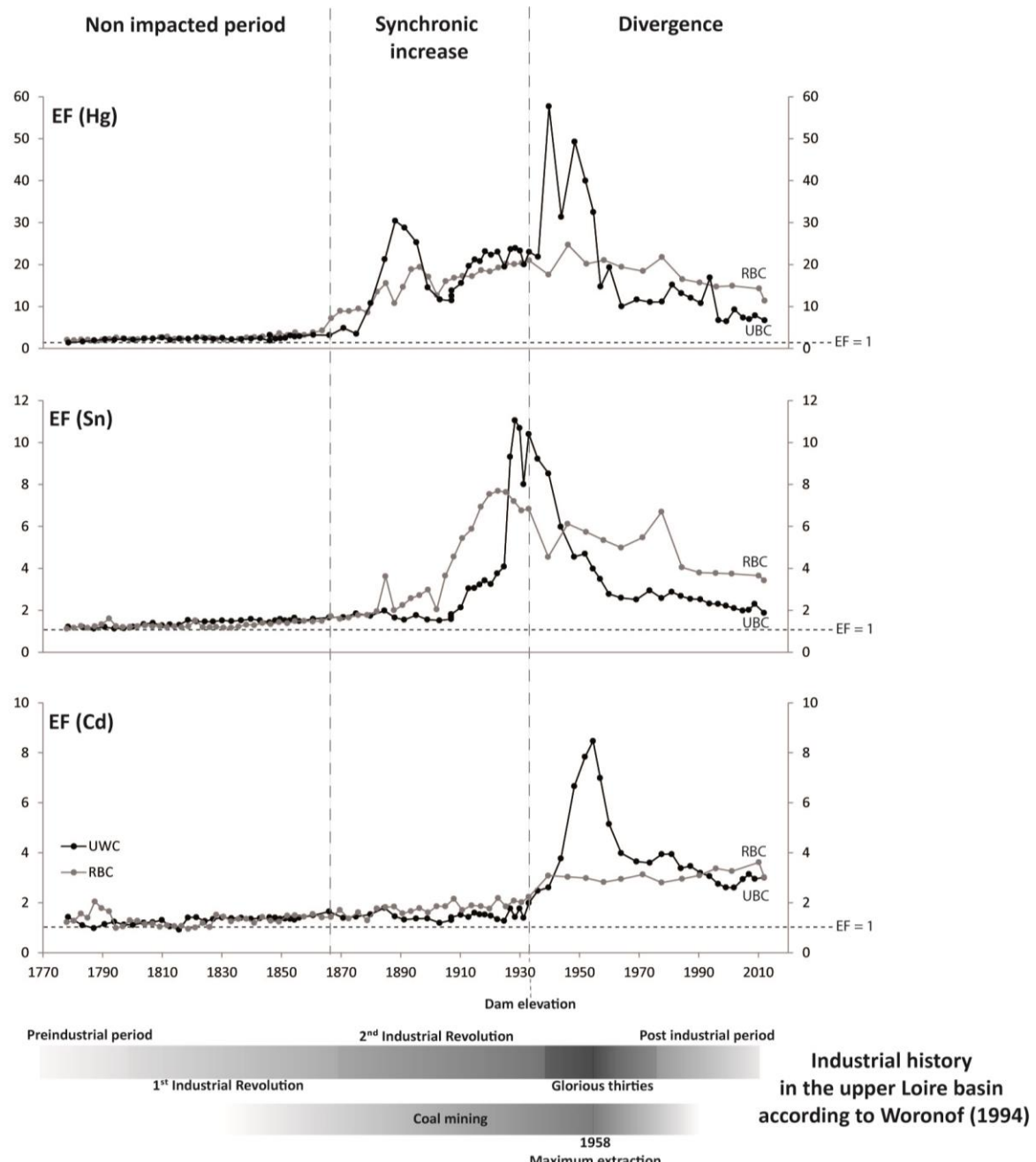


**Fig. 6.5.: Enrichment factor chronic of Hg, Sn and Cd for the two cores compared to the industrial history at the basin scale.**

As a result of water-depth control, the aggradation rate of the RBC is largely reduced. Therefore, less potential contaminated particles can settle down in this part of the floodplain. Additionally, some organic particles containing a significant part of the total S and chalcophil TE-rich (such as As, Cd, Co, Cu, Hg, Mo, Ni, Sb, U and Zn, all highly correlated,  $r = 0.9$ ,  $p < 0.05$ ,  $n = 8$ ) are trapped in the UWC between 34 and 50 cm and are absent in the RBC (Fig. 6.4). The dam elevation enhanced the connectivity degree for the UWC and archived conditions for these TE-rich particles compared to the RBC. These TOC-S increases could be related to metalliferous coal and blast furnace sludge activities in the study area. Bioturbation, organic matter degradation and post-depositional processes can be important factors to explain differences in recorded TE chronics between the UWC and the RBC. The upper unit of the RBC, from 70 cm to the surface, has pedogenetic characteristics with secondary porosity, roots and a bottom-up important increase of TOC content (Fig. 6.4). TE-TOC correlations are significant in this core interval ( $r > 0.6$ ,  $p < 0.05$ ,  $n = 63$ ). Surface

sediments (post 1990s,  $< 10$  cm deep) of the RBC, and TOC-rich ( $> 3\%$ ) with roots have higher contamination levels than the UWC. In a pedogenic context, the TE vertical distribution and contamination levels are more dependent on their high retention in surface because of an organic top soil and TE redistribution by biological activities than progressive archiving processes. These results have been shown by other authors (Palumbo *et al*, 2000; Fujikawa *et al*, 1998). At a long-term scale, this phenomenon should also be magnified by the high disconnection degree of the river bank and low sediment inputs induced by water depth control.

These results show a significant influence of the settling environment on archived long-term TE variations. In the paleochannel, TE temporal dynamics are archived with a well-defined time resolution and are not affected by connection degree variations. However, sediments cored in a river bank can be more influenced by river modifications and pedogenetic activities.

#### 6.4. Conclusions

To highlight the influences of fluvial depositional environments on sediment archiving processes, aggradation rates and recorded geochemical patterns, two cores were sampled on a ridge of the river bank and in a paleochannel. In the river bank core, two steps of the floodplain edification are archived, corresponding to two successive depositional environments. The oldest one corresponds to a proximal floodplain sedimentation archived during the earliest age of the floodplain during the end of the Little Ice Age. This sedimentary sequence shows a general fining upward sequence related to decreasing river energy during river bank accretion. Subsequently, a fine-grained material was homogenously settled during overbank floods to present day. Sediments in the underwater core of the paleochannel are similar to the upper unit of the river bank core. However, after the Decize dam elevation in 1933, slackwater depositions of fine sands have largely contributed to its aggradation.

The main differences between the two depositional environments highlighted in this study are

1. a better archiving capacity of sediments in a paleochannel as the river bank accretion is largely influenced by erosion episodes,
2. higher aggradation rates in the river bank, although more dependent on connection degree variations, with the aggradation rate significantly reduced after water depth regulation in this environment,
3. preindustrial geochemical concentrations are more dependent on river energy in proximal than distal areas because of the sorting of heavy minerals, and
4. in the paleochannel, trapped contaminated sediments are less selected and allow for a better time resolution of anthropogenic TE signals.

For this floodplain study, TE temporal dynamics archived in the paleochannel are more representative of an anthropogenic source history. However, TE temporal dynamics recorded in the river bank show similar trends than those of the paleochannel, with the divergences being caused by local water depth regulation and a biological redistribution of deposited TEs.

## Acknowledgments:

This work was financially supported by the Agence de l'eau Loire-Bretagne and is a part of the Observation Network of the Loire River Basin Sediments. Authors really appreciate the great quality of geochemical analyses and discussions with the Service d'Analyse des Roches et des Minéraux (SARM) in Nancy (France), a CNRS Analytical Research facility. Thanks to the two reviewers for their constructive comments.

## References:

- Arnaud-Fassetta, G., 2003. River channel changes in the Rhone Delta (France) since the end of the Little Ice Age: geomorphological adjustment to hydroclimatic change and natural resource management. *Catena*. 51, 141–172.
- Bábek, O., Faměra, M., Hilscherová, K., Kalvoda, J., Dobrovolný, P., Sedláček, J., Machát, J., Holoubek, I., 2011. Geochemical traces of flood layers in the fluvial sedimentary archive; implications for contamination history analyses. *Catena*. 87, 281–290.
- Bábek, O., Hilscherová, K., Nehyba, S., Zeman, J., Famera, M., Francu, J., Holoubek, I., Machát, J., Klánová, J., 2008. Contamination history of suspended river sediments accumulated in oxbow lakes over the last 25 years. *Journal of Soils and Sediments*. 8, 165–176.
- Babonaux, Y., 1970. *Le Lit de la Loire – Etude d'hydrodynamique fluviale*, Paris, Bibliothèque Nationale, 252 p.
- Baborowski, M., Büttner, O., Morgenstern, P., Krüger, F., Lobe, I., Rupp, H., Tümlpling, W. V., 2007. Spatial and temporal variability of sediment deposition on artificial-lawn traps in a floodplain of the River Elbe. *Environmental Pollution*, 148, 770–778.
- Benedetti, M. M., 2003. Controls on overbank deposition in the Upper Mississippi River. *Geomorphology*. 56, 271–290.
- Berner, Z. A., Bleeck-Schmidt, S., Stüben, D., Neumann, T., Fuchs, M., Lehmann, M. 2012, Floodplain deposits: A geochemical archive of flood history – A case study on the River Rhine, Germany. *Applied Geochemistry*. 27, 543–561.
- Birch, G. F., Taylor, S. E., Matthai, C., 2001. Small-scale spatial and temporal variance in the concentration of heavy metals in aquatic sediments: a review and some new concepts. *Environmental pollution* (Barking, Essex : 1987), 113, 357–72.
- Bradley, S.B., Cox, J.J., 1990. The significance of the floodplain to the cycling of metals in the river Derwent Catchment, U.K. *Science of The Total Environment*. 97–98, 441–454.
- Bravard, J.-P., Goichot, M., Tronchère, H., 2014. An assessment of sediment-transport processes in the Lower Mekong River based on deposit grain sizes, the CM technique and flow-energy data. *Geomorphology*. 207, 174–189.
- Bravard, J.-P., Peiry, J.-L., 1999. The CM pattern as a tool for the classification of alluvial suites and floodplains along the river continuum. In Marrott S.B. and Alexander J. (eds.), *Floodplains*:

*interdisciplinary approaches.* Geological Society Special Publication 163, 259-268.

Bridge, J., 2003, Rivers and Floodplains Forms, processes, and Sedimentary Record, (Eds) Blackwell Science Ltd, pp. 487

Dacharry M., 1974. Hydrologie de la Loire en amont de Gien. Paris, N.A.L., 2 vol. 334 & 285 p.

Delfour J., Isnard P., Lecuyer E., Lemiere B., Lhote F., Moine B., Piboule M., Picot P., Ploquin A., Tegyey M., 1984 - Etude du gîte de pyrite de Chizeuil (Saône-et-Loire) et de son environnement volcanosédimentaire dévonien et dinantien. Document BRGM, n° 73, 37 p.

De Cort, G. Dubois, S.D. Fridman, M.G. Germenchuk, Yu A. Izrael, A. Janssens, A.R. Jones, G.N. Kelly, E.V. Kvasnikova, I.I. Matveenko, I.M. Nazarov, Yu M. Pokumeiko, V.A. Sitak, E.D. Stukin, L.Ya Tabachny, Yu S. Tsaturov, S.I. Avdyushin. 1998. The Atlas of Caesium Deposition on Europe after the Chernobyl Accident: M. Luxembourg, EUR 16733, ISBN 92-828-3140-X.

Desmet, M., Mourier,B., Mahler, B.J.,Van Metre, P.C., Roux, G.,Persat, H., I. Lefèvre, Peretti,A., Chapron, E., Simonneau, A., Miège, C., Babut, M. 2012, Spatial and temporal trends in PCBs in sediment along the lower Rhône River, France. The Science of the total environment, 433, 189–97.

Détriché, S., Rodrigues S., Macaire, J.-J., Bonté, P., Bréhéret, J.-G., Bakyno, J.-P., Jugé, P. 2010, Caesium-137 in sandy sediments of the River Loire (France): Assessment of an alluvial island evolving over the last 50 years. Geomorphology, 115, 11–22.

Dhivert, E., Grosbois, C., Coynel, A., Desmet, M., 2015. Sedimentary and geochemical evidences in a core age model to highlight flood-event dynamics in a reservoir infill (Upper Loire basin, France). Catena, 126, 75-85

Dieras, P. L., Constantine, J. A., Hales, T. C., Piégay, H., Riquier, J., 2013. The role of oxbow lakes in the off-channel storage of bed material along the Ain River, France. Geomorphology, 188, 110–119.

Dill, H. G., 2010. The “chessboard” classification scheme of mineral deposits: Mineralogy and geology from aluminum to zirconium. Earth-Science Reviews, 100, 1–420.

Du, P., Walling, D. E., 2012. Using  $^{210}\text{Pb}$  measurements to estimate sedimentation rates on river floodplains. Journal of environmental radioactivity, 103, 59–75.

Euler, T., Zemke, J., Rodrigues, S., Herguet, J., 2014. Influence of inclination and permeability of solitary woody riparian plants on local hydraulic and sedimentary processes, Hydrol. Process. 28, 1358–1371.

Ferrand, E., Eyrolle, F., Radakovitch, O., Provansal, M., Dufour, S., Vella, C., Raccasi, G., Gurriaran, R., 2012. Historical levels of heavy metals and artificial radionuclides reconstructed from overbank sediment records in lower Rhône River (South-East France). Geochimica et Cosmochimica Acta. 82, 163-182.

Förstner, U., Heise, S., Schwartz, R., Westrich, B., Ahlf, W., 2004. Historical contaminated sediments and soils at the river basin scale. Journal of soils and sediments. 4, 247-260.

Fujikawa, Y., Fukui, M., Kudo, A., 2000. VERTICAL DISTRIBUTIONS OF TRACE

METALS IN NATURAL SOIL. Water, Air and Soil pollution, 123, 1–21.

Fuller, I. C., 2008. Geomorphic impacts of a 100-year flood: Kiwitea Stream, Manawatu catchment, New Zealand. *Geomorphology*. 98, 84–95.

Gasowski, Z., 1994. L'enfoncement du lit de la Loire/The entrenchment of the Loire's river bed. *Revue de géographie de Lyon*. 69, 41-45.

Gocht, T., Moldenhauer, K., Pu, W., 2001. Historical record of polycyclic aromatic hydrocarbons (PAH) and heavy metals in floodplain sediments from the Rhine River (Hessisches Ried, Germany). *Applied Geochemistry*. 16, 1707–1721.

van Griethuysen, C., Luitwieler, M., Joziasse, J., Koelmans, A. A., 2005. Temporal variation of trace metal geochemistry in floodplain lake sediment subject to dynamic hydrological conditions. *Environmental Pollution*. 137, 281-294.

Grivel, S., Gautier, E., 2012. Mise en place des îles fluviales en Loire moyenne, du 19<sup>e</sup> siècle à aujourd'hui, *Cybergeo : European Journal of Geography*, 615 Grosbois, C., Meybeck, M., Lestel, L., Lefèvre, I., Moatar, F., 2012. Severe and contrasted polymetallic contamination patterns (1900-2009) in the Loire River sediments (France). *The Science of the total environment*. 435-436, 290–305.

Grosbois, C., Meybeck, M., Lestel, L., Lefèvre, I., Moatar, F., 2012. Severe and contrasted polymetallic contamination patterns (1900–2009) in the Loire River sediments (France). *Science of the Total Environment*. 435, 290-305.

Grousset, F. E., Jouanneau, J. M., Castaing, P., Lavaux, G., Latouche, C., 1999. A 70 year Record of Contamination from

Industrial Activity Along the Garonne River and its Tributaries (SW France). *Estuarine, Coastal and Shelf Science*. 48, 401–414.

Grygar, M.T., Elznicová, J., Bábek, O., Hošek, M., Engel, Z., Kiss, T., 2014. Obtaining isochrones from pollution signals in a fluvial sediment record: A case study in a uranium-polluted floodplain of the Ploučnice River, Czech Republic. *Applied Geochemistry*.

Grygar, T., Světlík, I., Lisá, L., Koptíková, L., Bajer, A., Wray, D. S., Smetana, M. (2010). Geochemical tools for the stratigraphic correlation of floodplain deposits of the Morava River in Strážnické Pomoraví, Czech Republic from the last millennium. *Catena*. 80, 106-121.

He, Q., Walling, D. E., 1996. Interpreting Particle Size Effects in the Adsorption of <sup>137</sup>Cs and Unsupported <sup>210</sup>Pb by Mineral Soils and Sediments. *Earth surface processes and landforms*. 30, 117–137.

Heaven,S., Ilyushchenko,M.A., Tanton, T.W., Ullrich, S.M., Yanin, E.P.,2000. Mercury in the River Nura and its floodplain, Central Kazakhstan: I. River sediments and water, *Science of The Total Environment*. 260, 35-44.

Hoffmann, T., Thorndycraft, V. R., Brown, A. G., Coulthard, T. J., Damnati, B., Kale, V. S., Middelkoop, H., Notebaert, B., Walling, D.E., 2010. Human impact on fluvial regimes and sediment flux during the Holocene. Review and future research agenda: *Global and Planetary Change*. 72, 87–98.

Hostache, R., Hissler, C., Matgen, P., Guignard, C., Bates, P., 2014. A 2-D hydro-morphodynamic modelling approach for predicting suspended sediment propagation and related heavy metal contamination in floodplain: a sensitivity

analysis. *Hydrology and Earth System Sciences Discussions*. 11, 1741-1776.

Houben, P., 2007. Geomorphological facies reconstruction of Late Quaternary alluvia by the application of fluvial architecture concepts. *Geomorphology*. 86, 94–114.

Hughes, A. O., Croke, J. C., Pietsch, T. J., Olley, J. M., 2010. Changes in the rates of floodplain and in-channel bench accretion in response to catchment disturbance, central Queensland, Australia. *Geomorphology*, 114, 338–347.

Knox, J. C., 2006. Floodplain sedimentation in the Upper Mississippi Valley: Natural versus human accelerated. *Geomorphology*. 79, 286–310.

Landon N., 1999, L'évolution contemporaine du profil en long des affluents du Rhône moyen. Constat régional et analyse d'un hydrosystème complexe, la Drôme, Paris, pp. 560

Latapie, A. 2011. Modélisation de l'évolution morphologique d'un lit alluvial: application à la Loire moyenne. PhD thesis, Tours univ., 277 pp.

Latapie, A., Camenen, B., Rodrigues, S., Paquier, A., Bouchard, J.P., Moatar, F., 2014. Assessing channel response of a long river influenced by human disturbance, *Catena*, 121, 1-12.

Le Cloarec, M.-F., Bonte, P. H., Lestel, L., Lefèvre, I., Ayraut, S., 2011. Sedimentary record of metal contamination in the Seine River during the last century. *Physics and Chemistry of the Earth, Parts A/B/C*. 36, 515–529.

Lecce, S. A., Pavlowsky, R. T., 1997. Storage of mining-related zinc in floodplain sediments, Blue River,

Wisconsin. *Physical Geography*. 18, 424-439.

Lecce, S. A., Pavlowsky, R. T., 2004. Spatial and temporal variations in the grain-size characteristics of historical flood plain deposits, Blue River, Wisconsin, USA. *Geomorphology*. 61, 361-371.

Lecce, S. A., Pavlowsky, R. T., 2014. Floodplain storage of sediment contaminated by mercury and copper from historic gold mining at Gold Hill, North Carolina, USA. *Geomorphology*. 206, 122-132.

Leteinturier B., Engels P., Petit F., Chiffaut A., Malaisse F., 2000. Morphodynamisme d'un tronçon de Loire bourbonnaise depuis le XVIII<sup>e</sup> siècle / Changing dynamics of the Loire river in Burgundy (France) during the last 200 years. In: *Géomorphologie : relief, processus, environnement*. 4, 239-251.

Macaire, J. J., Gay-Ovejero, I., Bacchi, M., Cocirla, C., Patryl, L., Rodrigues, S., 2013. Petrography of alluvial sands as a past and present environmental indicator: Case of the Loire River (France). *International Journal of Sediment Research*. 28, 285-303.

Macklin, M. G., Klimek, K., 1992. Dispersal, storage and transformation of metal contaminated alluvium in the upper Vistula basin, southwest Poland. *Applied Geography*. 12, 7-30.

Martin, C. W., 2000. Heavy metal trends in floodplain sediments and valley fill, River Lahn, Germany. *Catena*, 39, 53–68.

Matisoff, G., Ketterer, M. E., Rosén, K., Mietelski, J. W., Vitko, L. F., Persson, H., Lokas, E., 2011. Downward migration of Chernobyl-derived radionuclides in soils in Poland and Sweden. *Applied Geochemistry*. 26, 105–115.

- Meitzen, K. M., Doyle, M. W., Thoms, M. C., Burns, C. E., 2013. Geomorphology within the interdisciplinary science of environmental flows. *Geomorphology*. 200, 143–154.
- Mourier, B., Desmet, M., Van Metre, P. C., Mahler, B. J., Perrodin, Y., Roux, G., Bedell, J.-P., Lefèvre, I., Babut, M., 2014. Historical records, sources, and spatial trends of PCBs along the Rhône River (France). *The Science of the total environment*. 476-477, 568–576.
- Nanson, G.C., Croke, J.C., 1992. A genetic classification of floodplains. *Geomorphology*. 4, 459–486.
- Nanson, G. C., Page, K., 1983. Lateral Accretion of Fine-Grained Concave Benches on Meandering Rivers, in Modern and Ancient Fluvial Systems (eds J. D. Collinson and J. Lewin), Blackwell Publishing Ltd.
- Owens, P. N, Walling, D. E., Leeks, G.J.L., 1999. Use of floodplain sediment cores to investigate recent historical changes in overbank sedimentation rates and sediment sources in the catchment of the River Ouse, Yorkshire, UK. *Catena*. 36, 21–47.
- Palumbo, B., Angelone, M., Bellanca, A., Dazzi, C., Hauser, S., Neri, R., Wilson, J., 2000. Influence of inheritance and pedogenesis on heavy metal distribution in soils of Sicily, Italy. *Geoderma*. 95, 247–266.
- Passega, R., 1957. Texture as characteristic of clastic deposition. *Bull. Am. Assoc. Pet. Geol.*. 41, 1952–1984.
- Passega, R., 1964. Grain-size representation by CM pattern as a geological tool. *J. Sediment. Petrol.*. 34, 830–847.
- Pye, K., Blott, S. J., 2004. Particle size analysis of sediments, soils and related particulate materials for forensic purposes using laser granulometry. *Forensic science international*. 144, 19–27.
- Rodrigues S., Breheret J.-G., Macaire J.-J., Greulich, S., Villar, M., 2007. In-channel woody vegetation controls on sedimentary processes and the sedimentary record within alluvial environments: a modern example of an anabranch of the River Loire (France). *Sedimentology*. 54, 223-242.
- Rodrigues, S., Bréhéret, J.-G., Macaire, J.-J., Moatar, F., Nistoran, D., Jugé, P., 2006. Flow and sediment dynamics in the vegetated secondary channels of an anabranching river: The Loire River (France). *Sedimentary Geology*. 186, 89–109.
- Schulz-Zunkel, C., Krueger, F., Rupp, H., Meissner, R., Gruber, B., Gerisch, M., & Bork, H. R. (2013). Spatial and seasonal distribution of trace metals in floodplain soils. A case study with the Middle Elbe River, Germany. *Geoderma*. 211, 128-137.
- Thompson, C., Croke, J. 2013, Geomorphic effects, flood power, and channel competence of a catastrophic flood in confined and unconfined reaches of the upper Lockyer valley, southeast Queensland, Australia. *Geomorphology*. 197, 156–169.
- Valverde, L., Jugé, P., Handfus, T., 2013. Résultats granulométriques et localisation des points dures en Loire, rapport InfoSed 2, pp. 180
- Van Metre, P.C., Wilson, J.T., Fuller, C.C., Callender, E., Mahler, B.J., 2004. Collection, analysis, and age-dating of sediment cores from 56 U.S. lakes and reservoirs sampled by the U.S. geological

survey, 1992–2001 USGS Scientific Investigations Report–5184

Vrel, A., Boust, D., Lesueur, P., Deloffre, J., Dubrulle-Brunaud, C., Solier, L., Rozet, M., Thouroude, C., Cossonet, C., Thomas, S., 2013. Dating of sediment record at two contrasting sites of the Seine River using radioactivity data and hydrological time series. *Journal of environmental radioactivity.* 126, 20-31

Walling, D.E, He, Q., 1998. The spatial variability of overbank sedimentation on river floodplains. *Geomorphology.* 24, 209–223.

Walling, D. E., He, Q., 1997. Use of fallout  $^{137}\text{Cs}$  in investigations of overbank sediment deposition on river floodplains. *Catena.* 29, 263-282.

Walling, D. E., Owens, P. N., G. J.L. Leeks., 1998. The role of channel and floodplain storage in the suspended sediment budget of the River Ouse, Yorkshire, UK. *Geomorphology.* 22, 225–242.

Walling, D.E., Owens, P.N., Leeks, G.J.L., 1997. The characteristics of overbank deposits associated with a major flood event in the catchment of the River Ouse, Yorkshire, UK. *Catena.* 31, 53–75.

Werritty, A, Paine, J. L., Macdonald, N., Rowan, J. S., McEwen, L. J., 2006. Use of multi-proxy flood records to improve estimates of flood risk: Lower River Tay, Scotland. *Catena.* 66, 107–119.

Woronoff D.,1994, *Histoire de l'industrie en France, Du 16e siècle à nos jours*, Paris. Le Seuil. 671 p.



Félix Thiollier

### **Partie 3 - Variabilité spatiale de l'enregistrement sédimentaire des contaminations à l'échelle du bassin de la Loire**

## **Chapitre 7 - Synthèse**

### **Points importants :**

- Comparaison de l'enregistrement sédimentaire des contaminations entre les parties amont et aval du bassin de la Loire
- Contaminations sédimentaires localisées à la partie amont du bassin de la Loire
- Contaminations sédimentaires enregistrées avec un délai entre les parties amont et aval du bassin
- Caractérisation des sources anciennes de contamination à partir des signatures géochimiques archivées dans les sédiments des berges

### **Mots clés :**

dynamique temporelle, éléments traces, variabilité spatiale, bassin versant, caractérisation des sources de contaminations

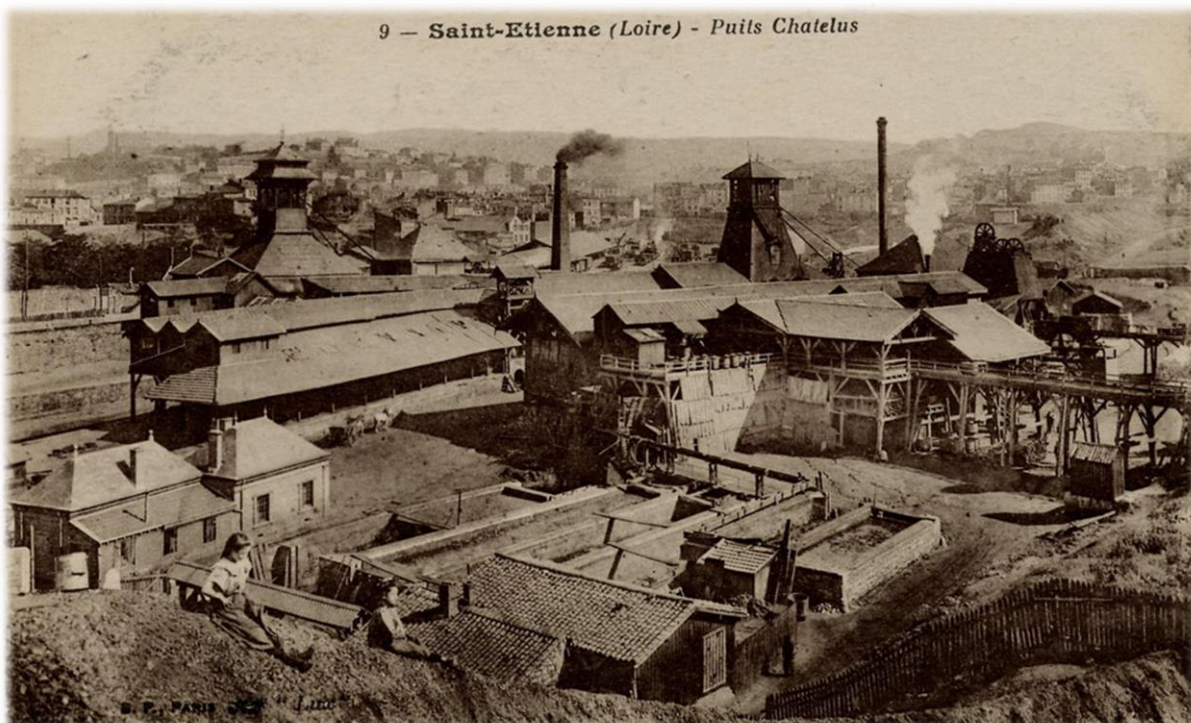


**Illustration 3 :** Carte postale de la fin du XIX<sup>ème</sup> siècle montrant les mines de charbon à Saint Etienne et les activités industrielles connexes. Le bassin houiller de Saint Etienne était l'un des plus anciens foyers industriels et l'un des plus importants en France jusqu'à la fin des années 1950. (source : [www.delcampe.fr](http://www.delcampe.fr))

## **7.1. Objectifs et méthodes analytiques**

Dans le précédent chapitre, la variabilité spatiale des enregistrements sédimentaires des contaminants métalliques a été étudiée à l'échelle de l'environnement fluviatile. Cette troisième partie s'intéresse **aux variabilités spatiales et temporelles de l'archivage des contaminations sédimentaires à l'échelle du bassin de la Loire**. Cette étude comporte quatre objectifs majeurs :

- (i) **reconstituer les évolutions temporelles des contaminations métalliques** dans les sous-bassins de la Loire Amont et de l'Allier accueillant les plus anciens et les plus importants foyers industriels et miniers
- (ii) **comparer les dynamiques temporelles de contaminations** enregistrées dans ces sous-bassins avec celles archivées dans la partie aval du bassin
- (iii) **caractériser les sources historiques** de contamination
- (iv) **caractériser l'héritage des sources anciennes** sur la contamination actuelle des sédiments.

Deux archives sédimentaires prélevées dans les sous-bassins de la Loire Amont et de l'Allier ont donc été analysées. En Loire Amont, l'archive sédimentaire utilisée est celle prélevée dans le paléochenal de Decize (décrise dans la partie précédente). Elle permet de retracer l'histoire des contaminations métalliques depuis la fin du XVIII<sup>ème</sup> siècle. Pour reconstituer les dynamiques temporelles dans le bassin de l'Allier, une archive sédimentaire a été échantillonnée dans le canal d'Apremont-sur-Allier en 2012. Les enregistrements les plus anciens datent des années 1940 pour cette carotte. Des **fenêtres temporelles basées sur l'évolution temporelle des niveaux de contaminations et sur les corrélations interélémentaires** ont été définies dans ces enregistrements.

Les signaux géochimiques enregistrés dans les archives des sous-bassins de la Loire Amont et de l'Allier ont été comparés à ceux décrits dans une archive prélevée **tout en aval du domaine fluviatile**, en 2009. Cette approche multi-site et délimitée par fenêtres temporelles permet de mettre en évidence **les différences tendancielles** des contaminations entre les parties amont et aval du bassin.

D'autre part, les sources anciennes de contamination ont été caractérisées en comparant les signatures géochimiques archivées dans les carottes sédimentaires à celles enregistrées dans les sédiments des berges des affluents de la Loire (amont et aval) et de l'Allier drainant les principaux foyers industriels et miniers. Les signatures géochimiques représentent ici des relations interélémentaires caractérisant les phases temporelles de contaminations et les activités anthropiques échantillonnées.

Les séquences de crues archivées dans le réservoir de Villerest ont été utilisées pour caractériser l'héritage des sources anciennes sur la contamination actuelle des sédiments.

Les résultats des analyses géochimiques réalisées sur les sédiments des archives sédimentaires et des berges sont présentés en annexe 2.2.

## 7.2. Principaux résultats

L'analyse de l'évolution temporelle des contaminations sédimentaires enregistrées en Loire amont atteste de

faibles influences des activités anthropiques sur la composition géochimique des sédiments jusqu'à la fin du XIX<sup>ème</sup> siècle.

Trois fenêtres temporelles de contaminations peuvent être définies dans les sous-bassins de la Loire Amont et de l'Allier depuis les années 1880 correspondant à:

- (i) **de forts enrichissements en Hg, Sb et Sn entre les années 1880 et la fin des années 1930 en Loire Amont**
- (ii) **une phase de contamination polymétallique entre les années 1940 et la fin des années 1950** enregistrées dans les deux sous-bassins, exposant les niveaux de contaminations maximum (Bi, Cd, Hg et Sb sont les éléments les plus enrichis au cours de cette période)
- (iii) **une phase de diminution des enrichissements enregistrée depuis les années 1960** dans les deux sous-bassins.

La comparaison de ces enregistrements avec l'archive prélevée tout en aval du bassin permet de montrer

## Influence de la cascade sédimentaire

A l'échelle d'un bassin, les processus géomorphologiques peuvent en partie contrôler la distribution spatiale et temporelle des métaux dans les sédiments.

La comparaison des enregistrements entre les sous-bassins les plus fortement industrialisés du bassin de la Loire (la Loire Amont et l'Allier) et la partie aval permet de mettre en évidence l'influence de ces processus.

On différencie des phases de contamination localisées dans les sous-bassins amont (Sb et Sn) et d'autres enregistrés aussi bien dans les parties amont qu'en aval du bassin (Hg, Bi et Cd).

Une phase de contamination polymétallique présentant les enrichissements maximum est enregistrée au cours de la période d'activité minière et industrielle maximale dans la partie amont du bassin, entre les années 1940 et 1950, et entre les années 1950 et 1980 dans la partie aval, soit un décalage d'au moins 10 à 20 ans.

Cette comparaison met ici en évidence l'influence de la cascade sédimentaire, contrôlant la propagation des sédiments par l'alternance de phase de transport et de stockage temporaire. Ces processus limitent l'influence spatiale des contaminations en fonction de la capacité de transport des sédiments contaminés et imposent un délai d'environ 20 ans dans l'archivage des phases de contaminations entre les sous-bassins proches des sources et la partie aval du bassin.

l'existence de **contaminations sédimentaires locales** n'affectant que les sous-bassins de la Loire Amont (Sn, Sb) et de l'Allier (Sb).

La caractérisation des sources anciennes de contaminations permet de définir **l'influence locale des retombées atmosphériques issues des verreries** implantées à proximité du site de Decize entre les années 1910 et la fin des années 1930 (corrélation Sb-Sn). Durant cette période, la **métallurgie de l'étain** en Loire amont est aussi responsable de forts enrichissements en Sn localisés dans le sous-bassin du Furan (Loire Amont). D'autre part, les enrichissements en Sb enregistrés dans les sous-bassins de la Loire Amont et de l'Allier dans les années 1940 - 1950 peuvent être attribués aux **effluents issus des mines de charbons** (districts de St Etienne – Loire Amont, Epinac-Blanzy-La Machine – Loire Amont, Brassac-les-mines - Allier) et **d'antimoine** (district de Brioude-Massiac - Allier) dont l'activité était maximale au cours de cette période. De la même manière, des enrichissements extrêmes sont enregistrés dans les sédiments des berges du Vicoin en aval du district minier de La Lucette (Mayenne). Dans les effluents miniers, Sb est majoritairement associé aux phases

porteuses les plus denses, ce qui limite la propagation de la contamination en aval. De surcroit, Sb ayant une forte affinité pour la matière organique et les oxydes, le transport sous forme dissoute est limité lors de l'altération des phases porteuses.

Les enrichissements maximum en Hg, Bi et Cd sont archivés entre les années 1940 et 1950 dans les sous-bassins amont alors qu'ils **sont enregistrés avec un délai dans la partie aval du domaine fluviatile**, entre les années 1950 et 1980. Des différences amont-aval importantes concernant l'enregistrement temporel des contaminations sédimentaires sont ainsi mises en évidence dans le bassin de la Loire. Entre les années 1960 et 1980, alors que les enrichissements en ET décroissent de manière exponentielle dans les sous-bassins amont les plus fortement industrialisés, les niveaux de contaminations maximum sont enregistrés dans la partie aval du bassin. Ces niveaux de contaminations maximum enregistrés dans la partie aval du bassin sont comparables à ceux enregistrés durant la période 1940-1950 dans la partie amont pour Hg et sont plus élevés pour Bi et Cd.

Hg étant un métal volatil dont l'utilisation a été très répandue au cours

de l'ère industrielle, la caractérisation des sources est difficile. En effet, la contamination est **généralisée dans les sédiments du bassin de la Loire** pouvant être à la fois attribuée à des **sources globales et diffuses à l'échelle du bassin**. Cependant des enrichissements extrêmes sont archivés dans les sédiments de l'Anzieux (Loire Amont) en aval d'anciennes **chapelleries**, du Furan en aval d'anciennes **usines d'armement** et de la Vienne en aval de **tanneries**. Ces activités sont connues pour avoir constitué de fortes sources de contaminations en Hg avant les années 1960.

D'autre part, **les retombées globales et locales issues de la combustion du charbon** ont pu constituer des sources de **contaminations diffuses contribuant à la contamination polymétallique des sédiments**. Cependant, les sédiments des berges du Furan, de l'Anzieux, du Bedat (Allier) et de la Vienne présentent des signatures géochimiques similaires à celles enregistrées au cours de la période 1940 – 1950 dans les sous bassins de la Loire Amont et de l'Allier et entre les années 1950 et 1980 dans l'archive la plus aval.

## Influence des sources de contamination

Entre la seconde moitié du XIX<sup>ème</sup> siècle et la fin des années 1950, les activités polluantes qui étaient implantées dans le bassin de la Loire ont potentiellement influencé la géochimie des sédiments.

L'influence spatiale et temporelle des sources a été définie en faisant concorder les signatures géochimiques des phases de contaminations enregistrées dans les carottes avec celles des principales activités anthropiques de l'époque archivées dans les berges.

Dans la partie amont du bassin, cette analyse met en évidence l'influence des industries textiles, extractives et métallurgiques, maximale entre les années 1880 et la fin des années 1930, ainsi que des effluents miniers, maximale entre les années 1940 et les années 1950.

D'autre part cette analyse montre l'influence de l'utilisation locale du charbon dans les industries lourdes, maximale entre les années 1940 et 1950 dans la partie amont du bassin, et entre les années 1950 et 1980 dans la partie aval du bassin. D'autres sources, diffuses à l'échelle mondiale, ont aussi contribué aux contaminations généralisées à l'échelle du bassin.

De nos jours, les rejets sont mieux maîtrisés. Dans ce contexte, des sources anciennes peuvent être réactivées lors des événements hydrosédimentaires majeurs *via* l'érosion des sédiments contaminés stockés dans les berges.

**Des industries lourdes et notamment les aciéries** étaient implantées jusqu'à la fin des années 1950 dans ces affluents. La signature géochimique des effluents de hauts-fourneaux est comparable à celles enregistrées dans les sédiments des sous-bassins précédemment cités. La propagation des sédiments contaminés de ces sources vers la partie aval du bassin a été conditionnée par **les capacités de rétention sédimentaire du bassin**. Les aménagements des cours d'eau au cours de l'ère industrielle ont amplifié **le stockage des sédiments**, ce qui peut certainement expliquer le délai dans l'enregistrement de la phase de contamination.

Les séquences de crues archivées dans le réservoir de Villerest présentent une signature géochimique similaire à celle des sédiments contaminés des berge du Furan. De nos jours, les activités polluantes ont cessé leurs activités et les rejets anthropiques sont maîtrisés. Dans ce contexte **l'érosion des sédiments contaminés stockés dans les berges constitue une source importante de contaminations** lors des épisodes hydrosédimentaires majeurs.

### 7.3. Conclusion

L'analyse de la variabilité spatiale de l'enregistrement des contaminations sédimentaires a permis de mettre en évidence l'existence de phases de contaminations locales n'affectant que leurs sous-bassins sources et d'autres enregistrées aussi bien dans les parties amont qu'à l'aval du bassin. La propagation des sédiments contaminés des sous-bassins sources vers la partie aval du bassin de la Loire a imposé un délai dans l'archivage du signal géochimique. Ces résultats soulignent **l'importance d'une étude multi-site pour reconstituer les dynamiques temporelles à l'échelle du bassin.**

L'utilisation des signatures géochimiques des contaminations anciennes archivées dans les sédiments

des berges a permis de reconstituer l'historique des sources au cours de l'ère industrielle. Avant les années 1940, les métaux enrichis sont essentiellement Hg, Sb et Sn, liés aux **industries textiles, extractives et métallurgiques**. Entre les années 1940 et 1950 de très forts enrichissements en Bi, Cd, Hg et Sb sont enregistrés, associés aux **activités minières** (Charbons et minerais) ainsi qu'aux **industries lourdes**. Après les années 1960, le progressif abandon des extractions minières et la délocalisation des industries lourdes permet une décroissance progressive des niveaux de **contaminations sédimentaires**. De nos jours, **l'érosion des sédiments contaminés** archivés dans les berges constitue une **source importante de contamination lors des épisodes hydrosédimentaires**.

## **Chapitre 8 – Spatial variability of trace element sedimentary contaminations archived in sediments of the Loire basin**

*This chapter will be part of a paper in preparation*

### **Highlights:**

- Comparison of the archiving of sedimentary contamination between the upstream and the downstream part of the Loire basin
- Local sedimentary contaminations only affecting the upstream part of the Loire basin
- Sedimentary contaminations archived with a delay between the upstream and the downstream part of the basin
- Old sources characterization with geochemical signatures archived in river bank sediments

## **Abstract:**

From the 19<sup>th</sup> century, the Loire basin (France) contains important mining and industrial complexes mostly located in the upstream part of the basin and main tributaries. The geographical distribution of anthropogenic activities is potentially a factor of spatial and temporal variability of sedimentary contaminations. This paper proposes a basin-scale approach of the history of trace element sedimentary contaminations by comparing archived TE signals recorded in sedimentary cores recovered in the most industrialized sub-basins and the most downstream part of the Loire basin. In addition, contamination sources were characterized by comparing geochemical signatures archived in river bank sediments downstream of industrialized sub-basins and in sedimentary cores. This approach highlights influences of industrial and coal/TE-mining complexes on the sedimentary contamination of the Upper Loire and the Allier sub-basins between the 1880s and the late 1950s. During this period, mining effluents and local TE fallout are responsible of TE contaminations affecting only these two sub-basins. By contrast, local and global emission sources like coal combustion and blast furnace sludge from heavy industries implanted in the upstream part of the basin and in the Vienne tributary affect the upstream like the downstream part of Loire basin. The dispersion time for polluted sediments induces a decade delay in the archiving of contamination phases in the most downstream part of the basin. Since the 1960s in upstream sub-basins and since the 1980s in the most downstream part of the Loire basins, TE enrichments exponentially decrease. In this context, the erosion of highly polluted river bank sediments during major hydrosedimentary events is a factor of reactivation of old sources.

## **Keywords:**

trace elements, sedimentary contamination, temporal evolution, spatial variability, basin-scale approach, fingerprints

## 8.1. Introduction

Industrial Revolutions of the 19<sup>th</sup> and 20<sup>th</sup> century mark a transition in the Earth history. From this epoch a new geological era can be defined - the Anthropocene - corresponding to a period when Human imprint on the global environment largely concurrences the great force of Nature (Crutzen, 2000; Steffen *et al*, 2007; Steffen *et al*, 2011). At basin-scale, dramatic intensifications of anthropogenic pressures on the environment result in important disturbances like among others on:

- (i) the geochemical composition of water and sediments (*e.g.* for trace elements: Martin and Meybeck, 1979; Meybeck and Helmer, 1989; Darnley *et al*, 1995; Vink *et al*, 1999; Meybeck, 2002; Viers *et al*, 2009),
- (ii) and the sedimentary transport (Arnaud-Fassetta, 2003; Bridge, 2003; Vörösmarty *et al*, 2003 ; Knox, 2006; Hoffmann *et al*, 2010; Hughes *et al*, 2010).

Hence, in highly anthropized basins, the major part of metal inputs has been stored and is still retained in basin sediments (Walling and Owens, 2003;

Audry *et al*, 2004; Meybeck *et al*, 2007; Lestel *et al*, 2007; Thevenot *et al*, 2007).

As trace elements (TE) are mostly associated with fine-grained sediments during the sedimentary transport, the spatial distribution of a contamination is largely controlled by settling and erosional capacities in fluvial environments (Horowitz and Elrick, 1987; Walling *et al*, 2003). In detailed, storage of fine-grained sediments and associated pollutants in river bed is only limited at interflood periods (Walling *et al*, 2003; Estrany *et al*, 2011 ; Reis *et al*, 2014). Conversely, sediments and pollutants can be stored at more or less long-term in floodplain (Bradley and Cox, 1990; Martin, 2000; Heaven *et al*, 2000; Walling *et al*, 2003; Lecee and Pavlowsky, 2014; Dhivert *et al*, 2015) and dam reservoirs environments (Ye *et al*, 2011; Vukovic *et al*, 2014; Dhivert *et al*, 2015). Archiving capacities of these two last storage compartments are often used to build temporal dynamics of pollutants at basin scale (*e.g.* for neighboring basins: Grousset *et al*, 1999; Gocht *et al*, 2001; Audry *et al*, 2004; Castelle *et al*, 2007; Le Cloarec *et al*, 2011; Berner *et al*, 2012; Desmet *et al*, 2012; Ferrand *et al*, 2012; Mourier *et al*, 2014).

The Loire basin contains important coal and TE-mining districts which constituted ones of foci of development during Industrial Revolutions in France (Woronoff, 1994). The Loire River offers good opportunities to study the long-term evolution of TE contaminations archived in sediments (Grosbois *et al*, 2012; Dhivert *et al*, 2015). Geographical distribution of anthropogenic activities and potential contamination sources is contrasted at the Loire basin scale (Fig. 8.1). Indeed, industrial and mining complexes and the most important urban areas are essentially located in the upstream part of the Loire basin (in the Upper Loire and the Allier sub-basins), and lesser in main tributaries in the downstream part.

Regarding these observations, the aim of this paper is to study spatial and temporal variabilities of TE sedimentary contaminations in the entire Loire basin. Historical contamination sources were characterized at the entire basin scale and over the industrial period using geochemical signatures archived in river bank sediments. This study is then based on a comparison of TE signals archived in sediments downstream of the oldest and the most industrialized sub-basins and in

the most downstream part of the Loire basin.

## 8.2. Study area and methodology

### 8.2.1. Physical and hydrological characteristics of the Loire basin

The Loire River is the largest French basin with a total surface area of 117 800 km<sup>2</sup> (the ten largest of W-European basins) and 1013 km long from the spring to the estuary. In its upstream part, the basin is composed of the Upper Loire (480 km long, 17 570 km<sup>2</sup> of surface area) and the Allier sub-basins (421 km; 14 310 km<sup>2</sup>). The downstream part of the Loire basin drains three main tributaries as the Cher (368 km, 13 920 km<sup>2</sup>), the Vienne (372 km, 21 161 km<sup>2</sup>) and the Maine (23 314 km<sup>2</sup>) sub-basins.

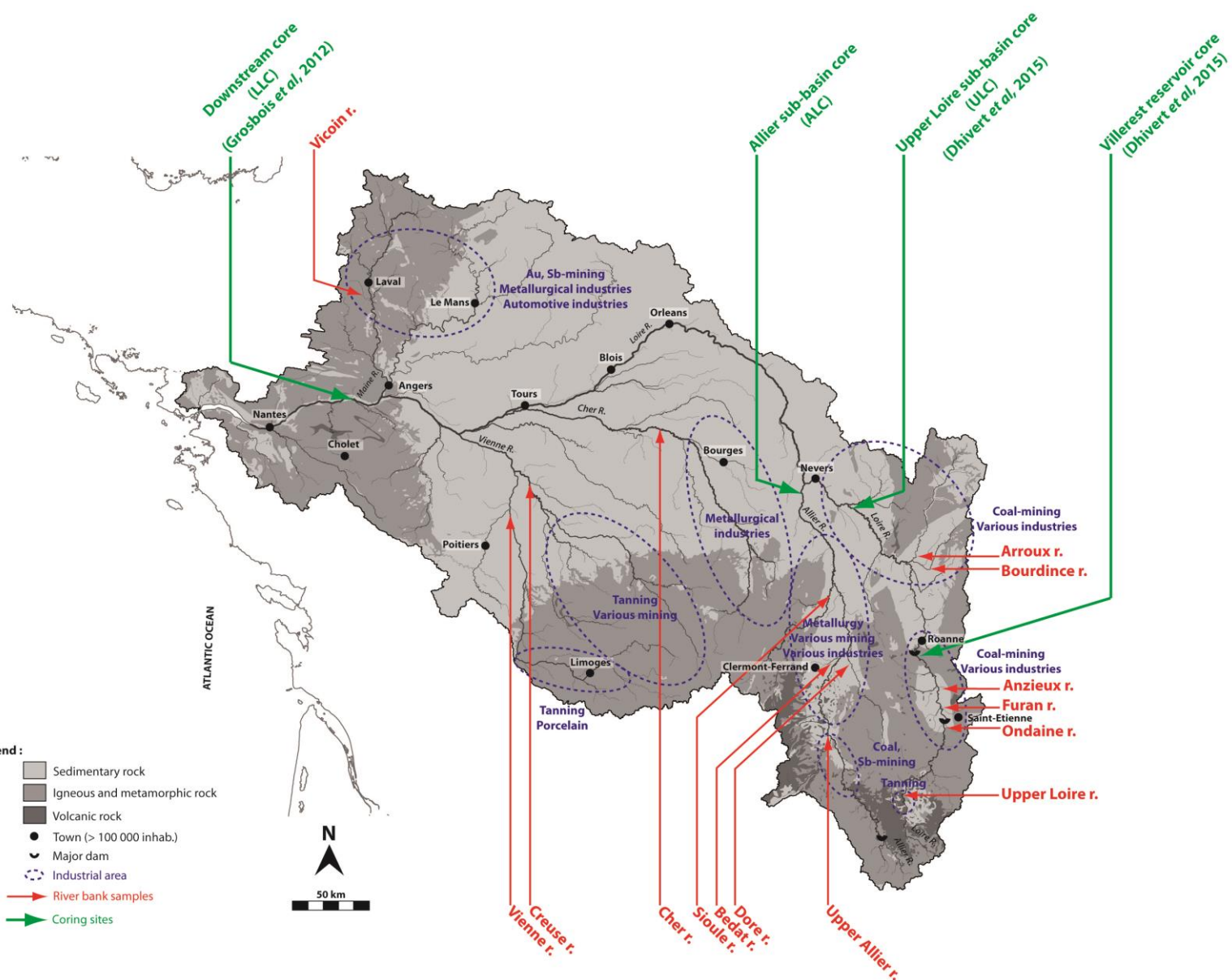
Hydrology of the Loire basin is influenced by a balance of oceanic and Mediterranean rainfalls during autumn and winter completed by snow-melt in spring (Dacharry, 1974). At the downstream gauging station (near to the most downstream coring site noted LLC in Fig. 8.1), the annual hydrological cycle is characterized by a high flow period from November to May (maximum averaged

monthly discharge of  $1530 \text{ m}^3.\text{s}^{-1}$  in February) and a low flow during summer time (minimum of  $250 \text{ m}^3.\text{s}^{-1}$  in August; calculated over 147 years). Hydrology is very similar between the Upper Loire and the Allier sub-basins, presenting at their downstream gauging stations, maximum monthly discharges of  $325 \text{ m}^3.\text{s}^{-1}$  in February and minimum of  $48 \text{ m}^3.\text{s}^{-1}$  in August (calculated over 60 years). During the second part of the 20<sup>th</sup> century, water discharge was controlled by important dams in the upstream part of Loire basin (dams > 50 m high, Fig. 8.1, since 1957 and 1984 the Grangent and the Villerest dams respectively in the Upper Loire River and since 1983 the Naussac dam in the Allier River). Hydrology of the main tributaries of the Lower Loire basin is sensitively similar to the two upstream rivers (averaged monthly discharges ranged from 28 to  $196 \text{ m}^3.\text{s}^{-1}$  for the Cher River, from 62 to  $362 \text{ m}^3.\text{s}^{-1}$  for the Vienne River and from 35 to  $267 \text{ m}^3.\text{s}^{-1}$  for the Maine River ([www.hydro.eaufrance.fr](http://www.hydro.eaufrance.fr))).

Geology of the Loire basin is contrasted (Fig. 8.1). The upstream part of the

hydrosystem drains the E-part of the French Central Massif (Fig.8.1). This old massif is inherited from the Variscan orogeny (480-290 Ma) and it is composed of (i) Variscan plutonic bedrocks (granites, gneiss and micaschists), (ii) volcanic areas dating from the Tertiary to the Holocene (65 Ma and 3.5 ka), and (iii) sedimentary facies from Carboniferous and Oligocene-Miocene (mainly sandstones, marls and clays). Downstream the confluence between the Upper Loire and the Allier Rivers, the Loire River runs over the S-part of the Paris basin, a sedimentary basin infilled from the Trias to the Tertiary and composed of limestone, chalk, marl and detrital siliceous rocks. Springs of main tributaries are all located in the French Central Massif. The Cher and the Vienne Rivers start in the central part of the massif essentially composed of Variscan plutonic bedrocks. The Maine basin drains the N-W part of the massif composed of a mix of plutonic bedrocks and Primary sedimentary facies (mostly sandstones and partially metamorphized marls) and the central part of the Paris basin.

**next page - Fig. 8.1:** Map of the entire Loire basin showing: i) geology (BRGM), ii) major dams (> 50 m high), iii) major urban areas (> 100 000 inhab., INSEE), iv) major industrial and mining areas (various historical archives), v) the three coring sites of this study and vi) sampled river banks



### **8.2.2. Industrialization of the Loire basin**

From the 16<sup>th</sup> century, proto-industrial activities were present in the Loire basin, essentially based on textile, leather and fur tanning and manufacturing (Woronoff, 1994). The industrialization of the Loire basin fully began in the second part of the 19<sup>th</sup> with the industrial exploitation of geological resources in the French Central Massif. Old mining districts of the upstream part of the basin constitute emergence points of this industrial development (Fig. 8.1). Indeed, three of the major coal-mining districts at the French scale were implanted in Carboniferous sedimentary facies of the E-part of the massif:

- (i) the Saint Etienne and the Blanzy-Epinac-La Machine districts located in the Furan and the Arroux-Aron tributaries respectively (Upper Loire sub-basin)
- (ii) and the Brassac-les-Mines district located in the Allagnon tributary (Allier sub-basin, Fig. 1).

From the Middle-Age to the early 1980s, they produced more than 1.5 Gt of

coal, corresponding to 30% of the national production. In details, industrial coal extraction really began in the 1830s and strongly increased in the 1870s to reach a maximum production between the early 1930s and the late 1950s. After then, coal-mining activities slowly decreased down to the early 1980s, the last mine closing in 1983 ([www.charbonnagesdefrance.fr](http://www.charbonnagesdefrance.fr)). Smaller coal-mining sites were also in activities during the between the second part of the 19<sup>th</sup> century and the late 1950s in similar geological units located in the central and the N-W part of the massif.

Between the second part of the 19<sup>th</sup> and the end of the 1950s, TE-mining constituted the second factor of industrial development for the Loire basin. As a result of hydrothermal mineralization during the Variscan orogeny, TE enrichments are present in bedrock of the French Central Massif (Delfour *et al*, 1984; Sizaret, 2002). TE-ores due to sulfide mineralization were largely exploited in the upstream basin (notably pyrite deposits) as the Cu-mining district of Chizeuil (about 1 000 t extracted between 1854-1963) or the Ag-Pb-mining district of Pontgibaud (50 kt extracted between 1826 and 1897; Fig. 8.1). In addition, during the first part of the 20<sup>th</sup> century, the Loire

basin contained two of the most important Sb-mining districts in the world, exploiting stibine deposits in the Allier basin (Brioude-Massiac district, 40 kt extracted between 1880s and 1968) and in the Maine basin (La Lucette district, 42 kt extracted between 1900 and 1934). Both of them provided more than 60% of the total French production ([www.sigminesfrance.brgm.fr](http://www.sigminesfrance.brgm.fr); [www.societechimiquedefrance.fr](http://www.societechimiquedefrance.fr); Fig. 8.1).

Associated with coal and TE-mining, raw materials and energy were locally used for industrial activities. Hence, the most important part of the Loire basin economy was based on industrial and mining complexes implanted near to geological resources. TE-ores were locally smelted using coal extracted nearby, as in districts of Pontgibaud, Brioude-Massiac and La Lucette. In complement of local production, ores from Europea countries around were often imported to be smelted in these structures (Garçon, 1995). In addition, heavy industries were also implanted near of mining sites like steel factories and glassware (Fig. 8.1). In the early 1960s, after the mining productions slowdown, many heavy industries relocated their production units

near to international harbors on seashores.

Since the late 19<sup>th</sup>, industrial and mining foci also correspond to the oldest and the most important urban areas of the Loire basin (Woronoff, 1994). Nowadays, the Saint Etienne (508 847 inhabitants in 2010) and the Clermont-Ferrand agglomerations (468 891 inhab.) are still the major urban areas at the Loire basin scale. Four other important urban areas are also located in the Lower Loire basin *i.e.* Limoges (282 873 inhab.), Orléans (419 271 inhab.), Tours (477 438 inhab.) and Angers (397 435 inhab.; [www.insee.fr](http://www.insee.fr)).

### 8.2.3. *Geochemical analysis*

Stream, floodplain and reservoir sediments of the Loire bassin can be very heterometric (Valverde *et al*, 2013; Dhivert *et al*, 2015; Dhivert *et al*, 2015), therefore geochemical analyses were carried out on the < 63 µm fraction in order to limit grain-size influences (Horowitz and Elrick, 1987).

Geochemical analyses were carried by the SARM-CRPG laboratory (France; [www.helium.crgc.cnrs-nancy.fr/SARM](http://www.helium.crgc.cnrs-nancy.fr/SARM)). Material was completely digested with LiBO<sub>2</sub>-Li<sub>2</sub>B<sub>4</sub>O<sub>7</sub> on a tunnel oven and placed

in an acid solution before to be analyzed by ICP-OES (ICap 6500, Thermo Scientific) for total contents of major and minor elements by ICP-MS (Thermo Elemental X7, Thermo Scientific) for trace elements, except for Hg done by DMA-80 (Milestone). Total organic carbon (TOC) after a HCl attack and total sulfur (TS) were analyzed by O<sub>2</sub> flow combustion at 1350°C with a SC 144-DRPC (Leco). Analytical error taking into account accuracy of digestion process and analyses was within 1% for major elements and within 10% for trace elements.

In order to compare anthropogenic TE enrichments at the entire basin scale, recorded TE concentrations must be compared to representative natural concentrations. By calculating enrichment factors (EF) with a double normalization to Al concentrations and to preindustrial concentrations, a comparative analysis of contamination levels in sediments can be representative at a basin scale. Despite a contrasted geology, preindustrial sedimentary concentrations in the upstream (Dhivert *et al*, 2015) and the downstream part of the Loire River (Grosbois *et al*, 2012) are similar, except local influences of geochemical anomalies.

#### **8.2.4. Sedimentary archive descriptions**

In order to study spatial and temporal variabilities of TE contaminations archived in sediments, TE temporal signals were compared in sedimentary archives sampled

- (i) downstream the oldest and the most important industrial and mining complexes on the Upper Loire river and on the Allier river
- (ii) and in the most downstream part of the fluvial domaine.

The Cher, the Vienne and the Maine sub-basins should have been sampled as industrialized areas. However, appropriate coring sites (settling spots downstream of anthropized sub-basins) are hard to find in these sub-basins because of embankments and canalization of river channels.

The Upper Loire Core (ULC) was sampled in 2012 in a paleochannel at Decize (46°49'37"N, 3°27'38"E, noted UWC in Dhivert *et al*, 2015, Fig 8.1). The 160 cm long core of ULC is essentially composed of fine-grained sediments, with a low enrichment in very fine-grained sands from 50 cm deep towards the surface. More than two centuries are registered in this sedimentary archive

(bottom sediments dating from  $1780 \pm 11$ a). For the ULC, sedimentary transitions related to well documented hydrosedimentary events allowed a detailed dating (*i.e.* extreme flood records related to the 1846, 1856, 1866 and 1907 events and a transition in aggradation processes related to the Decize dam elevation in 1933).

In 2012, another core was sampled in the downstream part of the Allier basin (ALC). The ALC was recovered in the Appremont-sur-Allier water supply canal ( $46^{\circ} 55' 36''$  N,  $03^{\circ} 03' 29''$  E; Fig. 8.1 and Fig. 8.2 a). Since 1840, this hydraulic structure supplies water from the Allier River to the Loire lateral shipping canal. Since the 1940s, the structure is equipped for retaining the coarsest particles in the lock (coarse sediments being evacuated by

opening of the downstream door). In order to limit the influence of dead biomass deposits, the coring site is located close to the supply lock. According to canal managers, sediments have never been dredged.

As for the ULC, dating and geochemistry analyses of the ALC were performed with 2 cm-slices of core sediments. Material and method are detailed in Dhivert *et al.* (2015). Grain-size measurements were performed using a laser microgranulometer (Mastersizer 2000, Malvern). According to a visual and textural sedimentary analysis, the ALC can be divided in two sedimentary units (Fig. 8.2 b). The deepest unit (28-116 cm) is dark and composed of very poorly sorted sediments in a balanced proportion of very fine-grained sands and silts.

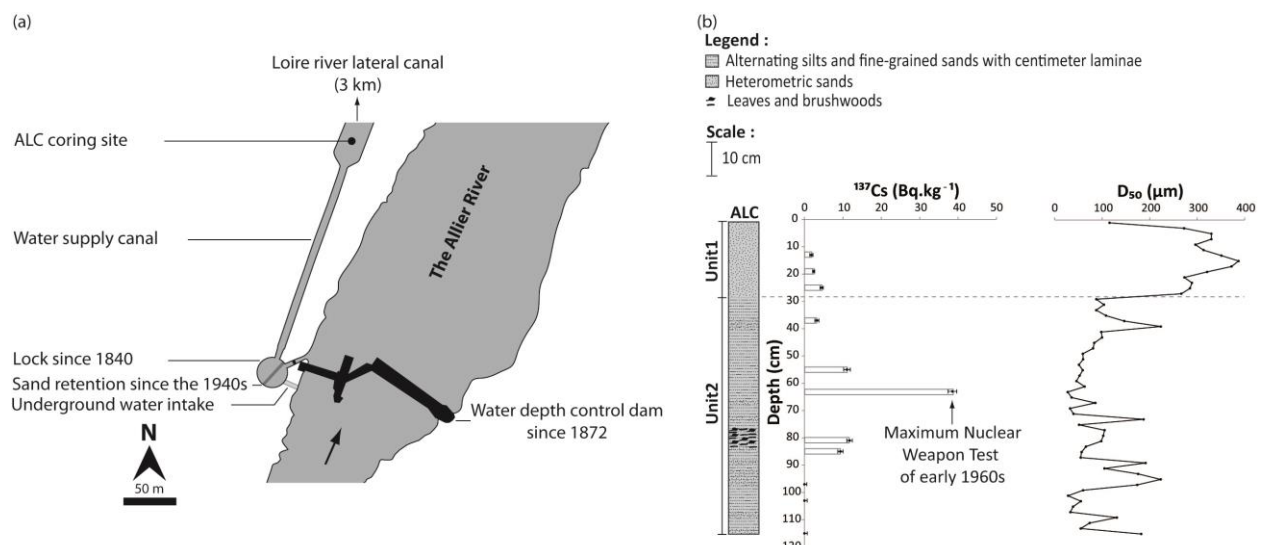


**Fig. 8.2:** a) Coring site of the Allier core (ALC) showing the sampled hydraulic structure; b) the sedimentary log of the ALC, median grain-size evolution and  $^{137}\text{Cs}$  vertical profile

The 78-88 cm sedimentary layer is composed of compacted leaves and brushwood and is therefore not integrated in this study. The median grain-size of this unit averages 88 µm ( $n = 44$ ) but the grain-size variability is high (RDS = 58%) because of heterometric sandy layers archived at 114-116; 108-110; 88-98; 72-74 and 36-40 cm deep (Fig. 8.2 b). The upper unit (0-28 cm) is homogenously composed of sands moderately sorted, median grain-size equals to 298 µm (RDS = 12%,  $n = 14$ ). Sandy sedimentary layers at 92-96 cm, 70-72 cm and 0-28 cm contain rich-Hf sediments (ranges from 39.5 to 138.5 ppm compared to the rest of the core:  $20.9 \pm 8.0$  ppm). In the Loire basin, Hf concentrations can be used as a tracer of heavy minerals and thus detrital inputs especially during floods (Dhivert *et al*, 2015). TE signal being potentially influenced by these detrital inputs, these sandy layers were not considered to build long-term evolution of sedimentary contaminations in the ALC.

The core datation was built regarding vertical distribution of the  $^{137}\text{Cs}$  radionuclide, measured by gamma spectrometry with very low-background detectors, coaxial HP Ge N-type (8000 channels, low back-ground). In this studied

core, a detailed dating was not possible because of a non-linear sedimentation rate resulting of undated sandy layers. They should be attributed to overfull episodes for the sand retention structure, when the coarsest particles could spread in the water supply canal. Unfortunately, any information about such events was recorded in archives of the canal manager. However, the  $^{137}\text{Cs}$  dating can be used to define absolute time markers, even in the sandy fraction of the Loire basin sediments (Détriché *et al*, 2010). There is no  $^{137}\text{Cs}$  under 96 cm deep attesting sediment deposits before 1950, date of the first significant Nuclear Weapon Test (NWT; Fig. 8.2 b; Tab. 8.2). The  $^{137}\text{Cs}$  vertical profile shows an extended peak between 86 and 54 cm deep with a maximum of  $39 \pm 1.1 \text{ Bq}.\text{kg}^{-1}$  at 62-64 cm and a low activity ( $< 4 \pm 0.4 \text{ Bq}.\text{kg}^{-1}$ ) from 38 cm deep to the surface. According to the shape of this vertical profile and the low influence of the Chernobyl Nuclear Power Plant Disaster (C-NPPD) in the study area (De Cort *et al*, 1998; Dhivert *et al*, 2015), the  $^{137}\text{Cs}$  peak can be attributed to the maximum fallout of NWT, in the early 1960s.

The most downstream core (the Lower Loire Core, LLC) was sampled in 2009 in

the alluvial island of Montjean-sur-Loire ( $47^{\circ}23'34''N$ ,  $0^{\circ}51'23''E$ ; Grosbois *et al.*, 2012; Fig. 8.1). For this 400 cm long sedimentary archive, only sediments down to 230 cm deep are composed of fine-grained sediments and were considered to build TE temporal dynamics at the entire basin scale. The time interval covers by the LLC ranges from the early 20<sup>th</sup> at 198 cm deep to 2009 for surface sediments. In addition, pre-industrial TE concentrations in sediments were measured in a clayey layer sampled between 360 and 400 cm deep (much older than the 1900s, Tab. 8.1).

#### **8.2.5. Sampling strategy for anthropogenic source characterization**

As described in § 8.2.2., old anthropogenic activities are no longer in operation in the Loire basin because of the phasing-out of an economy based on industrial and mining complexes after the early 1960s. Moreover, since the 1980s the development of urban and industrial effluent treatment plants has largely improved the quality of aquatic environments in W-Europe (Meybeck and Helmer, 1989; Vink *et al.*, 1999; Meybeck, 2002). Therefore, old contamination sources are not necessarily active nowadays, and characterizing former

anthropogenic end-members may not be available. Nevertheless, their geochemical signatures archived in sedimentary storage areas can be characterized.

To select representative stations with a potential anthropogenic impact, documentation were provided by the French environmental ministry and the French geological survey (BASIAS, BASOL and SIGMines databases [www.basias.brgm.fr](http://www.basias.brgm.fr), [www.basol.developpement-durable.gouv.fr](http://www.basol.developpement-durable.gouv.fr) and [www.sigminesfrance.brgm.fr](http://www.sigminesfrance.brgm.fr)), by industrialists ([www.acier.org](http://www.acier.org); [www.societechimiquedefrance.fr](http://www.societechimiquedefrance.fr), [www.charbonnagedefrance.fr](http://www.charbonnagedefrance.fr), [www.atelierdeprojet.loire.equipement.gouv.fr](http://www.atelierdeprojet.loire.equipement.gouv.fr)) and by local municipal archives or museums (St Etienne, Gueugnon, Decize, Le Puy Guillaume municipal archives; Hat-making museum of Chazelles sur Lyon).

Stream sediments can be sampled to characterize active contamination sources (e.g. Förster and Salomons, 1980; Teixeira *et al.*, 2000; Möller and Einax, 2013). Indeed, the storage of sediments and associated contaminants are limited to interflood periods in river bed, because of important erosion episodes occurring during high discharge events (Birch *et al.*,

2001; Walling *et al*, 2003; Estrany *et al*, 2011; Bednarova *et al*, 2013; Reis *et al*, 2014). In this study, some stream sediments were collected downstream former and actual polluting or potentially polluting activities of the Loire basin (99 sites were sampled annex 3.1). Even if some of actual and former anthropogenic activities still constitute active contaminations sources, this database does not contains accurate information to characterize geochemical signatures of old contamination sources (Fig. 8.3.).

Hence, river bank sediments were sampled downstream important mining districts or/and industrialized areas (Fig. 8.1; Tab. 8.3). Sediments were sampled in the outer part of meanders, after refreshing the erosional surface. Two situations were selected for this sampling campaign:

- (i) the river bank was visually homogenous, sediments were then sampled continuously on 20 cm - slices all over the vertical profile,
- (ii) the river bank presents visual transitions, each layer was individually sampled.

All across the Loire basin, 14 rivers were sampled (Tab. 8.3). River bank

sediments used in this study are essentially composed of fine-grained sediments and present similar Hf concentrations (average of 15.4 ppm, RDS = 53%, data not shown).

## 8.3. Results

### 8.3.1. *Temporal evolution of trace element enrichments in sediments of the Upper Loire sub-bassin*

#### 8.3.1.1. < 1880s: non-impacted period

In this study, the TE signal comparison is based on the description of temporal windows, defined according to the temporal evolution of enrichment levels and to association of TE with similar behaviours.

In the Upper Loire sub-basin, a detailed dating is available for the ULC. Therefore, short-time variations of TE temporal dynamics can be precisely described.

The first temporal window in this sub-basin corresponds to a non-contaminated period defined between the 1780s and the end of the 1870s (Fig.8.4). During this time interval enrichment factors ranges between 1 and 2 for all TE except for Sb ( $4 < EF < 6$ ) which locally

present higher geochemical backgrounds (Dhivert *et al*, 2015, Tab. 8.1). Hg also shows light enrichments ( $2 < EF < 5$ ), with a slow increase from the 1846 flood sedimentary sequence to the late 1870s (Fig. 8.4; Tab. 8.1). As and W, enrichment factors do not exceed 2 all along the recording period (Tab. 8.1).

Since the 1830s and the beginning of industrial coal-mining, the Upper Loire basin was one of the emergence points of the First Industrial Revolution in France (*c.a* 1789-1880s, Woronoff, 1994). During this period, influence of anthropogenic activities on the geochemical composition of Upper Loire sediments is very light.

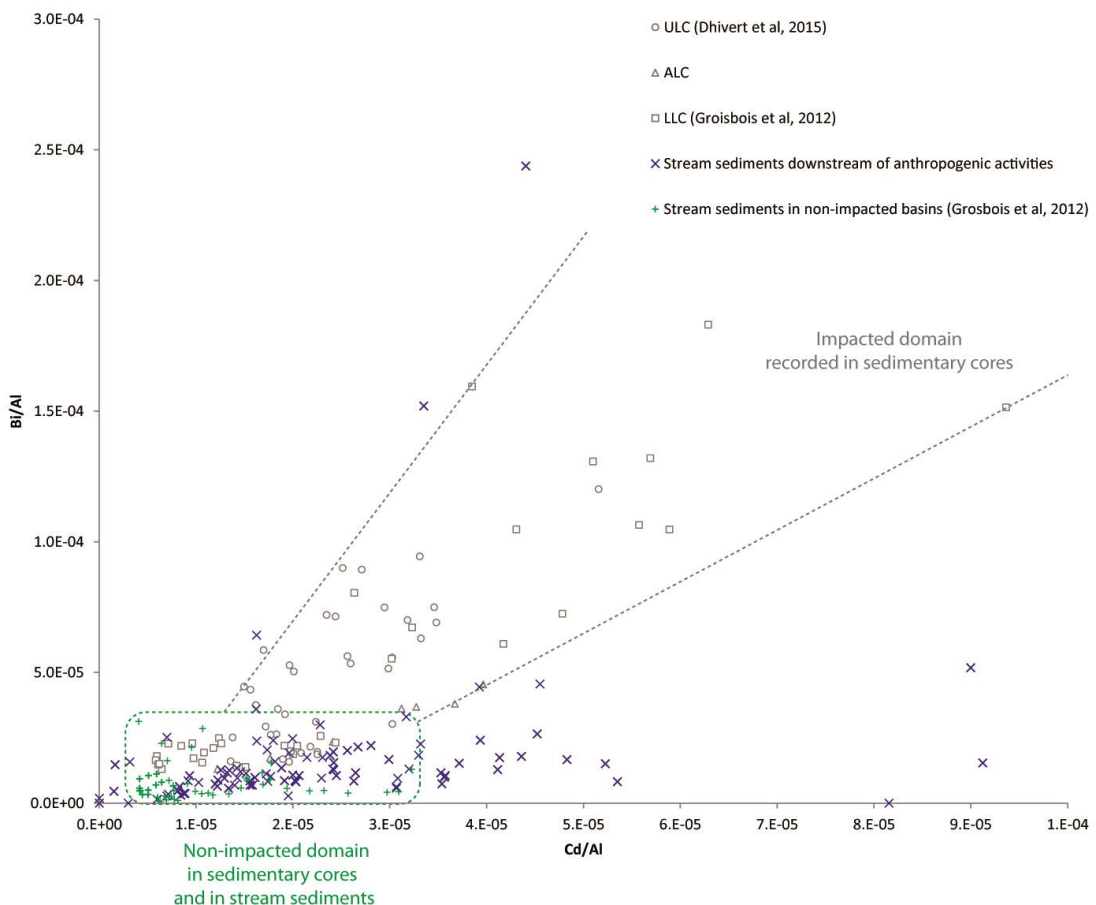


**Fig. 8.3. : Cd- Bi relationships in sedimentary cores, in stream sediments of non-impacted sub-basins in the Loire basin (Grosbois *et al*, 2012) and in stream sediments downstream of anthropogenic activities. Most of stream sediments sampled downstream of anthropogenic activities present geochemical compositions similar to non-impacted sediments. Bi/Cd ratios in impacted stream sediments are different from ratios in sedimentary cores.**

### *8.3.1.2. 1880s - late 1930s: Hg, Sb, Sn enrichments in sediments of the Upper Loire sub-basin*

The second temporal window in the ULC is defined between the early 1880s and the late 1930s. This temporal window corresponds to the first contaminated period, concerning Hg, Sb and Sn (Fig. 8.4, Tab. 8.1). Hg is the first and the most enriched TE. This element draws a sharp peak between the 1880s and the 1900s (maximum EF = 30 in the late 1880s; Fig. 8.4). The second enrichment increase in this temporal window is archived between the 1907 flood sequence and the late 1930s and concerns Hg, Sb and Sn. During this period, Hg follows a second gradual increase to reach EF close to 23 during the 1930s. Sb and Sn enrichments are gradually amplified until the late 1920s (maximum EF c.a. 9 between late 1920s and the late 1930s; Fig. 8.4). During this period, Sb and Sn and Pb are correlated ( $r = 0.9, p < 0.05, n = 14$ ). However, Pb shows very light enrichments (maximum EF = 3 between the late 1920s and the late 1930s; Tab. 8.1). In sediments deposited between the 1880s and the late 1930s, Cd, Cr, Cu, Mo, Ni, Pb, Sb, Sn and Zn are significantly correlated with TOC and S. ( $r > 0.6, p < 0.05, n = 24$ )

This defined time interval covers the Second Industrial Revolution (Woronoff, 1994). During this period mining activities and heavy industry developments are largely enhanced in the Loire basin (§ 8.2.2).

### *8.3.1.3. 1940s - late 1950s: maximum trace element enrichments in sediments of the Upper Loire sub-basin*

Between the early 1940s and the late 1950s, all TE are strongly enriched and defined a polymetallic contamination phase with maximum contamination levels over the recorded period (Fig. 8.4, Tab. 8.1). Pb are lowly enriched during this period (EF ranges between 3 and 4) but maximum enrichments are recorded after the 1960s (EF = 9). By contrast, Sn follows a progressive decreasing trend since the 1940s up to the early 1960s (EF c.a. 2 from the early 1960s to 2012; Fig. 8.4, Tab. 8.1).

During this time interval, Hg is not correlated with any other TE nor any major element evolution and shows very important enrichments with a maximum EF of 57 in the early 1940s. For other TE, a significant correlation can be highlighted between TOC, TS, Fe and chalcophil TE as As, Cu, Mo, Sb and U ( $r > 0.8, p > 0.05, n = 6$ ). Sb is the most enriched element of

these correlated TE showing a maximum EF of 13 in the late 1950s. Another significant correlation concerns Bi, Cd, Cr, Ni, W and Zn ( $r > 0.9$ ,  $p > 0.05$ ,  $n = 6$ ) in this time interval. These latter cited TE do not present any significant correlation with major element.

In the industrial history of France, this time interval corresponds to the beginning of the Glorious Thirty. For the Loire basin, maximum activities for mining districts and heavy industries occurred during this period (§ 8.2.2).

#### *8.3.1.4. > 1960s: general decreasing trends for trace element enrichments in sediments of the Upper Loire sub-basin*

From the early 1960s, temporal trajectories of TE contaminations are reversed. TE enrichments follow an exponential decrease, drawing the last temporal window up to the coring date (Fig. 8.4, Tab. 8.1). By contrast, Pb enrichments are maximum between the early 1960s and the early 1980s (EF c.a. 8). This maximum Pb contamination phase is synchronous with maximum global fallout related to leaded petrol combustion but only isotopic

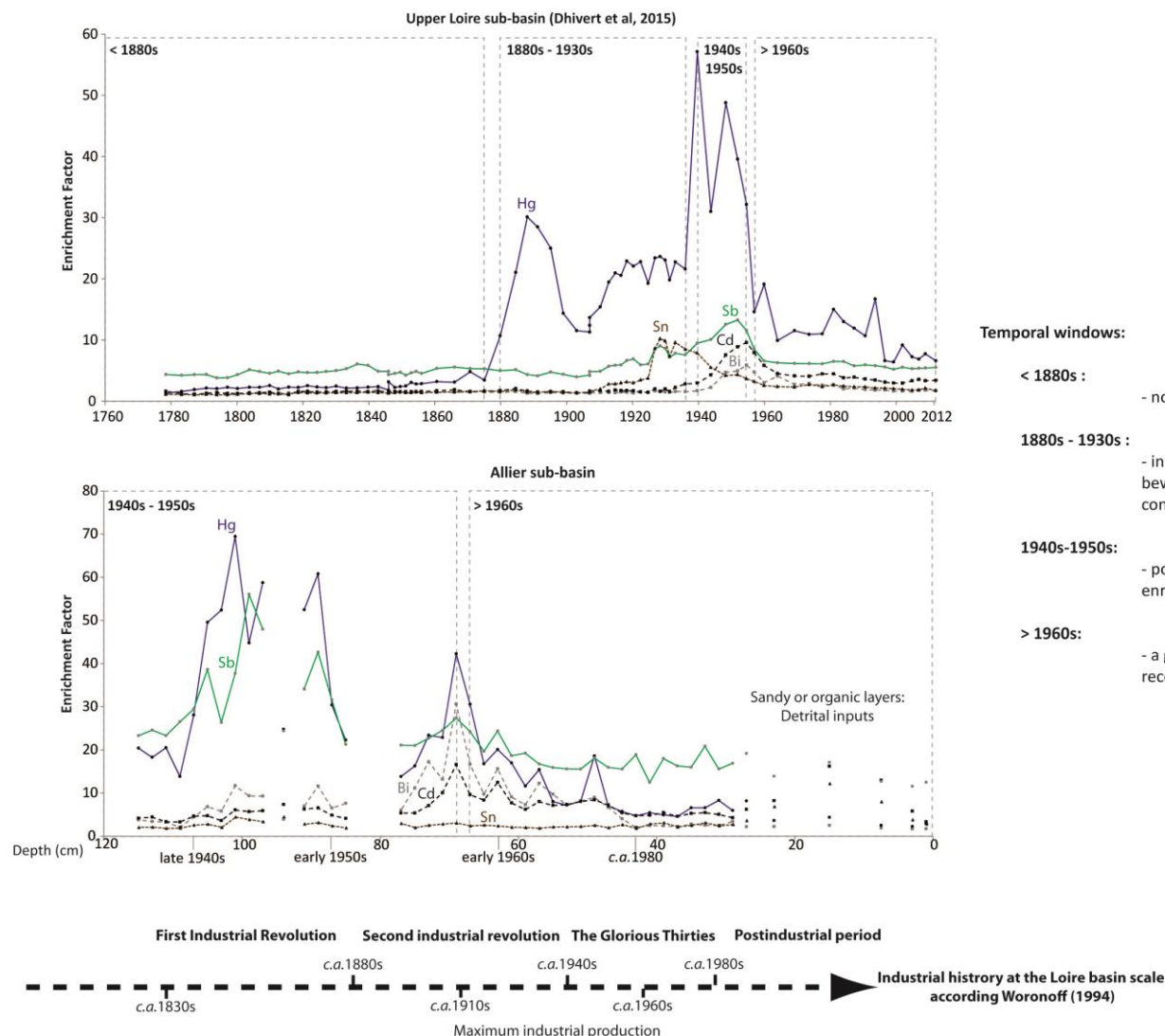
analyses could really trace sources (e.g. Hong *et al.*, 1994; Shotyk *et al.*, 1998; Monna *et al.*, 2000).

During this period Al, TS, Bi, Cd, Cr, Cu, Mo, Ni, Sb, Sn and Zn are significantly correlated ( $r > 0.7$ ,  $p < 0.05$ ,  $n = 18$ ). TE enrichments follow a significant decreasing trend up to the early 1980s ( $r > 0.8$ ;  $p < 0.05$ ;  $n = 7$ ). After the early 1980s, TE enrichments do not follow significant temporal evolutions ( $p > 0.05$ ). As, Bi, Cr, Cu, Ni, Pb, Sb, Sn, U, W and Zn recover EF range between 1 and 2 from the early 1980s. Mo and Sb enrichments average 3 and 5 respectively, close to during the preindustrial period. Cd presents enrichments range between 3 and 4.

After the 1950s, Hg enrichments sharply decrease up to 1964. Hg enrichments stay high until the early 1990s (EF ranges between 10 and 17) before to secondly decline (EF ranges between 6 and 9 from the early 1990s).

In summary, four temporal windows can be defined:

- (i) the non-contaminated period of 1780s-1870s,



#### Temporal windows:

##### < 1880s :

- non-contaminated period for the Upper Loire basin

##### 1880s - 1930s :

- in the Upper Loire sub-basin a Hg contamination phase between the 1880s and the 1900s and a Hg, Sb, Sn contamination phase between the 1910s and the 1930s

##### 1940s-1950s:

- polymetallic contamination phases with maximum enrichments levels for the Upper Loire and the Allier sub-basins

##### > 1960s:

- a general decreasing trend for TE enrichments recorded in the Upper Loire and the Allier sub-basins

**Fig. 8.4. : TE temporal evolution recorded in sedimentary cores of the Upper Loire sub-basin (ULC; Dhivert et al, 2015) the Allier sub-basin (ALC), and the historical evolution of industrial and mining activities in the Loire basin according to Woronoff (1994)**

- (ii) the 1880s-1930s period with high to moderate contamination levels for Hg, Sb and Sn,
- (iii) the 1940s-1950s period corresponding to a polymetallic contamination phase with maximum TE enrichments
- (iv) and the 1960s-2012 period drawing an exponential decrease of TE enrichments. The only exception is for Pb showing maximum enrichments during this period. Since the early 1980s, TE contaminations are low compared to the most contaminated period but all TE do not recover preindustrial concentrations

### **8.3.2. Temporal evolution of trace element enrichments in sediments of the Allier sub-bassin**

#### **8.3.2.1. 1940s – late 1950s: maximum trace element enrichments in sediments of the Allier sub-basins**

Temporal evolutions of TE enrichments in sediments of the Allier sub-basin can be described in the ALC according to temporal windows defined in the ULC.. Because of the non-linear

aggradation rate, a detailed dating is not established for this core. However, according to the  $^{137}\text{Cs}$  vertical profile, temporal windows can be defined.

The oldest temporal window of the ALC is archived between 106 and 68 cm deep. In this interval, TE enrichments are maximum (Fig. 8.4, Tab. 8.2). In detail, W enrichments draw a sharp peak between 98 and 106 cm deep (EF c.a. 6). Sb and Hg enrichments are maximum between 88 and 106 cm deep, and show very high contamination levels (EF range between 24 and 69). TOC and TS are also maximum in this interval. In this interval Bi and Cd present moderate to high enrichments (EF range between 4 and 12) and other TE low to moderate enrichments (EF ranges between 2 and 5). Between 78 and 68 cm deep, all TE enrichments sharply increase (except Cr and Ni). Bi, Cd, Hg, and Sb are the most enriched TE reaching high to very high contamination levels (maximum EF = 31 for Bi, 17 for Cd, 42 for Hg, and 27 for Sb at 68-70 cm deep). In 68-78 cm and 88-106 cm intervals, a correlation can be highlighted between TOC, TS, Bi, Cd, Cu, and Zn ( $r > 0.8$ ,  $p < 0.05$ ,  $n = 16$ ).

According to the  $^{137}\text{Cs}$  date-bounded (the early 1960s maximum at 62–64 cm and its deepest detection at 94–96 cm) the 68–106 cm sedimentary layer should be deposited between the 1940s and the 1950s. This time interval corresponds to the maximum acitivity period for the Brioude-Massiac Sb-mining district, the Brassac-les-Mines coal-mining district and the Echassières W-mining district located in the Allier sub-basin. TOC, TS, Hg, Sb and W maximum enrichments can be related to these anthropogenic activities (§ 8.4.1.2).

### *8.3.2.2. > 1960s: general decrease of enrichements in sediments of the Allier sub-basin*

From 68 cm to 44 cm deep a general TE decontamination trend is archived drawing the second temporal window (Fig. 8.4, Tab. 8.2). Al, TOC, As, Bi, Cd, Cu, Pb and Zn are all significantly correlated in this interval ( $r > 0.8$ ,  $p < 0.05$ ,  $n = 12$ ). For all elements except Cr, Ni, Sn, U and W, a significant exponential decreasing trend is archived from 68 cm to 44 cm deep ( $r > 0.7$ ,  $p < 0.05$ ,  $n = 12$ ). As and Cu recover preindustrial concentrations, and other TE present EF range between 2 and 4 for Bi, Cr, Ni, Pb, Sn, U, W and Zn, between 4 and 6 for Cd and Mo and between 5 and 8 for Hg. Sb

enrichments stay high, ranging between 12 and 21. Between 44 cm and 28 cm deep, TE contaminations do not follow a significant temporal evolution ( $p > 0.05$ ,  $n = 14$ ), except for Hg which enrichments are slightly amplified between 34 cm and 28 cm deep (EF c.a. 8).

In the sandy sedimentary unit 1 (0–28 cm), Cd, Sn and U enrichments are enhanced (maximum EF = 16 for Cd, 12 for Sn and 8 for U; Fig. 8.4). As explaind in § 8.2.4, heavy minerals can be more abundant in this sandy layer which may influence enrichments for these TE.

In the Upper Loire and in the Allier sub-basins draining the oldest and the most important mining and industrial complexes of the Loire basin, archived temporal windows are synchronous and enrichments levels are similar. For both upstream sub-basins:

- (i) TE pollutions are maximum between the 1940s and the late 1950s (EF > 50 for Hg), a first group of TE is represented by chalcophil elements (Sb and Hg are the most enriched TE), the second group corresponding to an association of Bi, Cd, Pb and Zn (Bi

- and Cd are the most enriched TE in this group)
- (ii) a general decrease of TE enrichments is recorded between the 1960s and the early 1980s
  - (iii) from the 1980s TE enrichments do not follow significant temporal evolutions .

### **8.3.3. *Upstream-downstream comparison of recorded temporal signals***

#### **8.3.3.1. *Spatial and temporal variations of sedimentary contaminations in sediments of the Loire basin***

Using temporal windows defined in the most industrialized sub-basins, temporal variations of TE sedimentary contaminations can be compared between the upstream and the downstream part of the Loire basin.

- The 1880s-1930s temporal windows (Fig.8.5):

The beginning of the sedimentary record dates from the early 20<sup>th</sup> century in the LLC. During this time interval, two contaminations phases can be described in the Upper Loire sub-basin affecting Hg, Sb and Sn (Fig. 8.4). During this time interval, Hg shows high enrichments (EF range between 23 and 36) in the LLC, similar to the ULC (Fig. 8.5). However,

unlike in the ULC, Hg enrichments follows a significant decreasing trend in the most downstream core before the 1930s ( $r=0.6$ ,  $p < 0.05$ ,  $n = 10$ ). In the most downstream core, temporal variations of Sb and Sn enrichments are also different to the ULC. These TE follows a significant decreasing trend all over the recorded period in the LLC (EF range between 2 and 6;  $r = 0.8$ ,  $p < 0.05$ ,  $n = 25$ ; Fig. 8.5). By contrast, in the ULC Sb and Sn show an increasing trend from the 1910s to the late 1930s (§ 8.3.1.2). Before the 1930s, other TE present enrichments range between 1 and 4 in the LLC like in the ULC.

- Between the 1940s and the 1950s (Fig. 8.5):

A polymetallic contamination phase is recorded in the ULC like in the ALC. Bi, Cd, Hg and Sb are the most enriched TE (Fig.8.4). In the LLC, Hg enrichments significantly increase from 22 in the 1940s to 46 in the early 1950 ( $r = 0.9$ ;  $p < 0.05$ ,  $n = 4$ ; Fig. 8.5). However, enrichments of Bi, Cd and other TE are very low (between 1 and 4) in comparison to the ULC and the ALC (Fig. 8.5).

Depth cm	Date	$^{137}\text{Cs}$ activity Bq.kg $^{-1}$	Median grain-size $\mu\text{m}$																															
				ppm	ppm	EF	ppm	EF	ppm	EF	ppm	EF	ppm	EF	ppm	EF	ppm	EF	ppm	EF	ppm	EF	ppm	EF	ppm	EF	ppm	EF						
0-2	2012	6±0,7	30,1	0,10	2,92	11,8	27,9	2	0,9	2	1,0	3	96	1	27	2	0,110	7	0,9	3	33	1	61,5	2	1,8	6	10,8	2	7,4	1	6,0	1	159	2
2-4	2009±6a	n.d.	31,2	0,09	3,11	11,0	29,1	2	1,0	2	1,0	3	101	1	33	2	0,130	8	0,8	3	35	1	68,4	2	1,8	5	13,4	2	7,9	1	6,7	1	174	2
4-6	2007±6a	n.d.	28,6	0,10	2,83	11,4	25,1	2	1,0	2	1,0	4	101	1	31	2	0,115	7	0,8	3	35	1	66,2	2	1,8	5	11,7	2	7,6	1	6,4	1	166	2
6-8	2005±6a	n.d.	31,2	0,09	2,49	13,1	24,4	1	0,9	2	1,0	3	101	1	29	2	0,120	7	0,7	2	34	1	65,2	2	1,8	5	11,4	2	8,3	1	6,1	1	160	2
8-10	2002±6a	n.d.	27,8	0,08	2,18	15,2	24,0	1	0,9	2	0,8	3	99	1	29	2	0,150	9	0,7	3	35	2	66,6	2	1,8	6	11,9	2	8,7	1	6,0	1	155	2
10-12	1999±6a	7±0,7	44,9	0,08	2,09	15,0	23,7	1	0,9	2	0,8	3	99	1	28	2	0,105	6	0,8	3	34	1	66,2	2	1,7	5	12,6	2	8,7	1	6,3	1	149	2
12-14	1997±6a	5±0,5	45,5	0,09	2,21	13,3	23,2	1	1,0	2	0,9	3	103	1	28	2	0,110	7	0,8	3	35	1	66,7	2	1,9	6	13,3	2	8,5	1	6,4	1	161	2
14-16	1994±6a	7±0,8	39,2	0,10	2,21	15,7	24,4	1	1,0	2	1,0	3	119	1	30	2	0,280	17	0,9	3	40	2	78,9	3	1,9	6	13,5	2	9,6	1	6,5	1	170	2
16-18	1991±6a	n.d.	39,5	0,11	2,19	14,7	26,4	2	1,0	2	1,1	4	162	2	34	2	0,180	11	1,1	4	48	2	104,2	4	2,0	6	14,8	2	9,1	1	6,8	1	194	2
18-20	1987±6a	9±0,5	36,8	0,10	2,15	16,3	25,5	2	1,2	2	1,2	4	167	2	30	2	0,200	12	1,1	4	50	2	112,2	4	1,9	6	14,8	2	10,1	1	6,5	1	196	3
20-22	1984±6a	9±0,7	41,8	0,10	2,24	15,9	25,4	2	1,1	2	1,1	4	177	2	36	2	0,220	13	1,1	4	52	2	143,6	5	2,2	6	15,7	2	9,6	1	6,7	1	212	3
22-24	1981±6a	n.d.	42,1	0,11	2,31	15,0	28,4	2	1,5	3	1,3	4	209	2	40	2	0,255	15	1,1	4	57	2	199,5	7	2,2	7	16,9	3	9,1	1	6,8	1	238	3
24-26	1978±6a	12±0,8	36,8	0,11	2,17	16,6	26,7	2	1,4	3	1,3	4	202	2	36	2	0,185	11	1,1	4	57	2	252,9	9	2,1	6	15,0	2	9,3	1	6,7	1	229	3
26-28	1974±6a	13±0,4	41,2	0,11	2,05	14,9	26,8	2	1,6	3	1,2	4	181	2	35	2	0,185	11	1,1	4	52	2	255,4	9	2,1	6	17,3	3	9,0	1	7,7	2	225	3
28-30	1969±6a	14±0,5	40,1	0,12	2,04	15,0	24,8	1	1,5	3	1,2	4	161	2	33	2	0,195	12	1,0	3	49	2	201,8	7	2,1	6	14,8	2	9,0	1	6,7	1	231	3
30-32	1964	17±0,8	43,1	0,11	1,98	16,1	25,4	2	2,3	4	1,4	5	156	2	34	2	0,170	10	1,1	4	47	2	193,7	6	2,2	6	15,4	2	10,0	1	7,2	1	239	3
32-34	1960±6a	12±0,6	41,6	0,14	2,22	17,1	28,9	2	1,7	3	1,8	6	178	2	42	2	0,330	19	1,2	4	58	2	170,0	6	2,3	7	16,6	3	11,1	2	7,4	1	359	4
34-36	1957±6a	12±0,6	44,3	0,20	2,68	15,4	33,6	2	2,7	5	2,4	8	222	3	57	3	0,255	15	1,4	4	77	3	133,9	4	3,0	8	21,2	3	10,6	1	7,7	1	536	7
36-38	1955±6a	9±0,7	32,6	0,38	3,74	12,9	39,4	2	3,4	6	3,0	10	240	3	89	5	0,575	32	2,0	6	89	4	107,2	3	4,1	12	24,7	4	15,4	2	8,8	2	614	7
38-40	1952±6a	n.d.	39,7	0,47	4,61	12,0	41,7	2	2,9	5	2,8	9	244	3	110	6	0,720	40	2,4	8	93	4	106,2	3	4,8	13	29,6	4	19,2	3	8,8	2	599	7
40-42	1948±6a	< d.l.	69,9	0,45	4,85	11,7	41,1	2	2,8	5	2,4	8	218	2	114	6	0,895	49	2,3	7	83	3	96,6	3	4,6	13	29,0	4	18,2	2	8,4	2	543	6
42-44	1944±6a	n.d.	36,4	0,35	4,14	16,0	33,4	2	1,3	2	1,4	4	129	1	95	5	0,570	31	1,5	5	51	2	84,9	3	3,7	10	38,1	6	12,2	2	7,2	1	292	3
44-46	1940±6a	n.d.	49,7	0,30	3,02	13,3	32,4	2	1,0	2	1,0	3	127	1	66	3	1,080	57	1,2	4	41	2	91,2	3	3,6	9	55,8	8	10,4	1	7,3	1	200	2
46-48	1936±6a	< d.l.	31,1	0,18	2,62	13,7	27,6	1	1,0	2	0,9	3	126	1	52	3	0,410	22	0,9	3	39	1	87,0	3	2,9	8	60,7	9	10,4	1	6,7	1	180	2
48-50	1933	n.d.	32,4	0,21	2,89	11,7	32,7	2	1,0	2	0,8	2	132	1	48	2	0,450	23	1,0	3	40	1	90,7	3	3,1	8	71,3	10	9,6	1	6,8	1	179	2
50-52	1931±11a	n.d.	17,7	0,15	2,31	8,6	30,1	1	1,0	1	0,6	2	171	2	43	2	0,420	20	0,9	3	45	2	91,7	2	3,0	7	58,9	7	8,3	1	5,8	1	162	2
52-54	1930±11a	< d.l.	17,5	0,13	2,65	8,5	31,7	2	1,0	2	0,7	2	181	2	45	2	0,480	23	0,9	2	43	1	109,4	3	3,6	9	77,2	10	8,2	1	5,6	1	160	2
54-56	1928±11a	n.d.	13,7	0,11	2,58	7,5	29,3	1	1,1	2	0,6	2	172	2	69	3	0,505	24	1,0	3	41	1	114,0	3	3,9	9	81,9	10	8,5	1	6,1	1	181	2
56-58	1928±11a	n.d.	18,0	0,10	2,37	8,8	29,2	1	1,1	2	0,7	2	177	2	38	2	0,470	23	1,0	3	38	1	112,2	3	3,4	9	64,9	1	8,6	1	6,5	1	157	2
58-60	1925±11a	< d.l.	16,7	0,07	2,04	8,7	23,3	1	0,9	1	0,5	1	159	2	34	2	0,395	19	0,8	2	41	1	84,2	2	2,5	6	29,0	4	8,7	1	6,0	1	140	1
60-62	1922±11a	n.d.	19,6	0,08	2,21	9,5	23,4	1	1,0	1	0,5	2	157	2	35	2	0,465	23	0,9	2	40	1	80,5	2	2,4	6	26,6	3	9,0	1	5,7	1	142	1
62-64	1920±11a	n.d.	27,8	0,07	2,12	11,7	22,9	1	0,9	1	0,6	2	158	2	33	2	0,435	22	0,8	2	37	1	79,3	2	2,7	7	22,2	3	9,4	1	5,9	1	132	1
64-66	1918±11a	n.d.	19,0	0,09	2,17	10,5	27,0	1	0,9	1	0,6	2	175	2	36	2	0,450	23	0,8	2	38	1	78,1	2	2,6	7	23,3	3	9,4	1	6,3	1	145	2
66-68	1917±11a	n.d.	21,1	0,09	2,26	10,0	29,4	2	1,0	1	0,6	2	165	2	37	2	0,405	21	0,7	2	39	1	75,1	2	2,3	6	22,1	3	8,8	1	6,0	1	143	2
68-70	1915±11a	n.d.	20,1	0,09	2,37	10,3	29,4	2	0,9	1	0,6	2	157	2	36	2	0,410	21	0,8	2	40	1	73,5	2	2,3	6	20,8	3	9,0	1	5,9	1	140	2
70-72	1913±11a	n.d.	20,0	0,10	2,26	9,8	29,7	2	0,9	1	0,6	2	152	2	36	2	0,385	19	0,8	2	39	1	73,5	2	2,3	6	20,9	3	9,1	1	6,1	1	141	2
72-74	1910±11a	n.d.	20,3	0,11	2,29	9,4	28,6	1	0,9	1	0,6	2	120	1	32	2	0,315	15	1,1	3	41	1	66,1	2	2,0	5	15,1	2	8,9	1</td				

Depth cm	Date	<sup>137</sup> Cs activity Bq.kg <sup>-1</sup>	Median grain-size μm																														
				TS	TOC	Hf	As	Bi		Cd		Cr		Cu		Hg		Mo		Ni		Pb		Sb		Sn		U		W		Zn	
%	%	ppm	ppm	EF	ppm	EF	ppm	EF	ppm	EF	ppm	EF	ppm	EF	ppm	EF	ppm	EF	ppm	EF	ppm	EF	ppm	EF	ppm	EF	ppm	EF	ppm	EF			
100-102	1861±11a	21,4	0,05	1,12	12,4	30,2	1	1,0	2	0,6	2	93	1	24	1	0,066	3	0,9	2	36	1	60,2	2	2,2	5	11,4	1	9,6	1	6,5	1	109	1
102-104	1856	25,9	0,08	1,14	9,9	31,4	2	1,1	2	0,6	2	91	1	24	1	0,060	3	0,9	2	37	1	60,2	2	1,9	5	10,8	1	8,5	1	6,6	1	114	1
104-106	1854±11a	15,7	0,07	1,00	9,6	29,6	1	1,1	2	0,5	1	91	1	23	1	0,058	3	0,9	2	35	1	61,7	2	2,0	5	11,8	2	8,6	1	7,0	1	110	1
106-108	1853±11a	18,0	0,06	1,08	9,7	28,4	1	1,0	2	0,6	2	89	1	23	1	0,063	3	0,8	2	35	1	59,4	2	1,9	5	10,8	1	8,1	1	6,4	1	109	1
108-110	1851±11a	15,5	0,06	0,99	10,7	28,9	1	1,0	1	0,6	2	89	1	22	1	0,051	2	0,8	2	35	1	58,0	2	1,7	4	10,8	1	8,5	1	6,2	1	108	1
110-112	1850±11a	21,3	0,06	0,99	10,4	31,9	2	1,0	1	0,6	2	101	1	24	1	0,049	2	0,9	2	41	1	59,6	2	2,0	5	11,4	1	8,9	1	6,0	1	117	1
112-114	1848±11a	17,7	0,04	0,95	10,9	29,4	2	0,9	1	0,6	2	91	1	21	1	0,045	2	0,9	3	38	1	55,9	2	1,8	5	10,5	1	8,5	1	6,1	1	106	1
114-116	1846	21,0	0,04	1,07	9,2	31,7	2	1,0	1	0,6	2	97	1	25	1	0,067	3	1,0	3	41	1	58,7	2	1,8	4	10,4	1	8,4	1	5,8	1	120	1
116-118	1846	24,2	0,05	0,88	10,8	29,7	2	0,9	1	0,5	2	89	1	20	1	0,036	2	0,8	2	33	1	56,7	2	1,9	5	9,9	1	9,1	1	6,3	1	100	1
118-120	1843±11a	15,1	0,06	1,09	8,9	33,1	2	1,2	2	0,6	2	90	1	22	1	0,049	2	0,9	3	37	1	59,2	2	2,0	5	10,9	1	8,4	1	6,3	1	112	1
120-122	1840±11a	14,9	0,06	1,10	9,2	35,4	2	1,1	2	0,6	2	94	1	22	1	0,047	2	0,9	2	36	1	62,3	2	2,4	6	11,3	1	8,6	1	7,3	1	116	1
122-124	1837±11a	12,8	0,06	1,08	9,2	35,6	2	1,1	2	0,6	2	89	1	23	1	0,045	2	0,9	2	35	1	63,3	2	2,5	6	10,9	1	8,8	1	7,5	1	118	1
124-126	1833±11a	16,2	0,05	1,01	9,4	33,0	2	1,1	2	0,6	2	91	1	22	1	0,043	2	0,8	2	36	1	60,4	2	2,2	5	10,5	1	8,6	1	6,9	1	111	1
126-128	1833±11a	14,7	0,06	1,03	8,5	32,7	2	1,0	2	0,6	2	92	1	25	1	0,051	2	0,8	2	36	1	61,4	2	2,1	5	10,9	1	8,6	1	7,1	1	126	1
128-130	1827±11a	13,2	0,06	1,27	8,7	32,6	2	1,0	2	0,6	2	89	1	23	1	0,046	2	0,9	2	37	1	58,5	2	2,0	5	10,6	1	8,5	1	6,8	1	116	1
130-132	1824±11a	13,1	0,07	1,13	7,7	37,1	2	1,1	2	0,5	1	97	1	26	1	0,050	2	1,0	3	40	1	60,1	2	2,0	5	11,0	1	7,9	1	6,9	1	127	1
132-134	1821±11a	11,1	0,07	1,31	7,5	35,7	2	1,1	2	0,6	2	92	1	25	1	0,055	3	0,9	2	38	1	61,2	2	2,0	5	11,1	1	7,9	1	7,4	1	125	1
134-136	1819±11a	10,1	0,05	1,27	7,0	36,3	2	1,1	2	0,6	2	93	1	25	1	0,049	2	0,9	2	38	1	61,4	2	2,1	5	11,7	1	7,8	1	7,4	1	127	1
136-138	1816±11a	12,9	0,07	1,25	7,1	33,4	2	1,0	1	0,4	1	103	1	27	1	0,051	2	1,0	2	44	1	54,2	1	2,0	4	10,1	1	8,4	1	6,5	1	139	1
138-140	1813±11a	7,8	0,07	1,23	6,8	36,5	2	1,0	1	0,5	1	96	1	26	1	0,044	2	1,0	2	38	1	58,4	2	2,2	5	10,2	1	8,4	1	6,7	1	132	1
140-142	1810±11a	12,7	0,07	1,29	8,1	31,5	2	0,9	1	0,5	1	94	1	23	1	0,053	3	0,8	2	37	1	55,0	2	1,9	5	9,2	1	8,2	1	6,0	1	128	1
142-144	1807±11a	18,1	0,06	1,14	10,4	28,9	1	0,8	1	0,5	1	95	1	23	1	0,046	2	0,8	2	36	1	54,7	2	2,0	5	9,8	1	9,0	1	6,0	1	125	1
144-146	1804±11a	15,6	0,06	1,13	9,5	28,3	1	0,8	1	0,5	1	96	1	23	1	0,047	2	0,8	2	37	1	56,4	2	2,1	5	9,6	1	9,2	1	6,2	1	130	1
146-148	1800±11a	16,1	0,05	1,01	10,7	26,7	1	0,8	1	0,5	1	93	1	22	1	0,042	2	0,7	2	36	1	52,4	1	1,8	4	8,6	1	9,2	1	5,8	1	119	1
148-150	1797±11a	13,8	0,05	1,02	9,7	27,0	1	0,8	1	0,5	1	103	1	24	1	0,047	2	0,8	2	41	1	52,4	1	1,6	4	8,2	1	8,7	1	5,2	1	125	1
150-152	1794±11a	13,0	0,06	0,98	10,6	26,7	1	0,8	1	0,5	1	99	1	22	1	0,042	2	0,8	2	39	1	52,7	1	1,6	4	8,0	1	9,0	1	5,3	1	120	1
152-154	1791±11a	15,5	0,05	0,97	10,7	27,5	1	0,9	1	0,5	1	100	1	23	1	0,044	2	0,8	2	40	1	57,8	2	1,8	4	8,6	1	9,2	1	5,6	1	121	1
154-156	1787±11a	17,6	0,02	0,88	11,2	26,5	1	0,8	1	0,4	1	102	1	22	1	0,039	2	0,9	3	39	1	51,4	1	1,8	4	8,1	1	9,1	1	5,3	1	117	1
156-158	1783±11a	21,1	0,03	0,85	13,0	24,5	1	0,8	1	0,4	1	100	1	21	1	0,032	2	0,8	2	39	1	52,4	1	1,7	4	8,3	1	10,2	1	5,1	1	112	1
158-160	1778±11a	29,7	0,03	0,75	18,3	23,2	1	0,7	1	0,5	2	98	1	18	1	0,026	1	0,7	2	36	1	50,9	2	1,7	4	8,1	1	12,8	2	5,5	1	105	1
d.l.				0,01	0,01	0,1	1,5	0,1	0,2	4	5	0,001	0,5	5	0,7	0,2	0,5	0,1	0,3	11													

**Tab. 8.1 – continued from previous page**

Depth cm	Date	<sup>137</sup> Cs activity Bq/kg	Median grain-size µm	TS		TOC	Hf	As		Bi		Cd		Cr		Cu		Hg		Mo		Ni		Pb		Sb		Sn		U		W		Zn	
				%	%	ppm	ppm	EF	ppm	EF	ppm	EF	ppm	EF	ppm	EF	ppm	EF	ppm	EF	ppm	EF	ppm	EF											
0-2		n.d.	115,6	0,08	1,5	24,2	23,5	1	1,0	2	1,0	3	138	2	22	1	0,048	3	1,1	4	44	2	48,3	2	4,3	13	19,1	3	11,5	2	10,1	2	137	2	
2-4		n.d.	272,5	0,06	0,8	51,5	19,5	1	0,9	2	1,7	6	168	2	19	1	0,037	2	0,9	3	50	2	45,1	2	3,8	12	23,8	4	22,6	3	16,8	3	132	2	
4-10		n.d.	318,8	< l.d.	0,8	106,1	17,9	1	1,0	2	3,6	13	196	2	21	1	0,040	2	1,1	4	57	3	47,5	2	4,1	13	48,1	8	42,6	7	30,9	6	155	2	
10-20		2±0,4	349,0	< d.l.	1,1	138,5	21,2	1	1,3	2	4,7	16	218	3	28	2	0,072	4	1,5	5	59	3	55,4	2	5,6	17	75,4	12	54,4	8	23,0	5	191	2	
20-26		4±0,4	282,3	0,06	0,8	69,6	20,3	1	1,2	2	2,4	8	170	2	24	1	0,060	4	1,1	4	50	2	52,7	2	4,6	14	42,7	7	30,3	5	10,2	2	148	2	
26-28		n.d.	266,7	0,07	0,9	50,8	22,3	1	1,2	2	1,9	6	161	2	25	1	0,140	8	1,2	4	48	2	52,6	2	6,6	19	23,5	4	21,4	3	13,0	3	142	2	
28-30		n.d.	87,7	0,09	1,3	22,5	26,9	2	1,9	3	1,3	4	155	2	31	2	0,105	6	1,2	4	47	2	58,0	2	6,0	17	18,3	3	12,8	2	10,4	2	162	2	
30-32		n.d.	103,7	0,09	1,1	31,9	23,4	1	1,4	2	1,5	5	168	2	29	2	0,145	8	1,3	4	49	2	54,7	2	5,5	16	16,2	2	15,7	2	10,0	2	150	2	
32-34		n.d.	87,5	0,09	1,3	25,6	25,9	2	1,4	3	1,7	5	162	2	32	2	0,115	7	1,8	6	48	2	57,5	2	7,3	21	20,7	3	12,9	2	13,2	3	161	2	
34-36		n.d.	108,1	0,09	1,3	23,3	24,7	1	1,6	3	1,6	5	151	2	30	2	0,115	7	1,4	5	45	2	57,9	2	5,6	16	16,9	3	12,2	2	8,5	2	161	2	
36-38		3±0,5	146,7	0,08	1,0	32,9	22,0	1	1,2	2	1,4	5	161	2	26	2	0,078	5	1,1	4	46	2	52,9	2	5,6	16	14,4	2	15,4	2	8,8	2	145	2	
38-40		n.d.	223,5	0,08	0,9	30,9	22,3	1	1,4	2	1,6	5	158	2	25	1	0,085	5	1,2	4	45	2	57,0	2	6,2	18	20,3	3	14,3	2	7,2	1	147	2	
40-42		n.d.	98,1	0,09	0,8	25,8	21,0	1	1,3	2	1,4	5	160	2	24	1	0,092	5	1,1	4	45	2	49,7	2	4,2	12	18,3	3	11,8	2	7,0	1	147	2	
42-44		n.d.	99,8	0,12	0,6	28,3	18,7	1	1,1	2	1,4	5	152	2	20	1	0,080	5	1,1	4	43	2	45,1	2	6,4	19	11,8	2	13,3	2	9,2	2	129	2	
44-46		n.d.	83,4	0,18	0,9	26,0	25,0	1	2,3	4	1,7	5	173	2	26	1	0,100	6	1,2	4	47	2	52,2	2	5,4	16	17,9	3	13,2	2	12,7	2	150	2	
46-48		n.d.	80,9	0,10	1,3	23,1	29,7	2	3,9	7	2,2	7	188	2	36	2	0,125	7	1,5	5	48	2	61,1	2	5,7	16	13,6	2	11,8	2	8,8	2	187	2	
48-50		n.d.	59,3	0,12	1,5	17,6	35,0	2	5,3	9	2,7	8	184	2	41	2	0,340	19	1,7	5	50	2	66,9	2	6,6	18	17,7	3	9,8	1	9,1	2	206	2	
50-52		n.d.	59,9	0,09	1,3	21,9	32,0	2	4,8	8	2,5	8	188	2	39	2	0,145	8	1,4	5	51	2	63,3	2	5,6	16	15,5	2	10,9	1	8,8	2	199	2	
52-54		n.d.	51,1	0,10	1,2	18,4	30,4	2	4,2	7	2,3	7	184	2	38	2	0,130	7	2,2	7	47	2	61,4	2	5,6	16	15,1	2	9,8	1	8,4	2	189	2	
54-56		11±0,9	59,1	0,10	1,2	21,1	30,0	2	5,7	10	2,3	7	183	2	39	2	0,145	8	1,3	4	49	2	64,0	2	5,8	16	15,1	2	11,2	2	9,0	2	190	2	
56-58		n.d.	52,4	0,10	1,5	15,4	33,7	2	7,4	12	2,6	8	165	2	44	2	0,285	15	1,2	4	45	2	67,8	2	6,2	17	13,3	2	8,7	1	8,7	2	207	2	
58-60		n.d.	45,9	0,07	1,0	20,2	25,2	1	4,3	7	2,0	6	158	2	33	2	0,210	12	1,3	4	45	2	60,2	2	7,0	19	14,1	2	10,7	1	9,0	2	176	2	
60-62		n.d.	63,1	0,09	1,4	16,5	28,6	2	5,5	9	2,5	8	160	2	41	2	0,315	17	1,2	4	46	2	63,9	2	6,9	19	14,8	2	9,4	1	9,5	2	188	2	
62-64	1960s	39±1,1	27,4	0,15	1,7	17,5	40,3	2	9,2	16	4,0	12	166	2	57	3	0,365	20	1,8	6	49	2	75,4	2	8,9	24	16,6	2	10,0	1	9,6	2	231	3	
64-66		n.d.	35,7	0,12	1,5	19,5	31,7	2	5,8	10	2,7	8	165	2	44	2	0,305	17	2,4	7	47	2	66,9	2	7,2	20	17,9	3	10,4	1	10,7	2	200	2	
66-68		n.d.	85,5	0,12	2,1	14,1	40,1	2	10,2	17	3,2	10	167	2	63	3	0,575	31	2,5	8	46	2	82,6	3	9,1	24	17,3	2	9,1	1	11,8	2	251	3	
68-70		n.d.	32,5	0,18	2,6	14,4	51,4	3	16,5	31	4,8	17	150	2	90	5	0,700	42	2,3	8	47	2	94,3	3	9,1	27	19,3	3	8,6	1	9,1	2	323	4	
70-72		n.d.	39,6	0,13	1,9	39,5	35,2	2	7,4	13	3,0	10	172	2	65	4	0,395	23	2,7	9	53	2	73,7	2	8,5	25	18,7	3	18,4	3	13,9	3	264	3	
72-74		n.d.	187,3	0,14	2,3	20,1	38,3	2	10,2	17	2,2	7	159	2	87	5	0,425	23	1,6	5	53	2	83,6	3	8,3	23	17,6	3	11,1	1	11,4	2	291	3	
74-76		n.d.	51,4	0,12	2,0	17,4	32,5	2	6,6	11	1,7	5	147	2	59	3	0,295	16	1,3	4	51	2	72,0	2	7,6	21	14,0	2	9,6	1	11,3	2	246	3	
76-78		n.d.	105,0	0,11	2,0	24,5	31,4	2	3,5	6	1,7	5	164	2	50	3	0,250	14	1,2	4	52	2	68,5	2	7,6	21	20,4	3	12,5	2	234	3			
78-80		n.d.	102,4	n.d.	n.d.	n.d.	n.d.	n.d.	n.d.	n.d.	n.d.	n.d.	n.d.	n.d.	n.d.	n.d.	n.d.	n.d.	n.d.	n.d.	n.d.	n.d.	n.d.	n.d.	n.d.	n.d.	n.d.	n.d.	n.d.	n.d.	n.d.	n.d.			
80-82		11±0,7	98,1	n.d.	n.d.	n.d.	n.d.	n.d.	n.d.	n.d.	n.d.	n.d.	n.d.	n.d.	n.d.	n.d.	n.d.	n.d.	n.d.	n.d.	n.d.	n.d.	n.d.	n.d.	n.d.	n.d.	n.d.	n.d.	n.d.	n.d.	n.d.	n.d.			
82-84		n.d.	65,9	n.d.	n.d.	n.d.	n.d.	n.d.	n.d.	n.d.	n.d.	n.d.	n.d.	n.d.	n.d.	n.d.	n.d.	n.d.	n.d.	n.d.	n.d.	n.d.	n.d.	n.d.	n.d.	n.d.	n.d.	n.d.	n.d.	n.d.	n.d.	n.d.			
84-86		9±0,7	56,6	n.d.	n.d.	n.d.	n.d.	n.d.	n.d.	n.d.	n.d.	n.d.	n.d.	n.d.	n.d.	n.d.	n.d.	n.d.	n.d.	n.d.	n.d.	n.d.	n.d.	n.d.	n.d.	n.d.	n.d.	n.d.	n.d.	n.d.	n.d.	n.d.			
86-88		n.d.	54,7	n.d.	n.d.	n.d.	n.d.	n.d.	n.d.	n.d.	n.d.	n.d.	n.d.	n.d.	n.d.	n.d.	n.d.	n.d.	n.d.	n.d.	n.d.	n.d.	n.d.	n.d.	n.d.	n.d.	n.d.	n.d.	n.d.	n.d.	n.d.	n.d.			
88-90		n.d.	191,5	0,13	2,5	13,6	55,0	3	6,8	12	2,1	7	152	2	85	5	1,100	61	1,5	5	54	2	118,0	4	15,5	43	21,6	3	10,0	1	19,8	4	381	5	
90-92		n.d.	104,6	0,14	2,3	20,7	45,6	3	3,9	7	1,9	6	146	2	58	3	0,905	52	1,3	4	51	2	87,7	3	11,8	34	18,6	3	11,1	2	19,2	4	301	4	
92-96		n.d.	199,5	< d.l.	1,3	54,1	32,1	2	2,3	4	2,3	7	167	2	41	2	0,440	25	1,2																

- After the 1960s (Fig. 8.5):

The increasing trend of TE enrichments begin in the early 1950s, in the LLC until the early 1980s. Temporal evolutions are significant for Bi, Cd, Cr, Cu, Ni, Pb and Zn ( $r > 0.6$ ,  $p < 0.05$ ,  $n = 10$ ). Maximum Hg enrichments occur in the late 1960s ( $EF = 53$ ) before to exponentially decline until the coring date ( $r = 0.8$ ,  $p < 0.05$ ,  $n = 18$ ; Fig. 8.5). From the early 1950s to the coring date, Cd and Bi are correlated with Cr, Cu, Ni, Pb and Zn ( $r < 0.7$ ,  $p < 0.05$ ,  $n = 21$ ). All these TE reach maximum enrichments between the 1960s and the 1980s (maximum  $EF = 24$  for Bi and Cd), before to decline up to the coring date (significant decrease,  $r > 0.8$ ;  $p < 0.05$ ,  $n = 10$ ; Fig. 8.5). By contrast, after the 1960s a general decrease of TE enrichments is recorded in sedimentary archives recovered in upstream sub-basins (Fig. 8.4). However, in the three cores ET enrichments are higher than preindustrial references in post-1980 sediments ( $EF \text{ c.a.} = 10$  for Hg, 4 for Cd as the most enriched TE).

These results highlight an important upstream-downstream difference concerning TE temporal

dynamics archived in sedimentary cores. Indeed, Sn and Sb are only enriched in sediments of upstream sub-basins. These TE constitute local sedimentary contaminations affecting:

- (i) the Upper Loire sub-basin between the 1910s and the 1930s for Sb and Sn
- (ii) the Upper Loire and the Allier sub-basins between the 1940s and the late 1950s for Sb only.

Bi, Cd and Hg can be considered as tracers of sedimentary contaminations recorded in upstream sub-basins as well as in the most downstream part of the Loire basin. Maximum enrichments for these TE are recorded:

- (i) between the 1940s and the late 1950s in the oldest and most industrialized upstream sub-basins
- (ii) between the early 1950s and the early 1980s in the most downstream part of the basin.

A decade delay can be calculated between the archiving of these generalized sedimentary contaminations in the upstream and downstream parts of the Loire basin. Consequently, while a general

decrease of TE enrichments characterizes the last temporal window in upstream sub-basins (after the 1960s), enrichments

are maximum in the downstream part of the Loire basin before to decline.

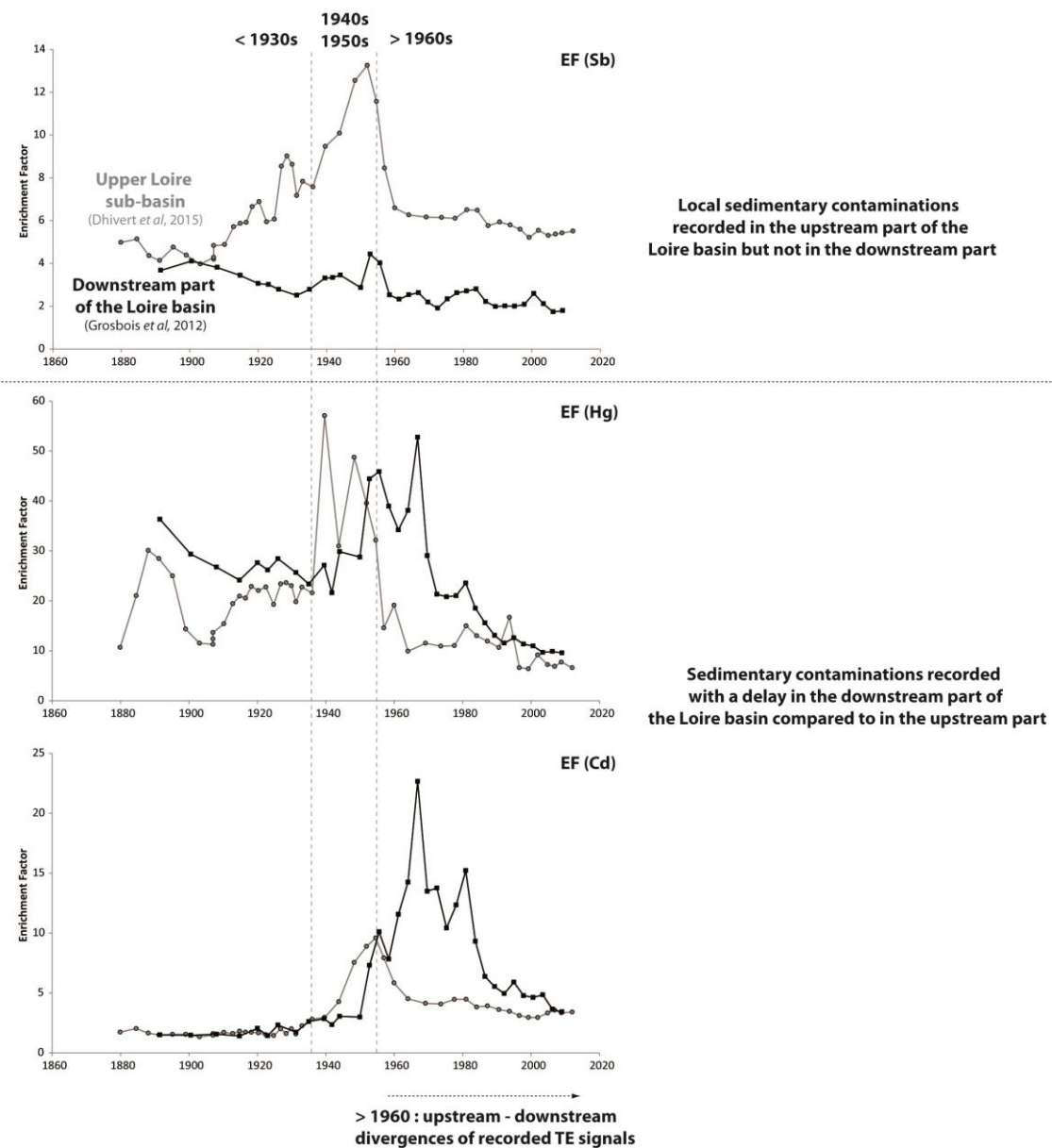


**Fig. 8.5. : Upstream-downstream comparison of TE signal recorded in sediments of the Loire basin (upstream core, Dhivert et al, 2015; downstream core : Grosbois et al, 2012)**

### *8.3.3.2. Inter-basin comparisons of the spatial and temporal variations of TE contaminations in sediments of various European basins*

This study highlights divergence of TE temporal dynamics archived in sedimentary cores between upstream sub-basins and the most downstream part of the Loire basin. As explained in § 8.2.1.1, maximum activity period for mining and industrial complexes occurred between the end of the World War II and the late 1950s in French continental industrial foci. This time interval corresponds to the most polluted period recorded in cores sampled in the most industrialized sub-basins. Do such differences in recorded TE signals exist in neighbor basins?

The Igeo index (Müller, 1979; eq. 1.1 p. 20) allows an inter-basin comparison of pollution levels in sediments (Fig. 8.6). In this study, temporal evolutions of sedimentary contaminations in the Loire are compared in cores sampled:

- (i) in the most downstream part of the Seine, the Garonne (Grouset et al, 1999, Le Cloarec et al, 2011)
- (ii) in highly industrialized sub-basins as the Oise (Seine basin, Le Cloarec

*et al, 2011), the Lippe (Rhin basin, Heim et al, 2004).*

TE temporal dynamics, commonly described for W-European Rivers, attest a maximum pollution level during the Glorious Thirty (1945 - 1980s), followed by a general decontamination phase related to anthropogenic releases control (Meybeck and Helmer, 1989 ; Vink et al, 1999 ; Meybeck et al, 2002 ). Contamination levels recorded between the 1940s and the 1980s in sediments of the Loire, the Garone and the Rhine basins are similar (Igeo ranges between 1 and 5 for Cd and Hg i.e. moderately to highly polluted; Fig. 8.6). In the downstream part of Seine basin and in the Oise tributary sediments deposited during this period are highly to extremely polluted (Igeo ranges between 5 and 10 for Cd and Hg).

Maximum TE sedimentary contaminations are recorded between the 1950s and the late 1960s for Hg in the downstream part of the Loire and the Seine basin. For Cd, maximum contamination levels are recorded between the late 1950s/early 1960s and the 1980s for Cd in the downstream part of the Loire, the Garonne and the Seine basins (Fig. 8.6). Hence, maximum contamination phases were archived

during the same time interval in the downstream part of these European basins.

In industrialized Upper Loire and Oise sub-basins maximum pollutions are synchronous, archived more early than in the downstream part of basins (between the 1940s and the late 1950s; Fig. 8.6.). For the Lippe sub-basin, a first Cd contamination phase is recorded during the 1940s – 1950s time interval and another occurred at the end of the 1970s.

This inter-basin comparison shows that the decade delay in the archiving of contamination phases between the most industrialized sub-basins and the downstream part of fluvial domains is not specific to the Loire basin. Large divergences of recorded temporal evolutions of TE sedimentary contaminations are also present in neighbor basins.

In addition, in basins where the density of anthropogenic activities follows upstream-downstream gradients, the multiplication of sources contributions can induce a spatial increasing trend of pollutions levels in suspended matters and in river bank deposits (*e.g.* for the Seine and the Rhône Rivers: Santiago *et al*, 1994;

Horowitz *et al*, 1999; Meybeck *et al*, 2004; Grosbois *et al*, 2006; Le Cloarec *et al*, 2011; Desmet *et al*, 2012; Le Pape *et al*, 2012; Mourier *et al*, 2014). In the Loire basin maximum Hg contamination levels are similar in the upstream and the downstream part of the fluvial domaine (Fig. 8.5). However, Cd and Bi contaminations are higher in the downstream part of the basin than in the Upper Loire; they are more similar with contamination levels recorded in sediments of the Allier sub-basin.

## 8.4. Discussion

### 8.4.1. Characterization of anthropogenic sources: local TE sedimentary contaminations

#### 8.4.1.1. Sn-Sb enrichments in sediments of the Upper Loire sub-basin before the 1930s

This first part of the discussion is focused on local anthropogenic impacts, affecting the Upper Loire and the Allier sub-basins (not observed in the downstream part of the basin). Between the 1910s and the 1930s, moderate to high Sb and Sn enrichments are recorded in the Upper Loire sub-basin. These TE are correlated with Pb showing light enrichments during this period. A significant geochemical signature can be

calculated in sediments deposited during this period in the ULC ( $\text{Sb}/\text{Al} = 2.0 \cdot 10^{-2} \cdot \text{Sn}/\text{Al} + 2.3 \cdot 10^{-5}$ ,  $r = 0.9$ ,  $p < 0.05$ ,  $n = 14$ , Fig. 8.7). For comparison, the Sb-Sn relationship in sediments deposited

before the 1880s in the ULC is  $\text{Sb}/\text{Al} = 1.2 \cdot 10^{-1} \cdot \text{Sn}/\text{Al} + 8.8 \cdot 10^{-6}$ ,  $r = 0.7$ ,  $p < 0.05$ ,  $n = 33$  (Fig. 8.7) and since the early 1940s, Sb and Sn do not follow the same temporal trajectory (see § 8.3.1.3).

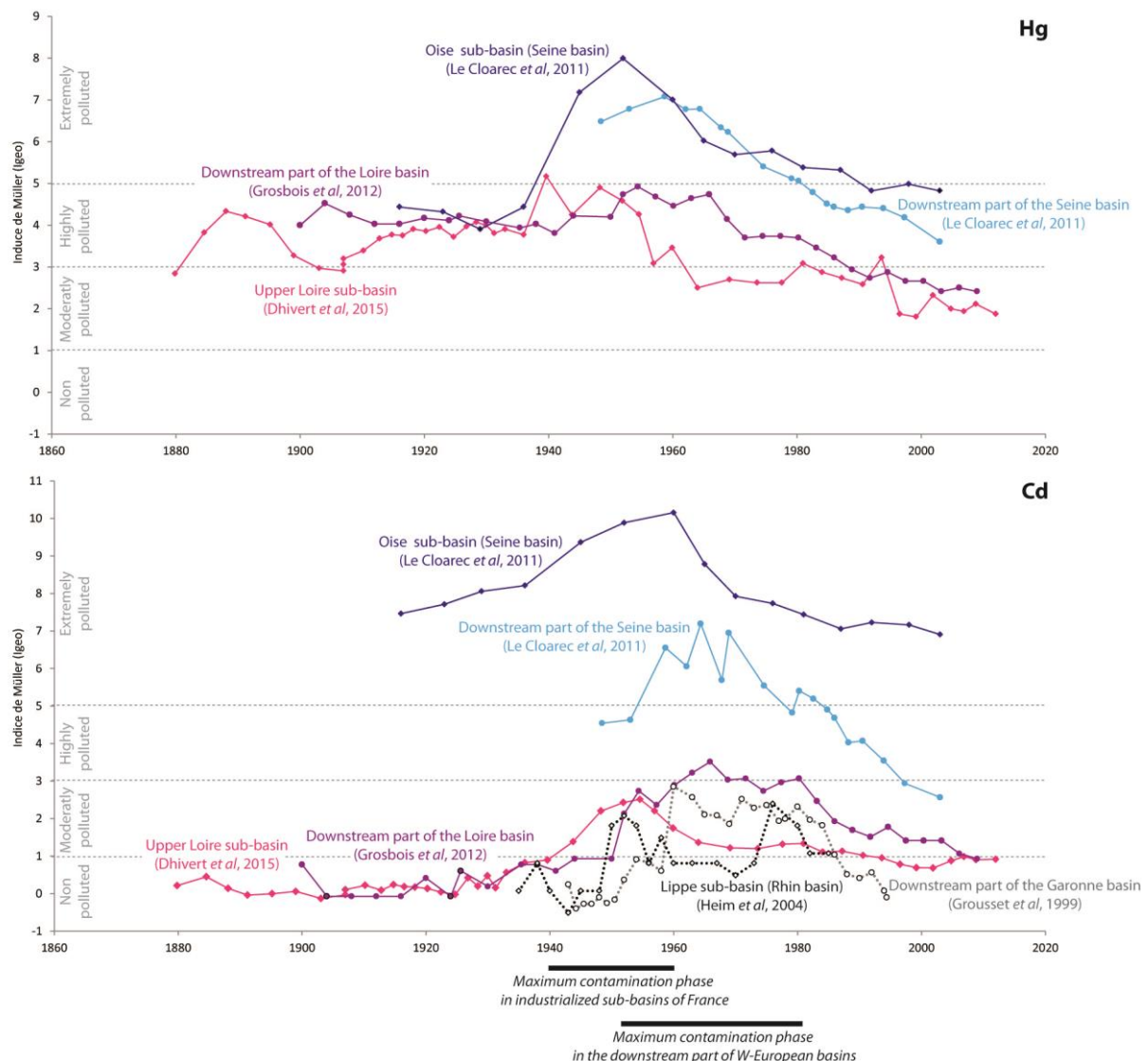


**Fig. 8.6:** Comparison of temporal evolutions of TE sedimentary contaminations recorded in sedimentary archived sampled in W-European industrialized sub-basins (the Upper Loire, Dhivert et al., 2015; the Oise, Le Cloarec et al., 2011, and the Lippe sub-basins, Heim et al., 2004) and in the downstream part of fluvial domain (the Loire, Grosbois et al., 2012; the Seine, Le Cloarec et al., 2011; the Garonne basins, Grousset et al., 1999)

In river bank sediments sampled in the Upper Loire sub-basin, any significant geochemical signature could correspond to the Sb/Sn of the ULC during the 1910-1930 period. Even, high Sb and Sn enrichments are archived in sediments of the Furan river bank (maximum EF = 73 for Sb and 160 for Sn; Tab. 8.3), but the Sb-Sn ratio would not correspond, ranging between  $6.0 \cdot 10^{-3}$  and  $6.4 \cdot 10^{-2}$ . Atmospheric releases of metallurgical activities are known to be important Sn pollution sources (average of 1187 ppm in atmospheric particles, Querol *et al*, 2007). Such industries were present in the Furan sub-basin from the First Industrial Revolution in the early 19<sup>th</sup> (Woronoff, 1994; Saint Etienne municipal archives). Moreover, before the end of the War World II and the expansion of stainless steel productions, important tin-planting factories were implanted around St Etienne and the Furan sub-basin (St Etienne municipal archives; [www.acier.org](http://www.acier.org)). Such industries were also implanted during this period in the Arroux sub-basin (Gueugnon municipal archives). However, Sn enrichments stay light in river bank sediments of this sub-basin (tab. 8.3).

Tin and antimony oxides ( $\text{SnO}_2$ ;  $\text{Sb}_2\text{O}_3$ ) were also largely used as pigments for glass and ceramic, in addition to Pb (Eppler 1987; [www.societechimiquedefrance.fr](http://www.societechimiquedefrance.fr)). Near to the ULC coring site (< 1km), industrial glass and ceramic production units were in operation during the Second Industrial Revolution. The maximum activity period occurred between the 1910s and the 1930s period (Decize municipal archives). Therefore, the 1910s-1930s contamination phase archived in the ULC may be influenced by the local fallout of Sb and Sn polluted particles emitted by these extractive industries. Moreover, river bank sediments of the Dore River (Allier Basin) show a similar geochemical signature between 20 and 80 cm deep (EF ranges between 5 and 7 for Sb and Sn, 3 for Pb;  $\text{Sb}/\text{Al} = 2.4 \cdot 10^{-2} \cdot \text{Sn}/\text{Al} + 1.5 \cdot 10^{-5}$ ,  $r = 0.9$ ,  $p < 0.05$ ,  $n = 3$ ; Fig. 8.7). Since the 1900s, important glassware was also implanted at less than 2 km of the sampling site (Le Puy Guillaume municipal archives).

In summary, Sn-metallurgy and glass industries can be considered as active contamination sources during the Second Industrial Revolution (1880s - 1930s) in the ULC.

**Legend:**

- Upper Loire sub-basin core sediments dating from the < 1900s period
- Upper Loire sub-basin sediments dating from the 1910s - 1930s period
- ✖ River bank sediments

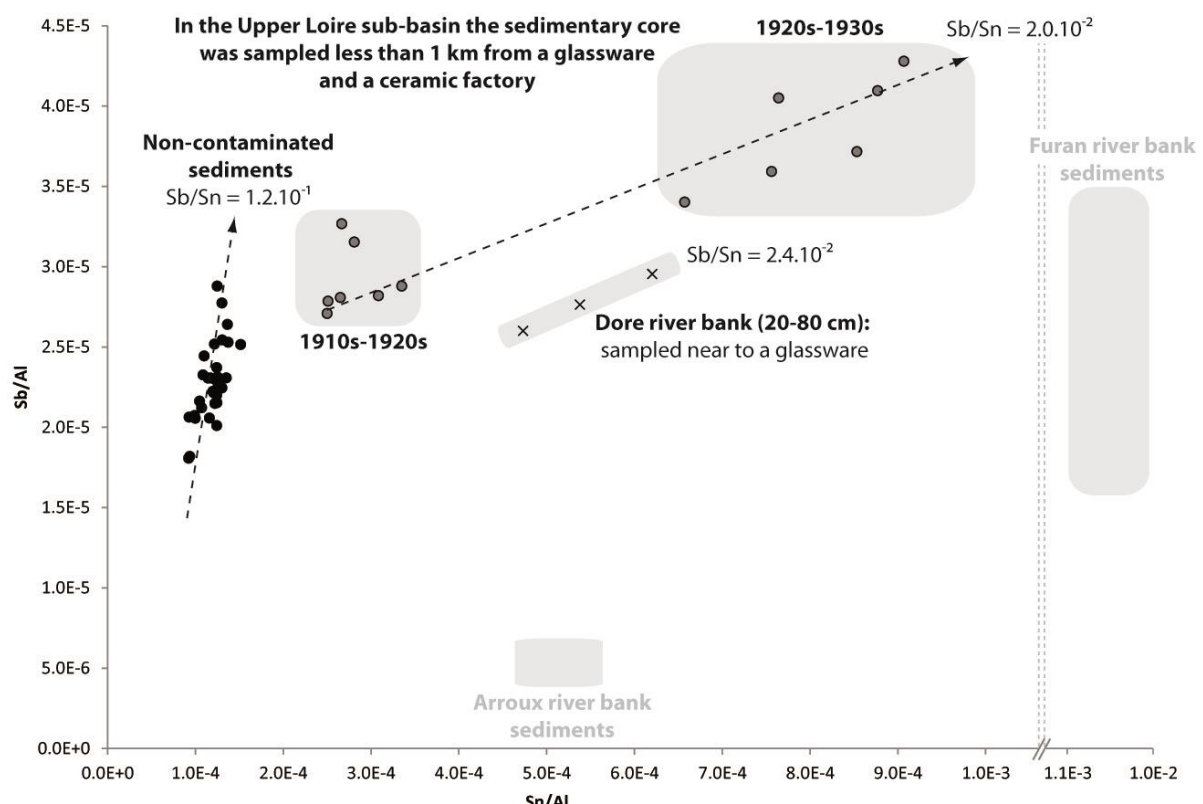


**Fig. 8.7. : Sb-Sn relationship for the Upper Loire sub-basin core (ULC) during the 1910s-1930s period and in river bank sediments**

Any similar Sn-Sb – Pb enrichments nor Sn/Sb ratios were identified in the LLC sediments. Proximal fallout of polluted particles, should certainly explain the local influence of these contamination phases.

#### 8.4.1.2. *Sb enrichments in sediments of the Upper Loire and the Allier sub-basins between the 1940s and the 1950s*

Between the 1940s and the 1950s, chalcophil TE and especially Sb are enriched in both upstream sub-basins in association with TOC and TS.

In the ULC, this contamination phase is characterized by a strong Sb-TOC correlation defining a significant relationship of  $Sb/Al = 9.10^{-6} \text{ TOC} + 1.7.10^{-5}$ ,  $r = 0.9$ ,  $p < 0.05$ ,  $n = 6$  (maximum concentrations : 4.9 % for TOC, EF = 13 for Sb, Fig. 8.8). In this core, microscopic coal particles were visually identified in sediments deposited during this time interval. Any significant Sb-TOC relationship has been identified in sedimentary layers archived before the 1940s and after the 1960s ( $r < 0.6$ ,  $p > 0.05$ ). In the ALC, Sb/Al does not present significant correlations with TOC ( $r < 0.5$ ,  $p > 0.05$ ,  $n = 37$ ). However, during this period, Sb is very highly enriched and TOC also show maximum concentrations (maximum concentrations of 2.5 % for TOC, EF of 56 for Sb; Tab. 8.2, Fig. 8.8).

In the most downstream core of the Loire basin, TOC and Sb/Al ratios do not present significant correlations over the recorded period ( $r = 0.15$ ,  $p > 0.05$ ,  $n = 35$ ).

Downstream the coal-mining district of St Etienne, Furan river bank sediments are also rich in coal particles (especially for the black sediments layer). Furan river bank sediments present the

most important Sb and TOC enrichments at the Upper Loire sub-basin scale (maximum concentration of 26.1 % for TOC, EF of 73 for Sb, Tab. 8.3). The geochemical composition of these dark river bank sediments is very heterogeneous (Fig. 8.8). At the Allier basin scale, the Upper Allier river bank contains the most enriched sediments in TOC and Sb (maximum concentrations of 3.6 % for TOC, EF of 51 for Sb, Tab. 8.8). The geochemical composition of these river bank sediments presents similarity with those archived between the 1940s and the 1950s in the ALC (Fig. 8.8).

In the Furan and the Allagnon sub-basins were implanted two of the most important coal-mining districts at a national scale (see § 8.2.1.2). Maximal mining period occurred between the 1940s and the late 1950s. Coals and more especially their pyrite contents can be important host for chalcophil TE and mining effluents can constitute solid TE contamination sources for aquatic environments (Finkelman, 1993; Tiwary and Dhar, 1994ab; Ghose and Majee, 2000ab; Yudovich and Ketris, 2005ab; Mishra *et al.*, 2008; Seredin and Finkelman, 2008; Karamanis *et al.*, 2009; Kolker, 2012).

Code	Sampled sub-basin	Depth cm	TS	COT	Hf	As		Bi		Cd		Cr		Cu		Hg		Mo		Ni		Pb		Sb		Sn		U		W		Zn	
			%	%	ppm	ppm	EF	ppm	EF	ppm	EF	ppm	EF	ppm	EF	ppm	EF	ppm	EF	ppm	EF	ppm	EF	ppm	EF	ppm	EF	ppm	EF	ppm	EF		
1	Loire River	0-50	0,05	1,04	64,3	10,4	1	0,9	2	2,4	8	240	3	32	2	0,035	2	1,5	5	82	3	47,8	2	0,7	2	20,1	3	38,6	5	3,7	1	152	2
		50-100	0,05	1,26	46,7	10,5	1	0,7	1	2,0	6	236	3	32	2	0,036	2	1,9	6	80	3	47,3	2	1,5	4	14,9	2	29,0	4	3,4	1	144	2
		100-150	0,06	2,36	20,7	13,7	1	0,8	1	1,0	3	207	2	36	2	0,053	3	1,2	4	69	3	48,9	2	0,7	2	12,4	2	12,3	2	3,9	1	148	2
		150-200	0,06	2,24	25,4	13,4	1	1,1	2	1,1	3	227	3	39	2	0,074	4	1,4	5	70	3	58,3	2	0,9	2	13,3	2	15,5	2	3,8	1	155	2
		200-250	0,05	2,17	18,6	13,0	1	0,9	2	0,9	3	319	4	43	2	0,115	6	1,5	5	72	3	64,4	2	1,2	3	13,6	2	12,5	2	3,7	1	165	2
		250-300	0,06	2,4	26,5	12,9	1	1,0	2	1,3	4	302	3	37	2	0,090	5	1,6	5	72	3	64,3	2	0,9	2	14,7	2	17,8	2	4,3	1	163	2
		300-350	0,07	2,45	15,4	14,4	1	0,9	1	0,8	2	225	2	39	2	0,076	4	1,1	3	72	3	51,7	2	1,0	3	14,6	2	10,2	1	3,5	1	162	2
		350-400	0,06	1,77	22,6	14,0	1	0,9	1	1,0	3	191	2	35	2	0,079	4	1,1	3	70	3	53,1	2	1,4	4	18,8	3	14,5	2	3,6	1	158	2
		0-20	0,03	1,35	8,7	45,7	2	1,3	2	0,5	1	89	1	27	1	0,033	1	1,0	2	38	1	35,6	1	3,3	7	15,7	2	10,0	1	9,1	1	145	1
2	Ondaine	20-40	0,03	1,35	11,6	47,5	2	1,2	1	0,6	1	89	1	28	1	0,039	2	1,0	2	37	1	37,8	1	2,8	6	15,2	2	12,1	1	9,1	1	137	1
		40-60	0,03	1,24	9,6	47,8	2	1,2	2	0,5	1	87	1	27	1	0,042	2	1,1	2	36	1	37,1	1	2,8	6	15,2	2	11,5	1	9,1	1	132	1
		60-80	0,03	1,17	10,2	39,5	2	1,2	2	0,5	1	82	1	24	1	0,041	2	1,1	3	33	1	34,1	1	2,4	5	15,4	2	12,8	1	8,3	1	122	1
		80-100	0,02	0,87	10,4	30,1	1	1,0	1	0,5	1	72	1	21	1	0,042	2	0,8	2	33	1	29,6	1	1,8	4	14,1	2	12,4	1	7,6	1	109	1
		100-120	0,01	0,55	14,9	29,0	1	0,8	1	0,6	2	79	1	20	1	0,040	2	0,9	2	30	1	31,7	1	1,7	4	13,5	2	9,0	1	122	1		
3*	Furan	0-5	0,14	7,45	9,6	92,8	4	10,0	14	5,1	13	253	2	116	5	0,790	36	5,0	13	95	3	176,3	5	3,7	8	99,0	12	9,0	1	23,1	3	368	4
		20-25	0,06	1,32	11,2	136,6	6	0,9	1	0,4	1	103	1	37	2	0,120	5	1,2	3	61	2	61,5	1	0,5	1	20,0	2	7,0	1	8,1	1	165	1
		25-50	0,08	1,11	23,5	24,9	1	0,8	1	0,3	1	123	1	29	1	0,100	4	0,9	2	51	2	32,4	1	0,3	1	18,0	2	19,4	2	4,2	1	106	1
		90-95	0,27	18,86	6,5	92,0	5	4,6	7	1,2	4	130	1	179	9	3,650	186	2,1	6	63	2	245,6	7	5,5	14	924,0	126	9,2	1	14,4	2	332	4
		110-115	0,23	19,37	7,0	217,5	12	3,2	5	0,7	2	116	1	201	11	3,430	182	2,2	7	58	2	291,1	9	6,4	17	1129,0	160	8,2	1	13,7	2	402	5
		130-135	0,07	5,18	13,2	146,6	6	1,3	2	0,4	1	109	1	105	4	1,350	57	1,7	4	51	2	113,7	3	4,5	9	212,0	24	10,8	1	12,4	2	237	2
		150-155	0,04	2,43	10,6	141,8	6	1,0	1	0,2	0	109	1	76	3	0,510	20	1,7	4	54	1	71,0	2	4,0	8	83,0	9	9,9	1	12,7	2	186	2
		170-175	0,06	3,14	10,8	167,7	7	1,2	1	0,4	1	109	1	88	3	2,010	77	4,0	9	55	1	91,5	2	4,2	8	110,0	11	11,8	1	12,4	2	179	1
		190-195	0,04	1,89	16,9	104,0	4	0,9	1	0,1	0	109	1	60	2	0,610	24	2,9	6	48	1	51,4	1	3,8	7	25,0	3	12,4	1	12,6	2	141	1
		210-215	0,04	2,29	11,7	129,3	5	1,0	1	0,3	1	103	1	74	3	0,870	33	3,2	7	52	1	69,8	2	4,0	8	51,0	5	10,9	1	13,0	2	166	1
4	Anzieux	230-235	0,04	1,74	18,1	96,5	4	0,8	1	0,1	0	109	1	54	2	0,350	14	2,5	6	44	1	48,9	1	4,1	8	18,0	2	12,8	1	132	1		
		250-255	0,03	1,76	10,5	101,1	4	1,0	1	0,1	0	109	1	53	2	0,340	13	2,6	6	41	1	53,7	1	3,8	7	23,0	2	10,3	1	12,3	2	119	1
		270-275	0,03	1,81	14,4	72,3	3	1,0	1	0,2	0	103	1	50	2	0,280	11	2,1	5	42	1	50,4	1	2,7	5	23,0	2	11,3	1	14,9	2	114	1
		dark levels	0,37	26,06	7,3	130,2	9	23,5	47	8,6	32	526	7	97	6	1,490	97	22,3	83	76	3	352,5	13	11,0	36	108,6	19	8,1	1	154,4	33	255	4
			0,18	8,59	13,4	593,4	36	10,9	20	18,3	63	893	11	411	25	2,060	123	50,4	172	157	7	782,3	27	24,3	72	376,6	60	10,3	2	437,0	87	770	10
			0,17	10,44	18,7	247,1	14	6,6	11	12,6	39	849	9	224	12	1,775	96	35,0	108	152	6	558,1	17	17,7	48	379,2	55	12,4	2	345,0	62	529	6
			0,2	13,45	9,1	169,4	8	17,5	26	7,6	21	289	3	124	6	1,145	56	8,5	24	74	3	200,5	6	14,1	35	97,4	13	9,0	1	50,2	8	301	3
			0,14	6,84	16,7	240,6	14	2,4	4	1,2	4	94	1	225	12	1,955	108	4,5	14	57	2	611,3	19	26,7	73	709,4	104	11,3	2	32,2	6	361	4
		0-20	0,04	1,61	23,4	109,8	5	6,4	9	1,5	4	137	1	305	15	19,780	947	1,5	4	107	4	242,1	7	8,9	21	24,2	3	10,6	1	10,3	2	179	2
		20-40	0,04	1,54	21,6	128,9	7	2,8	4	1,4	4	101	1	86	4	22,630	1128	1,4	4	71	3	132,7	4	7,7	19	18,9	3	8,9	1	7,8	1	166	2
		40-60	0,01	0,49	22,2	219,6	11	0,9	1	0,9	2	96	1	21	1	0,245	12	1,1	3	30	1	42,3	1	5,6	13	9,5	1	9,9	1	6,1	1	96	1
		60-80	0,06	0,63	18,9	101,4	5	0,9	1	0,8	2	95	1	17	1	0,125	6	0,8	2	29	1	47,3	1	6,0	14	10,0	1	8,4	1	6,3	1	99	1
5*	Bourdince	5-15	0,06	9,18	8,8	23,7	1	1,5	2	0,6	2	82	1	32	2	0,220	12	1,4	4	33	1	51,9	2	0,4	1	10,0	1	8,5	1	7,7	1	180	2
		15-40	< d.l.	1,07	11,2	17,5	1	0,5	1	0,1	0	75	1	15	1	0,040	2	0,6	2	23	1	33,2	1	0,2	0	7,0	1	8,7					

Code	Sampled sub-basin	Depth cm	TS %	COT %	Hf ppm	As ppm	Bi EF	Cd ppm	Cr EF	Cu ppm	Hg EF	Mo ppm	Ni EF	Pb ppm	Sb EF	Sn ppm	U EF	W ppm	Zn EF														
7	Upper Allier River	0-20	0,05	2,27	19,4	49,7	3	1,2	2	1,3	4	117	1	28	2	0,054	3	0,8	2	47	2	50,3	2	14,5	38	9,9	1	11,1	1	8,0	1	138	2
		20-40	0,04	2,1	18,6	58,3	3	1,0	2	1,2	4	122	1	26	1	0,055	3	0,8	2	48	2	57,4	2	16,6	42	10,8	1	10,9	1	6,6	1	149	2
		40-60	0,04	1,73	25,5	50,9	3	0,8	1	1,4	4	121	1	27	1	0,042	2	0,8	2	49	2	57,1	2	19,7	51	9,7	1	13,6	2	6,1	1	144	2
		60-80	0,05	2,37	18,6	67,2	3	0,9	1	1,4	4	121	1	33	2	0,062	3	1,2	4	49	2	66,8	2	19,0	48	13,7	2	11,8	1	6,6	1	165	2
8	Bedat	80-100	0,08	3,61	13,3	59,9	3	0,9	2	1,4	4	119	1	37	2	0,099	5	0,9	3	54	2	59,6	2	19,8	51	11,3	2	11,2	1	6,9	1	179	2
		0-20	0,09	2,77	6,6	56,0	3	11,0	19	2,6	8	84	1	122	7	0,660	37	3,4	11	38	2	161,5	5	20,0	56	26,1	4	5,1	1	11,7	2	1330	16
		20-40	0,04	1,16	7,4	36,7	2	1,6	3	0,7	2	71	1	36	2	0,110	6	1,5	5	33	1	41,9	1	4,7	13	8,5	1	4,0	1	5,2	1	240	3
		40-60	0,02	0,67	8,0	31,8	2	0,7	1	0,5	2	71	1	26	1	0,058	3	1,3	4	32	1	34,8	1	3,2	9	7,5	1	4,0	1	5,0	1	128	1
		60-80	0,03	0,77	8,6	41,4	2	0,7	1	0,5	1	72	1	28	2	0,063	3	1,5	5	34	1	32,5	1	2,9	8	8,0	1	4,1	1	5,4	1	124	1
9	Dore	80-100	0,03	1,02	8,2	41,5	2	1,2	2	0,7	2	69	1	34	2	0,097	5	1,5	5	33	1	39,4	1	4,0	11	8,8	1	4,0	1	5,4	1	187	2
		0-20	0,04	1,98	16,8	90,2	5	2,2	4	0,7	2	55	1	12	1	0,074	4	1,2	4	14	1	100,2	3	3,0	8	39,3	6	12,0	2	20,4	4	85	1
		20-40	0,01	0,28	24,3	61,6	3	2,1	3	0,8	2	64	1	13	1	0,042	2	0,9	3	16	1	82,9	3	2,3	6	49,2	7	17,3	2	20,7	4	75	1
		40-60	0,01	0,31	22,7	56,4	3	1,9	3	0,8	2	71	1	15	1	0,043	2	1,1	3	19	1	84,2	3	2,2	6	43,6	6	16,4	2	16,5	3	86	1
		60-80	0,01	0,35	16,6	63,0	3	1,9	3	0,6	2	71	1	16	1	0,056	3	1,1	3	20	1	84,0	2	2,2	5	39,9	5	15,2	2	15,9	3	94	1
		80-100	0,01	0,3	19,5	54,4	3	1,6	2	0,7	2	90	1	18	1	0,060	3	1,0	3	26	1	73,4	2	2,5	6	24,9	3	15,2	2	13,4	2	99	1
		100-120	0,02	0,49	21,1	32,0	2	0,9	1	0,8	2	163	2	25	1	0,024	1	1,2	3	49	2	48,2	1	5,6	14	12,6	2	11,4	1	7,5	1	124	1
		120-140	0,02	0,44	21,5	62,4	3	0,9	1	1,0	3	162	2	28	1	0,032	2	2,0	5	64	2	48,4	1	4,3	11	9,6	1	13,8	2	7,2	1	133	1
		140-160	0,01	0,43	30,1	43,6	2	0,9	1	1,2	4	188	2	28	1	0,019	1	1,4	4	56	2	49,0	1	5,8	15	13,5	2	6,8	1	127	1		
		160-180	0,03	0,93	29,1	52,0	3	1,8	3	1,2	3	116	1	23	1	0,190	10	1,2	3	32	1	75,8	2	3,6	9	41,1	6	17,4	2	13,5	2	120	1
10	Sioule	0-20	0,06	3,87	16,0	61,5	3	1,4	2	1,7	5	67	1	25	1	0,079	4	0,8	2	28	1	102,4	3	4,8	13	42,1	6	8,9	1	32,4	6	223	3
		20-40	0,03	1,59	16,3	67,9	3	1,0	2	1,2	3	77	1	25	1	0,070	3	0,7	2	30	1	102,2	3	6,2	15	31,7	4	9,1	1	12,5	2	152	2
		40-60	0,02	0,66	18,2	72,7	4	1,2	2	1,0	3	82	1	28	1	0,032	2	0,7	2	32	1	90,0	2	5,6	14	41,0	5	8,8	1	13,6	2	122	1
		60-80	<d.l.	0,74	24,2	55,0	3	0,9	1	1,2	3	77	1	19	1	0,020	1	0,7	2	30	1	56,2	2	4,3	11	28,0	4	11,2	1	12,2	2	100	1
11*	Cher	0-5	0,08	4,07	9,0	20,8	1	0,7	1	0,7	2	75	1	23	1	0,290	18	0,4	1	30	1	42,7	1	0,2	1	9,0	1	4,4	1	3,9	1	135	2
		25-30	0,05	3,08	11,2	17,7	1	0,7	1	0,6	2	89	1	25	2	0,290	18	0,6	2	31	1	51,8	2	0,3	1	9,0	1	4,7	1	3,6	1	133	2
		55-60	0,05	3,03	10,2	15,9	1	0,7	1	0,7	2	89	1	25	2	0,350	22	0,4	1	29	1	53,8	2	0,2	1	8,0	1	3,8	1	2,9	1	140	2
		85-90	0,05	3,54	8,9	12,4	1	0,8	2	0,7	3	82	1	32	2	0,410	27	0,5	2	32	1	57,0	2	0,2	1	9,0	2	3,3	1	2,7	1	158	2
		115-120	0,06	3,59	8,4	8,4	1	0,8	2	0,6	2	89	1	31	2	0,420	27	0,5	2	31	1	61,4	2	0,2	1	9,0	2	3,6	1	3,2	1	156	2
		185-190	0,16	3,72	9,7	11,6	1	0,7	1	0,4	1	89	1	29	2	0,330	21	0,5	2	33	1	62,7	2	0,4	1	8,0	1	5,1	1	3,3	1	125	2
		0-5	0,04	4,8	17,4	29,6	2	0,8	1	0,8	2	130	1	33	2	0,310	16	1,0	3	40	1	60,3	2	0,5	1	15,0	2	9,2	1	6,1	1	170	2
		25-30	0,03	3,38	13,1	32,6	2	1,1	2	0,9	3	123	1	39	2	0,360	18	1,2	3	42	1	247,3	7	1,5	4	20,0	3	8,4	1	4,8	1	170	2
		50-55	<d.l.	2,83	9,4	33,6	2	1,3	2	0,9	3	123	1	42	2	0,450	22	1,4	4	43	1	79,3	2	0,6	1	20,0	3	8,3	1	4,9	1	180	2
12*	Creuse	50-55	<d.l.	1,93	13,4	35,3	2	0,9	1	0,4	1	116	1	37	2	0,260	12	0,9	2	44	1	60,7	2	0,4	1	16,0	2	9,5	1	5,1	1	138	1
		75-80	<d.l.	1,93	13,4	35,3	2	0,9	1	0,4	1	109	1	33	1	0,140	6	0,8	2	39	1	47,6	1	0,4	1	15,0	2	9,1	1	4,8	1	120	1
		105-110	<d.l.	1,45	13,4	32,7	2	0,8	1	0,2	1	109	1	33	1	0,140	6	0,8	2	39	1	47,6	1	0,4	1	15,0	2	9,1	1	4,8	1	120	1
		130-135	<d.l.	1,36	11,2	31,8	1	0,7	1	0,1	0	116	1	31	1	0,110	5	1,0	3	37	1	41,7	1	0,4	1	12,0	1	7,8	1	4,5	1	116	1
		150-155	0,02	2,12	9,6	42,2	2	0,8	1	0,1	0	116	1	32	1	0,120	5	1,5	4	39	1	44,4	1	0,5	1	11,0	1	7,8	1	4,6	1	114	1
		170-175	<d.l.	1,21	14,4	11,0	0	0,8	1	0,1	0	123	1	37	2	0,070	3	0,4	1	40	1	43,5	1	0,4	1	11,0	1	8,7	1	5,2	1	123	1
		0-5	0,06	3,89	15,5	39,7	2	1,8	3	1,9	5	116	1	52	3	0,520	26	1,3	4	45	2	62,7	2	0,5	1	16,0	2	10,7	1	7,3	1	200	2
13*	Vienne	30-35	0,05	4,33	14,0	42,2	2	2,8	4	2,3	7	130	1	85	4	0,710	35	1,3	4	47	2	87,2	2	0,7	2	20,0	3	12,0	1	9,1	2	262	3
		60-65	0,04	4,11	11,5	51,9	3	4,3	6	2,0	5	137	1	103	5	0,880	42	1,4	4	45	2	98,7	3	0,7	2	17,0	2	12,0	1	8,9	1	277	3

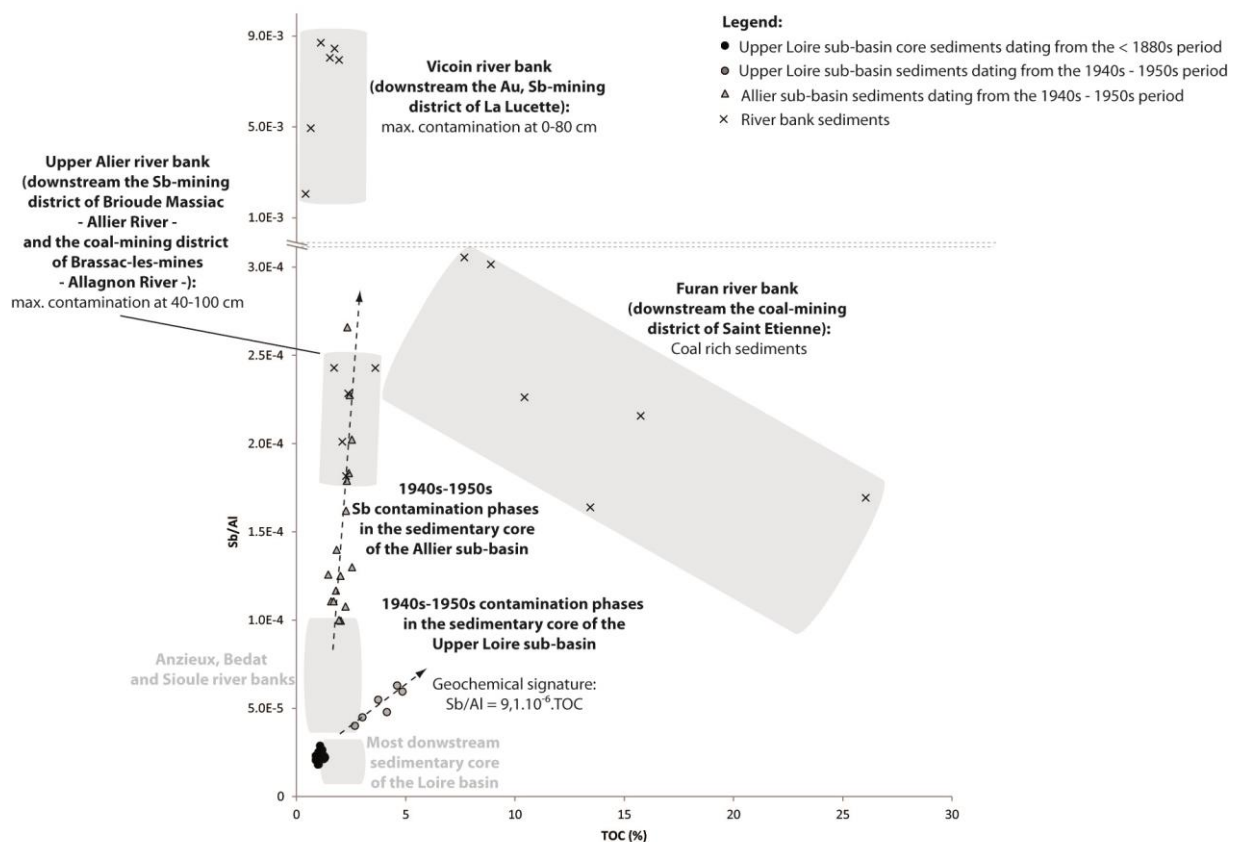


**Fig. 8.8. : Sb-TOC realtionships in the Upper Loire (ULC) and the Allier sub-basin cores (ALC) for the 1940s-1950s period and river bank sediments**

At global scale, Sb concentrations in coals average 0.92 ppm, about 0.98 ppm in Europe (Querol *et al*, 1995; Seredin and Finkelman, 2008). However, Sb concentrations are heterogeneous in coals and can locally be very important (*e.g.* average 7.06 ppm, max 348 ppm for Chinese coals, Qi *et al*, 2008; average 134 ppm, max 2347 ppm for Gokler coals in Turkey, Karayigit *et al*, 2000). Unfortunately, none information about TE

contents in coals of the French Central Massif have been found for this study. As shown by Querol *et al* (1995), the geochemical composition of coals depends on the selected density fraction. For these authors concentrations can ranges between 0.69 ppm for Sb,  $Sb/Al = 1.10^{-6} \cdot TOC$  in the less dense fraction (1.3-1.4) and reach 3.7 ppm for Sb,  $Sb/Al = 2.10^{-5} \cdot TOC$  in the densest fraction (> 2.8). During archiving processes, coal particles

are subjected to a storage according to density like other minerals, and associated geochemical signals depend on depositional environments (Dhivert *et al*, 2015). Therefore, the difference between geochemical signatures archived in Furan river bank sediments and the ULC can be explained by

- (i) the local influence of various industries accompanying coal-mining in the St Etienne district
- (ii) and/or by controlled depositional environment of the coring site selecting archived coal particles and thus archiving only a partial geochemical signature of coal-mining effluents.

Nonetheless, Sb concentrations being more important in the densest coal particles, the dispersion is limited and coal-mining effluents may only affect locally upstream sub-basins.

Moreover in the upstream part of the Allier basin was present one of the most important Sb-mining and smelting complexes at a national scale. Maximum activity period for this district also corresponds to the 1940s-1950s interval (see § 8.2.1.2.). At the entire Loire basin scale, maximum Sb contaminations are

archived in Vicoin river bank sediments, downstream the important Au-Sb-mining and smelting complex of La Lucette district (maximum EF = 1833, Fig. 8.7, Tab. 8.3). The dispersion of polluted sediments coming from TE-mining effluents can be spatially limited because of the low transport of TE-carrier phases (influences from 10 to  $10^2$  km, e.g. Jung *et al*, 2002; Maclin *et al*, 2006; Grosbois *et al*, 2007; Lecce and Pawlowski, 2014). For instance, for the largest Sb-mining and smelting complex of Xikuangshan (China), maximum concentrations reach 7316 ppm downstream of the site and rapidly decrease to 57 ppm in less than 10 km (Wang *et al*, 2011). In mining districts of Brioude-Massiac and La Lucette, Sb is associated to a sulfide mineralization and is mostly present as stibnite ( $Sb_2S_3$ , density 4.6). As for coal-mining effluents, the low dispersion of Sb contaminated sediments can be explained by the high density and the low transport of Sb-ores. Moreover, Sb levels are limited in the dissolved fraction because of its tendency to be sorbed to Fe, Al, Mn hydroxides, clays and organic matters (Ure and Berrow, 1982; Fillela *et al*, 2002ab, Wang *et al*, 2011). Nevertheless, during major hydrosedimentary events, Sb mobility can be enhanced, Sb-bearing minerals being

transported and altered several km downstream of mining sites (Craw *et al*, 2004). In highly contaminated areas, biological activity can also magnify the Sb solubility in soils and thus its transport during soils erosions events (Okkenhaug *et al*, 2011).

In addition, high Sb enrichments can be highlighted in river bank sediments of the Anzieux, the Bedat, and the Sioule Rivers (EF ranged between 11 and 21; Tab. 8.3). In the two first sub-basins, Sb is significantly correlated with all TE, except As and U ( $r > 0.8$ ,  $p < 0.05$ ). In sediments of the Sioule sub-basin, Sb is only correlated with As and Pb ( $r > 0.7$ ,  $p < 0.05$ ,  $n = 4$ ). From the 19<sup>th</sup> century, various TE-smelters were implanted in these sub-basins (especially Cu, Pb smelters in cited sub-basins; Garçon, 1995). In industrialized areas, smelting activity of chalcophil TE associated to sulfide ores can constitute solid Sb contamination sources, especially by the local fallout of emitted ashes (Crecelius *et al*, 1974; Takaoka *et al*, 2005).

In addition, after coal combustion, Sb is enriched by a factor close to 2 in ashes (Ondov *et al*, 1989; Clarke, 1993; Querol *et al*, 1995; Seredin and Finkelman, 2008). Therefore, fallout of ashes from

coal combustion should also largely contribute to Sb sedimentary contaminations. As shown by Shortyk *et al* (1996) the maximum fallout of Sb polluted particles at a W-European scale occurred between the 1920s and the 1950s and is attributed to coal and heavy industries ashes.

In summary, between the 1910s and the late 1950s Sb and Sn sedimentary contaminations were limited to upstream sub-basins and be realted to:

- (i) local fallout of contaminated ashes coming from glass industries, chalcophil TE smelters and metallurgy
- (ii) the low dispersion of dense Sb-rich particles from coal and Sb-mining effluents.

#### **8.4.2. Characterization of generalized anthropogenic sources**

##### **8.4.2.1. Various Hg contamination sources since the 1880s**

From the end of the 19<sup>th</sup> century, Hg is the most enriched TE in sediments of the whole Loire basin, showing very high enrichments in the three studied cores. Maximum contamination levels are reached during the 1940s-1950s in the upstream part

(maximum EF= 57 in the Upper Loire and 69 in the Allier sub-basins) and between 1950s - 1970s for the downstream part (maximum EF = 53). The Hg sedimentary contamination is generalized at the entire basin, most of sampled river bank sediments presenting high Hg enrichments (Tab. 8.3). At basin scale, diffuse local and global Hg emission sources contribute to the sedimentary contamination during the industrial period (Meybeck *et al*, 2007; Thevenot *et al*, 2007; Lestel *et al*, 2007; Le Cloarec *et al*, 2011).

Indeed, Hg is a highly volatile TE and compared to the preindustrial period, the Hg global fallout has increased of a factor 2 to 10 in the most industrialized areas (Martinez-Cortizas *et al*, 1999). Some important Hg-mining sites are older than 5 centuries but industrial production dates from the 1850s at global scale and gradually increases up to the 1960s; this TE was used in various industries (Lumb, 1995; Hylander and Meili, 2003; Bank, 2012). Moreover, Hg volatilization during coal combustion has constituted from the 19<sup>th</sup> century the major Hg contamination source at global scale (1534 t emitted in 2003; Querol *et al*, 1995; Hylander and Meili, 2003; Mukherjee *et al*, 2008)

At the Loire basin scale, coal-mining effluents and more generally the transport of coal particles should also be part of important Hg contamination sources during the industrial period. Hg concentrations in coals generally ranges between 0.1 and 1.0 ppm but can locally reach 1000 ppm at maximum (Seredin and Finkelman, 2008; Mukherjee *et al*, 2008). As for Sb, Hg concentrations depend on density of coal particles (1.34 ppm for a density of 2.8; Querol *et al*, 1995). Moreover, blast furnace effluents from heavy industries could also largely contribute to this sedimentary contamination, Hg concentrations ranging from 0.006 to 20.8 ppm in European blast furnace sludge, (average 1.63 ppm; Földi *et al*, 2014). In Europe, high Hg enrichments can be highlighted in soils and sediments sampled in old metallurgical areas (*e.g.* maximum of 4.6 ppm in soil, Jasmina and Robert, 2011; 35 ppm in reservoir sediments, Castelle *et al*, 2007).

In summary, Hg contamination archived in sediments of the Loire basin is related to various global and local anthropogenic activities, more or less synchroic. Hence, specific contributive sources are hard to characterized with

elementary ratios (any TE-Hg relationship was significant), isotopic analyses of Hg would be more discriminant; Feng *et al*, 2010 ; Yin *et al*, 2010).

Extreme enrichments were measured in river bank sediments of the Anzieux (0-40 cm, maximum EF = 1128), the Furan (maximum EF = 186) and the Vienne Rivers (maximum EF = 220). They correspond to fingerprints of anthropogenic releases coming from well-known Hg contamination sources located in these sub-basins.

In the Anzieux sub-basin, hat-making factories were in operation between the second part of the 19<sup>th</sup> century and 1997, with a maximum production period occurring at the end of the 19<sup>th</sup> century (Hat-making museum of Chazelles-sur-Lyon). Up to the 1940s, the fur-felting process in the hat-making used mercuric nitrate ( $Hg_2(No_3)_2$ ; this process was abandoned because of the human health impact (e.g. Neal, 1938; Lumb, 1995). Solid contaminations of soils were highlighted near to these hat-making factories (maximum Hg concentrations = 370 ppm, [www.basol.developpement-durable.gouv.fr](http://www.basol.developpement-durable.gouv.fr)). Therefore, high Hg enrichments archived between the 1880s and the 1900s in the Upper Loire sub-

basin core should certainly be associated to this activity (maximum EF = 30 in the late 1880s).

At the same time, at global scale, Hg production peak occurred during World War II related to the important bomb and explosive production (Hylander and Meili, 2003). In the Furan sub-basin one of the most important weapon factories of France was implanted, largely active during this period (St Etienne municipal archives). Hence, weapon industries can be here a solid Hg sources, explaining maximum Hg enrichments (EF = 57) recorded during the 1940s in the Upper Loire sub-basin. During this period, bombing should also contribute to Hg contaminations (Wang *et al*, 2004).

In addition, since the 18<sup>th</sup> century, important glass and ceramic factories are implanted close to Limoges in the Vienne sub-basin, producing porcelain. Traditionally, porcelain decorations are made of mercuric oxides (HgO) or mercuric amalgam with Au or Ag for instance (Neal, 1938). In addition, important tanning industries were implanted in this sub-basin, using Hg for skins treatments (Neal, 1938). These old anthropogenic activities should influence

Hg concentrations in archived sediments of the Vienne sub-basin.

#### 8.4.2.2. Heavy industries releases

Polymetallic sedimentary contaminations are recorded in sediments of the Upper Loire and the Allier sub-basins between the 1940s and the 1950s. These contamination phases can be characterized by two significant geochemical signatures *i.e.*  $\text{Bi}/\text{Al} = 1.2.\text{Cd}/\text{Al} - 1.9.10^{-6}$ ,  $r = 0.9$ ,  $p < 0.05$ ,  $n = 6$  in the Upper Loire sub-basin and  $\text{Bi}/\text{Al} = 4.0.\text{Cd}/\text{Al} - 2.7.10^{-5}$ ,  $r = 0.9$ ,  $p < 0.05$ ,  $n = 16$  in the Allier sub-basin (Fig. 8.9). For sediments archived after the late 1950s in the ULC and the ALC, similar geochemical signature can be highlighted (but in a decreasing trend,  $\text{Bi}/\text{Al} = 1.4.\text{Cd}/\text{Al} - 4.3.10^{-6}$ ,  $r = 0.8$ ,  $p < 0.05$ ,  $n = 17$  for the ULC;  $\text{Bi}/\text{Al} = 3.5.\text{Cd}/\text{Al} - 4.7.10^{-6}$ ,  $r = 0.9$ ,  $p < 0.05$ ,  $n = 19$  for the ALC). In the ULC, any significant geochemical signature can be calculated in sediments deposited before the 1940s ( $r = 0.4$ ,  $p > 0.05$ ,  $n = 57$ ).

Between the 1950s and the 1980s, a polymetallic contamination phase is also recorded in the most downstream part of the Loire basin showing similarities with those archives 20 years before in the upstream part. Indeed, Bi/Cd ratios of sedimentary layers dating from the 1950s-

1980s period in the LLC range between those archived during the 1940s-1950s period in the ULC and the ALC (Fig. 8.9). A significant geochemical signature can be characterized in the 1950s-1980s sequence of the LLC ( $\text{Bi}/\text{Al} = 1.6.\text{Cd}/\text{Al} + 2.6.10^{-5}$ ,  $r = 0.7$ ,  $p < 0.05$ ,  $n = 14$ ). In the LLC, a similar Cd-Bi relationship can be calculated during the general decrease phase (post 1980s;  $\text{Bi}/\text{Al} = 1.1.\text{Cd}/\text{Al} - 1.5.10^{-6}$ ,  $r = 0.9$ ,  $p < 0.05$ ,  $n = 10$ ). Any significant Cd-Bi association can be calculated in sediments deposited before the 1950s in the LLC.

In the Loire basin, Bi and Cd are moderately to highly enriched in sediments archived in river bank sediments of the Furan (especially in the black sedimentary layer and between 90 and 115 cm deep, maximum EF = 47 for Bi, 63 for Cd), the Anzieux in the 0-20 cm sedimentary layer (EF = 9 for Bi, 4 for Cd), the Bedat in the 0-20 cm sedimentary layer (EF = 19 for Bi, 8 for Cd) and the Vienne sub-basins (under 95 cm deep; maximum EF = 6 Bi, 7 for Cd; Tab. 8.3.). The Bi/Cd ratio in sediments of the Furan (90-115 cm), the Anzieux and the Bedat river bank is close to 4 as in the ALC (Fig. 8.9). Dark sediments of the Furan and the Vienne river bank present heterogeneous Bi/Cd ratios ranging between 1 and 3.

In mining and industrial complexes of the Loire basin, coal was locally used in industry. Coal particles can contain high Cd and Bi concentrations, but during combustion these TE are largely enriched in fly ashes (*e.g.* average concentrations in European coals: Bi = 0.1 to 0.3 ppm, Cd = 0.2 to 1.4 ppm; average concentrations in fly ashes Bi = 0.3 to 0.7 ppm, Cd = 0.6 to 1.2 ppm; average Bi/Cd ratio = 0.7; Querol *et al*, 1995). Currently, in important urban and industrial areas of China, where energy is essentially produced by coal combustion, Bi and Cd concentrations reach 12.3 ppm for Bi and 41.4 ppm for Cd in deposited dusts (Li *et al*, 2013). Therefore, important fallout of ashes associated to the massive coal combustion during the 1940s and the 1950s may constitute a solid contamination source affecting the entire basin and more again the most industrialized areas. In addition, coal was also largely used for pig-iron and steel productions. Blast furnace sludge contain high TE concentrations, notably for Bi and Cd (average concentrations 98.3 ppm for Bi, 36.2 ppm for Cd, average Bi/Cd ratio close to 3, Földi *et al*, 2014). Up to the late 1950s, steel production units, based on coal combustion and coke used in cracking processes, were implanted in the Furan, the Anzieux, the Bedat and the

Vienne sub-basins. Effluents of metallurgical activities should also constitute important contamination sources during the 1940s-1950s period.

Identified sources attributed to the polylmetallic sedimentary contamination are located in the Upper Loire, the Allier and the Vienne sub-basin. The delay for the archiving of the polymetallic contamination phases highlighted in the most downstream part of the Loire basin can be explained by the dispersion time of polluted sediments. Indeed at basin scale, sediments – and thus associated substances - are transported from eroded bedrocks to estuaries like a sedimentary cascade, by alternate episodes of deposition and erosion (Burt and Allisson, 2010). Therefore, spatial and temporal distributions of sedimentary contaminations do not only depend on the geography and the history of anthropogenic releases.

This study highlights that spatial and temporal variabilites of recorded TE signals do not only depend on sources history. The dispersion capacity of contaminated sediments plays a key role in the spatial and the temporal distribution of the sedimentary contamination.

**Legend:**

- Upper Loire sub-basin core sediments dating from the < 1880s period
- Upper Loire sub-basin sediments dating from the 1940s - 1950s period
- △ Allier sub-basin sediments dating from the 1940s - 1950s period
- Lower Loire basin sediments dating from the 1950s - 1980s period
- × River bank sediments

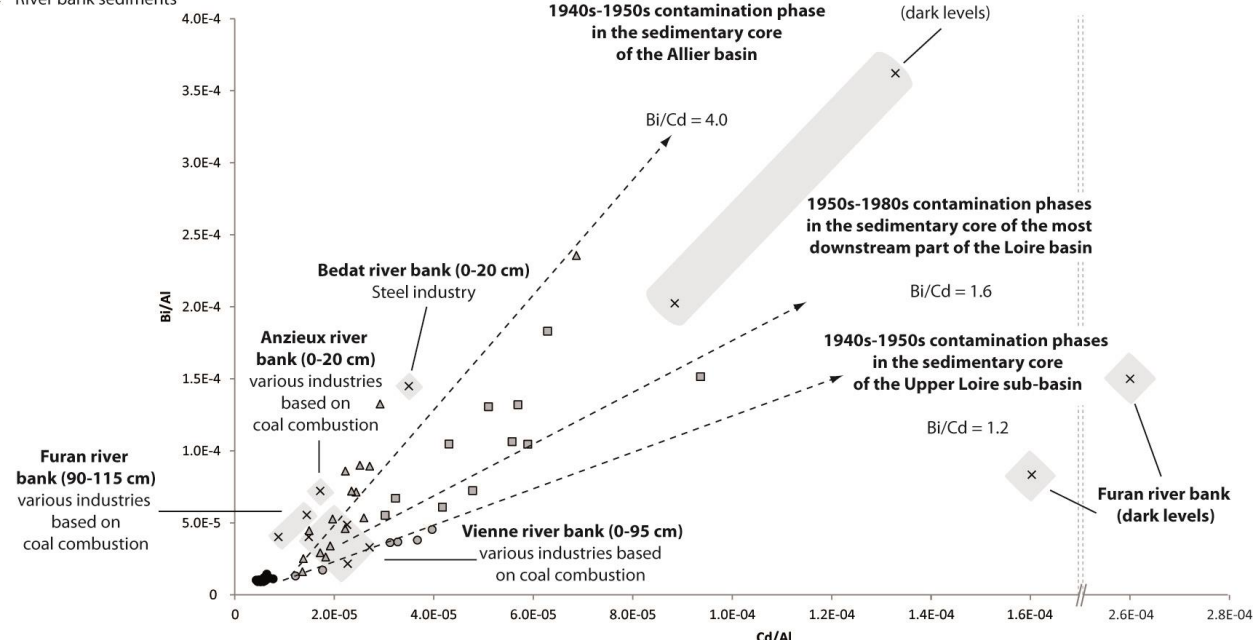


**Fig. 8.9. : Cd-Bi relationships in the Upper Loire (ULC) and the Allier sub-basin cores (ALC) during the 1940s-1950s period; during the 1950s-1980s period in the most downstream core (LLC) and in river bank sediments**

The nature of carrier phases is an important factor influencing the transport and the post-depositional remobilization of pollutants (*e.g.* for mining wastes: Courtin-Nomade *et al*, 2005; Grosbois *et al*, 2007; Lecee and Pavlowsky, 2014).

Moreover, geomorphological processes control storage / transport conditions and therefore the fate of sediments and associated contaminants

(Miller, 1997; Walling *et al*, 2003; Macklin *et al*, 2006). For the largest W-European basins ( $>13\ 500\ km^2$ ) residence time of fine-grained sediments is very heterogeneous, generally comprise between 1 and 60 years (Wallbrink *et al*, 1998, Skalak and Pizzuto, 2010, Koiter *et al*, 2013). Since the 19<sup>th</sup> century, embankments and other hydraulic structures controlling water discharge have

largely disturbed the continuity of the sedimentary transport by amplifying sediments storage in out of channel forms and dam reservoirs (*e.g.* Vörösmarty *et al*, 2002; Arnaud-Fassetta, 2003; Bridge, 2003; Houben, 2007).

In the Loire basin, since the late 18<sup>th</sup> century, river bed has been largely managed by longitudinal and lateral hydraulic structures (Dion, 1961; Lino *et al*, 2000). Moreover, according to the Loire Water Agency, up to the 1990s more than 5 Mm<sup>3</sup> of alluvial sediments were extracted at an annual rate 20 times higher than the sedimentary transport. As the result of this anthropization, the river geomorphology have changed and the sediment storage capacity of the Loire basin has been enhanced (Babonaux, 1970; Leteinturier *et al*, 2000; Rodrigues *et al*, 2007; Détriché *et al*, 2010; Grivel and Gauthier, 2012; Dhivert *et al*, 2015; Dhivert *et al*, 2015), while incision of the river bed has increased (Gasowski, 1994; Latapie, 2011; Latapie *et al*, 2014). In this context, dispersion of contaminated sediments should largely be slowdown.

#### **8.4.3. Evidence of old sources reactivation during major hydrosedimentary events**

In the current context of controlled TE releases, the erosion of contaminated sediments has became one of the major contamination sources for the hydrosystem (Macklin and Kilmer, 1992 ; Lecce and Pavlowsky, 1997 ; Förstner, 2004 ; Lecce and Pavlowsky, 2014). In the Loire basin, the annual erosion yield for fine-grained sediments ranges between 2.9 and 32.4 t.km<sup>-2</sup>.year<sup>-1</sup> (Grosbois *et al*, 2001; Gay *et al*, 2014). Regarding this observation, what is the influence of river bank erosion on the current TE sedimentary contamination?

In the Upper Loire basin, sediments of the Villerest Dam reservoir located 30 km downstream of the St Etienne agglomeration have trapped highly polluted sediments since the early 1980s (maximum EF *c.a.* 30 for Cd and Hg; Dhivert *et al*, 2015; Fig.8.1). Sedimentary inputs of three major flood events (average daily discharge higher than a 20 year return value) occurred in 1996, 2003 and 2008 and have largely contributed to the sedimentary infill of this reservoir. While a general decrease of TE enrichmentsis recorded in sediments deposited during interflood periods, flood

sequences present the highest TE enrichments. This attests the activation of specific sources during these hydrosedimentary events.

Before the 2000s, sediments deposited during interflood period are affected by a local Cd Hg contamination sources in the Villerest core. The geochemical signature of this sedimentary sequence is  $\text{Hg}/\text{Al} = 2.8 \cdot 10^{-2} \cdot \text{Cd}/\text{Al} + 2.4 \cdot 10^{-6}$ ,  $r = 0.8$ ,  $p < 0.05$ ,  $n = 11$  (Fig. 8.10). In other cores such an Hg - Cd relationship is not recorded over registered periods (Fig. 8.10). Hg and Cd are highly enriched close to metallurgical sites (Audry *et al*, 2004; Castelle *et al*, 2007; Jasminka and Robert, 2011; Louriño-Cabana *et al*, 2011). Between the 1980s and the

Sediments, archived during important hydro-sedimentary events, show a different significant geochemical signature of  $\text{Hg}/\text{Al} = 1.5 \cdot 10^{-1} \cdot \text{Cd}/\text{Al} + 3.4 \cdot 10^{-7}$ ,  $r = 0.9$ ;  $p < 0.05$ ;  $n = 20$  (Fig. 8.10). The dark sedimentary layers, stored in the Furan river bank, present a similar geochemical signature (Fig. 8.10). Therefore, during major flood event, highly polluted sediments can be eroded

from the Furan river bank before to be trapped in the Villerest reservoir.

These results highlight contribution of river bank erosion to the current sedimentary contamination. Hence, at the Loire basin scale old sources can be reactivated during major hydro-sedimentary events *via* the erosion of highly polluted sediments archived in storage areas.

## 8.5. Conclusions

In order to study spatial and temporal variabilities of TE sedimentary contaminations at the Loire basin scale, three sedimentary archives were compared. The two upstream cores were sampled in the most industrialized sub-basins (*i.e.* the Upper Loire and the Allier sub-basins) and the third one was sampled in the most downstream part of the fluvial domain. In addition old sources were characterized by comparing geochemical signatures archives in river bank sediments recovered downstream of the major industrial and mining areas to those recorded in sedimentary cores.

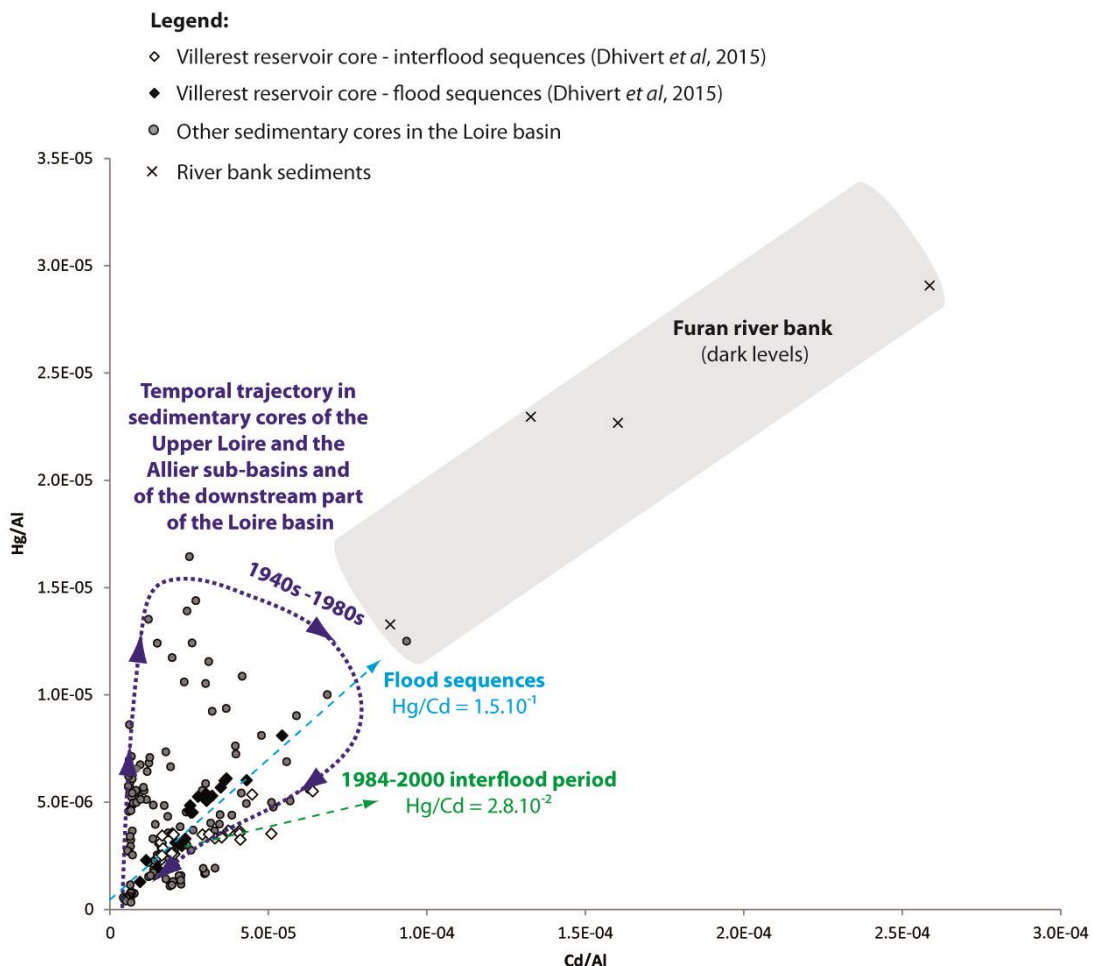


**Fig. 8.10.** : Cd-Hg relationships in the Villerest reservoir core (Dhivert et al, 2015), in the ULC, the ALC and the LLC and in Furan river bank sedimenst

Four temporal windows based on enriched TE associations and contamination levels were defined corresponding to:

- i) a non-contaminated period recorded in the Upper Loire sub-basin during the First Industrial Revolution from the late 18<sup>th</sup> century to the late 1870s and

before << 1900s in the downstream part of the basin  
ii) Hg, Sb and Sn contaminations during the Second Industrial Revolution (1880s-1930s) in the Upper Loire basin related to hat-making factories and local fallout of polluted ashes from glass industries implanted near to the coring site; in the downstream part of the Loire basin only Hg is

- enriched during this period showing a decreasing trend.
- iii) polymetallic contamination phase corresponding to maximum enrichments over the recording period between the 1940s and the late 1950s in the Upper Loire and the Allier sub-basins, recorded with a delay and lasting longer in the downstream part of the basin (between the 1950s and 1980s) ; these contamination phases can be related to the influence of mining effluents (in upstream sub-basins only) and to global and local emission sources as coal combustion and heavy industries releases
  - iv) and a general decrease of TE enrichments since the early 1960s for the both upstream sub-basins and from the 1980s in the downstream part of the basin ; in this context, river bank erosion during major hydrosedimentary events is a factor of reactivation of old contamination sources

This basin-scale approach of the history of the sedimentary contamination highlighted the spatial and temporal variability of recorded TE signals in

archived sediments and the difference of spatial and temporal influences of contamination sources. These variability factors must be considered to build historical reconstitution of pollutant dynamics and sources at an entire basin scale.

## References :

- Arnaud, F., Serralongue, J., Winiarski, T., Desmet, M., Paterne, M., 2006. Pollution au plomb dans la Savoie antique (II-III<sup>e</sup> s. ap. J.-C.) en relation avec une installation métallurgique de la cité de Vienne. Comptes Rendus Géosciences. 338, 244-252.
- Arnaud-Fassetta, G., 2003. River channel changes in the Rhone Delta (France) since the end of the Little Ice Age: geomorphological adjustment to hydroclimatic change and natural resource management. Catena, 51, 141-172.
- Audry, S., Schäfer, J., Blanc, G., Bossy, C., Lavaux, G., 2004. Anthropogenic components of heavy metal (Cd, Zn, Cu, Pb) budgets in the Lot-Garonne fluvial system (France). Applied Geochemistry, 19, 769-786.
- Audry, S., Schäfer, J., Blanc, G., Jouanneau, J. M., 2004. Fifty-year sedimentary record of heavy metal pollution (Cd, Zn, Cu, Pb) in the Lot River reservoirs (France). Environmental Pollution, 132, 413-426.
- Babonaux Y., 1970. Le lit de la Loire - Etude d'hydrodynamique fluviale, Paris, Bibliothèque Nationale, 252 p.

- Bank, M. S., 2012. Mercury in the environment: pattern and process. Univ of CaliforniaPress.237p.
- Bednarova, Z., Kuta, J., Kohut, L., Machat, J., Klanova, J., Holoubek, I., Hilscherova, K., 2013. Spatial patterns and temporal changes of heavy metal distributions in river sediments in a region with multiple pollution sources. *Journal of Soils and Sediments*, 13, 1257-1269.
- Berner, Z. A., Bleeck-Schmidt, S., Stüben, D., Neumann, T., Fuchs, M., Lehmann, M. 2012, Floodplain deposits: A geochemical archive of flood history – A case study on the River Rhine, Germany. *Applied Geochemistry*. 27, 543–561.
- Birch, G. F., Taylor, S. E., & Matthai, C., 2001. Small-scale spatial and temporal variance in the concentration of heavy metals in aquatic sediments: a review and some new concepts. *Environmental Pollution*, 113, 357-372.
- Bradley, S. B., Cox, J. J., 1990. The significance of the floodplain to the cycling of metals in the river Derwent catchment, UK. *Science of the Total Environment*, 97, 441-454.
- Bridge, J. S., 2003. Rivers and floodplains: forms, processes, and sedimentary record. John Wiley & Sons. 491 p.
- Burt, T. P., Allison, R. J., 2010. Sediment cascades in the environment: An integrated approach. *Sediment cascades: An integrated approach*, 449 p.
- Castelle, S., Schäfer, J., Blanc, G., Audry, S., Etcheber, H., Lissalde, J. P., 2007. 50-year record and solid state speciation of mercury in natural and contaminated reservoir sediment. *Applied Geochemistry*, 22, 1359-1370.
- Clarke, L. B., 1993. The fate of trace elements during coal combustion and gasification: an overview. *Fuel*, 72, 731-736.
- Courtin-Nomade, A., Grosbois, C., Bril, H., Roussel, C., 2005. Spatial variability of arsenic in some iron-rich deposits generated by acid mine drainage. *AppliedGeochemistry*, 20, 383-396.
- Covelli, S., Faganeli, J., Horvat, M., Brambati, A., 2001. Mercury contamination of coastal sediments as the result of long-term cinnabar mining activity (Gulf of Trieste, northern Adriatic sea). *AppliedGeochemistry*, 16, 541-558.
- Coynel, A., Schäfer, J., Blanc, G., Bossy, C., 2007. Scenario of particulate trace metal and metalloid transport during a major flood event inferred from transient geochemical signals. *Applied Geochemistry*, 22, 821–836.
- Craw, D., Wilson, N., Ashley, P. M., 2004. Geochemical controls on the environmental mobility of Sb and As at mesothermal antimony and gold deposits. *Applied Earth Science: Transactions of the Institutions of Mining and Metallurgy: Section B*, 113, 3-10.
- Crecelius, E. A., Johnson, C. J., Hofer, G. C., 1974. Contamination of soils near a copper smelter by arsenic, antimony and lead. *Water, air, and soil pollution*, 3, 337-342.
- Crutzen P. J., Stoermer E. F., 2000. The Anthropocene. *Global Change Newslett.* 41.17–18.
- Dacharry M., 1974. *Hydrologie de la Loire en amont de Gien*. Paris, N.A.L., 2 vol. 334 & 285 p.

- Darnley, A. G., Bjorklund, A., Bolviken, B., Gustavsson, N., Koval, P. V., Steenfelt, Xuejing, X., 1995. A Global geochemical database. Recommendations for international geochemical mapping. Final report of IGCP project, 259 p.
- De Cort, M., Dubois, G., Fridman, Sh. D., Germenchuk, M. G., Israel, Yu. A., Janssens, A., Jones, A. R., Kelly, G.N., Kvasnikova, E. V., Matveenko, I. I., Nazarov, I. M., Pokumeiko, Yu. M., Sitak, V. A., Stukin, E. D., Tabachnyi, L. Ya., Tsaturov, Yu. S., & Avdyushin, S. I., 1998. Atlas of caesium deposition on Europe after the Chernobyl accident. EUR Report 16733, EC, Office for Official Publications of the European Communities, Luxembourg.
- Delfour J., Isnard P., Lecuyer E., Lemier B., Lhote F., Moine B., Piboule M., Picot P., Ploquin A., Tegyey M., 1984. - Etude du gîte de pyrite de Chizeuil (Saône-et-Loire) et de son environnement volcanosédimentaire dévonien et dinantien. Document BRGM, 73, 37 p.
- Desmet, M., Mourier, B., Mahler, B. J., Van Metre, P. C., Roux, G., Persat, H., Babut, M., 2012. Spatial and temporal trends in PCBs in sediment along the lower Rhône River, France. *Science of the Total Environment*, 433, 189-197.
- Détriché, S., Rodrigues, S., Macaire, J.-J., Bonté, P., Bréhéret, J.-G., Bakyono, J.-P., Jugé, P., 2010. Caesium-137 in sandy sediments of the River Loire (France): Assessment of an alluvial island evolving over the last 50 years: *Geomorphology*, 115, 11–22
- Dhivert, E., Grosbois, C., Coynel, A., Desmet, M., 2015. Sedimentary and geochemical evidences in a core age model to highlight flood-event dynamics in a reservoir infill (Upper Loire basin, France). *Catena*. 126, 75-85
- Dhivert, E., Grosbois, C., Rodrigues, S., Desmet M., 2015. Influences of fluvial environments on sediment archiving processes and temporal pollutant dynamics (Upper Loire River, France). *Science of the total Environment*, 1, 121-136.
- Dion. R., 1961. *Histoire des levées de la Loire*. Paris, 312 p.
- Eppler, R. A., 1997. Selecting ceramic pigments. *Materials & Equipment/Whitewares: Ceramic Engineering and Science Proceedings*, 8, 1139-1149.
- Estrany, J., Garcia, C., Walling, D. E., Ferrer, L., 2011. Fluxes and storage of fine-grained sediment and associated contaminants in the Na Borges River (Mallorca, Spain). *Catena*, 87, 291-305.
- Feng, X., Foucher, D., Hintelmann, H., Yan, H., He, T., Qiu, G., 2010. Tracing mercury contamination sources in sediments using mercury isotope compositions. *Environmental science & technology*, 44, 3363-3368.
- Ferrand, E., Eyrolle, F., Radakovitch, O., Provansal, M., Dufour, S., Vella, C., Gurriaran, R., 2012. Historical levels of heavy metals and artificial radionuclides reconstructed from overbank sediment records in lower Rhône River (South-East France). *Geochimica et Cosmochimica Acta*, 82, 163-182.
- Filella, M., Belzile, N., Chen, Y. W., 2002. Antimony in the environment: a review focused on natural waters: I. Occurrence. *Earth-Science Reviews*, 57, 125-176.

- Filella, M., Belzile, N., Chen, Y. W., 2002. Antimony in the environment: a review focused on natural waters: II. Relevant solution chemistry. *Earth-Science Reviews*, 59, 265-285.
- Finkelman, R. B., 1993. Trace and minor elements in coal. In *Organic geochemistry*). Springer US., 593-607
- Földi, C., Dohrmann, R., Mansfeldt, T., 2014. Mercury in dumped blast furnace sludge. *Chemosphere*, 99, 248-253.
- Förstner, U., 2004. Sediment dynamics and pollutant mobility in rivers: an interdisciplinary approach. *Lakes & Reservoirs: Research & Management*, 9, 25-40.
- Förstner, U., Salomons, W., 1980. Trace metal analysis on polluted sediments: Part I: Assessment of sources and intensities. *Environmental Technology*, 1, 494-505.
- Garçon, A. F., 1995. Les métaux non-ferreux en France aux XVIII<sup>e</sup> et XIX<sup>e</sup> siècles: Ruptures, blocages, évolutions au sein des systèmes techniques, PhD thesis, Ecoles des Hautes Etudes en Sciences Sociales, Paris, 282p.
- Garçon, M., Chauvel, C., Chapron, E., Fain, X., Mingfang L., Campillo, S., Bureau, S., Desmet, M., Bailly-Maitre, M.C., Charlet, L., 2012. Silver and lead in high altitude lake sediments : proxies for climate changes and human activities. *Applied geochemistry*, 27, 760-773
- Gasowski, Z., 1994. L'enfoncement du lit de la Loire/The entrenchment of the Loire's river bed. *Revue de géographie de Lyon*, 69, 41-45.
- Gay, A., Cerdan, O., Delmas, M., Desmet, M., 2014. Variability of suspended sediment yields within the Loire river basin (France), *Journal of Hydrology*, 519, 1225-1237.
- Ghose, M. K., Majee, S. R., 2000. Sources of air pollution due to coal mining and their impacts in Jharia coalfield. *Environment international*, 26, 81-85.
- Gocht, T., Moldenhauer, K. M., Püttmann, W., 2001. Historical record of polycyclic aromatic hydrocarbons (PAH) and heavy metals in floodplain sediments from the Rhine River (Hessisches Ried, Germany). *Applied Geochemistry*, 16, 1707-1721.
- Grivel, S., Gauthier, E., 2012. Mise en place des îles fluviales en Loire moyenne, du 19<sup>e</sup> siècle à aujourd'hui, Cybergeo. URL : <http://cybergeo.revues.org/25451>.
- Grosbois, C., Meybeck, M., Lestel, L., Lefèvre, I., Moatar, F., 2012. Severe and contrasted polymetallic contamination patterns (1900–2009) in the Loire River sediments (France). *Science of the Total Environment*, 435, 290-305.
- Grosbois, C., Courtin-Nomade, A., Martin, F., Bril, H., 2007. Transportation and evolution of trace element bearing phases in stream sediments in a mining – Influenced basin (Upper Isle River, France). *Applied Geochemistry*, 22, 2362-2374
- Grosbois, C., Meybeck, M., Horowitz, A., Ficht, A., 2006. The spatial and temporal trends of Cd, Cu, Hg, Pb and Zn in Seine River floodplain deposits (1994–2000). *Science of the total environment*, 356, 22-37.
- Grosbois, C., Négrel, P., Grimaud, D., Fouillac, C., 2001. An overview of dissolved and suspended matter fluxes in the Loire river basin: natural and anthropogenic inputs. *Aquatic Geochemistry*, 7, 81-105.

- Grousset, F. E., Jouanneau, J. M., Castaing, P., Lavaux, G., Latouche, C., 1999. A 70 year record of contamination from industrial activity along the Garonne River and its tributaries (SW France). *Estuarine, Coastal and Shelf Science*, 48, 401-414.
- Heaven, S., Ilyushchenko, M. A., Kamberov, I. M., Politikov, M. I., Tanton, T. W., Ullrich, S. M., Yanin, E. P., 2000. Mercury in the River Nura and its floodplain, Central Kazakhstan: II. Floodplain soils and riverbank silt deposits. *Science of the Total environment*, 260, 45-55.
- Heim, S., Schwarzbauer, J., Kronimus, A., Littke, R., Woda, C., Mangini, A., 2004. Geochronology of anthropogenic pollutants in riparian wetland sediments of the Lippe River (Germany). *Organic Geochemistry*, 35, 1409-1425.
- Hoffmann, T., Thorndycraft, V. R., Brown, A. G., Coulthard, T. J., Damnati, B., Kale, V. S., Walling, D. E., 2010. Human impact on fluvial regimes and sediment flux during the Holocene: Review and future research agenda. *Global and Planetary Change*, 72, 87-98.
- Hong, S., Candelone, J. P., Patterson, C. C., Boutron, C. F., 1994. Greenland ice evidence of hemispheric lead pollution two millennia ago by Greek and Roman civilizations. *Science*, 265, 1841-1843.
- Horowitz, A. J., Meybeck, M., Idlafkikh, Z., Biger, E., 1999. Variations in trace element geochemistry in the Seine River Basin based on floodplain deposits and bed sediments. *Hydrological processes*, 13, 1329-1340.
- Horowitz, A. J., Elrick, K. A., 1987. The relation of stream sediment surface area, grain size and composition to trace element chemistry. *Applied Geochemistry*, 2, 437-451.
- Houben, P., 2007. Geomorphological facies reconstruction of Late Quaternary alluvia by the application of fluvial architecture concepts. *Geomorphology*, 86, 94-114.
- Hughes, A. O., Croke, J. C., Pietsch, T. J., Olley, J. M., 2010. Changes in the rates of floodplain and in-channel bench accretion in response to catchment disturbance, central Queensland, Australia. *Geomorphology*, 114, 338-347.
- Hylander, L. D., Meili, M., 2003. 500 years of mercury production: global annual inventory by region until 2000 and associated emissions. *Science of the Total Environment*, 304, 13-27.
- Jasminka, A., Robert, Š., 2011. Distribution of chemical elements in an old metallurgical area, Zenica (Bosnia and Herzegovina). *Geoderma*, 162, 71-85.
- Jung, M. C., Thornton, I., Chon, H. T., 2002. Arsenic, Sb and Bi contamination of soils, plants, waters and sediments in the vicinity of the Dalsung Cu-W mine in Korea. *Science of the Total Environment*, 295, 81-89.
- Karamanis, D., Ioannides, K., Stamoulis, K., 2009. Environmental assessment of natural radionuclides and heavy metals in waters discharged from a lignite-fired power plant. *Fuel*, 88, 2046-2052.
- Karayigit, A. I., Gayer, R. A., Querol, X., Onacak, T., 2000. Contents of major and trace elements in feed coals from Turkish coal-fired power plants. *International Journal of Coal Geology*, 44, 169-184.
- Knox, J. C., 2006. Floodplain sedimentation in the Upper Mississippi

Valley: Natural versus human accelerated. *Geomorphology*. 79, 286–310.

Koiter, A. J., Owens, P. N., Petticrew, E. L., Lobb, D., 2013. The Behavioural Characteristics of Sediment Properties and their Implications for Sediment Fingerprinting as an Approach for Identifying Sediment Sources in River Basins. *Earth-Science Reviews*, 125, 24–42.

Kolker, A., 2012. Minor element distribution in iron disulfides in coal: a geochemical review. *International Journal of Coal Geology*, 94, 32-43.

Latapie, A., Camenen, B., Rodrigues, S., Paquier, A., Bouchard, J.P., Moatar, F., 2014. Assessing channel response of a long river influenced by human disturbance, *Catena*, 121,1-12.

Latapie, A., 2011. Modélisation de l'évolution morphologique d'un lit alluvial: application à la Loire moyenne. PhD thesis, Tours univ., 277 p.

Le Cloarec, M. F., Bonte, P. H., Lestel, L., Lefèvre, I., Ayrault, S., 2011. Sedimentary record of metal contamination in the Seine River during the last century. *Physics and Chemistry of the Earth*, 36, 515-529.

Le Pape, P., Ayrault, S., Quantin, C., 2012. Trace element behavior and partition versus urbanization gradient in an urban river (Orge River, France). *Journal of Hydrology*, 472, 99-110.

Lecce, S. A., Pavlowsky, R. T., 2014. Floodplain storage of sediment contaminated by mercury and copper from historic gold mining at Gold Hill, North Carolina, USA. *Geomorphology*, 206, 122-132.

Lecce, S. A., Pavlowsky, R. T., 1997. Storage of mining-related zinc in floodplain sediments, Blue River,

Wisconsin. *Physical Geography*. 18, 424-439.

Lestel, L., Meybeck, M., Thevenot, D. R., 2007. Metal contamination budget at the river basin scale: an original Flux-Flow Analysis (F2A) for the Seine River. *Hydrology and earth system sciences*, 11, 1771-1781.

Leteinturier B., Engels P., Petit F., Chiffaut A., Malaisse F..Morphodynamisme d'un tronçon de Loire bourbonnaise depuis le XVIIIe siècle / Changingdynamics of the Loire river in Burgundy (France) during the last 200 years. In: *Géomorphologie : relief, processus, environnement*, 6, 239-251.

Li, Z., Feng, X., Li, G., Bi, X., Zhu, J., Qin, H., Sun, G., 2013. Distributions, sources and pollution status of 17 trace metal/metalloids in the street dust of a heavily industrialized city of Central China. *Environmental Pollution*, 182, 408-416.

Lino, M., Mériaux, P., Royet, P., 2000. Méthodologie de diagnostic des digues appliquée aux levées de la Loire moyenne. Editions Quae.

Louriño-Cabana, B., Lesven, L., Charria, A., Billon, G., Ouddane, B., Boughriet, A., 2011. Potential risks of metal toxicity in contaminated sediments of Deûle river in Northern France. *Journal of hazardous materials*, 186, 2129-2137.

Lumb, A. J., 1995. Mercury (a Review with Special Emphasis on Pollution Effects from Gold Mining). British Geological Survey.

Macaire, J. J., Gay-Ovejero, I., Bacchi, M., Cocirat, C., Patryl, L., Rodrigues, S., 2013. Petrography of alluvial sands as a past and present environmental indicator: Case of the Loire River (France). *International Journal of Sediment Research*, 28, 285-303.

- Macklin, M. G., Brewer, P. A., Hudson-Edwards, K. A., Bird, G., Coulthard, T. J., Dennis, I. A., Turner, J. N., 2006. A geomorphological approach to the management of rivers contaminated by metal mining. *Geomorphology*, 79, 423-447.
- Macklin, M. G., Klimek, K., 1992. Dispersal, storage and transformation of metal contaminated alluvium in the upper Vistula basin, southwest Poland. *Applied Geography*. 12, 7-30.
- Martin, C. W., 2000. Heavy metal trends in floodplain sediments and valley fill, River Lahn, Germany. *Catena*, 39, 53-68.
- Martin, J. M., Meybeck, M., 1979. Elemental mass-balance of material carried by major world rivers. *Marine chemistry*, 7, 173-206.
- Martinez-Cortizas, A., Pontevedra-Pombal, X., Garcia-Rodeja, E., Novoa-Munoz, J. C., Shotyk, W. (1999). Mercury in a Spanish peat bog: archive of climate change and atmospheric metal deposition. *Science*, 284, 939-942.
- Meybeck, M., Lestel, L., Bonté, P., Moilleron, R., Colin, J. L., Rousselot, O., Thévenot, D. R., 2007. Historical perspective of heavy metals contamination (Cd, Cr, Cu, Hg, Pb, Zn) in the Seine River basin (France) following a DPSIR approach (1950–2005). *Science of the Total Environment*, 375, 204-231.
- Meybeck M, Horowitz A, Grosbois C., 2004. The geochemistry of Seine River basin particulate matter: distribution of an integrated metal pollution index. *Science of the Total Environment*, 328, 219–36.
- Meybeck, M., 2002. Riverine quality at the Anthropocene: Propositions for global space and time analysis, illustrated by the Seine River. *Aquatic Sciences*, 64, 376-393.
- Meybeck, M., Helmer, R., 1989. The quality of rivers: from pristine stage to global pollution. *Global and Planetary Change*, 1, 283-309.
- Miller, J. R., Lechler, P. J., Bridge, G., 2003. Mercury contamination of alluvial sediments within the Essequibo and Mazaruni river basins, Guyana. *Water, Air, and Soil Pollution*, 148, 139-166.
- Miller, J. R., 1997. The role of fluvial geomorphic processes in the dispersal of heavy metals from mine sites. *Journal of Geochemical Exploration*, 58, 101-118.
- Mishra, V. K., Upadhyaya, A. R., Pandey, S. K., Tripathi, B. D. , 2008. Heavy metal pollution induced due to coal mining effluent on surrounding aquatic ecosystem and its management through naturally occurring aquatic macrophytes. *Bioresource technology*, 99, 930-936.
- Möller, S., Einax, J. W., 2013. Metals in sediments—spatial investigation of Saale River applying chemometric tools. *Microchemical Journal*, 110, 233-238.
- Monna, F., Clauer, N., Toulkeridis, T., Lancelot, J. R., 2000. Influence of anthropogenic activity on the lead isotope signature of Thau Lake sediments (southern France): origin and temporal evolution. *Applied Geochemistry*, 15, 1291-1305.
- Mourier, B., Desmet, M., Van Metre, P. C., Mahler, B. J., Perrodin, Y., Roux, G., Babut, M., 2014. Historical records, sources, and spatial trends of PCBs along the Rhône River (France). *Science of the total environment*, 476, 568-576.
- Mukherjee, A. B., Zevenhoven, R., Bhattacharya, P., Sajwan, K. S., Kikuchi, R., 2008. Mercury flow via coal and coal

utilization by-products: A global perspective. *Resources, Conservation and Recycling*, 52, 571-591.

Neal, P. A., 1938. Mercury Poisoning from the Public Health Viewpoint\*. *American Journal of Public Health and the Nations Health*, 28, 907-915.

Negrel, P., Kloppmann, W., Garcin, M., Giot, D., 2004. Lead isotope signatures of Holocene fluvial sediments from the Loire River valley. *Applied geochemistry*, 19, 957-972.

Négrel, P., Grosbois, C., 1999. Changes in chemical and  $^{87}\text{Sr}/^{86}\text{Sr}$  signature distribution patterns of suspended matter and bed sediments in the upper Loire river basin (France). *Chemical Geology*, 156, 231-249.

Okkenhaug, G., Zhu, Y. G., Luo, L., Lei, M., Li, X., Mulder, J., 2011. Distribution, speciation and availability of antimony (Sb) in soils and terrestrial plants from an active Sb mining area. *Environmental Pollution*, 159, 2427-2434.

Ondov, J. M., Choquette, C. E., Zoller, W. H., Gordon, G. E., Biermann, A. H., Heft, R. E., 1989. Atmospheric behavior of trace elements on particles emitted from a coal-fired power plant. *Atmospheric Environment*, 23, 2193-2204.

Oyarzun, R., Lillo, J., López-García, J. A., Esbrí, J. M., Cubas, P., Llanos, W., Higuera, P., 2011. The Mazarrón Pb-(Ag)-Zn mining district (SE Spain) as a source of heavy metal contamination in a semiarid realm: Geochemical data from mine wastes, soils, and stream sediments. *Journal of Geochemical Exploration*, 109, 113-124.

Qi, C., Liu, G., Chou, C. L., Zheng, L., 2008. Environmental geochemistry of antimony

in Chinese coals. *Science of the total environment*, 389, 225-234.

Querol, X., Fernández-Turiel, J., Lopez-Soler, A., 1995. Trace elements in coal and their behaviour during combustion in a large power station. *Fuel*, 74, 331-343.

Querol, X., Viana, M., Alastuey, A., Amato, F., Moreno, T., Castillo, S., Zabalza, J., 2007. Source origin of trace elements in PM from regional background, urban and industrial sites of Spain. *Atmospheric Environment*, 41, 7219-7231.

Reis, A., Parker, A., Alencão, A., 2014. Storage and origin of metals in active stream sediments from mountainous rivers: A case study in the River Douro basin (North Portugal). *Applied Geochemistry*, 44, 69-79.

Resongles, E., Casiot, C., Freydier, R., Dezileau, L., Viers, J., & Elbaz-Poulichet, F., 2014. Persisting impact of historical mining activity to metal (Pb, Zn, Cd, Tl, Hg) and metalloid (As, Sb) enrichment in sediments of the Gardon River, Southern France. *Science of the Total Environment*, 481, 509-521.

Rodrigues S, Bréhéret JG, Macaire JJ, Greulich S, Villar M., 2007. In-channel woody vegetation controls on sedimentary processes and the sedimentary record within alluvial environments: a modern example of an anabranch of the River Loire, France. *Sedimentology*, 54, 223–242.

Santiago, S., Thomas, R. L., Larbaigt, G., Corvi, C., Rossel, D., Tarradellas, J., Vernet, J. P., 1994. Nutrient, heavy metal and organic pollutant composition of suspended and bed sediments in the Rhone River. *Aquatic sciences*, 56, 220-242.

- Seredin, V. V., Finkelman, R. B., 2008. Metalliferous coals: a review of the main genetic and geochemical types. *International Journal of Coal Geology*, 76, 253-289.
- Shotyk, W., Weiss, D., Appleby, P. G., Cheburkin, A. K., Frei, R., Gloor, M., Van Der Knaap, W. O., 1998. History of atmospheric lead deposition since 12,370 14C yr BP from a peat bog, Jura Mountains, Switzerland. *Science*, 281, 1635-1640.
- Sizaret, S., 2002. Genèse du système hydrothermal à fluorine-barytine-fer de Chaillac, (Indre, France) (Doctoral dissertation, Université d'Orléans).
- Skalak, K., Pizzuto, J., 2010. The distribution and residence time of suspended sediment stored within the channel margins of a gravel-bed bedrock river. *Earth Surface Processes and Landforms*, 35, 435-446.
- Steffen, W., Grinevald, J., Crutzen, P., McNeill, J., 2011. The Anthropocene: conceptual and historical perspectives. *Philosophical Transactions of the Royal Society A: Mathematical, Physical and Engineering Sciences*, 369, 842-867.
- Steffen, W., Crutzen, P. J., McNeill, J. R., 2007. The Anthropocene: are humans now overwhelming the great forces of nature. *Ambio: A Journal of the Human Environment*, 36, 614-621.
- Stutter, M. I., Langan, S. J., Lumsdon, D. G., Clark, L. M., 2009. Multi-element signatures of stream sediments and sources under moderate to low flow conditions. *Applied Geochemistry*, 24, 800-809.
- Takaoka, M., Fukutani, S., Yamamoto, T., Horiuchi, M., Satta, N., Takeda, N., Tanaka, T., 2005. Determination of chemical form of antimony in contaminated soil around a smelter using X-ray absorption fine structure. *Analytical Sciences*, 21, 769.
- Teixeira, E. C., Sanchez, J. C. D., Migliavacca, D., Binotto, R. B., Fachel, J. M. G., 2000. Environmental assessment: study of metals in fluvial sediments in sites impacted by coal processing and steel industry activities. *Fuel*, 79, 1539-1546.
- Thévenot, D. R., Moilleron, R., Lestel, L., Gromaire, M. C., Rocher, V., Cambier, P., Meybeck, M., 2007. Critical budget of metal sources and pathways in the Seine River basin (1994–2003) for Cd, Cr, Cu, Hg, Ni, Pb and Zn. *Science of the total environment*, 375, 180-203.
- Tiwary, R. K., Dhar, B. B., 1994. Effect of coal mining and coal based industrial activities on water quality of the river Damodar with specific reference to heavy metals. *International Journal of Surface Mining and Reclamation*, 8, 111-115.
- Tiwary, R. K., Dhar, B. B., 1994. Environmental pollution from coal mining activities in Damodar River Basin, India. *Mine water and the Environment*, 13, 1-10.
- Ure, A. M., Berrow, M. L., 1982. Environmental chemistry. Spec. Period. Rep, 2, 94-204.
- Valverde, L., Jugé, P., Handfus, T., 2013. Résultats granulométriques et localisation des points dures en Loire, rapport InfoSed 2,180 p.
- Viers, J., Dupré, B., Gaillardet, J., 2009. Chemical composition of suspended sediments in World Rivers: new insights from a new database. *Science of the total environment*, 407, 853-868.

- Vink, R., Behrendt, H., Salomons, W., 1999. Development of the heavy metal pollution trends in several European rivers: an analysis of point and diffuse sources. *Water Science and Technology*, 39, 215-223.
- Vörösmarty, C. J., Meybeck, M., Fekete, B., Sharma, K., Green, P., Syvitski, J. P., 2003. Anthropogenic sediment retention: major global impact from registered river impoundments. *Global and Planetary Change*, 39, 169-190.
- Vukovic, D., Vukovic, Z., Stankovic, S., 2014. The impact of the Danube Iron Gate Dam on heavy metal storage and sediment flux within the reservoir. *Catena*, 113, 18-23.
- Wallbrink, P. J., Murray, A. S., Olley, J. M., Olive, L. J., 1998. Determining sources and transit times of suspended sediment in the Murrumbidgee River, New South Wales, Australia, using fallout  $^{137}\text{Cs}$  and  $^{210}\text{Pb}$ . *Water Resources Research*, 34, 879-887..
- Walling, D. E., 2005. Tracing suspended sediment sources in catchments and river systems. *Science of the total environment*, 344, 159-184.
- Walling, D. E., Owens, P. N., 2003. The role of overbank floodplain sedimentation in catchment contaminant budgets. *Hydrobiologia*, 494, 83-91.
- Walling, D. E., Owens, P. N., Carter, J., Leeks, G. J. L., Lewis, S., Meharg, A. A., Wright, J., 2003. Storage of sediment-associated nutrients and contaminants in river channel and floodplain systems. *Applied Geochemistry*, 18, 195-220.
- Wang, Q., Kim, D., Dionysiou, D. D., Sorial, G. A., Timberlake, D., 2004. Sources and remediation for mercury contamination in aquatic systems—a literature review. *Environmental pollution*, 131, 323-336.
- Wang, X., He, M., Xi, J., Lu, X., 2011. Antimony distribution and mobility in rivers around the world's largest antimony mine of Xikuangshan, Hunan Province, China. *Microchemical Journal*, 97, 4-11.
- Woronoff Denis, *Histoire de l'industrie en France, Du 16e siècle à nos jours*, Paris, Le Seuil, 1994, 671 p.
- Ye, C., Li, S., Zhang, Y., Zhang, Q., 2011. Assessing soil heavy metal pollution in the water-level-fluctuation zone of the Three Gorges Reservoir, China. *Journal of hazardous materials*, 191, 366-372.
- Yin, R., Feng, X., Shi, W., 2010. Application of the stable-isotope system to the study of sources and fate of Hg in the environment: A review. *Applied Geochemistry*, 25, 1467-1477.
- Yudovich, Y. E., Ketrus, M. P., 2005. Mercury in coal: a review: Part 1. *Geochemistry. International Journal of Coal Geology*, 62, 107-134.
- Yudovich, Y. E., Ketrus, M. P., 2005. Mercury in coal: a review: Part 2. Coal use and environmental problems. *International Journal of Coal Geology*, 62, 135-165.

## Conclusions et perspectives

Au cours de cette thèse, une étude multiscalaire de la **variabilité spatiale des enregistrements sédimentaires des contaminations métalliques** a été menée, intégrant des **approches géochimiques et sédimentologiques**.

L'étude des **mécanismes et les modalités de l'archivage des sédiments et contaminants** associés a permis de répondre aux verrous scientifiques concernant la représentativité des enregistrements sédimentaires. Ce travail met en évidence des variabilités spatiales concernant l'archivage des signaux géochimiques à une double échelle *i.e.* celle de l'environnement fluviatile et celle du bassin versant.

Au cours de cette étude, il a été montré que **l'environnement de dépôt conditionne :**

- (i) **les taux d'aggradation,**
- (ii) **la continuité des enregistrements,**
- (iii) **l'archivage des sédiments et contaminants associés en fonction**

- (iv) **de leur granulométrie, de leur densité et de leurs origines et les processus de redistribution des ET au sein de la colonne sédimentaire.**

Ces facteurs influencent l'enregistrement sédimentaire des dynamiques temporelles des contaminants. Les paléochenaux et les réservoirs de barrages sont des **environnements de stockage des sédiments fins** permettant l'établissement de chroniques de contaminations représentatives. L'activation de fortes sources de contaminations et l'apport massif de sédiments lors **des épisodes hydrosédimentaires majeurs** peuvent influencer le signal géochimique enregistré.

D'autre part, ces travaux témoignent de **l'homogénéité les états de référence dans les sédiments fins à l'échelle du domaine fluviatile ligérien**. Par contre, des **différences significatives** concernant les concentrations préindustrielles ont été mises en évidence à l'échelle de l'environnement

**fluviatile**, liées à la variabilité spatiale des processus d'alluvionnements.

A l'échelle du **bassin versant**, deux archives sédimentaires ont été analysées afin de reconstituer les évolutions temporelles des contaminations dans les sous-bassins les plus industrialisés (la Loire Amont et l'Allier). Ces enregistrements ont été comparés aux chroniques des contaminations sédimentaires établies dans le partie aval du bassin. Cette étude multi-sites a permis de discriminer les **contaminations sédimentaires locales**, seulement enregistrées dans les sous-bassins de la Loire Amont et de l'Allier, **de celles affectant aussi bien les parties amont et aval du bassin**. Ces phases temporelles de contaminations sédimentaires sont enregistrées avec **un délai et sur une plus large fenêtre temporelle dans la partie aval du domaine fluviatile**. La propagation des sédiments contaminés depuis les sources, localisées dans la partie amont du bassin et dans les principaux affluents de la Loire, vers la partie aval du bassin peut expliquer ces différences.

Ces résultats montrent qu'à l'échelle du bassin de la Loire **les processus de transport et d'archivage des**

**sédiments et contaminants associés jouent un rôle important en ce qui concerne les distributions spatiales et temporelles des contaminants sédimentaires.**

D'autre part, les **sources historiques de contaminations** ont été caractérisées à l'aide de leurs **signatures géochimiques archivées dans les sédiments des berges** en aval des principaux foyers industriels et miniers.

L'histoire des sources de contaminations métalliques du bassin de la Loire fait état d'une **faible influence des activités protoindustrielles et de la Première Révolution Industrielle** (*c.a.* 1800 - *c.a.* 1880) sur la géochimie des sédiments. De **forts enrichissements en Hg** sont enregistrés depuis les années **1880** dans la Loire Amont et généralisés à l'échelle du bassin depuis au moins le début du XX<sup>ème</sup> siècle. En Loire Amont, la Seconde Révolution Industrielle (*c.a.* 1880 – fin des années 1930) est caractérisée par des enrichissements élevés en **Hg, Sb et Sn** associés aux rejets industriels des chapelleries (Hg) ainsi que des verreries et des industries métallurgiques (Sb, Sn). Pour les sous-bassins de la Loire Amont et de l'Allier, une phase de contamination

**polymétallique est enregistrée au début des Trente Glorieuses** (entre les années 1940 et 1950) présentant les plus importants enrichissements pour l'ensemble des ET (sauf Sn et Pb). **Bi, Cd, Hg et Sb sont les métaux les plus enrichis** au cours de cette période et sont associés aux effluents miniers (mines de charbon et ET) ainsi qu'aux rejets des industries lourdes (essentiellement des aciéries) utilisant localement les matières premières extraites du sous-sol. Suite au ralentissement des activités minières et à la relocalisation des industries lourdes à proximité des ports internationaux **dans les années 1960, les niveaux de contaminations sédimentaires ont diminué de façon exponentielle** dans la partie amont du bassin de la Loire. Les enrichissements maximum sont enregistrés entre les années 1950 et 1980 dans la partie aval du bassin. Depuis les années 1980, les niveaux de contaminations enregistrés dans les sédiments du bassin de la Loire sont beaucoup plus faibles que durant la période 1940-1980. Dans ce contexte, **l'érosion des sédiments contaminés stockés dans les berges est un facteur de réactivation des sources anciennes et une source de contamination importante** lors des épisodes hydrosédimentaires majeurs.

Entre les années 1880 et la fin des années 1950 les **activités industrielles et minières du bassin de la Loire ont été sources d'importants rejets en ET** en partie stockés avec les sédiments des berges et des réservoirs. De nos jours, **des événements de déstockage de ces sédiments contaminés peuvent induire un réel risque pour les écosystèmes.**

Les résultats de ces travaux de thèse portent sur les mécanismes et modalités de l'archivage des contaminations sédimentaires et ils permettent formuler **plusieurs recommandations en termes de gestion des sédiments de la Loire.**

En ce qui concerne **l'évaluation des tendances temporelles des contaminations**, cette étude souligne l'intérêt de sélectionner **des sites localisés à proximité des sources de contamination et permettant un dépôt régulier et continu de sédiments fins.** La variabilité granulométrique et minéralogique associée à l'évolution du degré de connectivité des environnements de dépôts influence directement les niveaux de contamination et donc la représentativité de l'enregistrement. **La double normalisation des concentrations**

**aux teneurs en Al et au bruit de fond géochimique dans la fraction < 63 µm** permet en partie de limiter ces influences dans ce travail.

De plus, l'évolution temporelle des contaminations a montré qu'il peut être important de différencier les **apports des crues majeures** de celles plus fréquentes. Ces événements hydrosédimentaires majeurs peuvent concourir à la **sollicitation événementielle d'importantes sources de contamination** (directement par ruissellement, lessivage ou via le déstockage de sédiments très contaminés, archivés dans les environnements fluviatiles). **La variabilité du signal géochimique enregistrée alors pendant ces crues n'est pas représentative de l'évolution à long-terme des niveaux de contaminations.**

Depuis la fin du XIX<sup>ème</sup> siècle, la rétention de sédiments contaminés sur les berges et en amont d'ouvrages hydrauliques a constitué des **stocks de contaminants plus ou moins mobilisables**. Avant d'effectuer des travaux visant à **restaurer le fonctionnement naturel des hydrosystèmes** et la continuité du transport sédimentaire (arasement des

seuils et barrages, travaux sur les berges), il est important d'évaluer

- (i) **la qualité des sédiments piégés et la quantité de contaminants potentiellement remobilisables,**
- (ii) **les risques de relargage associés et**
- (iii) **la faisabilité de solutions de traitement ou de séquestration.**

Différentes perspectives peuvent être proposées à ces travaux de recherche.

De la même manière que pour le bassin de la Seine, une comparaison entre **l'évolution temporelle des flux de métaux** (introduits dans le système et extrait du sous-sol) **et les stocks sédimentaires de contaminants métalliques** pourrait apporter des informations importantes concernant **la capacité de rétention du système** (Lestel *et al*, 2007, Meybeck *et al*, 2007, Thevenot *et al*, 2007).

Dans cette perspective, les informations mis à jour au cours de cette étude concernant la contamination des sédiments et le délai amont-aval pour l'archivage des phases de contaminations

pourrait permettre de définir **le temps de résidences des sédiments fins au sein bassin de la Loire.**

D'autre part, la quantification des stocks de contaminants piégés avec les sédiments au sein des environnements fluviatiles et **la modélisation de leurs évolutions futures** constituent des objectifs de recherche majeurs pour **évaluer à plus ou moins long terme les risques auxquels sont soumis les sociétés et les écosystèmes** (objectifs de la directive-cadre européenne concernant la qualité des milieux aquatiques continentaux DCE ; Audry *et al*, 2004 ; Newham *et al*, 2004 ; Heise et Förstner, 2006 ).

Dans le bassin de la Loire, l'érosion des berges constitue une source de contamination importante lors des épisodes de crues majeurs. Dans cette perspective, la **caractérisation des phases porteuses** des ET permettraient d'analyser la **disponibilité environnementale des contaminants déstockés** (ex. pour des rejets miniers et de fonderies : Courtin-Nomade *et al*, 2005 ; Castelle *et al*, 2007 ; Grosbois *et al*, 2007 ; Audry *et al*, 2010). Des analyses sont actuellement en cours visant à caractériser les phases porteuses

et la disponibilité des ET dans les sédiments des archives du réservoir de Villerest et des berges du Furan (extractions sélectives, microscopie électronique par balayage; DRX). De surcroit, le projet MetMin porté par le laboratoire GRESE de l'université de Limoges vise à caractériser l'impact des sites miniers sur le milieu naturel et mène des analyses géochimiques comparables sur des sédiments de fonds en aval des districts miniers de l'Allier (Pontgibaud et Brioude-Massiac).

D'autre part, des analyses complémentaires pourraient être menées pour caractériser les sources de contaminations. En effet, dans le bassin de la Loire, les sources de Hg étaient multiples et synchrones au cours de l'ère industrielle, et leur caractérisation n'a été que partielle dans cette étude. La **caractérisation isotopique des sources de contaminations en Hg** pourrait permettre de mieux discriminer leurs contributions respectives (Feng *et al*, 2010 ; Yin *et al*, 2010). Dans ce cadre, le programme de recherche ISOP (BRGM) est actuellement en cours. Il a pour objectif de caractériser les signatures isotopiques des sources de contaminations actives du bassin de la Loire et de les confronter à celles des

sources anciennes enregistrées dans les archives de Villerest et Decize.

D'autre part, le projet de recherche SPAL (laboratoire GHeCO, université de Tours) a pour objectif de **spatialiser les contaminations métalliques dans les sédiments de fond** du bassin de la Loire et de **déterminer les facteurs explicatifs de la distribution spatiale des contaminations selon différentes plages temporelles**.

Dans le cadre du réseau d'observation des sédiments de la Loire et de ces affluents (OSLA), des recherches concernant la **distribution spatiale et temporelle des pollutions organiques** sont entreprises (MetOrg2). Des études sont en cours concernant les HAPs et PCBs archivés avec les sédiments du réservoir de Villerest (*Bertrand et al, in prep*, laboratoire GHeCO, université de Tours) et sur les composés pharmaceutiques des sédiments de surface de la Dore (sous-bassin de l'Allier) et du Clain (sous-bassin de la Vienne, laboratoire IC2MP – UMR CNRS 7285, université de Poitiers). Les résultats de cette thèse, en ce qui concerne les mécanismes d'archivage des sédiments et substances associées, les modèles d'âges des archives

sédimentaires et la caractérisation des sources peuvent être intégrés à ces programmes.

Dans le cadre de l'OSLA, le projet DYNAMICS développé par le laboratoire LMGE (UMR-CNRS 6023, université de Clermont-Ferrand) a pour objectif d'étudier **l'écotoxicité des sédiments** de l'archive de Villerest. Les résultats de cette thèse ainsi que ceux issus des recherches sur les polluants organiques et sur la caractérisation des phases porteuses sont intégrés à cette étude.

L'exposition des êtres vivants aux pollutions induit la sélection de gènes de résistances ou même l'apparition d'effets épigénétiques spécifiques (Feil, 2006 ; Baccarelli et Bollati, 2009, Feil et Fraga, 2012). Les connaissances concernant la pollution des sédiments de la Loire pourraient par la suite être intégrées pour développer des outils de diagnostics basés sur la recherche de **biomarqueurs de leur toxicité**.

## Bibliographie :

Audry, S., Grosbois, C., Bril, H., Schäfer, J., Kierczak, J., Blanc, G., 2010. Post-depositional redistribution of trace metals in reservoir sediments of a

mining/smelting-impacted watershed (the Lot River, SW France). Applied Geochemistry, 25, 778–794.

Audry, S., Blanc, G., Schäfer, J., 2004. Cadmium transport in the Lot–Garonne River system (France)—temporal variability and a model for flux estimation. Science of the Total Environment, 319, 197–213.

Baccarelli, A., Bollati, V., 2009. Epigenetics and environmental chemicals. Current opinion in pediatrics, 21, 243.

Courtin-Nomade, A., Grosbois, C., Bril, H., Roussel, C., 2005. Spatial variability of arsenic in some iron-rich deposits generated by acid mine drainage. Applied Geochemistry, 20, 383–396.

Castelle, S., Schäfer, J., Blanc, G., Audry, S., Etcheber, H., Lissalde, J. P., 2007. 50-year record and solid state speciation of mercury in natural and contaminated reservoir sediment. Applied Geochemistry, 22, 1359–1370.

Grosbois, C., Courtin-Nomade, A., Martin, F., Bril, H., 2007. Transportation and evolution of trace element bearing phases in stream sediments in a mining – Influenced basin (Upper Isle River, France). Applied Geochemistry, 22, 2362–2374

Feil, R., Fraga, M. F., 2012. Epigenetics and the environment: emerging patterns and implications. Nature Reviews Genetics, 13, 97–109.

Feil, R., 2006. Environmental and nutritional effects on the epigenetic regulation of genes. Mutation Research/Fundamental and Molecular Mechanisms of Mutagenesis, 600, 46–57.

Feng, X., Foucher, D., Hintelmann, H., Yan, H., He, T., Qiu, G., 2010. Tracing mercury contamination sources in sediments using

mercury isotope compositions. Environmental science & technology, 44, 3363–3368.

Heise, S., Förstner, U., 2006. Risks from historical contaminated sediments in the Rhine basin. In The Interactions Between Sediments and Water, Springer Netherlands. 261–272

Lestel, L., Meybeck, M., Thévenot, D. R., 2007. Metal contamination budget at the river basin scale: an original Flux-Flow Analysis (F2A) for the Seine River. Hydrology and earth system sciences, 11, 1771–1781.

Meybeck, M., Lestel, L., Bonté, P., Moilleron, R., Colin, J. L., Rousselot, O., Thévenot, D. R., 2007. Historical perspective of heavy metals contamination (Cd, Cr, Cu, Hg, Pb, Zn) in the Seine River basin (France) following a DPSIR approach (1950–2005). Science of the Total Environment, 375, 204–231.

Newham, L. T., Letcher, R. A., Jakeman, A. J., Kobayashi, T., 2004. A framework for integrated hydrologic, sediment and nutrient export modelling for catchment-scale management. Environmental Modelling & Software, 19(11), 1029–1038.

Thévenot, D. R., Moilleron, R., Lestel, L., Gromaire, M. C., Rocher, V., Cambier, P., Meybeck, M., 2007. Critical budget of metal sources and pathways in the Seine River basin (1994–2003) for Cd, Cr, Cu, Hg, Ni, Pb and Zn. Science of the total environment, 375, 180–203.

Yin, R., Feng, X., Shi, W., 2010. Application of the stable-isotope system to the study of sources and fate of Hg in the environment: A review. Applied Geochemistry, 25, 1467–1477





## Elie DHIVERT

### Mécanismes et modalités de la distribution spatiale et temporelle des éléments traces dans les sédiments du bassin versant de la Loire

#### Résumé

Cette étude correspond à une approche multiscalaire de la variabilité spatiale des contaminations métalliques enregistrées dans les sédiments du bassin de la Loire. Ce manuscrit est organisé en trois parties exposant la démarche et les résultats de ces travaux.

La première partie permet de formuler les problématiques de l'étude en proposant une synthèse des connaissances concernant l'archivage des contaminations sédimentaires dans les environnements fluviaitiles.

La seconde partie s'intéresse à l'influence des environnements de dépôts sur l'archivage des sédiments et contaminants associés. Les objectifs de ces recherches sont d'étudier la représentativité des signaux géochimiques enregistrés dans les compartiments de stockage sédimentaire.

La troisième partie permet de mettre en évidence la variabilité spatiale et l'origine des contaminations sédimentaires à l'échelle du bassin versant de la Loire.

#### Abstract

This multi-scale focuses on the spatial and temporal variability of the metallic contamination in sediments of the Loire basin. This manuscript presents methods and results in three sections.

The first section deals with scientific issues concerning the recording of sedimentary contaminations in fluvial environments.

The second section shows the influence of depositional environments on sediments and associated contaminants archiving. The aim of this study is to analyse the representation of geochemical signals recorded in sedimentary infills.

The third section highlights spatial variabilities of recorded sedimentary contaminations at the entire Loire basin-scale. Historical sources are here characterized.